DEVELOPMENT AND EVALUATION OF A NOVEL NANOPARTICULATE DELIVERY SYSTEM OF ARSENIC SULFIDES

WU JINZHU

((*M. Eng.*), Harbin Institute of Technology)

A THESIS SUBMITTED

FOR THE DEGREE OF DOCTOR OF PHILOSOPHY

DEPARTMENT OF PHARMACY

NATIONAL UNIVERSITY OF SINGAPORE

2008

Acknowledgements

First, I thank my supervisor Associate Professor (A/P) Ho Chi Lui, Paul, for his always supports throughout the whole course of my Ph.D study. Whenever I encountered difficulties and problems during my study and in my personal life, A/P Ho constantly gave his timely helps and directions and encouragements to me to fight this and that obstacles and clear them off finally. I am also deeply touched by A/P Ho's kind patience and considerations for my occasional poor performance.

I would like to appreciate A/P Li Shu Chuen and Dr Chui Wai Keung, who as my Ph.D qualifying examination examiners gave me valuable suggestions in the beginning of this project. I also would like to say thanks to A/P Chan Sui Yong for her cares for me.

I would like to express my thankfulness to Ms Ng Swee Eng, Ms Ng Sek Eng, Mr Tang Chong Wing, Mdm Tham-Wong Pheng, Josephine, and other laboratory officers of the Department of Pharmacy, for having given me assistances during my study. I also would like to thank Mdm Lee Hua Yeong and Mdm Lim Sing for their warm cares and helps and sistership.

I would like to thank my fellow postgraduate students, Liu Xin, Sam Wai Johnn, Su Jie, Lin Haishu, Huang Meng, Wang Zhe, Wang Chun Xia, Kang Lifeng, Hou Peiling and Yang Hong for their loyal friendship. I miss so much the good times we spent together in Singapore.

I would also like to acknowledge the National University of Singapore for the award of a research scholarship, which financially supported my study.

Finally, but not least, I thank so much my parents and two sisters and my own family for their great supports and selfless sacrifice throughout my whole life. I also would like to say thanks to my lovely twin girls, they always bring me so many

happiness and spiritual energies to face all kinds of difficulties in life.

Table of Contents

CONTENTS **PAGE**

Summary

Arsenicals were therapeutic mainstays for various diseases in the 18th, 19th and early 20th centuries. Fowler's solution (1% potassium arsenite) was a famous example, which was a key medicine for treatment of chronic myeloid leukemia (CML) until the 1930s, thereafter it was gradually replaced by radiotherapy and other cytotoxic chemotherapeutic agents. Decline in the medicinal use of arsenicals in the mid-20th century can be traced to the concerns about their toxicity and carcinogenicity. Arsenic trioxide (As_2O_3) was reintroduced as an anticancer agent after reports emerged from China of the success of an arsenic trioxide-contained herbal medicine for treatment of patients with acute promyelocytic leukemia (APL) in 1970s. Commercial available arsenic trioxide product, Trisenox™, was approved by the American Food and Drug Administration (FDA) in 2000 for treatment of patients with APL, who have not responded to or have relapsed following the use of all *trans*-retinoic acid (ATRA) and anthracycline-based chemotherapies.

Since arsenic trioxide can cause serious liver damage if given orally, it must be administered intravenously daily as an infusion over 1 to 4 hours, which makes consolidation and maintenance therapies difficult. Therefore, an alternative oral agent with similar therapeutic effects and fewer side effects would provide not only cost and quality-of-life benefits but also easy access to the consolidation and maintenance therapies. Moreover, such oral agent would give opportunity for further combination with other agents of interest. Realgar (As_2S_2) and orpiment (As_2S_3) could be such candidates. Both realgar and orpiment are reportedly the oldest drugs. The first mention of arsenicals was made by Hippocrates (460-370 BC), who used realgar and orpiment pastes to treat ulcers. Realgar and orpiment are defined as mild-toxic compounds. Recent years, mainly in China, realgar and orpiment became research

focus for their promising anticancer effects.

Although some clinical trials conducted in China reported that both realgar and orpiment achieved promising outcomes in treatment of patients with APL at different disease stages, there is extremely limited information of these arsenicals in terms of the mechanisms of action, toxicity, as well as pharmacokinetic and pharmacodynamic profiles. The lack of information could be caused by the water-insolubility of realgar and orpiment. Both realgar and orpiment are crystal with high native lattice energy, which results in the difficulty of breaking apart the respective molecules into surrounding media including aqueous and most organic solvents.

The water-insolubility of realgar and orpiment is a key obstacle for their investigation, development and final commercialization. In order to improve the poor water-solubility of realgar and orpiment, alkalization approach by directly dissolving both compounds into alkali solutions was usually applied. We established capillary zone electrophoresis (CZE) method to identify the exact composition of realgar and orpiment in sodium hydroxide solution. Our findings showed that realgar and orpiment would be converted to arsenite and arsenate with different proportions instead of intact molecules, suggesting that the conventional alkalization approach is not appropriate for enhancement of the water-solubility of realgar and orpiment.

Nanosized realgar and orpiment particles were prepared by cryo-grinding technique with the assistance of biocompatible water-soluble polymer polyvinylpyrrolidone (PVP) and surfactant sodium dodecyl sulphate (SDS). Improved water-solubility of nanosized reaglar and orpiment particles were achieved as indicated by the increased soluble arsenic contents, i.e. 134.20 ± 4.30 ppm and 152.80 ± 5.54 ppm, respectively, of R/PVP/SDS and O/PVP/SDS nanosuspensions compared with those, i.e. 0.52 ± 0.03 ppm and 0.51 ± 0.03 ppm, respectively, of original realgar

and orpiment filtrates. The effects of PVP and SDS not only increase the grinding efficiency but also effectively stabilize the realgar and orpiment suspensions through the formation of steric and ionic barriers on the surfaces of drugs particles.

Bioavailability of orally administered drugs with poorly water-soluble is usually poor and highly variable. In the *in vivo* study, bioavailability expressed by urinary arsenic recovery of orally administered reduced sized realgar and orpiment particles to rats were obviously improved when compared with the original coarse realgar and orpiment powders. For example, within 96h, up to 85.4 ± 24.4% of dose was recovered in urine after oral administration of R/PVP/SDS suspension, whereas original realgar course powders gave a urinary recovery of 31.9 ± 13.6%. In the case of orpiment administration, 75.8% ± 27.2% and 33.2% ± 14.2% were the respective recovery of orally administrations of O/PVP/SDS suspension and original orpiment course powders.

In the *in vitro* cytotoxicity study, nanosized realgar and orpiment particles inhibited proliferation of the selected gynecological cancer cell lines including the ovarian cancer cell lines of CI80-13S, OVCAR, OVCAR-3, and a cervical cancer cell line of HeLa, whilst leaving the chosen control cell lines of normal human lung fibroblast cell line of MRC-5 and normal human dermal fibroblast cell line of HF unaffected. IC_{50} values were estimated. Comparison analysis of IC_{50} values of realgar (4.06 ± 0.45 on OVCAR-3 cells; 3.51 ± 0.48 on HeLa cells), orpiment (3.11 ± 0.44 on OVCAR-3 cells; 3.21 ± 0.46 on HeLa cells), and arsenic trioxide (2.37 ± 0.33 on OVCAR-3 cells; 1.85 ± 0.54 on HeLa cells) on the representative OVCAR-3 and HeLa cell lines demonstrated that there were no significant differences among realgar and orpiment and arsenic trioxide in terms of anti-proliferation effect on OVCAR-3 cells ($p > 0.05$, arsenic trioxide vs realgar; $p > 0.05$, arsenic trioxide vs orpiment; $p >$

0.05, realgar vs orpiment); on HeLa cells, arsenic trioxide seemingly was more cytotoxic than both realgar ($p < 0.05$) and orpiment ($p < 0.05$) which had similar effect ($p > 0.05$). Apoptosis induced by the nanosized realgar and orpiment particles on both OVCAR-3 and HeLa certain cancer cell lines was observed and confirmed by cell morphology, flow cytometry and DNA fragmentation assay, which partially contributes to the anti-cancer activity of realgar and orpiment.

In order to discern the possible underlying mechanisms of action of realgar, orpiment, and arsenic trioxide, preliminary screening for the effects of the target arsenicals on Hela cells was conducted by use of microarray technology. Alterations of some cancer-related genes, including BHLHB2, CAP1, CDC25A, CKMT1B, CLK2, CTPS, DCN, CTSC, DHCR7, E2F1, ETV3, FOSL1, IGFBP3, LAMB1, MYC, NME3, NR2F1, PCNA, PCTK3, RAP1A, RBBP4, TFDP1, TNFRSF1B, and TP53, obviously regulated by the target arsenicals were observed, however, further confirmation works should be done before drawing a final conclusion. Microarray study also showed that the effects of the arsenicals are species-dependent and dose-dependent.

Arsenic is well defined human carcinogen, although the mechanisms of carcinogenicity are not fully elucidated yet. The *in vivo* toxicity of realgar and orpiment and arsenic trioxide were assessed by measuring 8-hydroxy-2'-deoxyguanosine (8-OH-dGuo) in urine, a biomarker of oxidative DNA damage, by means of isotope dilution high performance liquid chromatography coupled with tandem mass spectrometry (LC/MS/MS) after oral administrations of the test arsenic compounds to rats. The elevated formation of urinary 8-OH-dGuo in the rats was found after the arsenic compounds administrations compared with control rats ($p < 0.01$, arsenic trioxide vs control; $p < 0.01$, realgar vs control; $p < 0.01$, orpiment vs

control). The *in vivo* toxicity studies showed that realgar and orpiment might be less genotoxic than arsenic trioxide ($p < 0.001$, arsenic trioxide vs realgar; $p < 0.001$, arsenic trioxide vs orpiment). Although our study showed that realgar and orpiment are somewhat genotoxic in terms of induction of 8-OH-dGuo, which indeed rings a warning bell for future medicinal application, it is still too early to tell whether realgar and orpiment are carcinogens before further evidences could prove it.

In general, realgar and orpiment could be formulated as nanosized particles/nanosuspensions. Such formulations would contribute to improvement of bioavailability of orally administered drugs, and give opportunity for parenteral use as well. Nanosized realgar and orpiment effectively inhibited proliferation of some gynecologic cancer cell lines partially through induction of apoptosis, similar to arsenic trioxide. Multiple mechanisms are involved in the anticancer effects of realgar and orpiment as shown by the preliminary microarray study, which provides possibility for the combination therapy of realgar/orpiment with other therapies. Realgar and orpiment although are usually classified as mild-toxic compounds, both stimulate elevated production of 8-OH-dGuo, indicating the potential of genotoxicity.

List of Tables

List of Schemes & Figures

CHAPTER ONE

Introduction

CHAPTER ONE

1.1 Historical medicinal use of arsenical: One of the oldest drug in the world

Arsenic is the 20th most abundant element in the earth's crust with a natural abundance of 1.8 mg/kg [Frankenberger WT Jr, 2002a]. It has been estimated that more than 99% of total arsenic contained in the environment (such as oceans, soils, rocks, biota, and atmosphere) is associated with rocks and soils [Frankenberger WT Jr, 2002b]. Arsenic-contained soils, sediments, and sludge are the major sources of arsenic contamination in food chain, surface water, ground water, and drinking water. Exposure to arsenical (arsenic-contained compound) by the general population occurs mainly through ingestion of arsenical existing in food and drinking water.

The effect of arsenical on human health is an issue of global concern. The U.S. Environmental Protection Agency (EPA) has proposed a revision of the maximum contaminant level for arsenic in drinking water from 50 μg/L down to 10 μg/L [United States Environmental Protection Agency, 2001]. Total compliance costs for the regulation of 10 μg/L in USA have been estimated at $1.47 billion a year. However, it should be known that assessment of human health effects strictly based on total arsenic concentration intake is not reliable. Identification and quantification of individual chemical species of the element are required, because the environmental fate and behavior, absorption and bioavailability, toxicity and potential benefits to health vary dramatically with the chemical species in which arsenic exists. The importance of arsenic speciation will be discussed in detail in Chapter 2. The most often encountered arsenic forms are trivalent (3^+) and pentavalent (5^+) inorganic arsenic, and methylated organic arsenic compounds [Francesconi KA and Kuehnelt D, 2004]. Three main inorganic arsenic forms, i.e. white arsenic (arsenic trioxide, As_2O_3), red arsenic (realgar, α-As_4S_4, often written as As_2S_2), and yellow arsenic (orpiment, As_2S_3), are our research focus.

CHAPTER ONE

Arsenical is viewed paradoxically as both a poison and a therapeutic agent. Arsenic is considered as a toxic and life-threatening element. Indeed, some arsenicals are well-documented carcinogens and human exposure is associated with an increased risk of developing tumors of the skin [Argos M et al., 2006; Rossman TG et al., 2004], bladder [Patton SE et al., 2002; Sternmaus C et al., 2000], liver [Chen CJ et al., 1992; Dopp E et al., 2005], kidney [Kurttio P et al., 1999; Hopenhayn-Rich C et al., 1998], or lung [Lundstrom NG et al., 2006; Boffetta P, 2006], even though the precise mechanisms of arsenic's cancer-causing effects are not clearly elucidated. In 1979, the International Agency for Research on Cancer (IARC) introduced an overall classification system for carcinogens and placed arsenic and certain arsenicals in group 1, which is defined as agents that are carcinogenic to humans. Paradoxically, arsenic has never been shown to be carcinogenic in animal models [Goering PL et al., 1999; Basu A et al., 2001]. In other words, although significant effort has been made in recent decades in an attempt to understand arsenic carcinogenesis using animal models, including rodents and larger mammals and even transgenic animals, all models have failed to elucidate satisfactorily the actual mechanisms of arsenic carcinogenicity. Despite the hazards, the potential for adverse effects should not deter physicians, especially clinical oncologists, from using arsenicals to treat patients with life-threatening diseases.

Medicinal use of arsenicals dates back more than 2400 years to ancient Greece and China independently. The major historical medicinal use of arsenicals is described as follows. Hippocrates (460-370 BC) and Galen (130-200 AD) popularized arsenicals used as healing agents [Jolliffe DM, 1993]. In central and southern Asia, arsenic was already an ingredient of many folk remedies. Sun Simao (孙思邈, 581-682 AD) purified a medicine composed of realgar (雄黄), orpiment (雌黄) and arsenic

trioxide (砒霜) to treat malaria. Li Shizhen (李时珍, 1518-1593 AD) recorded the use of arsenic trioxide to treat a variety of diseases [Li SZ, 1593]. In Persian textbooks, Avicennes (980-1037 AD) wrote down the use of white arsenic to treat fevers. These texts, along with the writings by Paracelsus (1493-1541 AD) introduced arsenicals to Europe. William Withering (1741-1799), British physician, botanist and mineralogist who discovered digitalis, was a strong proponent of arsenic-based therapies. He argued, "Poisons in small doses are the best medicines; and the best medicines in too large doses are poisonous." In 1786, Fowler of Stafford (1777-1843), a physician in England, recommended use of potassium arsenite, called Fowler's solution, internally for the treatment of intermittent fever initially. Fowler's solution gained great renown and was used to treat many ailments, including paralytic afflictions, rheumatism, hypochondriasis, epilepsy, syphilis, ulcers, cancer, and dyspepsia [Waxman S and Anderson KC, 2001]. In 1911, Fowler's solution was utilized as a drug for pernicious anemia, asthma, psoriasis, pemphigus, and eczema. As indicated in the British Pharmaceutical and Therapeutic Products Handbook edited by Martindale in 1958, Fowler's Solution was used in the treatment of leukemia, skin conditions (psoriasis, dermatitis herpetiformism and eczema), stomatitis and gingivitis in infants, and Vincent's angina. It was also prescribed as a healthy tonic. Since the 18th century, arsenic-derived preparations began to flourish. Physicians prescribed arsenicals for both external and internal use throughout the 18th century worldwide. Arsenicals were key ingredients in antiseptics, antispasmodics, antiperiodics, caustics, cholagogues, hematinics, sedatives, and tonics [Waxman S and Anderson KC, 2001]. Approximately 60 different arsenic-contained preparations have been developed and distributed during the lengthy history of this agent. More than 20 of these preparations were still in use at the end of the 19th century, including Aiken's Tonic Pills and

Andrew's Tonic. Arsenic's popularity peaked in 1910 when Paul Ehrlich (1854-1915), a German physician and founder of chemotherapy, developed an organic arsenical, Salvarsan (Arsphenamine), which was effective in treating tuberculosis and syphilis. Arsphenamine was the standard therapy for syphilis for nearly 40 years before it was replaced by penicillin [Kasten FH, 1996]. In fact, until the introduction and use of modern chemotherapy and radiation therapy in the mid 1900's, arsenic was used as one of the standard remedies for chronic myeloid leukemia (CML) and other leukemia. As medicinal chemistry evolved, enthusiasm for arsenical waned.

1.2 Arsenic trioxide (ATO): An anticancer drug

Arsenic trioxide was revived as an anticancer agent after reports emerged from China of the success of an ATO-contained herbal medicine in the treatment of acute promyelocytic leukemia (APL). In 1971, a group from Harbin Medical University in China developed Ailing-1 (癌灵-1) which contained 1% ATO [Niu C et al., 1999; Zhu XH et al., 1999]. After studying the effects of Ailing-1 in more than 1000 patients, researchers found that Ailing-1 has achieved notable success in the treatment of APL in the clinical setting. Ailing-1 alone and in combination with other chemotherapies were able to induce high complete remission (CR) rates. Since 1994, clinical trials with pure As_2O_3 were performed in Shanghai Second Medical University in China [Shen ZX et al., 1997]. The efficacy of pure As_2O_3 in patients with APL who had undergone relapse after retinoic acid (RA) plus chemotherapy was confirmed. In addition, the absence of myelosuppression with ATO offers an advantage over conventional cytotoxic chemotherapeutic agents. Thereafter, similar outcomes were further achieved in clinical trials done in Japan, Europe, and the United States [Soignet SL et al., 1998].

Development of Trisenox™ was rapid. In 2000, the U.S. Food and Drug Administration (FDA) approved arsenic trioxide injection (Trisenox™) for the treatment of patients with APL who have not responded to, or have relapsed following the use of the all trans-retinoic acid (ATRA) and anthracycline-based chemotherapies, which is considered first line therapy. The drug was approved for marketing only 3 years after the study was first started in the US. Trisenox™ was approved as an orphan drug, a drug intended for the treatment of rare diseases or conditions. The drug is now globally used to treat patients with APL who have suffered relapse from their primary therapy.

1.2.1 Treatment of acute promyelocytic leukemia (APL)

APL is a cancer of the blood and bone marrow, and is first recognized as a distinctive clinical entity in the 1950s. It is classified as a subtype of acute myeloid leukemia (AML), accounting for approximately 10% of AML. It was formerly associated with a high risk of early mortality before treatment or in the early treatment phase. Mean age at diagnosis is about 40 years. The male to female ratio is balanced [Groopman J and Ellman L, 1979].

APL is characterized by rapid accumulation of immature granulocytes called promyelocytes resulting in anemia, susceptibility to infection, bleeding, and hemorrhage. There are two morphological types of APL: the hypergranular form (AML FAB M3) and the microgranular variant (AML FAB M3v). The morphological diagnosis is confirmed by the APL specific translocation t(15;17). This translocation generates a fusion between the PML gene and the RARα gene, which encodes a transcription factor. The resulting PML/RARα fusion protein blocks the expression of genes required for normal myeloid differentiation. PML is a tumor suppressor

involved in complex functions including growth arrest and apoptosis induction. Normally PML is located in the nucleus on a specific subdomain named PML nuclear body (NB). Expression of the PML/RARα fusion protein in leukemic cells disrupts the nuclear bodies, and the PML protein is dispersed into smaller fragments with loss of PML functions.

With initial therapeutic strategies which include induction with ATRA combined with anthracycline-based chemotherapy, followed by anthracycline-based consolidation and maintenance therapy, 70-80% of APL patients are alive and disease-free beyond 4 years [Degos L and Wang ZY, 2001]. Although the CR rate obtained is high, the toxicity of this approach is also high. Re-induction with ATRA in patients in first relapse after ATRA treatment leads to inconsistent results [Huang ME, 1988]. Furthermore, resistance to re-induction with ATRA is high, even in patients who have been off ATRA for more than one year. In addition, a deficiency of ATRA as a single agent is its inability to induce molecular remission in most patients, even in those patients with newly diagnosed disease and those who are ATRA naive.

More than 400 APL patients worldwide have received ATO treatment. The CR rates for newly diagnosed patients are 72-85% and 85-93% for relapsed APL patients [Zhang TD et al., 2001; Chen Z at al., 2001]. ATO is administered in the form of 1% solution at a dose of 0.16 mg/kg daily diluted with 5% glucose in normal saline given by intravenous injection over 1-4 h. Patients receiving treatment for 28-44 days (rarely 60 days) achieve CR. Advantages of single-agent ATO are the consistently high CR rates in many studies and low resistance to the drug. More importantly, because ATO as a single agent induces molecular remission in almost all patients in relapse, other chemotherapy is not required, making this a less toxic approach compared with ATRA with anthracycline-based chemotherapy. Therefore,

ATO offers advantages over ATRA with anthracycline-based chemotherapy in the treatment of relapsed or refractory APL, and becomes a standard induction treatment in patients with relapsed or refractory APL [Douer D, 2006].

The precise mechanisms of ATO action in APL are not completely elucidated yet. In general, a variety of *in vitro* studies suggest that several mechanisms may contribute to its effectiveness *in vivo*, mainly including induction of apoptosis, stimulation of differentiation, degradation of the specific PML/RARα fusion protein, and inhibition of angiogenesis [Zhu J et al., 2001; Miller WH Jr, 2002]. Numerous intracellular signal transduction pathways are involved.

Furthermore, *in vitro*, ATO exhibits dose-dependent effects on APL cells [Zhang TD et al., 2001]. For example, at the higher concentrations (1.0-2.0 μM) apoptosis is preferentially triggered; at the lower concentrations (0.1-0.5 μM) partial differentiation of APL cells is induced. At both high- and low-doses, ATO promotes the degradation of PML/RARα fusion protein.

It should be noted that because of its toxicity, As_2O_3 must be given at low concentrations, i.e. physiologically acceptable concentration < 5 μM; therapeutic index is therefore a key issue.

ATO impacts on many cellular and physiological pathways, a wide variety of malignancies may be susceptible to therapy with ATO. As well, the multiple actions of ATO give the potential for synergy between ATO and other chemotherapeutic agents, thus providing enhanced benefits in cancer therapy.

1.2.2 Treatment of other cancers

Inspired by the clinical success of ATO in APL, subsequently, intensive research efforts focused on whether these effects were unique to APL cells or a more

generalized response by different types of neoplastic cells would occur. Findings indicate that ATO is indeed active against many other cancer cells. Numerous studies highlight the potent cytotoxicity of ATO against a variety of hematologic malignancies such as chronic myelogenous leukemia (CML) [Jing HM et al., 2002], promonocytic leukemia [Park JW et al., 2001], T-cell leukemia [Mahieux R et al., 2001] and multiple myeloma [Rousselot P et al., 2004]. ATO also exerts potent cytotoxic activity against a large variety of cancer cells of solid tumor origin such as neuroblastoma [Cheung WM et al., 2006], esophageal carcinoma [Shen ZY et al., 2000], gastric cancer [Zhang TC et al., 1999], hepatocellular carcinoma [Chan JY et al., 2006], head and neck cancer [Huilgol NG, 2006], cervical cancer [Chun YJ et al., 2002], prostate [Lu M et al., 2004], transitional cell cancer [Pu YS et al., 2002], glioblastoma [Haga N et al., 2005], renal cell carcinoma [Vuky J et al., 2002], and breast cancer [Chow SK et al., 2004]. For example, in a phase II trial in hormone-refractory prostate cancer, treatment with ATO (0.2 mg/kg/d for two contiguous 5-day periods on a 28-day cycle or one cycle followed by twice a week thereafter) resulted in marked decreases in prostate-specific antigen levels in two of 15 assessable patients, and slowed the increase in prostate-specific antigen levels in another 12 patients [Lu M et al., 2004].

Mechanisms of action of ATO in cells without the PML/RARα fusion protein are summarized as below:

- Inhibition of signal transduction and angiogenesis [Anderson KC et al., 2002]
- Induction of oxidative stress, hydrogen peroxide, reactive oxygen species (ROS) and depletion of glutathione [Park MJ et al., 2005]
- Induction of apoptosis through depolarization of mitochondrial membrane, activation of caspase-9, caspase-3 and PARP [Akao Y et al., 1999]

- Engaging in the extrinsic pathway by up-regulation of surface expression of TRAIL and TRAIL receptors and activation of BID in cells expressing mutant p53 [Akay C et al., 2004]
- Induction of the release of mitochondrial AIF to the cytosol, translocation of AIF to the nucleus and onset of chromatin condensation [Kang YH et al., 2004]

1.2.3 Toxicity

The low therapeutic dose of ATO (about 0.15 mg/kg/d) used to treat APL is associated with a tolerable toxicity level without bone marrow hypoplasia or drug-induced alopecia [Wang ZY, 2001]. The common non-life-threatening adverse events reported include nausea, rash, fatigue, neuropathy, fever, headache, vomiting, diarrhea, tachycardia, and hypokalemia [Zhang P, 1999]. The most prominent adverse events are weight gain and fluid retention, leukocytosis, APL differentiation syndrome, and prolongation of QT interval on the electrocardiogram [Wang ZY, 2001]. Sudden death has also been reported. Overall, ATO is quite well tolerated, and toxicities are manageable and reversible. In the treatment of APL, adverse events are less common during consolidation and maintenance cycles. Generally, most adverse events do not require discontinuation of treatment.

A drawback of ATO treatment is that it must be administered intravenously daily as an infusion over 1 to 4 hours since it causes severe liver damage if given orally, which makes the consolidation and maintenance therapy difficult [Lu DP et al., 2002]. Thus, an oral agent with similar therapeutic effects and fewer side effects would provide not only cost and quality-of-life benefits but also easy access to consolidation and maintenance therapy. Moreover, such an oral agent would give

opportunity for further combination with other agents of interest. Realgar and orpiment could be such candidates. Both realgar and orpiment are considered as non- or less-toxic compounds [Lu DP et al., 2002].

1.3 Realgar

The first mention of arsenicals was made by Hippocrates, who used realgar and orpiment pastes to treat ulcers. Realgar is commonly used in traditional Chinese medicine (TCM) and available as pills, tablets, and other preparations. According to Chinese Pharmacopoeia (2000 edition), realgar-contained formulations (23) account for 5.67% of total TCM formulations. They are used for psoriasis, syphilis, asthma, rheumatism, haemorrhoids, cough, and pruritus, and are also prescribed as a health tonic, analgesic, anti-inflammatory agent, and as a treatment for some malignant tumors [Pan B et al., 2004].

Prompted by the success of ATO in the treatment of leukemia, along with medicinal application background of realgar, researchers turn their attentions to realgar. Huang SL et al first developed Chinese medicine Composite Indigo Naturalis tablets (复方青黛片) containing realgar, baphicanthus cusia, radix salviae mithiorrhyzae, radix pseudosatellariae, and pulverata levis to treat APL, achieving high CR rates [Huang SL et al., 1995]. Composite Indigo Naturalis is given orally at a dose of five tablets (0.25 g/tablet), three times daily. After one week, the daily dose is increased to 30 tablets. CR is achieved within 30-60 days in 60 APL patients enrolled including 43 newly diagnosed and 17 relapsed patients. Clinical trials of pure As_2S_2 alone in the treatment of APL patients have been conducted in China since 1990s. Lu DP et al have published the outcomes of realgar in the treatment of APL [Lu DP et al., 2002; Lu DP and Wang Q, 2002]. In this clinical trial study, a total of 129 patients

with APL were enrolled between December 1994 and December 2000. 19 of the patients had newly diagnosed APL, 7 had first relapse, and 103 had hematologic complete remission (HCR). HCR was achieved in all patients with newly diagnosed APL and in all those with hematologic relapse. In that study, chemically pure realgar (As_2S_2) was used together with an equal amount of ground *Seman Platycladi* as an excipient to make capsule containing 250 mg realgar. Realgar was orally administered at a dosage of 50 mg/kg of body weight per day, divided into 4 doses until HCR was achieved. For patients with HCR, the same daily dose was given on a treatment schedule of 2 weeks on and 2 weeks off in the first year. Thereafter, the treatment break was increased to one month within 4 years. Therapy was discontinued in the fifth year. Highly effective and safe for both remission induction and maintenance in all stages of APL have been observed. Table 1 and Table 2 outline the major results in newly diagnosed and relapsed APL patients after treatment with realgar, respectively.

Table 1. Results in patients with newly diagnosed APL after treating with As_2S_2.

Patient no./age (year)/gender	Days to HCR	Total As_2S_2 dose (g) till HCR
Case 1/32/M	38	37.50
Case 2/34/F	40	37.75
Case 3/48/M	90	145.75
Case 4/21/F	35	60.50
Case 5/29/F	51	98.00
Case 6/16/M	46	105.75
Case 7/29/F	38	110.25
Case 8/37/M	69	89.75
Case 9/41/M	53	141.75
Case 10/20/F	50	94.50
Case 11/35/M	55	135.00
Case 12/43/F	50	150.00
Case 13/22/M	75	97.50
Case 14/63/F	77	186.00

Case 15/42/M	101	312.50
Case 16/29/F	76	221.25
Case 17/32/M	57	193.50
Case 18/26/M	28	105.00
Case 19/41/M	33	138.75

Modifited from Lu DP et al., 2002.

In the newly diagnosed patient group, the estimated leukemia-free survival (LFS) for 1 and 3 years were 86.1% and 76.6%, respectively, with a median follow-up time of 13.5 months. .

Table 2. Results in patients with relapsed APL after treatment of As_2S_2.

Patient no./age (year)/gender	Days to HCR	Total As_2S_2 dose (g) till HCR
Case 1/38/F	42	15.7
Case 2/58/F	80	26.2
Case 3/43/M	32	15.7
Case 4/54/F	42	50.5
Case 5/36/F	55	277.0
Case 6/30/F	34	226.0
Case 7/48/F	71	418.7

Modified from Lu DP et al., 2002.

Cytogenetic and molecular CRs were achieved in five of the 7 relapsed patients.

In addition, in the HCR group, thirty five out of 44 patients with PML/RARα positive were rendered to negative. The calculated LFS for 1 and 3 years was 96.7% and 87.4%, respectively, with a median follow-up time of 23 months.

Even though the promising clinical efficacy of realgar in the treatment of APL was reported, the study of medicinal use of realgar is still in a very initial preclinical

stage. In this introduction, major representative studies related to realgar are summarized in Table 3, which are retrieved from the search engine PubMed.

Table 3. Results of *in vitro* and/or *in vivo* studies related to realgar.

Research group	Cell type	Findings
Chen SY et al., Center of Hematology, Xi'an Jiaotong University, PRC	ATRA resistant APL cell line: MR2 [Chen SY et al., 2002]	Inhibition of growth and induction of apoptosis.
	Myeloid leukemia cell line: NB4 [Wang H et al., 2003]	Gene expression profile changed by realgar treatment: 9 up-regulated and 37 down-regulated.
	Myeloid leukemia cell line: RPMI 8226 [Wang MC et al., 2006]	Gene expression changed after realgar treatment including 17 up-regulated (such as CCL2, CCL3, BTG1, TNFAIP3, TNFAIP8, SLC38A2, IGFBP4) and 3 down-regulated genes.
	NB4 and MR2 [Zhao XA and Liu SX, 2003]	Realgar could down regulate the membrane PCA, TF antigen and TF mRNA transcription of both cell lines in a time-dependent manner.
Deng Y et al., Department of Chemistry, Huazhong University of Science and Technology, PRC	Human umbilical vein endothelial cell line: ECV-304 [Deng Y et al., 2001]	Reduction of cell viability in response to treatment with realgar suspension with particle size of 100 and 150 nm and induction of apoptosis.
Ye HQ et al., College of Life Science and Technology, Huazhong University of Science and Technology, PRC	Myeloid leukemia cell line: HL-60 [Ye HQ et al, 2006 and 2005]	Inhibition of cell growth and induction of apoptosis. Realgar treatment especially with nanosize grade accelerated membrane lipid peroxidation and LDH leakage.
Li JE et al., Shanghai Institute of Hematology, Rujin Hospital, Shanghai Second Medical University, PRC	Myeloid leukemia cell line: K562 Fresh CML nomonuclear cells derived from CML patients [Li JE et al., 2002]	Inhibition of proliferation and induction of apoptosis in both cell lines. The decline of the Bcr-Abl protein and its PTK activity may contribute to the induced apoptosis.

Luo LY et al., Department of Chemical Biology, School of Parmaceutical Sciences, Peking University	HL-60 [Luo LY et al., 2006a and b]	Inhibition of viability and induction of monocytic differentiation involving some serine/threonine protein phosphatases.
Xiao YF et al., Department of Pediatrics, The Second Hospital, Xi'an Jiaotong University, PRC	HL-60 and lymphocytic cell line: Jurket [Xiao YF et al., 2005]	Survivin expression level decreased in both cell line during apoptosis induced by realgar probably through mitochondrial pathway.
Zhang C et al., TCM Hematology Institute of People's Liberation Army, PRC	T lymphocytic leukemia cell line: CEM [Zhang C et al., 2003]	Inhibition of cell viability and induction of apoptosis.
Zhang J et al., Department of Biochemistry and Molecular Biology, Fourth Military Medical University, PRC	NB4 and K562 [Zhang J et al., 2005]	K562 cells were much less sensitive than NB4 cells to apoptosis induced by realgar, which probably due to high expression of bcl-x(L) in K562 cells.
Wu JZ et al., Department of Pharmacy, National University of Singapore, Singapore	Human ovarian cell line: CI80-13S, OVCAR, OVCAR-3; Human cervical cell line: HeLa [Wu JZ and Ho PC, 2006]	Inhibition of growth and promotion of apoptosis

Observations of the clinical utility of realgar in the treatment of APL have triggered investigations into the mechanisms of action by which realgar produces clinical benefits. Considerable preclinical evidences support the potential effects of realgar against a number of different malignancies. Studies in cultured cells showed that realgar inhibits growth and promotes apoptosis in myeloid leukemia, multiple myeloma, lymphocytic leukemia, and certain solid tumor cells, as shown in Table 3.

1.4 Orpiment

Nowadays, medicinal use of orpiment still mainly stays as folk remedy in traditional Chinese medicine. In recent years, researchers in China were attracted by

the promising outcomes of ATO and realgar in the treatment of leukemia and low toxicity of orpiment compared to ATO, and turned to orpiment, exploring its potential therapeutic effects for the treatment of cancer. Lu DP et al treated a single patient with newly diagnosed APL with pure orpiment (As_2S_3), and found that this patient entered HCR in 38 days and molecular CR in 128 days [Lu DP and Wang Q, 2002]. Table 4 summarizes the main investigational results related to orpiment obtained so far, which are retrieved from the PubMed. Similar to realgar, orpiment was also found to have anti-leukemic effect.

Table 4. Results of *in vitro* studies related to orpiment.

Research group	Cell type	Findings
Zhong L et al., Department of Leukemia Research, Shanghai Institute of Hematology, Renji Hospital, PRC	NB4 and HL-60 [Zhong L et al., 2003, 2001]	Inhibition of proliferation and induction of apoptosis. In detail, the fusion protein was no longer observed in NB4 cells, PML protein was degraded. In HL-60 cells, PML protein underwent a similar progress.
Hao HY et al., Institute of Hematology, People's Hospital, Peking University, PRC	NB4 [Hao HY et al., 2002]	Induction of apoptosis through degradation of PRM-RARα fusion protein and wild-type RARα.

1.5 Formulations to overcome absorption and bioavailability problems due to poor water-solubility

Both realgar and orpiment are crystals with high native lattice energy, which reduces the tendency of the crystals to dissolve in most surrounding aqueous or organic media. Water-insolubility of realgar and orpiment is a crucial obstacle for their investigation, development, and final commercialization.

Poorly water-soluble compounds are difficult to be developed as end products.

Thus, they are frequently abandoned in the early drug development stage [Prentis RA et al., 1998]. When these compounds are formulated using conventional approaches, their performance in preclinical screens is often erratic and highly variable. In clinics, the conventional formulations of poorly water-soluble drugs are frequently plagued with problems such as poor and weird absorption and bioavailability. In addition, the conventional approach is to achieve the solution state of drugs, which is especially difficult to attain for realgar and orpiment which are insoluble in both water and oils. In the last few years, a novel drug delivery approach for poorly water-soluble compounds has come to light. In this approach, poorly water-soluble compounds are formulated as nanometer-sized drug particles.

1.5.1 Nanonisation

Nanotechnology has a long history. The development of a wide spectrum of nanoscale technologies is beginning to change the foundations of disease diagnosis, treatment, and prevention. In the pharmaceutical field, the term “nanoparticle” has been rather loosely applied to structures less than 1 μm in diameter [Kipp JP, 2004]. They can be produced by either chemical or mechanical means, and characterized by conventional analytical methods such as microscopy or light scattering.

In pharmacology, bioavailability is one of the principal pharmacokinetic (PK) properties of drug. It is defined as the extent of a therapeutically active drug that reaches the systemic circulation and is available at the site of action. Drugs are commonly administered orally or parenterally by injection. Bioavailability of most orally administered drugs is less than 100%. For orally administered drugs, there are three major factors that could limit their bioavailability: (1) poor absorption from the gastrointestinal (GI) tract; (2) degradation of the drug prior to absorption; and (3)

hepatic first pass effect. In terms of oral absorption from the GI tract, the rate of dissolution is a crucial consideration. The theoretical basis of the dissolution velocity was established by Arthur Amos Noyes and Willis Rodney Whitney in 1897, as described by the Noyes-Whitney equation below:

$$\boldsymbol{dc/dt = DA(c_s - c_t)/h}$$

where: dc/dt is the dissolution velocity (rate of dissolution)

D is the diffusion coefficient

A is the surface area of the drug

c_s is the saturation solubility

c_t is the bulk concentration of the drug in the surrounding liquid

h is the diffusion distance above the drug particle surface

In general, drugs possessing poor solubility (c_s) exhibit a very low dissolution velocity. The dissolution velocity dc/dt is also a function of the surface area. According to this equation, there are two basic approaches to improve oral drug absorption:

1. Increasing dc/dt by enlarging the drug particle surface;
2. Increasing the saturation solubility, c_s, of the drug

This is a very simple traditional approach to increase the dissolution velocity by enlarging the surface, i.e. micronisation. The particle size of normally sized drug powders (approximately in the range of 20-100 μm) could be reduced to a size in a range of approximately 1-10 μm. However, many agents exhibit such a low solubility that the increase in surface area micronisation is not enough to achieve a sufficiently high dissolution velocity leading to therapeutic blood levels. Therefore, the next consequent step was taken, going from micronisation to nanonisation. Drug nanoparticles possess sizes of approximately 10-1000 nm, most production methods

yield a mean diameter somewhere between 200 and 400 nm. Nanonisation has an additional effect compared to micronisation, it increases not only the surface area, but also simultaneously increases the saturation solubility c_s. The solubility of normally sized powder is a compound specific constant, depending only on the temperature and the solvent. This changes when the particle size goes below a size of approximately 1 μm. The dissolution pressure increases due to the strong curvature of the particles resulting in an increase in c_s, based on the theoretical background provided by the Ostwald-Freundlich equation [Mosharraf MN, 1995] and the Kelvin equation [Simonelli AP et al., 1970]. According to Noyes-Whitney equation, this leads to a further increase in *dc/dt* in addition to the gain by an increased surface area. Therefore, nanosizing drug particles is a smart way to improve drug dissolution and bioavailability based on a universal principle that can be applied to any drug. The increase in the saturation solubility leads to the formation of a supersaturated solution compared to the solubility of normally sized powders.

Enhancement of oral bioavailability by using drug nanoparticles has been reported, e.g., the gonadotropin inhibitor danazol administered as commercial dispersion (microsuspension) had a relative bioavailability of 5.1%, whilst as a nanosuspension had an increased bioavailability to 82.3% [Liversidge GG and Cundy KC, 1995].

Besides oral administration, drug nanoparticles can also be injected intravenously as an aqueous dispersion. Dispersion of nanoparticles generally consists of water, drug, and stabilizer. In the absence of an appropriate stabilizer, the high surface energy of nanometer-sized particles would tend to agglomerate and/or aggregate. To be effective, the stabilizer must be capable of wetting the surface of the drug particle and providing steric and/or ionic barrier. The choice and concentration

of stabilizer are important to promote the particle size reduction process and generate physically stable formulations. Acceptable stabilizers for intravenous (i.v.) injection mainly include lecithin, Tween 80, Poloxamer 188, sodium glycocholate and low molecular weight polyvinylpyrrolidone (PVP) [Muller RH and Keck CM, 2004]. Stabilization of these formulations is often achieved using a combination of a non-ionic plus ionic stabilizer. Theoretically, using the nanoparticle technology, any drug can be made 100% bioavailability.

Furthermore, it has been reported that, i*n vivo*, nanoparticles are surprisingly well tolerated [de Garavilla L et al., 1996].

1.5.2 Methods for preparing solid drug nanoparticles

Complete solubilization of a drug with very low intrinsic solubility may be very difficult or untenable. Very low water-solubility affects the quantities of cosolvents or surfactants necessary for complete dissolution; the ability to form inclusion complexes with cyclodextrins is also limited for those compounds having very low intrinsic solubility; very low drug water-solubility also hamper preparation of an emulsion. Currently, there are a limited number of formulation approaches available for compounds which are poorly water-soluble. The most direct approach for enhancing solubility is to generate a salt. If, however, the compound is non-ionizable, solubility could be achieved by micronisation/nanonisation. Two commonly used preparation methods are described as follows:

- **Precipitation**

Precipitation has been applied for many years in the preparation of small particles, and within the last decade in the preparation of submicron particles for drug delivery [List M and Sucker H, 1988; Rasenack N and Muller BW, 2002]. Typically,

the drug is first dissolved in a solvent, and this solution is mixed with a miscible antisolvent. Simple precipitation methods, however, have numerous drawbacks. It is very difficult to control nucleation and crystal growth to obtain a narrow size distribution. Often a metastable solid, usually amorphous, is formed which is converted to more stable crystalline forms. Once nucleation occurs, crystal growth is spontaneous and difficult to control. Furthermore, non-aqueous solvents utilized in the precipitation process must be reduced to toxicologically acceptable levels in the end product.

- **Homogenization**

A simple process of particle diminution by high-pressure homogenization was developed at the beginning of 1990s [Keck CM and Muller RH, 2006; Krause KP and Muller RH, 2001]. When a suspension is homogenized, fluid shear, particle collision and cavitation are critical high-energy parameters. Microfluidization and piston-gap homogenization have been applied with success. In some cases, micronisation of the raw material was required before homogenization in order to obtain the desired final particle sizes. Jet milling or ball milling has been used for that purpose. In the liquid state, the dispersions are very stable, especially if the solubility of the drug is less than 1 mg/ml. Dispersions of nanoparticles can be post-processed as a dry powder for solid dosage development or lyophilized for injectable products. These dried powders are designed to re-disperse into nanometer-sized particles when placed in water or an alternate water-based environment.

1.6 Toxicity: Carcinogenicity

Chronic arsenic poisoning has been found in patients treated for long period with arsenical-based pharmaceuticals. Generally, the duration of arsenical-based

cancer therapy is prolonged, therefore, special concerns should be paid about the arsenical-induced toxicity. Arsenic is a well-established human carcinogen based on epidemiological studies [Boffetta P, 2004], though the mechanisms of carcinogenicity remain unclear. The lack of suitable animal models as well as poor understanding of its carcinogenic/genotoxic mechanisms hampers accurate risk assessment of the health effects of arsenic.

Several lines of evidence with cultured cells and experimental animals have indicated that arsenicals are capable of generating reactive oxygen species (ROS), especially superoxide and hydrogen peroxide, resulting in oxidative stress [Shi H et al., 2004; Harris GK and Shi X, 2003]. However, the underlying mechanisms for ROS regulation have not yet been fully identified. Recently, it has been proposed that arsenic may induce the formation of ROS through: (1) the ubiquinone site of the respiratory chain [Corsini E et al., 1999], (2) a decrease in cellular mitochondrial membrane potential [Woo SH et al., 2002], (3) alteration of glutathione (GSH) concentration [Dai J et al., 1999], (4) activation of NADH oxidase [Lynn S et al., 2000], and (5) the oxidation of arsenite to arsenate [Del Razo LM et al., 2001]. Arsenic-induced ROS has been demonstrated to cause DNA damage [Dong JT and Luo XM, 1993], lipid peroxidation [Lin TH et al., 1995], and protein modification [Dong JT and Luo XM, 1993], as well as alteration of antioxidant defenses [Lee TC and Ho IC, 1995].

However, it is not reported so far whether arsenic trioxide, realgar and orpiment could cause oxidative stress. Thus it is worth to investigate possible carcinogenicity of these compounds to provide valuable references to the field of arsenic carcinogenicity.

1.6.1 ROS and oxidative stress

ROS is a collective term often used by biologists for the intermediates formed during oxidative metabolism, including both oxygen radicals and non-radical reactive derivatives. Mitochondria (oxidative phosphorylation), leukocytes (oxidative burst), peroxisomes (degradation of fatty acids), and cytochrome P450 system (mixed function oxidation system) can all release ROS [Wu LL et al., 2004]. ROS includes superoxide [$O_2^{\cdot-}$], hydroxyl [$OH^{\cdot}$], peroxyl [$RO_2^{\cdot}$], alkoxyl [$RO^{\cdot}$]), and certain other nonradicals that are either potential oxidizing agents and/or are easily converted into radicals, such as hypochlorous acid (HOCl), ozone (O_3), peroxynitrite ($ONOO^-$), singlet oxygen ($^1O_2$), and hydrogen peroxide (H_2O_2) [Wiseman H et al., 1995]. Reactive nitrogen species (RNS) is a term becoming popular and encompasses nitrogen dioxide radical ($NO_2^{\cdot}$), peroxynitrite, nitrous acid (HNO_2), and related species [Wiseman H et al., 1995].

Cells can normally adapt to low physiological concentration of ROS/RNS with an elaborate antioxidant defense system consisting of enzymes such as catalase, superoxide dismutase, glutathione peroxidase, and numerous non-enzymatic antioxidants including vitamins A, E and C, glutathione, ubiquinone, and flavonoids [Urso ML and Clarkson PM, 2003]. In other words, under normal physiological conditions, there is a balance maintained between endogenous oxidants and antioxidants. When an imbalance occurs, created by the excessive generation of oxidants or a decrease of antioxidants, the abnormal oxidant system then enters what is called oxidative stress. In the presence of oxidative stress, ROS/RNS generated *in vivo* can cause oxidative damage to lipids, proteins and nucleic acids [Lunec J et al., 1994]. Oxidative stress has been linked to neurological disorders, atherosclerosis, diabetes, cancer, and other age-related diseases [Wu LL et al., 2004].

1.6.2 Oxidative DNA damage and repair products of 8-hydroxy-2'-deoxyguanosine and 8-hydroxy-2'-deoxyadenosine

DNA is probably the most biologically significant target of oxidative attack, and it is widely thought that continuous oxidative damage of DNA is a significant contributor to the age-related development of some cancers, such as those of the colon, breast, rectum, and prostate [Cooke MS et al., 2003]. Damage to DNA by reactive oxygen, chlorine, and nitrogen species generates a multiplicity of different base oxidation and other base modification products, which are repaired by a complex system of enzymes. It should also be noted that DNA oxidative damage can also occur from exogenous ROS, such as cigarette smoking, UV radiation, and ionizing radiation.

Guanine and guanosine most readily undergo oxidation for possessing the lowest oxidation potential of the four purine nucleobases and nucleosides [Kasai H, 1997]. The presence of the modified nucleobase, 8-hydroxyguanine (8-OH-Gua), and nucleoside 8-OH-dGuo during DNA replication can cause G:C-T:A transversion mutations [Cheng KC et al., 1992]. Therefore, oxidative lesions not repaired before replication can become mutagenic.

Direct measurement of reactive species and free radicals is impractical because they are short-lived, due to their highly reactive nature. Thus, biomarkers have been used to reflect the degree of oxidative damage. Various markers of oxidative damage have been identified. In the past, the most popular markers were designed for lipid peroxidation, such as malondialdehye (MDA), oxidized low-density lipoprotein (LDL), MDA-modified LDL, auto-antibodies against oxidized LDL and MDA-modified LDL, F2-isoprostane, and conjugated diene [Wu LL et al., 2004]. The

detection of a new carbonyl group, dityrosine and oxidized histidine has been measured to indicate protein oxidation [Wu LL et al., 2004].

Markers for DNA oxidation were few. The repair product, such as 8-hydroxy-2'-deoxyguanosine (8-OH-dGuo), is poor substrate for the enzymes involved in nucleotide synthesis, fairly water-soluble, and generally excreted into the urine without further metabolism [Cooke MS et al., 2003]. Indeed, animal experiments have shown that injected 8-OH-dGuo is readily excreted unchanged into the urine, whereas 8-OH-dGuo in the diet or oxidation of dGuo during excretion does not contribute. Consequently, the oxidized nucleoside, urinary 8-OH-dGuo, is the most often studied biomarker of oxidative DNA damage. The formation of 8-OH-dGuo was first reported in 1984 by Kasai and Nishimura [Kasai H and Nishimura S, 1984]. Detection of DNA oxidative adducts represents the dynamic equilibrium between DNA damage and their repair and also may provide an opportunity to evaluate the carcinogenesis potential. Therefore analysis of 8-OH-dGuo as a repair product in urine reflects the amount of total body oxidative DNA damage. Figure 1 summarizes the pathway of commonly measured biomarkers of oxidative stress, i.e. 8-OH-dGuo and 8-OHGua.

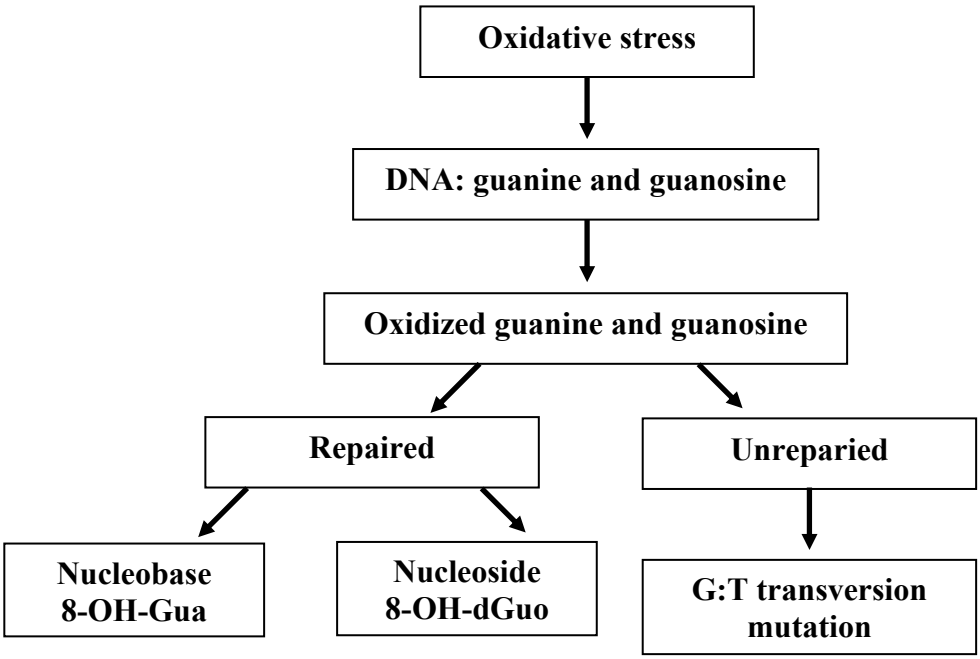

Figure 1. Pathway of commonly measured biomarkers of oxidative stress.

When deoxy-adenosine was oxidized by Fenton-type reagents, 8-hydroxy-deoxyadenosine (8-OH-dAdo) was detected as the major product [Jaruga P et al., 2001]. The yield of 8-OH-dAdo was comparable to that of 8-OH-dGuo. The presence of 8-OH-dAdo *in vivo* can cause GC-AT transition mutations are expected to occur in mammalian cells [Jaruga P et al., 2001].

1.7 Hypotheses and objectives of the thesis

In order to comprehend the activity and toxicity of arsenic, it is essential to understand its chemistry. Arsenic (atomic number 33, atomic weight 75) is a transitional element or metalloid under the nitrogen group in the Periodic Table. It can exist in four different valency states, including elemental (zero oxidation), divalent (As^{II}), trivalent (As^{III}), and pentavalent (As^{V}). Arsenic forms alloys with metals and also readily reacts with carbon, oxygen and hydrogen, forming covalent bonds.

Trivalent arsenics are more toxic than the pentavalent ones [Duker AA et al., 2005]. The activity and toxicity of an arsenical could also vary with the physical state of the compound, and the rate of absorption and elimination. Therefore, we hypothesize that the differences among arsenic trioxide and realgar and orpiment in the activity and the mechanisms of action and basis of toxicity could be due to the difference in the valency states of these compounds. The difference in the rate of absorption of arsenic trioxide, realgar and orpiment could lead to different metabolism profiles that would have profound impact on the toxicity.

For this study, we focus on four objectives:

1. To confirm conversion of arsenic sulfides to trivalent and pentavalent arsenic compounds through alkalinization, a usual step employed to solubilize arsenic trioxide.
2. To develop arsenic sulfides nanoparticles (based on the finding from Step 1) for the subsequent biopharmaceutical studies.
3. To compare the mechanisms of action of arsenic trioxide, realgar and orpiment based on the preliminary microarray study.
4. To establish a reliable high performance liquid chromatography coupled with tandem mass spectrometry (LC/MS/MS) method for detection of an oxidative DNA damage biomarker induced by the respective arsenic compounds and to compare their genotoxicity potential.

CHAPTER TWO

Speciation of inorganic and methylated arsenic compounds by capillary zone electrophoresis with indirect UV detection: with special application for analysis of alkali extracts of As_2S_2 (Realgar) and As_2S_3 (Orpiment)

CHAPTER TWO

2.1 Introduction

2.1.1 Importance of arsenic speciation

Arsenic compounds are ubiquitous in nature. The most commonly encountered arsenic forms are 3^+ and 5^+ valent states, including inorganic arsenite (iAs^{III}) and arsenate (iAs^{V}) as well as organic methylated species consisting of monomethylarsenic acid (MMA^{V}) and dimethylarsenic acid (DMA^{V}). Exposure to arsenic compounds by the general population occurs mainly through ingestion of arsenic existing in drinking water and food. In freshwater systems, iAs^{III} and iAs^{V} are major arsenic species, while minor amounts of MMA^{V} and DMA^{V} also exist [Frankenberger WT Jr, 2002c]. There is little information on the nature of arsenic species in human diet, except seafood. Most dietary arsenic originates from fish, shellfish, and seaweed products, where the major arsenic species found is nontoxic arsenobetaine (AB) [Frankenberger WT Jr, 2002d]. Ingested arsenic compounds can be readily absorbed through gastrointestinal (GI) tract into the blood stream [Le XC et al., 1994; Vahter M, 2002]. The reported urinary arsenic concentrations (mean ± standard deviation) from the general population are 9 ± 7 μg/L in America [Kalman DA et al., 1990], 17 ± 11 μg/L in Europe [Foa V et al., 1984], and 121 ± 101 μg/L in Japan [Yamauchi H et al., 1989]. It should be mentioned that the rate of absorption (absorbability) is dependent on the solubility and the chemical species of arsenic.

Most of the inorganic arsenic species are metabolized in humans and many mammalians to methylated arsenic species including MMA^{V} and DMA^{V}, which are more readily excreted into the urine than the inorganic arsenic species [Le XC et al., 1994]. Methylation of arsenical involves a stepwise process of two electron reduction of the pentavalent arsenic species to the trivalent arsenic species, followed by oxidative addition of a methyl group to the trivalent arsenic species as shown in

Scheme 1 [Benramdane L et al., 1999]. Glutathione, cysteine, and dithiothreitol act as reducing agents, and *S*-adenosylmethionine (SAM) is the methyl donor.

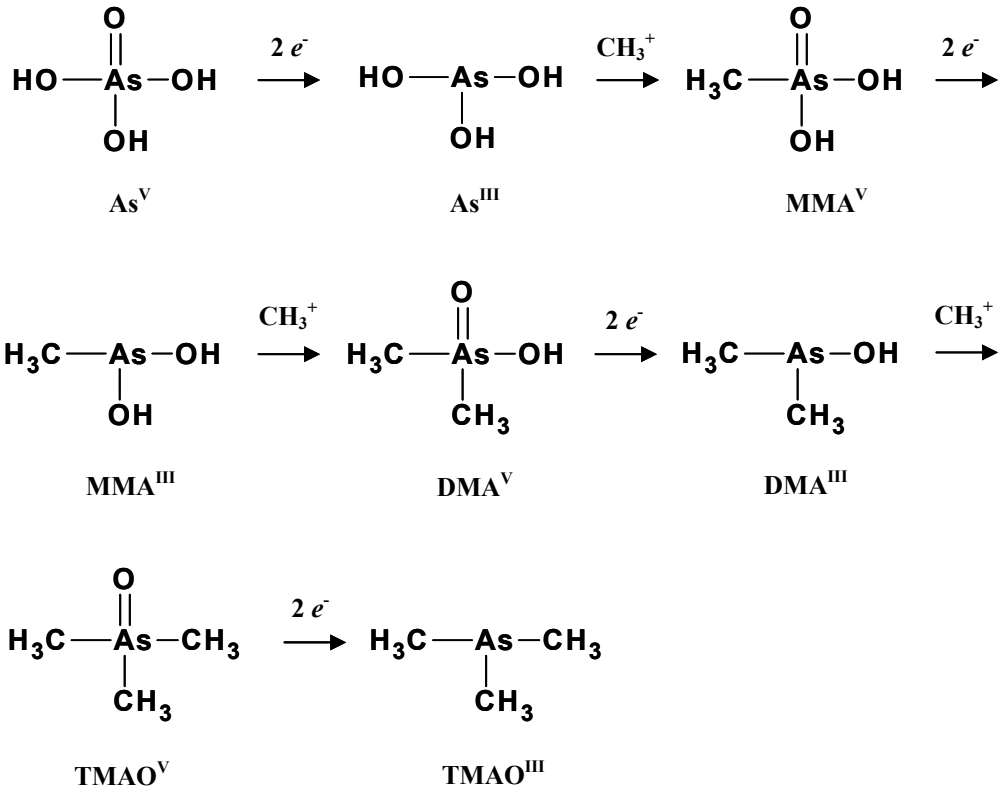

Scheme 1. Pathway of the biomethylation of inorganic arsenic species.

Association between acute and chronic exposures of humans to the arsenic compounds and various forms of cancers and other health problems has been well documented [Chen CJ et al., 1992], whereas the therapeutic actions of arsenic species have also been reported [Wang ZY, 2001; Niu C et al., 1999]. Conclusively, it is well established that the arsenicals present a paradox because they could act as both potential carcinogens and beneficial therapeutic agents mainly depending on their valent states and chemical forms. Therefore, arsenic speciation is of extensive research focus.

2.1.2 Analytical methods for arsenic speciation

In many studies, high performance liquid chromatography (HPLC) was used for separating arsenic compounds, and a variety of detectors including hydride generation atomic absorption/fluorescence spectrometry (HG-AAS/AFS) [Tseng WC et al., 2002; Ma M and Le XC, 1998], inductively coupled plasma-atomic emission spectrometry (ICP-AES) [Do B et al., 2000], and the more sensitive ICP mass spectrometry (ICP-MS) [Yoshida K et al., 2003; McSheehy S et al., 2002] were used for their detection. However, the separation efficiency of HPLC is relatively low particularly for analysis of inorganic arsenic compounds with low molecular weights [Huang YM and Whang CW, 1998; Sun B et al., 2002]. In contrast, capillary electrophoresis (CE) was found to be an efficient alternative to simultaneously separate and determine arsenic species owing to its very high efficiency, ease of operation, low cost, and universal availability compared to the HPLC method [Huang YM and Whang CW, 1998; Sun B et al., 2002].

From a historical perspective, CE appears to have arrived on analytical scene rather late. It was not introduced until early 1980s by Jorgenson and Lukacs [Jorgenson JW and Jukacs KD, 1981; 1983]. By the end of 1980s, the CE literature was expanding exponentially and three manufactures had introduced CE systems. To date, different modes of CE have been developed mainly consisting of capillary zone electrophoresis (CZE), micellar electrokinetic capillary chromatography (MECC), capillary isoelectric focusing (CIEF), capillary isotachophoresis (CITP), and capillary gel electrophoresis (CGE). Amongst, CZE is not only the simplest form of CE but also the most commonly used.

Simply speaking, the separation principle of CE is based on differences in electric-driven mobility of charged analytes, similar to conventional electrophoresis.

The basic instrumentation involves a high-voltage power supply (0 to 60 kV), a capillary with an internal diameter ≤ 200 μm, two buffer reservoirs that can accommodate the capillary and the electrodes connected to the power supply, and a detector (Figure 1).

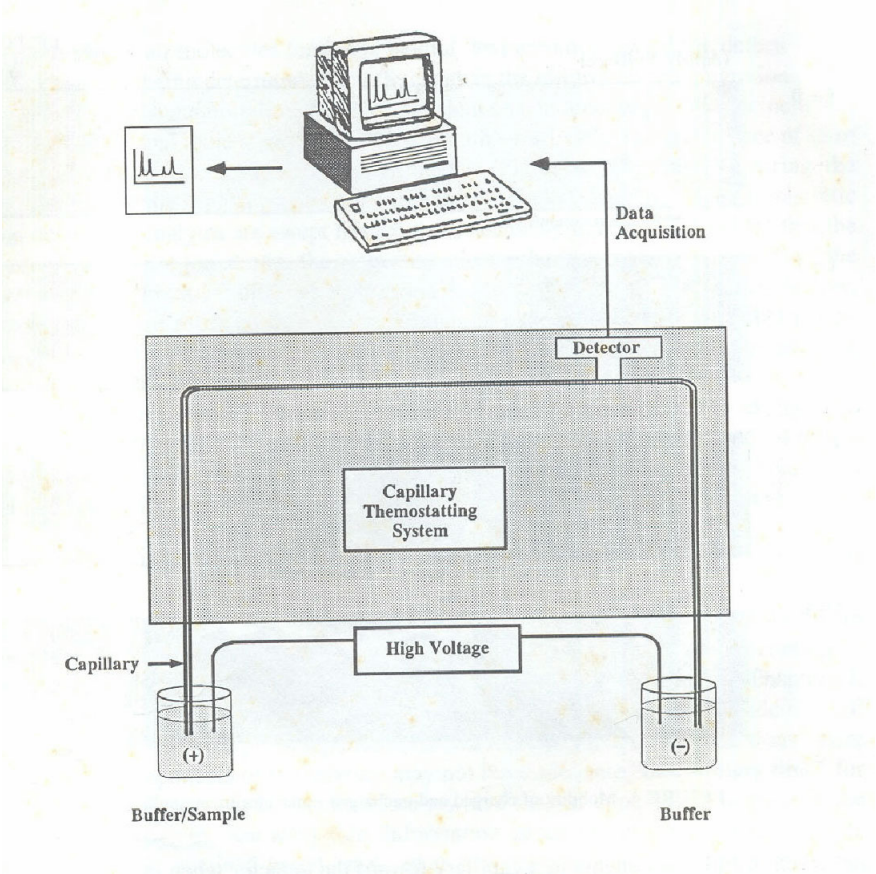

Figure 1. General schematic picture of a CE instrument.

In almost all instances, a detection technique is selected based on physical and chemical properties of the analyte and the requirements of the application being addressed. For example, the analyst uses UV absorbance for molecules that are highly absorbing UV. However, it is possible to indirectly detect analytes that lack desired physical and chemical properties. By incorporating a detectable molecule in the separation medium and monitoring the effect that the analyte has on the signal generated by this second molecule, one can indirectly observe the presence of the

analyte. Indirect detection has been applied to CE for UV absorbance [Foret F et al., 1990], fluorescence [Kuhr WG and Yeung ES, 1988], and electrochemical detection [Olefirowicz TM and Ewing AG, 1990].

2.1.3 Objectives of this study

Initially, we intended to establish a highly efficient capillary zone electrophoresis (CZE) method with indirect UV detection to separate the most commonly encountered inorganic and methylated arsenic compounds, that is, iAs^{III}, iAs^{V}, MMA^{V}, and DMA^{V}. The unique advantages of CZE method probably make it a routine analytical method for practical applications. Thereafter by using the well developed CZE method, the solution type of realgar and orpiment prepared would be analyzed.

Realgar (As_2S_2) and orpiment (As_2S_3) are minerals abundantly distributed in the earth's crust. The medicinal use of realgar and orpiment has been traced back thousands of years. Recently, the anticancer effects of realgar and orpiment particularly on leukemia have become the focus of research interests [Lu DP and Wang Q, 2002; Wang HY and Liu SX, 2002; Zhong L et al., 2003], partially prompted by the huge success of arsenic trioxide in the treatment of APL. Although their clinical efficacy especially on the treatment of CML and APL is evident, it is relatively unclear whether the effectiveness is due to the sulfides or the oxides formed from the parent compounds. The major difficulty limiting research in these areas is the lack of specific and sensitive analytical methods.

Realgar and orpiment are both water insoluble. Therefore, traditional usage formulations are external paste and internal suspension. It is believed that when these arsenic powders are administered orally, they are partially dissolved in the alkaline

intestinal fluids (pH 7-8) before absorption. The alkali extracts of realgar and orpiment have been analyzed by using ion chromatography (IC) with HG-AAS detector [He B et al., 2000]. The findings indicated that main components in the alkali extract of realgar were iAs^{III} and more iAs^{V}, and those in the alkali extract of orpiment were iAs^{III}, iAs^{V} and DMA^{V} with varying proportions [He B et al., 2000] instead of intact realgar or orpiment. It should be mentioned that realgar and orpiment used in that study were not pure and contained impurities, such as different types of iAs^{III}, arsenic trioxide and other trace elements.

In some practical applications, in order to improve their water solubility, researchers dissolved reaglar and orpiment in alkali solutions respectively to generate corresponding solutions [Zhong L et al., 2001]. However, the exact components in such alkali extractions were not identified. Therefore, in this study, the CZE method was chosen to identify the exact components in the alkali extracts of realgar and orpiment. In addition, to avoid interference of impurities to the analysis, in our study, As_2S_2 and As_2S_3 with high purity of above 98% were used.

2.2 Materials and methods

2.2.1 Materials

Potassium arsenate (KH_2AsO_4, iAs^{V}), dimethyl arsenic acid ($(CH_3)_2AsO(OH)$, DMA^{V}), arsenic trioxide (As_2O_3) were purchased from Sigma Chemical Co. (St. Louis, MO, USA). Sodium monomethyl arsonate ($CH_4AsNaO_3 \cdot {}^3/_2H2O$, MMA^{V}) was purchased from Chem Service Inc. (West Chester, PENN, USA). Sodium hydroxide and hydrochloric acid (fuming 37% extra pure) were purchased from Merck KGaA Co. (Darmstadt, Ger). The aqueous stock solutions of iAs^{V}, MMA^{V} and DMA^{V} each with a concentration of 1000 ± 5 ppm as molecule were respectively prepared by

dissolution in Milli-Q water. Sodium arsenite (iAs^{III}) stock solution (1000 ± 5 ppm as molecule of NaH_2AsO_3) was made by first dissolving 6.69 mg As_2O_3 in 10 ml 0.1 M NaOH and then being neutralized with concentrated HCl to pH 7.0 ± 0.2 measured by a pH meter (ION Check 10) from Radiometer Analytical SAS (Lyon, Fr). The accurate arsenic concentrations of all stock solutions were further measured by inductively coupled plasma-optical emission spectrometry (ICP-OES, Thermo Jarrell Ash, IRIS/AP, Ger). Before storage, all stock solutions were filtered through a 0.2 μm nylon filter membrane and degassed in ultrasonic bath for 15 min. The molecular structures and pK_a values of the arsenical analytes are shown in Table 1.

Table 1. Arsenic compounds of interest.

Chemicals with Symbolic name	Structure	pK_a
iAs^V	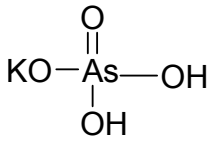	2.3 6.9 11.4
MMA	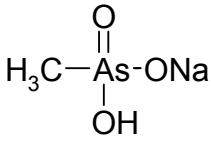	3.6 8.2
DMA	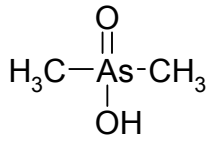	9.3
iAs^{III}	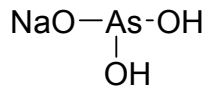	9.2 13.5

Pyridine 2,6-dicarboxylic acid (PDC) (≥98% in purity) was purchased from Fluka Chemicals (Buchs, Switzerland). n-Hexadecyltrimethylammonium hydroxide (CTAOH) (25% in methanol) was purchased from Tokyo Kasei Kogyo Co. Ltd.

(Tokyo, Japan).

Realgar (As_2S_2, 98% in purity) and orpiment (As_2S_3, 99.9% in purity) were purchased from Sigma Chemical Co. (St. Louis, MO, USA). The alkali extracts was prepared by ultrasonically extracting the respective compounds in 0.1 M NaOH for 30 min at an amount of 2 mg compound per 1 ml solution, and then being filtered through a 0.2 μm nylon filter membrane. The arsenic concentrations in the obtained alkali extracts were measured by ICP-OES, being 998 and 1338 ppm as As, respectively. All stock solutions were stored at 4 ^oC in dark.

2.2.2 CZE separation

2.2.2.1 Instruments

All CZE separations were performed on a CE-L1 Capillary Electrophoresis System (CE Resources Pte Ltd, Singapore). This system was equipped with a reversible-polarity power supply (0 – ±30 kV) and an on-column VUV-H22 UV detector. System control as well as data acquisition and analysis were processed by a CSW software (CE Resources Pte Ltd, Singapore). The separations were carried out on an uncoated fused-silica capillary (50 μm i.d. × 360 μm o.d. × 70 cm in length) with a detection window located 10 cm from its extremity. Negative potential applied at the injection port was referred to as negative polarity. A built-in temperature control system was designed to maintain separation temperature and minimize Joule heat generated, thus enabling the CE system to use high electric field and to achieve very low band dispersion. The system had both pneumatic and electrokinetic injection modes. In order to avoid sampling bias and achieve better reproducibility, the pressure-based injection mode was chosen. Sample plug was consistently injected at a low pressure of 0.36 psi for 10 s, which was equal to about 2.9 mm in length (L_{inj})

according to the Poiseulle-Hagen equation [User's Manual]:

$$L_{inj} = (d_{cap})^2 pt/(32\eta L_{cap})$$

where d_{cap} is the capillary inner diameter in μm, p is pressure in psi, t is the time of injection in s, η (0.000891 N·s /m^2) is the viscosity of water at 298 K, and L_{cap} is the length of capillary in cm.

2.2.2.2 Standard separation

PDC/CTAOH background electrolyte (BGE) containing 5 mM PDC and 0.5 mM CTAOH was freshly prepared at the beginning of each study day. Before use, it was vortexed for 2 min, filtered through a 0.45 μm filter membrane and degassed by ultrasonic for 15 min. In between runs, the capillary was subjected to preparation cycles including pre-rinse and precondition steps to ensure a clean and equilibrated surface for the following separations. At the end of the day, the capillary was rinsed for 3 min with 1 M NaOH and Milli-Q water for 5 min respectively and finally dried with air for 3 min. Milli-Q water produced by Ultra-Pure Water System (MilliPore Corp., Bedford, MA, USA) with a resistivity of 18 MΩ·cm was used throughout the experiment.

2.3 Results and Discussion

2.3.1 Separation of inorganic and organic arsenic species

The choice of a background electrolyte (BGE) is very important in method development employing CZE with indirect UV detection. In general, in CZE, ion migration velocity, separation, column efficiency, and peak shape are sensitive to changes in BGE characteristics. Typically, in indirect UV detection mode for anions, crucial BGE composition consists of electrolyte co-ion providing the UV

chromophore and suitable additives such as electroosmotic flow (EOF) modifiers.

The most widely used electrolyte co-ion for inorganic anions is chromate, which provides high mobility anions with a UV chromophore [Jeffrey RM and Khaledi MG, 1998]. It has been reported that band broadening and loss of resolution in the separation of some arsenic compounds were observed in a CZE method using a BGE containing chromate as a co-ion chromophore, borate buffer and n-hexadecyltrimethylammonium bromide (CTAB) as an EOF modifier (chromate/borate/CTAB) [Schlegel D et al., 1996]. In our preliminary study, although separation efficiency was improved and a baseline separation was obtained as using chromate/borate/CTAB BGE to separate arsenic compounds in a CZE method as shown in Figure 2, positive and negative signal peaks simultaneously appeared. The presence of the positive signal peaks disagreed with the separation principle of CZE with indirect detection and could not be clearly elucidated. In addition, the relative high limit of detection (LOD), e.g., around 10 ppm as molecule for iAs^{V}, limited the usage of such BGE in arsenic speciation analysis. Recently, the UV sensitive PDC with a medium mobility capacity was proven well suitable for the simultaneous analysis of both high and low mobility anions [Soga T and Imaizumi M, 2001]. Moreover, PDC has strong UV absorbance in a broad wavelength range at 200 to 400 nm.

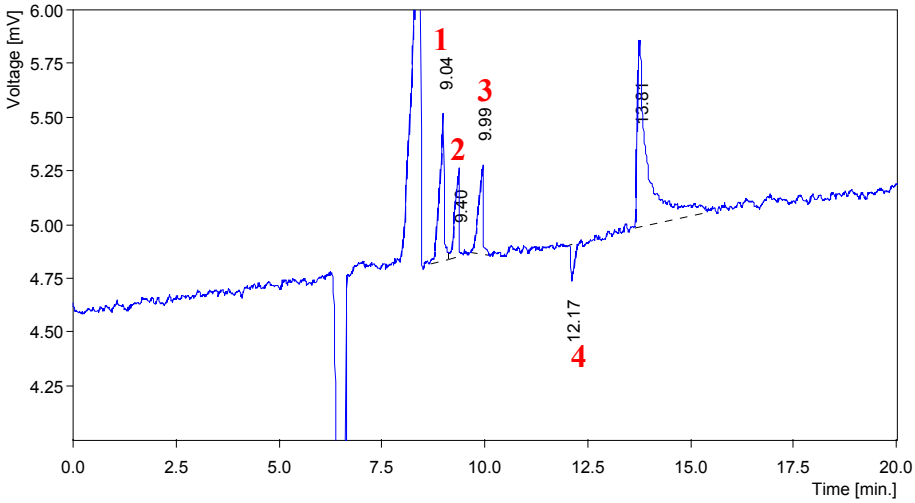

Figure 2. The electrophoretic separation of arsenic compounds each with concentration of 100 ppm as molecule. BGE composing of 10 mM chromate, 12.5 mM borate and 0.5 mM CTAB with pH 9.4; $U_{setting}$ = – 25 kV and $I_{setting}$ = 15 μA; detection wavelength at 216 nm; at temperature of 20 °C. Peaks: 1, iAs^{V}; 2, iAs^{III}; 3, MMA^{V}; and 4, DMA^{V}.

The EOF, which directs to cathode end, is especially adverse for anionic analyte detection at anode. Reducing/eliminating the EOF is required for detecting anions successfully. Among approaches currently applied to control the EOF, cationic surfactant CTAOH was reportedly effective to change capillary inner surface charge by adsorption and consequently the EOF direction [Soga T and Imaizumi M, 2001]. Therefore, PDC/CTAOH was selected as a BGE in this study, and no additional buffer component was used.

To select an optimum detection wavelength, a wavelength range of 195-225 nm was firstly tested. Figure 3 displays the electrophoregrams of iAs^{III} obtained by using 5 mM PDC/0.5 mM CTAOH BGE (pH 10.5) at various detection wavelengths. With an increase in the detection wavelength from 195 to 210 nm, the sensitivity of detection represented by the signal peak area increased, while the baseline noise decreased. Further increasing the detection wavelength to 225 nm, however, led to reduced detection sensitivity, with only a slight improvement in baseline. After

considering the detection sensitivity and baseline noise, 215 nm was thus selected as the detection wavelength for all experiments unless specified otherwise.

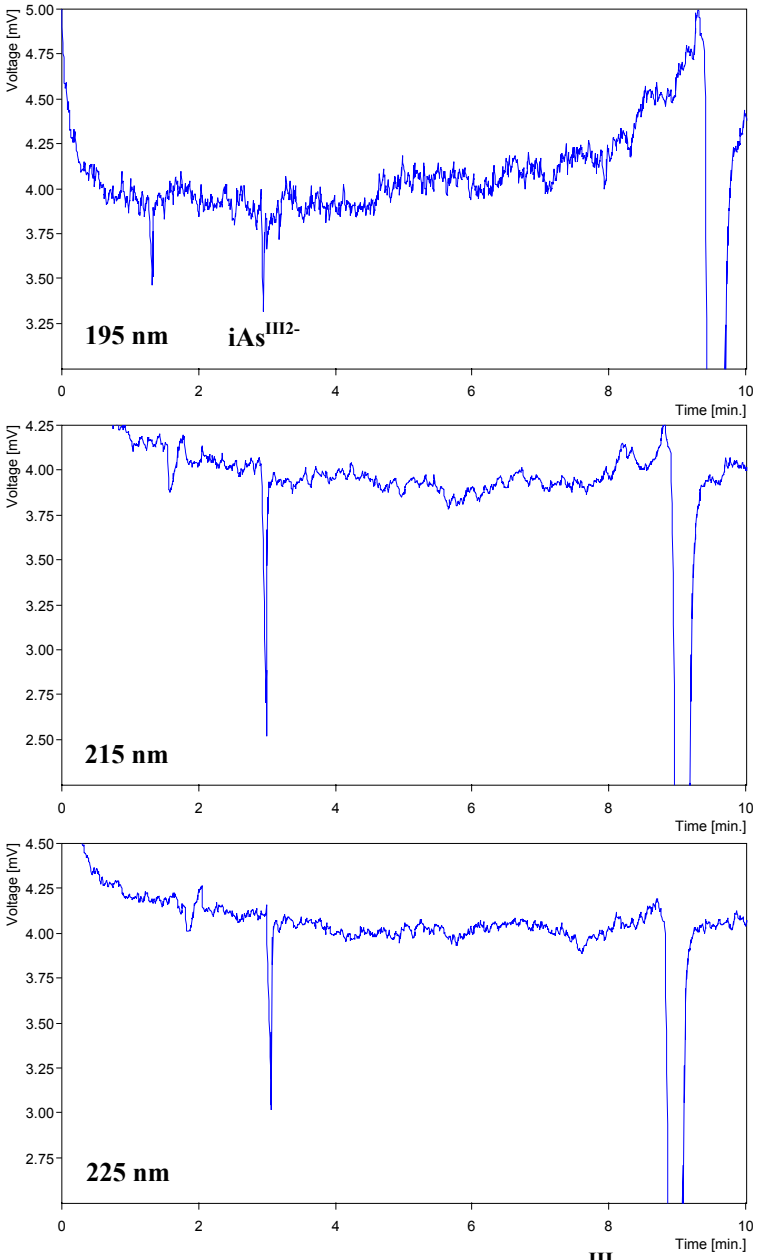

Figure 3. The electrophoregrams of iAs^{III} with concentration of 10 ppm as molecule obtained at different detection wavelengths. BGE with pH 10.5 containing 5 mM PDC and 0.5 mM CTAOH; $U_{setting}$ = – 30 kV and $I_{setting}$ = 8 µA; at temperature of 15 °C.

In the CZE, ionic species are separated based on their charges and sizes, therefore, BGE pH has a crucial impact on the separation. According to the pK_a

values of the analytes (Table 1), at pH 9.3 and above, theoretically, iAs^{V}, MMA^{V} and iAs^{III} have two negative charges, while DMA^{V} is negatively single-charged. Therefore, assuming the EOF has been successfully suppressed, iAs^{V}, MMA^{V} and iAs^{III} would first migrate towards the detector at the anode, while DMA migrates more slowly according to the electrophoretic separation principle. In other CZE studies [Soga T and Imaizumi M, 2001], a high pH up to 12.1 was used in the BGE containing PDC, implying that PDC was chemically stable in a strong basic environment. However, an extremely high BGE pH is not recommended because during an electrophoretic process, generally, an increase of the electrolyte pH will result in increasing the dissociation of silanol group of the capillary inner surface to silonate group, thus enhancing the capillary inner surface charges and the EOF consequently. Furthermore, iAs^{III} tends to be oxidized to iAs^{V} above pH 10 [Abernathy CO et al., 1997]. Therefore, a BGE pH range of 10.0 to 11.5 with a 0.5-step was selected and carefully adjusted.

Figure 4 shows the effects of different BGE pH values from 10.0 to 11.5 with a 0.5 (± 0.02)-step on the electrophoretic separations of arsenic species. Although in the above pH range, theoretically, each arsenic analyte was at the same ionization degree: iAs^{III2-}, iAs^{V2-}, MMA^{2-} and DMA^{-}, migration profiles were different. At low BGE pH of 10.0, the first two anions, iAs^{III2-} and iAs^{V2-}, partially overlapped. Increasing the BGE pH to 10.5, baseline separation was achieved, and the migration order was iAs^{III2-}, iAs^{V2-}, MMA^{2-} and DMA^{-}, and was confirmed by comparing with the electrophoregrams of the individual analytes. At higher BGE pH at 11.0, the whole migration suddenly became much slower in comparison with that at pH 10.5; however, with a further increase to pH 11.5, the migration pattern remained similar to that at pH 11.0. It was well established that the EOF would increase with increase in

the BGE pH. However, this situation can be changed with the addition of the EOF modifier CTAOH: the more negative capillary inner silica surface induced by higher BGE pH leads to attracting a greater amount of CTAOH till saturation. The resultant net charges of the capillary inner surface thus determine the actual EOF, which, in turn, affects the anionic analyte mobility. This could be the cause for the observed changes in the extent of the analyte migration time with the increasing BGE pH. The effects of pH on BGE resistance are shown in Table 2 and summarized as follow: resistance decreased with an increase in the amounts of hydroxide anions added, which was probably due to the high mobility of the small hydroxide anions. As a result, electric field strength that was represented by dividing the applied voltage by the total capillary length (V/cm) decreased with the decrease of the BGE resistance. Obviously, there was a close relationship between the actual migration times of the analytes and the applied electric field strength that could be affected by the BGE pH. It was reported that decreasing electric field strength would reduce the Joule heat and the convection currents in the electrophoretic medium, thus the peak would appear sharper and higher in the electrophoregram. Also from Figure 4, it was found that the detection sensitivity was improved at higher BGE pH such as at 11.0 and above. In the subsequent experiments, a BGE of pH 11.5 was thus selected. Although the chosen PDC/CTAOH BGE was not further adjusted with other buffer components, stable baseline and reproducible migrations were obtained within the pH range of 11.0 to 11.5, indicating their buffer capacity was high enough so that local pH and conductivity did not change as a result of sample injection and following separation.

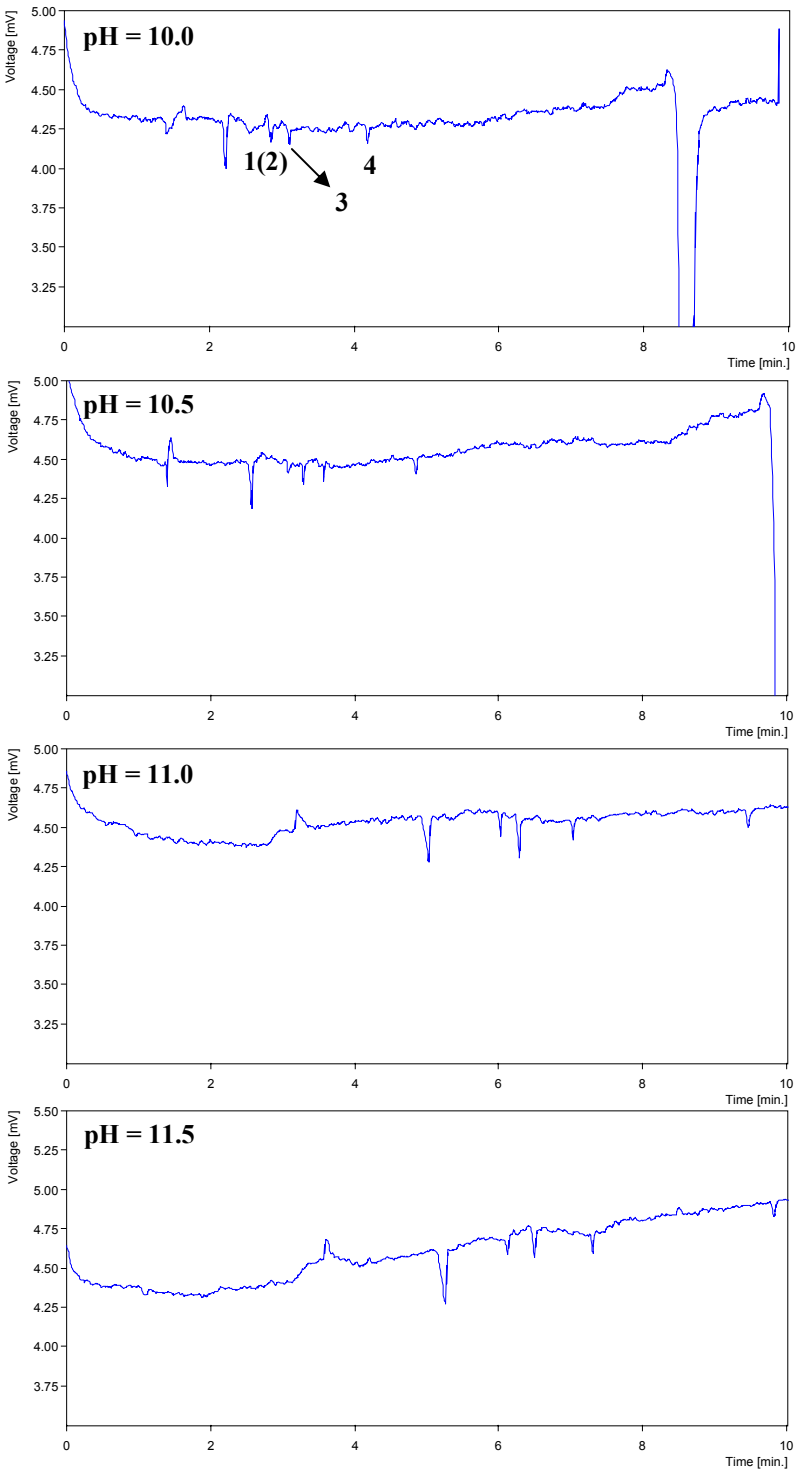

Figure 4. The effects of BGE pH on the electrophoretic separation of arsenic compounds each with concentration of 1 ppm as molecule. BGE composing of 5 mM PDC and 0.5 mM CTAOH; $U_{setting}$ = – 30 kV and $I_{setting}$ = 8 μA; at temperature of 15 ^{o}C. Peaks: 1, iAs^{III2-}; 2, iAs^{V2-}; 3, MMA^{V2-}; 4, DMA^{V-}.

Table 2. The influences of BGE pH on BGE resistance and electric field strength.

BGE pH	BGE resistance ($10^9\Omega$)	Electric field strength ($V.cm^{-1}$)
10.0	3.65	397.14
10.5	3.21	348.57
11.0	1.70	180.00
11.5	1.68	178.32

The driving force behind the migration of ions in CZE is the electric field strength applied across the capillary. Effects of the applied electric field strength on the separation were further demonstrated by directly changing the current settings while fixing the voltage settings as shown in Figure 5. The findings indicated that in the experimental range, increasing the applied electric field strength did not increase the detection sensitivity but did reduce the migration times, while it slightly increased the baseline noise probably due to Joule heat generated.

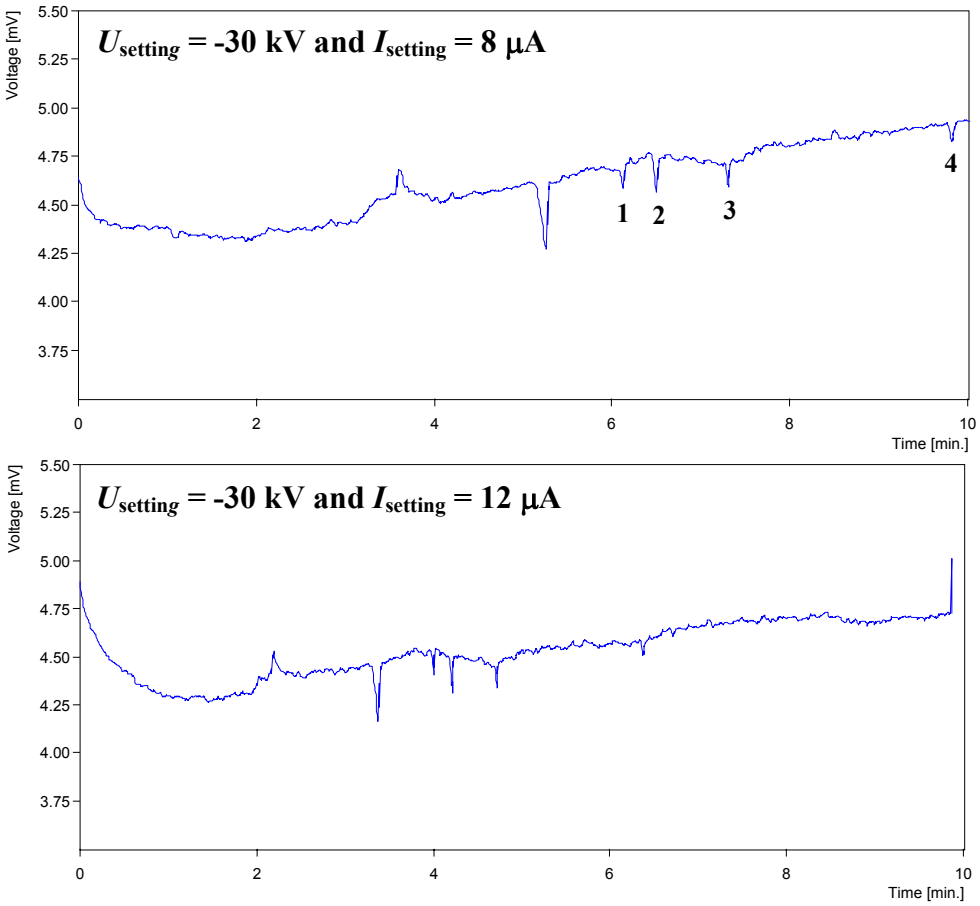

Figure 5. The electrophoretic separation of arsenic compounds each with concentration of 1 ppm as molecule under different applied voltage and current. 5 mM PDC/0.5 mM CTAOH BGE at pH 11.5; at temperature of 15 ^{o}C. Peaks: 1, iAs^{III2-}; 2, iAs^{V2-}; 3, MMA^{V2-}; 4, DMA^{-}.

Temperature plays an important role in many separations, because both analyte mobility and the level of EOF are temperature-related. In general, electrophoretic mobility increases with increasing the temperature by about 2% per 1 K [Foret F et al., 1993]. A temperature range of 20-35 ^{o}C was chosen and optimized. Figure 6 gives the electrophoretic separations of four arsenic species in the temperature range. In the temperature range selected, separation was almost not affected by the change of temperature, except the slightly faster migration and noisier baseline was observed with an increase in temperature.

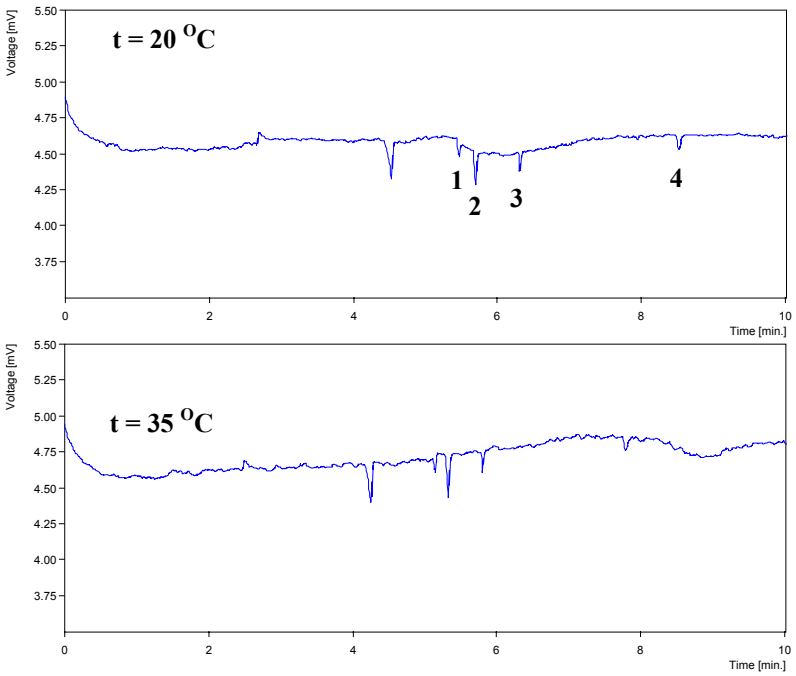

Figure 6. The electrophoretic separation of arsenic compounds each with concentration of 1 ppm as molecule under different operation temperature. 5 mM PDC/0.5 mM CTAOH BGE at pH 11.5; $U_{setting}$ = – 30 kV and $I_{setting}$ = 8 µA. Peaks: 1, iAs^{III2-}; 2, iAs^{V2-}; 3, MMA^{V2-}; 4, DMA^{-}.

2.3.2 Calibration Parameters

With 5 mM PDC/0.5 mM CTAOH BGE at pH 11.5, calibration curves were obtained for the respective arsenic species within the concentration range of 0.5 to 500 ppm. The sensitivity, linearity, intra-day and inter-day variation of the method were determined as shown in Table 3. The mean correlation coefficient (r^2) of each calibration curve with dynamic range of more than three orders of magnitude of concentration exceeded 0.99, indicating good linearity. Intra-day variation expressed as relative standard deviations (RSD%) with respect to migration times and peak areas from six successive injections at the analyte concentration of 10 ppm, was found to be 0.8 – 1.7% for migration times and 3.4 – 6.9% for peak areas, respectively. The inter-day variation for the same parameters was obtained by analyzing analyte species (10 ppm) on 3 successive days. RSD of 1.2 –2.2% for migration times and around 3.6 – 7.1% for peak areas were obtained for all analyte species.

Table 3. Parameters of the calibration curves [a].

Analyte	Detection limit [b] (ppm)	Linear dynamic range (order of magnitude)	r^2	Intra-day variation, RSD%		Inter-day variation, RSD%	
				Migration time (ppm)	Peak area (mV·s)	Migration time (ppm)	Peak area (mV·s)
iAs^{III}	0.23	> 3	0.9984	1.1	3.9	1.7	4.3
iAs^{V}	0.19	> 3	0.9993	0.8	3.4	1.2	3.6
MMA^{V}	0.19	> 3	0.9991	0.9	4.1	1.5	4.8
DMA^{V}	0.22	> 3	0.9987	1.7	6.9	2.2	7.1

[a] Conditions: injection 10s at low pressure; BGE, 5 mM PDC/0.5 mM CTAOH with pH 11.5; detection wavelength 215 nm; voltage setting of –30 kV and current setting of 8 μA.
[b] Relative detection limits were calculated as concentration that will give signals equivalent to three times the noise of the baseline.

2.3.3 Identification of arsenic species in the alkali extracts of realgar and orpiment

It was reported that the main components in the alkali extracts of realgar were iAs^{III} and iAs^{V}, and in the alkali extract of orpiment were iAs^{III}, iAs^{V} and DMA^{V} as identified by IC-HG-AAS method [He B et al., 2000]. By using the established CZE method the alkali extracts of realgar and orpiment were analyzed. By comparing with the migration times with the respective standards, the corresponding electrophoregrams indicated that there were two main components, iAs^{III} and iAs^{V} in the extracts. The alkali extracts were then spiked with standards. Figures 7(a) and (b) showed that no additional signal peak appeared after the samples were spiked separately with iAs^{III} and iAs^{V}, while the peak intensities of iAs^{III} and iAs^{V} respectively increased, supporting the above assumptions. These results were partially consistent with the other study [He B et al., 2000]. Although an amount of DMA^{V} was found in the alkali extract of orpiment in He's report [He B et al., 2000], it was reasonable to suspect that the DMA^{V} might be present as impurity in their samples. With the established calibration curves, the concentrations of iAs^{III} and iAs^{V} in both extracts with 1.5 ppm as As were determined. In the alkali extract of realgar (n = 3), there were 1.90 ± 0.10 ppm (84.61 ± 4.45%) of iAs^{III} and 0.39 ± 0.02 ppm (15.39 ± 0.78%) of iAs^{V}; whereas in the alkali extract of orpiment (n = 3), there were 1.61 ± 0.08 ppm (75.21 ± 3.61 %) of iAs^{III} and 0.60 ± 0.03 ppm (24.79 ± 1.34%) of iAs^{V}, respectively. This study is the first report on using CZE method to analyze the alkali extracts of realgar and orpiment, adding valuable information on the components constituting these compounds. Our finding indicated that the alkali extracting procedure could produce similar redox reactions between the respective As_2S_2 and As_2S_3 molecules and hydroxide to give arsenite (iAs^{III}) and arsenate (iAs^{V}).

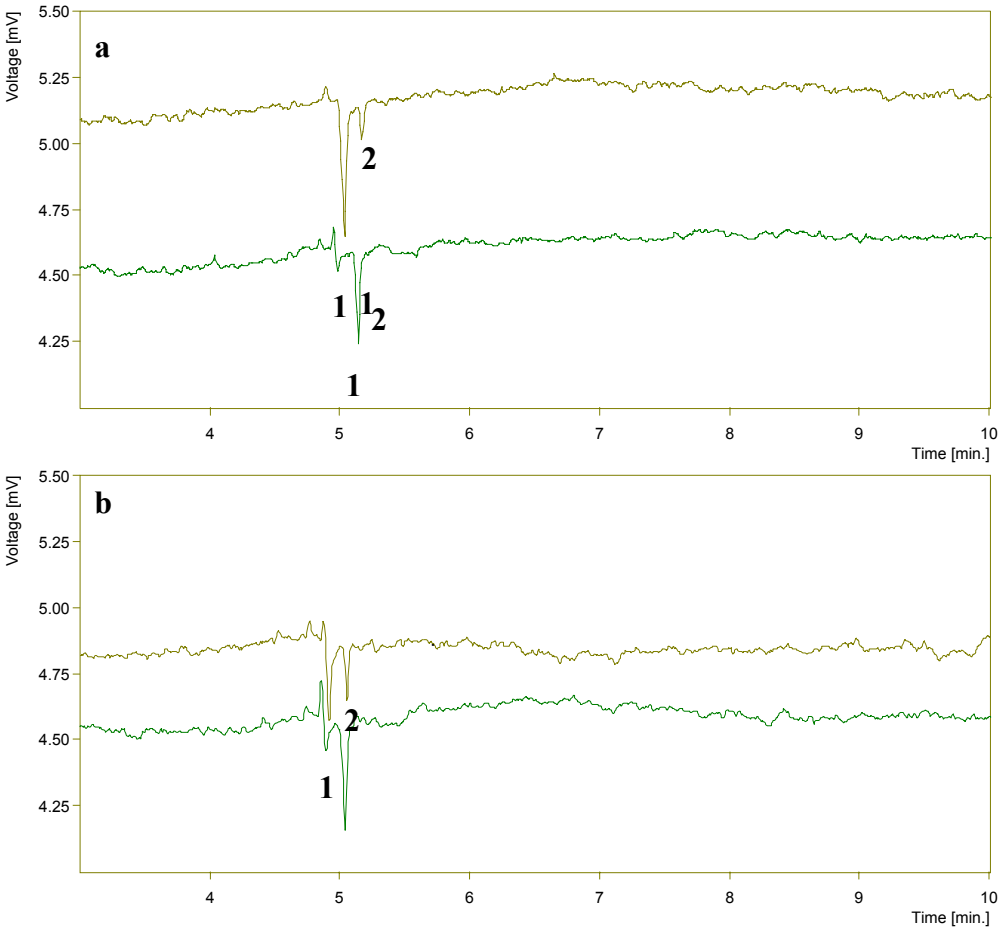

Figure 7. The electrophoregrams of the alkali extracts of realgar (1.5 ppm as As) (a) and orpiment (1.5 ppm as As) (b) respectively spiked with 1 ppm iAs^{III} (upper line) and 1 ppm iAs^{V} (lower line). 5 mM PDC/0.5 mM CTAOH BGE at pH 11.5; $U_{setting}$ = – 30 kV and $I_{setting}$ = 8 µA; at temperature 20°C. Peaks: 1, iAs^{III2-}; 2, iAs^{V2-}.

2.4 Conclusion

The proposed CZE method with indirect UV detection showed excellent suitability for the simultaneous separation and determination of the inorganic and organic arsenic compounds by using the PDC/CTAOH BGE. It provided excellent linearity, intra-day and inter-day variation to identify the components in the alkali extracts of realgar and orpiment as well. The main components in both extracts were found to be iAs^{III} and iAs^{V} instead of intact realgar and orpiment. Therefore, alkali extraction is not an appropriate approach to obtain realgar and orpiment solutions with

intact molecules. Other solubilization methods thus have to be considered.

CHAPTER THREE

Evaluation of the *in vitro* activity and *in vivo* bioavailability of realgar nanoparticles prepared by cryo-grinding

CHAPTER THREE

3.1 Introduction

3.1.1 Background of realgar

Realgar (R) (α-As_4S_4, also written as As_2S_2 or AsS) is a soft monoclinic crystal with orange-red color. The unit cell of realgar is shown as Figure 1. It is light sensitive, because realgar changes form to yellow pararealgar (β-As_4S_4) after a long period of exposure to light.

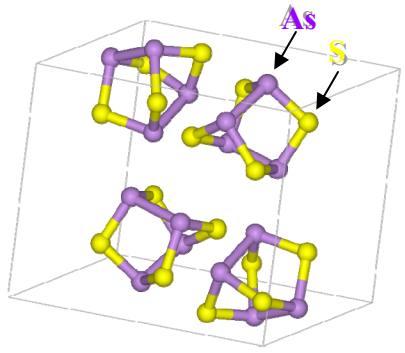

Figure 1. The unit cell of realgar.

As described earlier, a recent clinical trial study of orally administered realgar conducted in China showed that it was highly effective and safe for both remission induction and maintenance in all stages of APL [Lu DP et al., 2002]. In addition, in the corresponding clinical pharmacokinetics (PK) study, researchers observed that coarse realgar powder (in capsule formulation) was absorbed rapidly and excreted mostly within the first 24-h urine. However, realgar is so poorly water-soluble that the reported high oral bioavailability of the drug from the coarse powder needs to be confirmed. In fact, urgent needs always exist for safe and effective delivery of poorly water-soluble drugs.

The most direct approach to enhance the solubility of a compound is to generate a salt. Therefore, most researchers dissolved realgar in an alkali solution,

however, our previous study showed that realgar probably reacts with alkali to convert to trivalent arsenite and pentavalent arsenate instead. Other advanced approaches currently used to enhance the delivery of poorly water-soluble drugs are summarized in Table 1. In most cases, solution form of a drug either in aqueous environment or organic solvent is preliminarily required. Physically, the poor water-solubility of realgar is due to its high lattice energy, which leading to difficulty in breaking molecules apart into surrounding medium like aqueous or organic solvent environment. Generally, because of its too low intrinsic water-solubility, only particle size reduction by micronization/nanonization technique likely is a potential approach to improve the delivery of realgar.

Table 1. Current advanced approaches to enhance delivery of poorly water-soluble drugs.

Advanced approaches	Concept
Solid dispersions	Intimate mixture of drug substance and diluent, such as polyethylene glycol or polyvinylpyrrolidone. The modified drug is often in an amorphous, more soluble state. Due to the higher energy state, there is a potential for recrystallization.
Microemulsions	Micellular dispersion of oil/solvent-dissolved drug as nanometer size droplets in water. The drug can be directly absorbed from the droplets. There are some concerns about toxicity of high surfactant and cosolvent levels and the possibility of precipitation. Administered as a liquid.
Self-emulsifying systems	Mixture of drugs, oils, surfactants, and cosolvents that form an emulsion upon administration. phase inversion may further promote drug release. Can be administered as a solid dosage form.
Complexation	Formation of a reversible, noncovalent chemical complex of a drug with a carrier compound. Cyclodextrins are the most common complexing agents used to enhance drug absorption.
Liposomes	Encapsulation of a drug in uni- or multilayered vesicles of phospholipids. Specific sites can be targeted and certain drugs can be protected from inactivation.
Particle size reduction	Increased particle surface area enhances rate of solubilization.
1) wet milling	Particle size reduction to nano-sized particles through attrition in the presence of stabilizing agents.
2) homogenization	Particle size reduction by high-shear processing of an aqueous slurry of drug and stabilizing agents.

3.1.2 Nanonization

Nanotechnology has a long history. The first famous examples could be the nanosized heterogeneous catalysts developed in the early 19th century [Robertson AJB, 1983]. The most important scientific advancements have taken place in the last two decades in the fields of photography and semiconductor, where nanoparticles (less than 100 nm in diameter) were produced, exhibiting extraordinary and unique practical properties [Mendel J et al., 1999]. Indeed, the physical and chemical properties of materials can be significantly improved or radically changed as their size is scaled down to small clusters of atoms. Colloidal gold and iron oxide nanocrystals are examples of nanoparticles diagnostically applied in biology and medicine [Moghimi SM et al., 2005]. Nanoparticles have been extensively used for systemic and oral administration of different types of drugs and for different purposes including drug targeting [Stella B et al., 2000], drug bioavailability enhancement [Liversidge GG and Cundy KC, 1995], and protection against degradation [Roy K et al., 1999].

In pharmaceutical field, the term "nanoparticles" has been applied rather loosely to structures less than 1 μm in diameter [Kipp JP, 2004]. Present commercially or potentially commercially available nanoparticle engineering techniques of enhancement of dissolution of poorly water-soluble drugs involve the use of mechanical micronization techniques [Muller RH and Peters K, 1998], supercritical fluid processes [Tom JW and Bebenedetti PG, 1991], cryogenic spraying [Costantino HR et al., 2000], and solvent evaporation [Chen X et al., 2002]. Since realgar is not dissolved in almost all commonly used organic solvents, mechanical technique could be a suitable method to reduce its particle size. Co-grinding with water-soluble polymers and/or surfactants is one of the useful pharmaceutical approaches [Itoh K et al., 2003; Mura P et al., 2001; Otsuka M and Matsuda Y, 1995].

The co-grinding technique has the advantages of being simple and economical. The particles can also be produced without using organic solvents [Masaaki S et al., 1998].

3.1.3 Objectives of this study

In this study, realgar nanoparticles were firstly produced by means of cryo-grinding with water soluble and biocompatible polymer polyvinylpyrrolidone (PVP) and surfactant sodium dodecyl sulfate (SDS). *In vitro* and *in vivo* studies were carried out to characterize the realgar nanoparticles as a potential anticancer drug candidate. The *in vitro* cytotoxicity of the realgar nanoparticles was tested on human ovarian and cervical cancer cell lines with two normal human fibroblast cell lines as controls. For the *in vivo* study, a rat model was selected to examine the oral bioavailability of these realgar nanoparticles based on the urinary recovery of arsenic.

3.2 Materials and methods

3.2.1 Materials

PVP (K29-32, MW 40,000) and SDS (ultrapure, ≥ 99.8% in purity) were purchased from Sigma Chemical Co. (St. Louis, MO, USA). All other chemicals used were of analytical reagent grade. Milli-Q water was used throughout the experiment.

3.2.2 Methods

3.2.2.1 Preparation and characterization of cryo-ground realgar particles

(1) Preparation of cryo-ground realgar particles

A cryo-grinding equipment (6850-115 Freezer/Mill, SPEX CertiPrep Inc., Metuchen, NJ, USA) was used to reduce particle size of realgar powder. The equipment consisted of four grinding vials. The maximum capacity for samples with

moderate density was approximate 8 g in each vial. Liquid nitrogen was used as a coolant during grinding. Three physical mixtures (5.0 g each) i.e., R/PVP/SDS (1/3/1, w/w/w), R/PVP (1/3, w/w), and R/SDS (1/1, w/w), were weighed and added into the respective grinding vial, whilst 5.0 g realgar as purchased was put into the last sample vial. These four realgar preparations were ground simultaneously to produce fine particles under the same grinding conditions.

(2) Determination of arsenic content by using graphite furnace atomic absorption spectrometer (GFAAS)

Appropriate amount of each ground realgar preparation was dispersed into 10 ml Milli-Q water, giving a final concentration of 1 mg realgar/ml (1000 ppm as realgar). The dispersions were ultrasonically treated for 30 min and then shaken at 300 rpm for 24 h. Thereafter, the dispersions were filtered through a membrane filter (0.2 μm). Arsenic concentrations in the resulting filtrates were measured by GFAAS (AAnalyst 100, Perkin Elmer Corp., Norwalk, CT, USA).

An electrodeless discharge lamp (EDL) for arsenic operated at 5 mA was used, providing a 193.7 nm line with a spectral bandwidth of 1.3 nm. Argon gas was chosen as carrier and sheath gas. Typical analytical conditions were as follow: drying at 130 ^{o}C, ashing at 1300 ^{o}C, atomization at 2300 ^{o}C, and cleaning at 2600 ^{o}C. $Pd(NO_3)_2$-$Mg(NO_3)_2$ was used as a matrix modifier for such arsenic determinations. For each analysis, a 5 μl of matrix modifier was injected into graphite furnace tube together with 20 μl standard/sample solution. Three replicates were set for each standard/sample analysis. Five standard arsenic solutions with arsenic concentrations of 5, 10, 20, 30, and 50 ppb were prepared from an arsenic standard solution with a concentration of 997 ± 5 mg/L (E. Merck, Darmstadt, Germany) after appropriate

dilutions for calibration curve establishment together with a blank. A linear regression was used for calculation of arsenic content in standard and real samples. A correlation coefficient of 0.9984 was obtained for calibration curve by using linear regression across zero point.

(3) Powder X-Ray diffraction (XRD) measurement

Powder XRD was performed with a D8 advanced X-ray diffractometer (Bruker AXS, Cheshire, UK) using monochromatic CuK_α radiation at room temperature. Measurements were done at 40 kV voltage, 40 mA current, and a scanning angle (2θ) range from 10^o to 40^o.

(4) Particle size analysis and zeta potential measurement

Particle size distribution (mean diameter and polydispersity index (PI)) and zeta potential for each filtrate were determined by a Zetasizer 1000/2000/3000 (Malvern Instruments Ltd., Worcs, UK). Each batch of the realgar filtrate was analyzed in ten repeats. Mean values of three batches with the corresponding standard deviations (means ± SD) were presented.

(5) Transmission electron microscope (TEM) characterization

Transmission electron microscope (Philips CM10, Eindhoven, Netherlands) was used to examine the morphology of the realgar ground particles in the corresponding filtrate and also to physically measure the sizes of the ground realgar nanoparticles.

3.2.3 *In vitro* studies

3.2.3.1 Cells and cell culture.

Three human ovarian cancer cell lines (CI80-13S, OVCAR, OVCAR-3), a human cervical cancer cell line (HeLa), a human normal lung fibroblast cell line (MRC-5) and a dermal fibroblast cell line (HF) were used to test for the cytotoxicity of the realgar nanoparticles prepared. CI80-13S and OVCAR were obtained from Queensland Institute of Medical Research (Australia); HeLa, OVCAR-3 and MRC-5 from ATCC (Manassas, VA, USA), and HF from Skin Culture Laboratory, Singapore General Hospital (Singapore). The HeLa, MRC-5 and HF were grown as monolayer in Dulbecco's modified Eagle's medium (DMEM), and CI80-13S, OVCAR and OVCAR-3 in RPMI-1640, supplemented with 1% penicillin/streptomycin and 10% fetal bovine serum (FBS, HyClone Laboratories, Logan, Utah, USA) at 37 ^{o}C in a humidified atmosphere containing 5% CO_2. Cell viability of the stock cultures used for subsequent experiments was always above 95% as assessed by trypan blue exclusion test.

3.2.3.2 Cell viability assay: Fluorometric microculture cytotoxicity assay (FMCA)

MTT (3-(4,5-dimethylthiazol-2-yl)-2,5-diphenyltetrazolium bromide) assay is a standard colorimetric assay for measuring cellular proliferation [Mosmann T, 1983]. Although MTT assay probably is most prevalent *in vitro* assay used, there are some disadvantages/limitations of this test: 1) there are cell lines that do not metabolized the MTT well or have an acceptable colorimetric profile for control cells; 2) production of the MTT product is dependent on the MTT concentration in the culture medium. The kinetics and degree of saturation are dependent on cell type; 3) assay is less effective in the absence of cell proliferation; 4) MTT cannot distinguish between cytostatic and cytocidal effect; 5) test is less effective if cells have been cultured in

the same media that has supported growth for a few days, which leads to underestimated of control and untreated samples; and 6) certain types of drugs can induce formazan production (MTT) and/or mitochondrial activity. Increased production of formazan will potentially give false positives with these drugs.

Therefore, in this study, drug cytotoxicity and cell proliferation were determined using a previously described FMCA with minor modification [Larsson R and Nygren P, 1989]. The main advantages are its speed, high sensitivity and simplicity. FMCA is based on the measurement of fluorescence generated from the hydrolysis of fluorescein diacetate (FDA, Sigma Chemical Co., St. Louis, MO, USA) to fluorescein by cells with intact plasma membranes. Briefly, cells were seeded into 96-well microtiter plates. The plates were incubated till cells reach exponentially growing stage (80-85% confluence). The medium in the well was then changed to 200 μl of the respective fresh culture medium and culture medium containing the test compounds. After incubation period, the plates were washed with phosphate-buffered saline (PBS) buffer. A stock solution of FDA (10 mg/ml) was prepared in dimethyl sulphoxide (DMSO, ≥ 99.9% in purity, Sigma Chemical Co., St. Louis, MO, USA), kept frozen at -20 ^{o}C and protected from light. The FDA stock solution was freshly diluted to 2 μg/ml with PBS buffer and 200 μl of this solution was then added to each of the control, experimental and blank wells. The plates were incubated for another 30 min at 37 ^{o}C and the fluorescence generated from each well was measured by using a SpectruaFluor (Tecan Systems Inc., San Jose, CA, USA) at an excitation wavelength of 485 nm and an emission wavelength of 535 nm.

In a preliminary study, the fluorescence was found to be proportional to the number of viable cells in the well. Cell survival is presented as survival index (SI), which is defined as the fluorescence in experimental wells expressed as a percentage

of that in the control wells. IC_{50} was defined as the concentration giving a SI of 50%, and was estimated by using the software GraphPad Prism Version 4.00 (GraphPad Software Inc., San Diego, CA, USA).

Cell morphological change of adherent cells before and after drug treatment was observed by using phase-contrast microscope (Nikon Eclipse TE2000-U, Nikon Corp., Tokyo, JP).

3.2.3.3 Flow cytometry analysis of apoptosis and cell cycle distribution

Apoptosis was identified and quantified by flow cytometry on a Beckman Coulter Epics Alfa (Beckman Coulter Inc., Fullerton, CA, USA) after propidium iodine (PI, ≥ 95% in purity, Sigma Chemical Co., St. Louis, MO, USA) stained. PI stained the late apoptotic cells which had increased membrane permeability. Cells were treated with various realgar nanoparticles. At the end of the incubation, all cells were collected and fixed in 70% ice-cold ethanol at a cell density of 1×10^6/ml, and kept in fridge (-20 ^oC) at least overnight until analysis. Fixed cells were washed twice with PBS buffer and treated with 1 mg/ml RNAse (DNAse-free) (Sigma Chemical Co., St. Louis, MO, USA) for 30 min at 37 ^oC. PI was then added to the solution at a final concentration of 50 μg/ml. Samples were filtered through a 60 μm pore size nylon mesh before analysis. Obtained DNA histogram was analyzed using WinMDI Version 2.8. Cells with DNA content less than the cells in G_1 phase (sub-G_1) were taken as apoptotic cells.

3.2.3.4 DNA fragmentation assay

Following incubation with various realgar nanoparticles at the concentration of IC_{50} for 72 h, approximately 1×10^6 cells were harvested after centrifugation. The

harvested cells were washed twice with ice-cold PBS buffer, and then re-suspended in 0.5 ml lysis buffer (0.2% Triton X-100, 10 mM Tris pH 8.0, and 1 mM EDTA). After freshly added 0.25 mg Proteinase K (Sigma Chemical Co., St. Louis, MO, USA), the cell suspension was incubated at 55 ^{o}C for 1 h. After pelleting cell debris and proteins by centrifuging the cell suspension at 14,000 g at 4 ^{o}C for 20 min, the supernatant was saved. One-half volume of 3 M sodium acetate and 2.5 volumes of cold ethanol (99.7% in purity) were added to the supernatant followed by incubation overnight at -20 ^{o}C. DNA was collected by centrifugation at 14,000 g at 4 ^{o}C for 20 min. The DNA pellet was then dissolved in TE buffer (10 mM Tris pH 8.0 and 1 mM EDTA). The DNA sample was separated by electrophoresis in a 1.5% agarose gel containing 0.5 μg/ml ethidium bromide (EB, Bio-Rad Laboratories, Hercules, CA, USA) in Tris-acetate-EDTA (TAE) running buffer. The gels were then visualized under UV light with Quantity One mode 4.5.0 (Bio-Rad Laboratories, Hercules, CA, USA).

3.2.4 *In vivo* investigations

3.2.4.1 Animal

Healthy male Sprague Dawley (SD) rats (6-7 weeks of age, average weight of 200 ± 20 g) were purchased from Laboratory Animals Centre, Singapore. They were housed individually in polycarbonate metabolic cages and provided with a standard diet (Mouse pellets, Laboratory Animals Centre, Singapore) and water *ad libitum*. The room was kept on a 12/12-h light/dark cycle at a temperature of 23 ± 1 ^{o}C and relative humidity of 50 ± 10%. At least three days of acclimatization period was allowed for rats prior to drug administration experiments.

3.2.4.2 Bioavailability studies

The study protocol adhered to guidelines for the humane use of animals in scientific research, and all animal procedures were approved by the Institutional Animal Care and Use Committee (National University of Singapore, Singapore). The SD Rats were administered various realgar suspensions orally at a dose of 50 mg realgar/kg body weight using a gavage needle. Urine was collected at the end of intervals of 0-24, 24-48 and 48-96 h after single administration. The urine samples were centrifuged at 3000 g for 15 min to remove particulate materials and stored at – 80^{o}C till analysis. Arsenic concentrations in urine samples were measured by GFAAS.

3.2.4.3 Normalization of urine by creatinine assay

The concentration of creatinine in urine was measured by Jaffe method after slight modification [Chan MH et al., 2004]. Briefly, the formation of acid-sensitive chromogen after reduction of the urine sample with picrate was measured at absorbance of 500 nm. The urinary arsenic level was then normalized with creatinine concentration.

3.2.5 Statistical analysis

Data are presented as mean ± SD, and analyzed by one-way ANOVA with Tukey's multiple comparison test for post test (GraphPad Prism Version 4.00). Values of $p < 0.05$ were indicative of significant differences, and those of $p < 0.01$ were indicative of very significant differences.

3.3 Results and Discussion

3.3.1 Submicron/nanoparticles formation using cryo-grinding technique

Simultaneous adsorption of polymers and surfactants from their mixed

solutions onto solid particles has been extensively studied in recent years. Simultaneous adsorption of PVP and SDS onto alumina or titanium dioxide has been reported [Ma CM and Li CL, 1989]. The dispersion stability of alumina suspensions was enhanced due to the adsorption of PVP and SDS [Kunio E et al., 2000]. Both PVP and SDS are also used as grinding additives in a dry process to reduce particle sizes of poorly water-soluble drugs, such as griseofulvin, glibenclamide and nifedipine [Koichi I et al., 2003]. Stable drug/PVP/SDS aqueous suspensions were obtained due to inhibition of aggregation/agglomeration by the adsorption of PVP and SDS on the surfaces of drug crystals. Inspired by the fact that the PVP and/or SDS effectively enhance solubility of crystals in aqueous environments, they were chosen as grinding additives in the current study.

The filtrates from the binary R/PVP, R/SDS and ternary R/PVP/SDS ground mixtures were prepared as described in the Materials and Methods section. The filtrates from the ground alone realgar particles and the original coarse realgar powder (sieved through 150 μm pore size mesh before weighing) were also prepared. It might be noted that the filtrates from all co-ground mixtures were vague colloidal solutions and slightly yellowish in color, and the filtrates of the original realgar powder and ground realgar alone particles were clear solutions after 48 h standing at room temperature. Such difference probably results from the different realgar amount in the individual filtrate.

The arsenic concentrations of all filtrates were measured by GFAAS and the values are shown in Table 2. The arsenic concentration of the filtrate from the R/PVP/SDS preparation was highest to give a concentration of 134.20 ppm, about 250-fold higher than that of the filtrate from the original coarse realgar powder and about 50-fold higher than that of the filtrate from the realgar ground alone preparation,

and then followed by the binary R/PVP and R/SDS filtrates. The result indicated that the presence of PVP and/or SDS in the grinding mixtures facilitated the production of larger amounts of realgar fine particles of 200 nm or less.

Table 2. Physical properties of the realgar nanoparticles in the filtrates obtained after filtering the respective realgar preparation through a 0.2 μm filter membrane. Values are mean ± SD (*n* = 3 batches).

Analyte filtrate	Arsenic concentration (ppm)	Particle size (nm)	Polydispersity index (PI)	Zeta potential (mV)
Original realgar powder	0.52 ± 0.03	286.9 ± 17.5	0.874 ± 0.122	0.5 ± 0.1
Realgar ground alone particles	2.53 ± 0.09	328.9 ± 32.5	0.767 ± 0.373	0.6 ± 0.2
R/PVP (1/3, w/w)	121.00 ± 7.23	243.2 ± 5.3	0.184 ± 0.020	-4.3 ± 1.8
R/SDS (1/1, w/w)	53.81 ± 3.89	176.1 ± 4.5	0.116 ± 0.022	-14.9 ± 9.2
R/PVP/SDS (1/3/1, w/w)	134.20 ± 4.03	217.3 ± 4.9	0.209 ± 0.019	-8.7 ± 3.1

The particle size and distribution of all filtrates were evaluated by means of Zetasizer, and the results are shown in Table 2. With the assistance of PVP and/or SDS, the mean particle sizes were slightly decreased, to less than 250 nm, when compared with those of the original realgar powder and the realgar ground alone preparation. The PI value that represents the pattern of systematic particle distribution is equal to 0 for a monodisperse suspension and 1 for a polydisperse suspension. The PI values of the co-ground preparations were significantly lower than that of the ground realgar alone preparation ($p < 0.05$), suggesting that the particle distribution became more homogeneous after co-grinding with additive(s). As the values of the

particle size and PI of the co-ground preparations were determined after the complete dissolution of PVP and SDS, they might reflect the status of crystallization and/or aggregation of the realgar particles in the suspensions. The smaller mean particle sizes and PI values of all co-ground preparations might be partially attributed to the effective inhibition of the recrystallization and/or aggregation and/or agglomeration of realgar particles in water by PVP and/or SDS.

In order to study the surface physical properties of various nanosized realgar particles, the zeta potentials of the realgar fine particles were investigated by Zetasizer and the values are shown in Table 2. The zeta potential values of the original realgar powder and realgar ground particles without additive were almost same with mean values around zero. It is probably due to the fact that realgar is unionizable. After grinding with PVP and/or SDS, the zeta potential values became negative. This indicated that the negative charged PVP and SDS were partially adsorbed onto the particle surfaces. The zeta potential value of the ternary R/PVP/SDS preparation was between those of R/PVP and R/SDS preparations.

TEM was used to examine the morphologies of the different realgar ground preparations. Figure 2 displays the TEM images of the binary R/PVP, R/SDS and ternary R/PVP/SDS preparations. In comparison with the mean particle sizes of the corresponding filtrates determined by Zetasizer, the particle sizes observed by TEM were much smaller. This phenomenon was probably due to the particles observed by TEM were the individual core realgar particles, whilst the particles apparent to the Zetasizer were the realgar particles with PVP and/or SDS coating(s). Although the Zetasizer might not give very accurate measurements of the core particle size, it can give approximate estimates of the relative particle sizes.

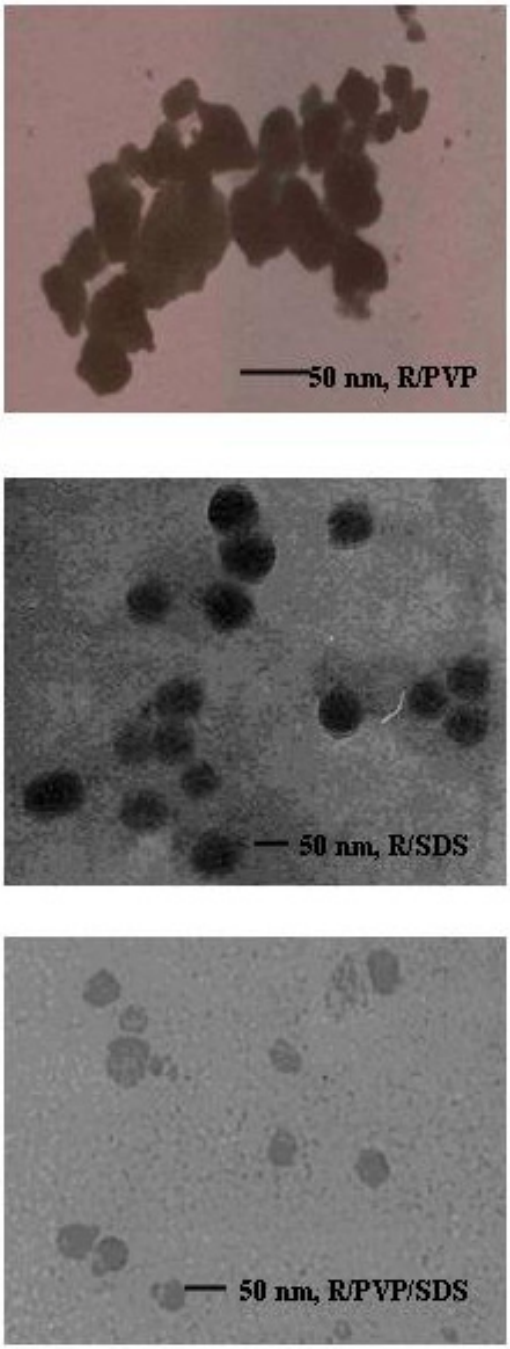

Figure 2. TEM pictures of the nanosized realgar particles from the binary R/PVP, R/SDS, and ternary R/PVP/SDS filtrates.

To study the crystallinity change of the realgar powder after cryo-grinding, the XRD of the respective realgar powder was scanned. Figure 3 shows the XRD patterns of the various realgar preparations. The characterized diffraction angles observed in

all realgar ground preparations were in agreement with that of the original realgar powder. The results suggested that the fine particles obtained from cryo-grinding included most crystalline form of realgar. This confirmed that the selected cryo-grinding technique did not change the crystallinity of the realgar powder. Although decrease in drug crystallinity till amorphization or formation of metastable polymorphic modification are possible factors responsible for the apparent increase in dissolution rate [Yonemochi E et al., 1999; Otsuka M et al., 1999], both approaches at the same time give rise to physical and/or chemical stability problems because the high-energy state of the drug can revert to the thermodynamically stable form of crystallinity or decompose more rapidly than the stable form under processing and storage conditions.

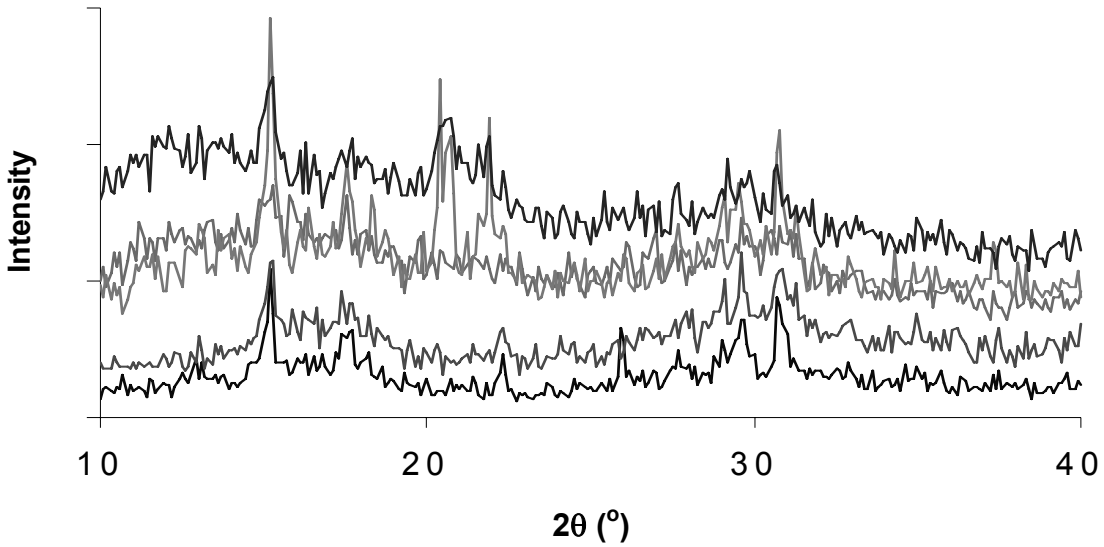

Figure 3. Powder XRD patterns of various realgar preparations (from top to bottom): R/PVP/SDS, R/PVP, R/SDS, R ground without additive, and original R.

In summary, nanocrystalline realgar particles were formed successfully by cryo-grinding. PVP and SDS not only enhanced the grinding efficiency, but also helped to de-aggregate the nanoparticles in solutions. It has been well known that the

choice and concentration of stabilizer can be selected to promote the particles size reduction process and generate physically stable formulations in nanocrystalline systems, mainly because the stabilizer is capable of wetting the surface of the drug crystals and providing steric and/or ionic barrier [Hu J et al., 2004]. In PVP/SDS system, the steric effect could arise from the long polyvinyl chains of PVP and the ionic repulsing barrier from the negative charged oxygen anion of SDS. In the absence of an appropriate stabilizer, the high surface energy of nanosized particles would tend to agglomerate and/or aggregate. It has also been reported that an appropriate amount of stabilizer is required to obtain stable nanocrystalline formulations, that is, too little stabilizer induces agglomeration and/or aggregation and too much promotes Ostwald ripening [Kibbe AH, 2000]. Many commonly used pharmaceutical excipients such as cellulosics, pluronics, polysorbates and povidones are acceptable stabilizers for generating physically stable nanoparticle dispersions [Kibbe AH, 2000; Liversidge GG et al., 1992].

Dispersion stability of co-ground preparations could be indicated by sedimentation rate with time, which could be observed by naked eye according to yellow color change and the appearance of yellow precipitate. After seven days standing in room temperature, R/PVP/SDS preparation showed the best stability than both R/PVP and R/SDS preparations. Further confirmation was done by a reducing order of R/PVP/SDS > R/PVP > R/SDS in terms of the arsenic concentration change in the top layer of the respective suspension.

3.3.2 *In vitro* activity of the nanosized realgar particles on human ovarian and cervical cancer cell lines

The potential *in vitro* activities of the various realgar nanoparticles on cell

growth and survival were tested on human ovarian (CI80-13S, OVCAR, and OVCAR-3) and cervical (HeLa) cancer cell lines. For comparison, two types of normal human fibroblast cell lines, lung fibroblast MRC-5 and skin fibroblast HF, were selected and tested as controls. Exposure of these cancer cell lines on exponentially growing stage to the corresponding filtrates with different concentrations was examined every 24 h for 3 days, inhibition of cell viability in a dose- and time-dependent manner was found. To estimate the IC_{50} values after 3-day drug treatment, the response-dose curves were fitted to the Sigmoidal dose-response (variable slope) equation using the software GraphPad Prism (V4.00). The results are summarized in Table 3. It was found that all realgar preparations had significant cytotoxic effect on the target gynecological cancer cell lines with IC_{50} values comparable to that of arsenic trioxide [Bode AM and Dong ZG, 2002]. By comparing the IC_{50} values of the respective realgar preparation on the cancer cell lines, CI80-13S was the most sensitive cell line to all realgar preparations (with IC_{50} values less than 1 μM as As_2S_2) ($p < 0.001$). The other caner cell lines had IC_{50} values in the range of 2-5 μM with insignificant differences among them ($p > 0.05$). In each cell line, there was no significant difference in the IC_{50} values ($p > 0.05$) among the different realgar formulations. The effects of PVP and SDS alone on the cells were also studied. Their IC_{50} values were around 25.0 mM and 0.3 M, respectively, indicating that PVP and SDS were not responsible for the cytotoxic effects within the working concentration ranges (i.e. maximum working concentration of about 0.12 mM for PVP; and around 0.04 mM for SDS). Our findings also showed that the normal human fibroblast cell lines, MRC-5 and HF, were relatively resistant to the various realgar preparations (IC_{50} values were all over 10 μM) (Table 3).

Table 3. IC_{50} (μM as As_2S_2) of various realgar particles and arsenic trioxide in different cell lines exposed for 3 days. Results are the mean ± SD from three independent experiments, and in each experiment there are six repeats.

	IC_{50} (μM as As_2S_2)					
	CI80-13S	**OVCAR**	**OVCAR-3**	**HeLa**	**MRC-5**	**HF**
Original realgar	0.77 ± 0.08	2.77 ± 0.23	3.63 ± 0.51	2.83 ± 0.35	14.76 ± 1.45	*
Realgar ground alone	0.80 ± 0.07	2.67 ± 0.30	3.44 ± 0.42	2.98 ± 0.29	12.67 ± 1.67	*
R/PVP	0.82 ± 0.08	2.81 ± 0.29	3.86 ± 0.35	2.57 ± 0.31	14.41 ± 1.44	*
R/SDS	0.78 ± 0.09	3.66 ± 0.36	4.37 ± 0.61	3.69 ± 0.34	11.41 ± 1.00	*
R/PVP/SDS	0.81 ± 0.07	3.44 ± 0.49	4.06 ± 0.45	3.51 ± 0.48	16.11 ± 2.01	*
As_2O_3**	2.10 ± 0.28	1.88 ± 0.49	2.37 ± 0.33	1.85 ± 0.54	ND	10.02 ± 0.37

* IC_{50} could not be reached in the test dose range.
** Data was obtained from the reference: Du YH and Ho PC, 2001.
ND: not determined.

3.3.3 Assessment of the apoptotic effects of the realgar nanoparticle

Cell death is an important variable in cancer development, cancer prevention and cancer therapy. In the treatment of cancer, the major approach is removal of the neoplasm by surgery, and/or the induction of cell death by radiation, toxic chemicals, antibodies and/or cells of the immune system [Zornig M et al., 2001; Kong AN et al., 2001]. However, the mechanisms underlying the cell death are still poorly understood. In the recent literatures, cell death is thought to occur by two alternative modes: apoptosis and necrosis. Figure 4 shows typical morphological characteristics of cells undergoing apoptosis or necrosis.

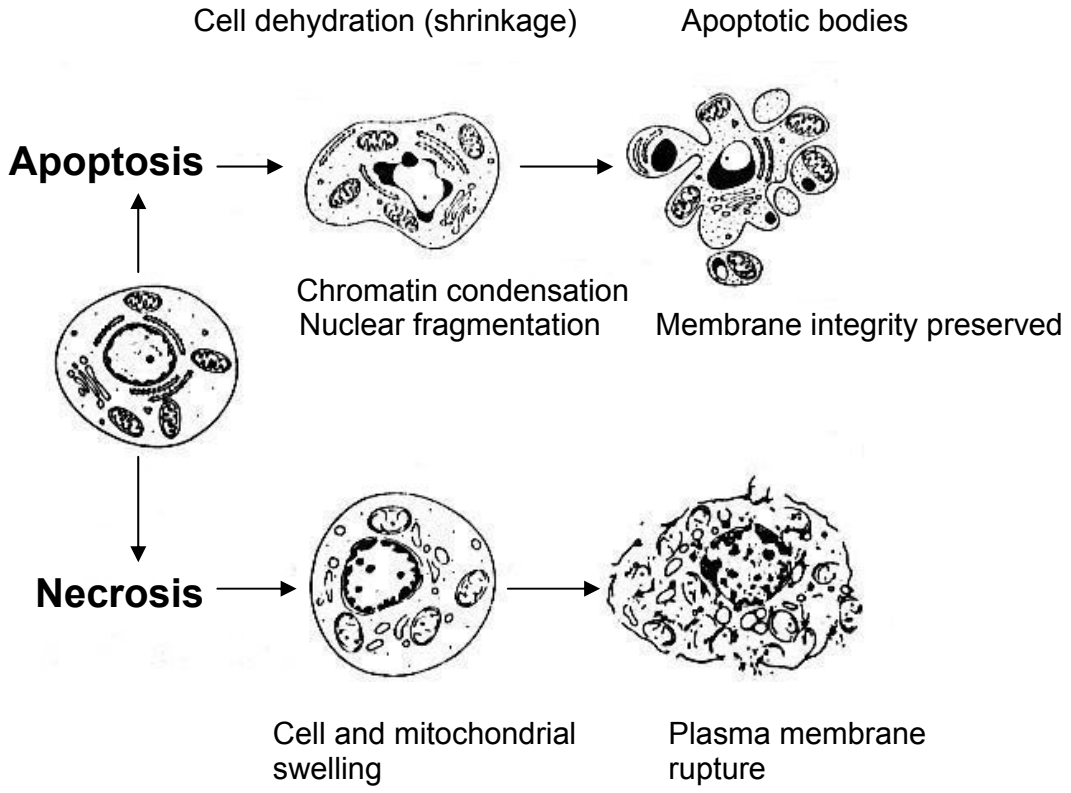

Figure 4. Morphological characteristics of cells undergoing apoptosis and necrosis.

Apoptosis (programmed cell death) has emerged as an important biological mechanism that contributes to the maintenance of the integrity of multicellular organisms [Kerr JF et al., 1972]. It has been shown that tumors develop not only from abnormal cell proliferation and the inhibition of differentiation, but also from reduced cell death due to the inhibition of apoptosis [Elmore S, 2007]. Evidence suggests that the failure of cells to undergo apoptosis might be a factor in the pathogenesis of a variety of human diseases, including cancer, autoimmune diseases, and viral infections [Elmore S, 2007]. Apoptosis has become a focus of interest in oncology. Specific therapies are being designed to enhance the susceptibility of individual cell type from a variety of human cancers to undergo apoptosis. An overwhelming amount of evidence indicates that arsenic compounds induce apoptosis in many cell types [Bode AM and Dong ZG, 2002; Seo T et al., 2005].

Generally, apoptosis can be recognized by its characteristic morphological features, including cell shrinkage, chromatin condensation, cytoplasmic membrane blebbing and formation of apoptotic bodies containing cytoplasm, organelles and nuclear fragments, phagocytosis of apoptotic bodies by neighboring cells or macrophages. Figures 5a and 5b shows the morphologies of the target cell lines treated with R/PVP/SDS nanoparticles at the concentration of IC_{50} for 72 h observed by phase-contrast microscope. After treatment, almost all cancer cells retracted from the neighboring ones. Some typical apoptotic features were observed, including chromatin condensation, blebbing of the plasma membrane or formation of apoptotic bodies. However, no significant changes in morphology appeared in the control fibroblast cell lines MRC-5 and HF after same treatment. It was also observed that all cell lines had similar responses to other realgar particle preparations to R/PVP/SDS in terms of morphological changes.

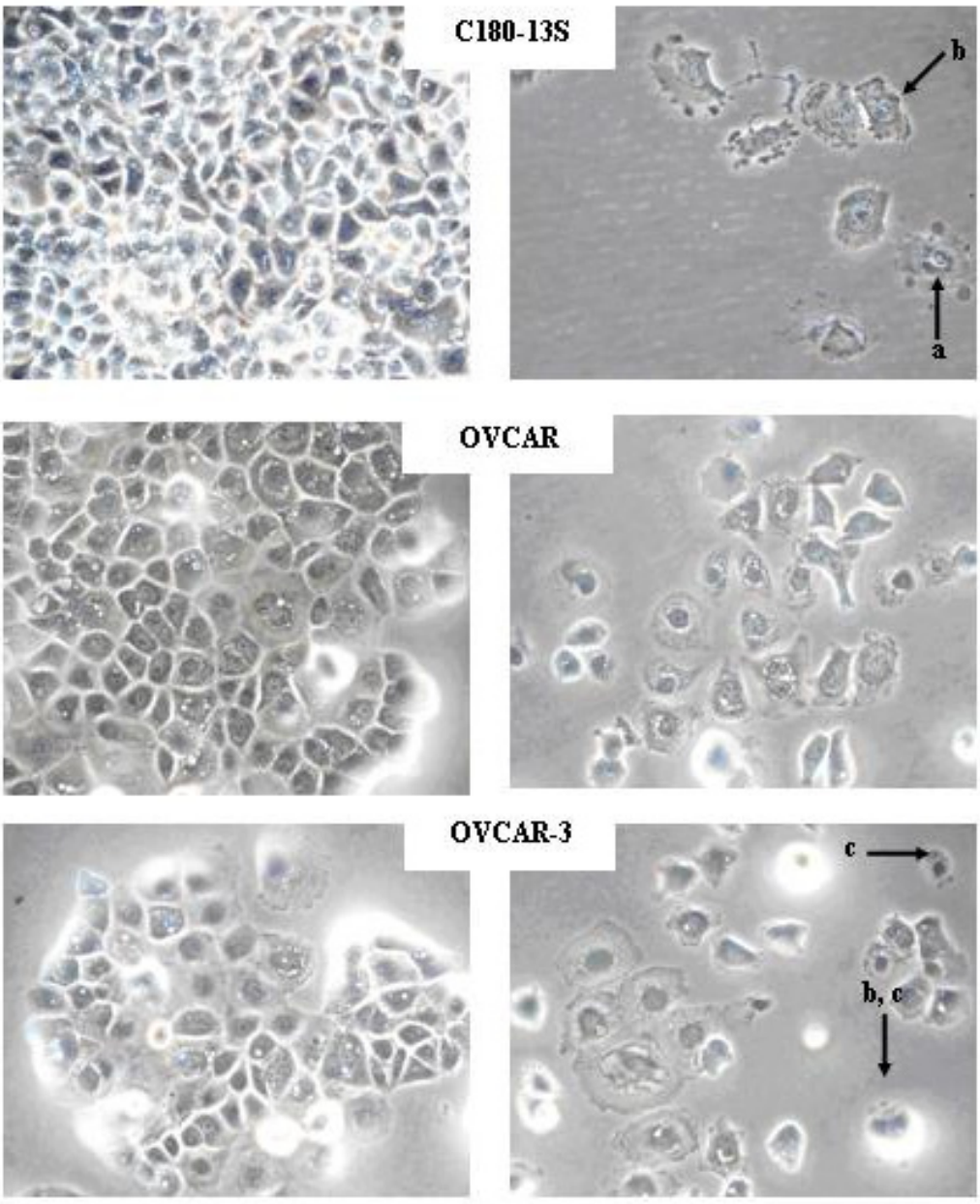

Figure 5a. Morphologies of CI80-13S, OVCAR and OVCAR-3 cell lines before (left, control) and after drug (R/PVP/SDS) treatment (right, treatment) for 72 h. All the photos were taken after removing the culture medium under a phase-contrast microscope. a: chromatin condensation; b: membrane blebbing; c: apoptotic body.

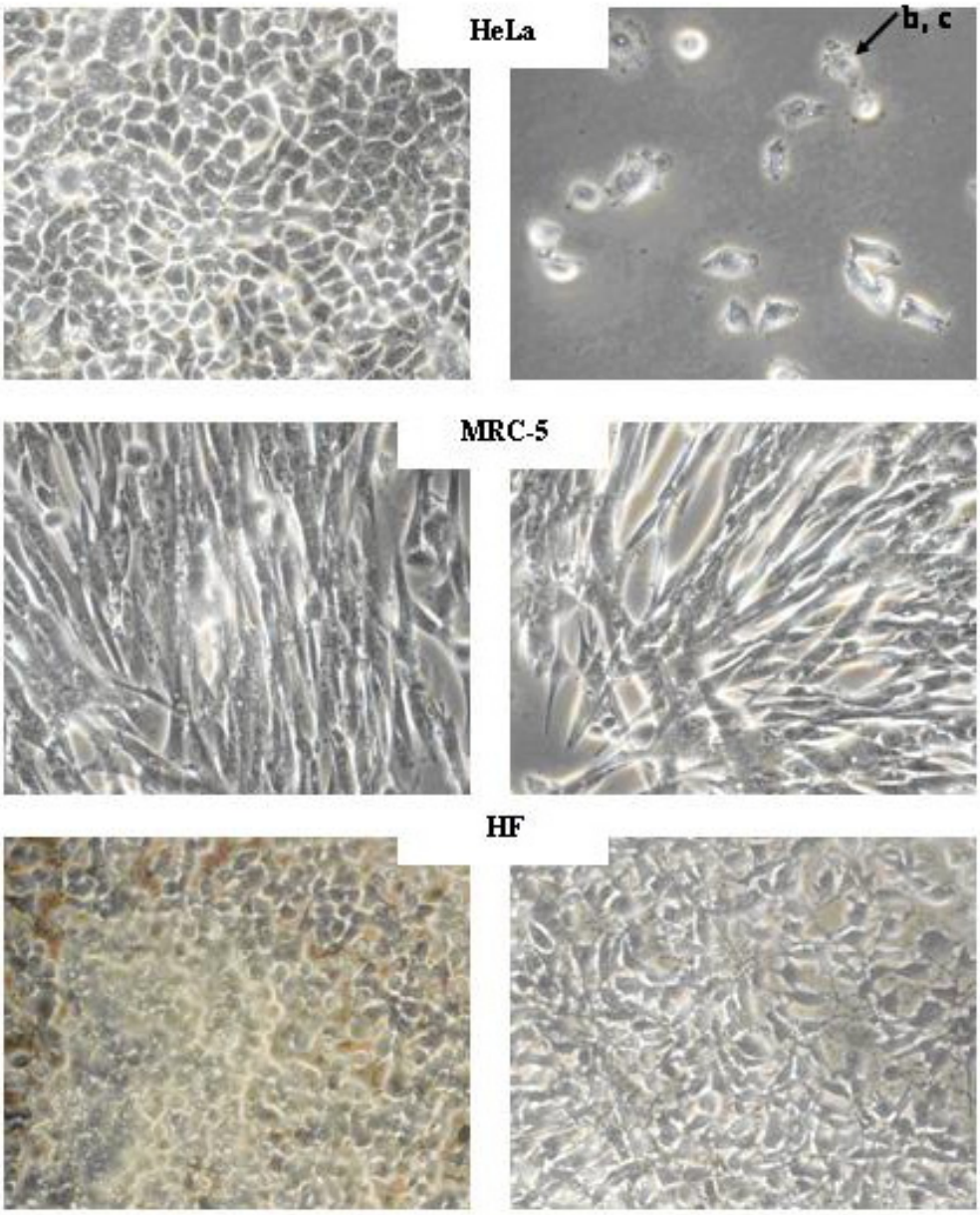

Figure 5b. Morphologies of HeLa, MRC-5 and HF cell lines before (left, control) and after drug (R/PVP/SDS) treatment (right, treatment) for 72 h. All the photos were taken after removing the culture medium under a phase-contrast microscope. a: chromatin condensation; b: membrane blebbing; c: apoptotic body.

The distribution of cells in the various phases of cell cycle were analyzed after treatment with the respective realgar preparation at a concentration around IC_{50} for 72 h. DNA content distribution histograms clearly indicated that exposure of all cancer

cell lines to realgar nanoparticles resulted in the appearance of cells with a fractional DNA content forming a well-defined sub-G_1 peak, a typical profile of apoptotic cells. The proportions of all cancer cell lines tested in the G_2/M phase were also increased. This result suggested that realgar induces apoptosis specifically through delay in G_2/M phase cell in the cell cycle. Figure 6 shows the typical cell cycle histograms of the target cancer cell lines treated with the R/PVP/SDS nanoparticles at the concentration of IC_{50} for 72 h. Other realgar nanoparticle preparations also showed similar effects on target cancer cells. Results are summarized in Figure 7. As for MRC-5 and HF cells, no major variation in the cell phase distribution was noted in them after realgar treatment even at the concentration around IC_{50} (Figure 7). To obtain enough cell amounts for flow cytometry analysis, 75 cm^2 culture flasks were used to grow the cells. It was found that for MRC-5 and HF cells, most cells survived even after drug treatment at concentrations around the IC_{50} values estimated from the FMCA experiments. This finding indicated that the cells could survive better in the larger culture flasks than in the smaller microtiter plates.

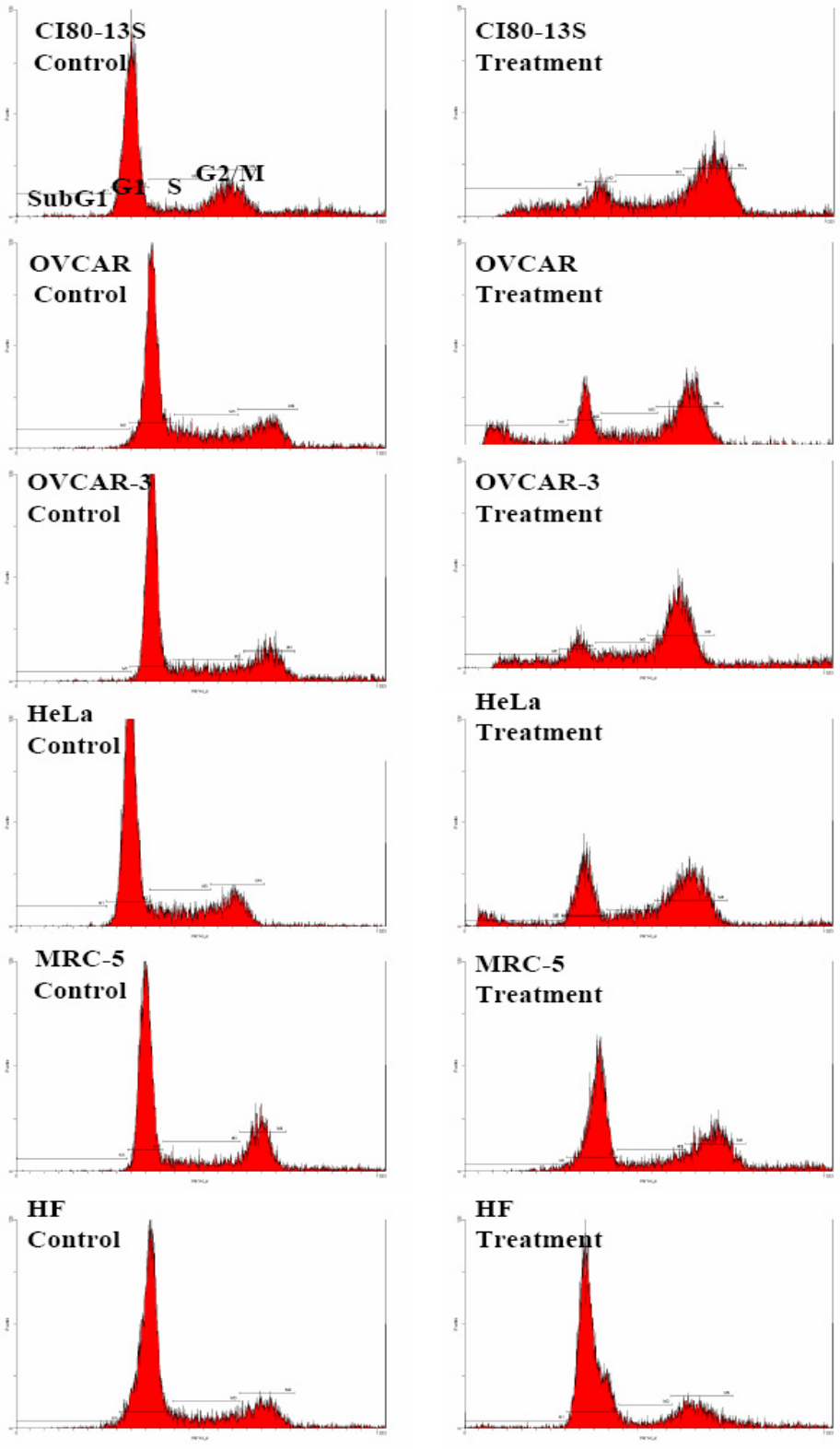

Figure 6. Histograms of the cell cycle distribution of the cell lines treated with the R/PVP/SDS nanoparticles at the concentration of IC_{50} for 72 h.

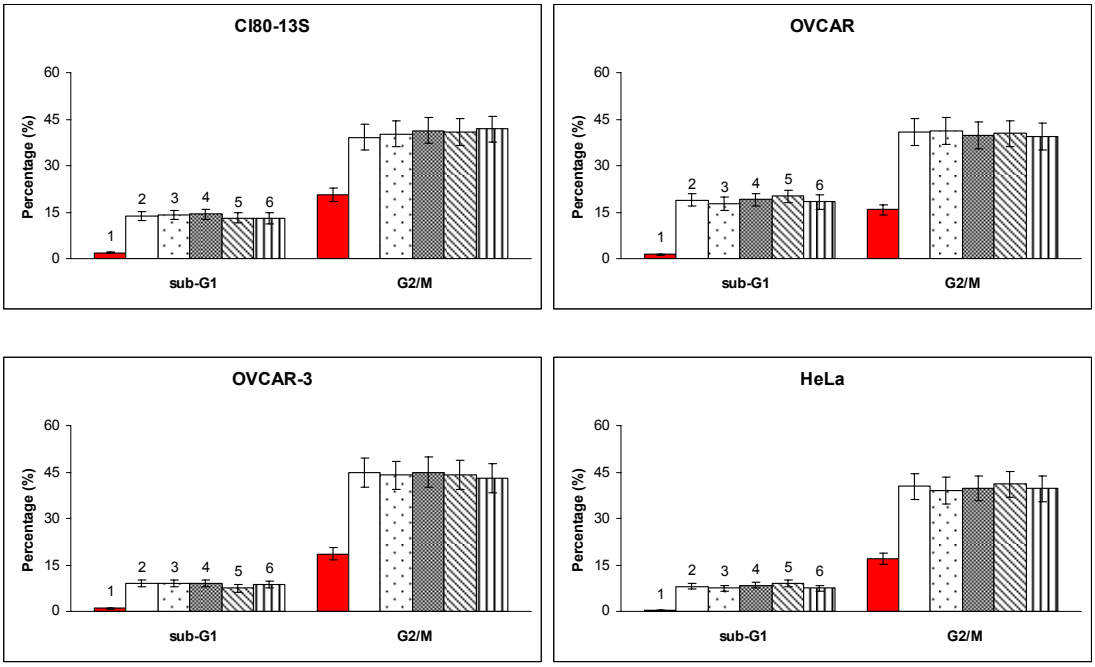

Figure 7. The changes of sub-G1 and G2/M phases after drug treatment. 1. Control; 2. Original realgar treatment; 2. Ground realgar particle treatment; 3. R/PVP treatment; 4. R/SDS treatment; 5; R/PVP/SDS treatment.

The activation of endogenous endonucleases resulting in double strand breaks in nuclear DNA at 180-200 bp-multiple intervals is a common event in apoptotic cascade [Alison MR and Sarraf CE, 1995]. To further confirm the induction of apoptosis by realgar, DNA degradation analysis by agarose gel electrophoresis was performed (Figure 8). After treatment for 72 h, the DNA extracted from all target cancer cell lines displayed the characteristic internucleosomal ladder of DNA fragments, suggesting apoptosis. In contrast, the MRC-5 and HF did not show any DNA fragmentation. Similar findings were previously obtained with nanosized realgar particles prepared by mechanically milling method [Deng Y et al., 2001; Ye HQ et al., 2005]. In their studies, nanosized realgar particles exhibited obvious anti-proliferation effect on selected promyelocytic leukemia cell line (HL-60) and human umbilical vein endothelial cell line (ECV-304) by triggering apoptosis. They attributed the apoptotic effects to the membrane toxicity induced by the realgar

nanoparticles on HL-60 cells.

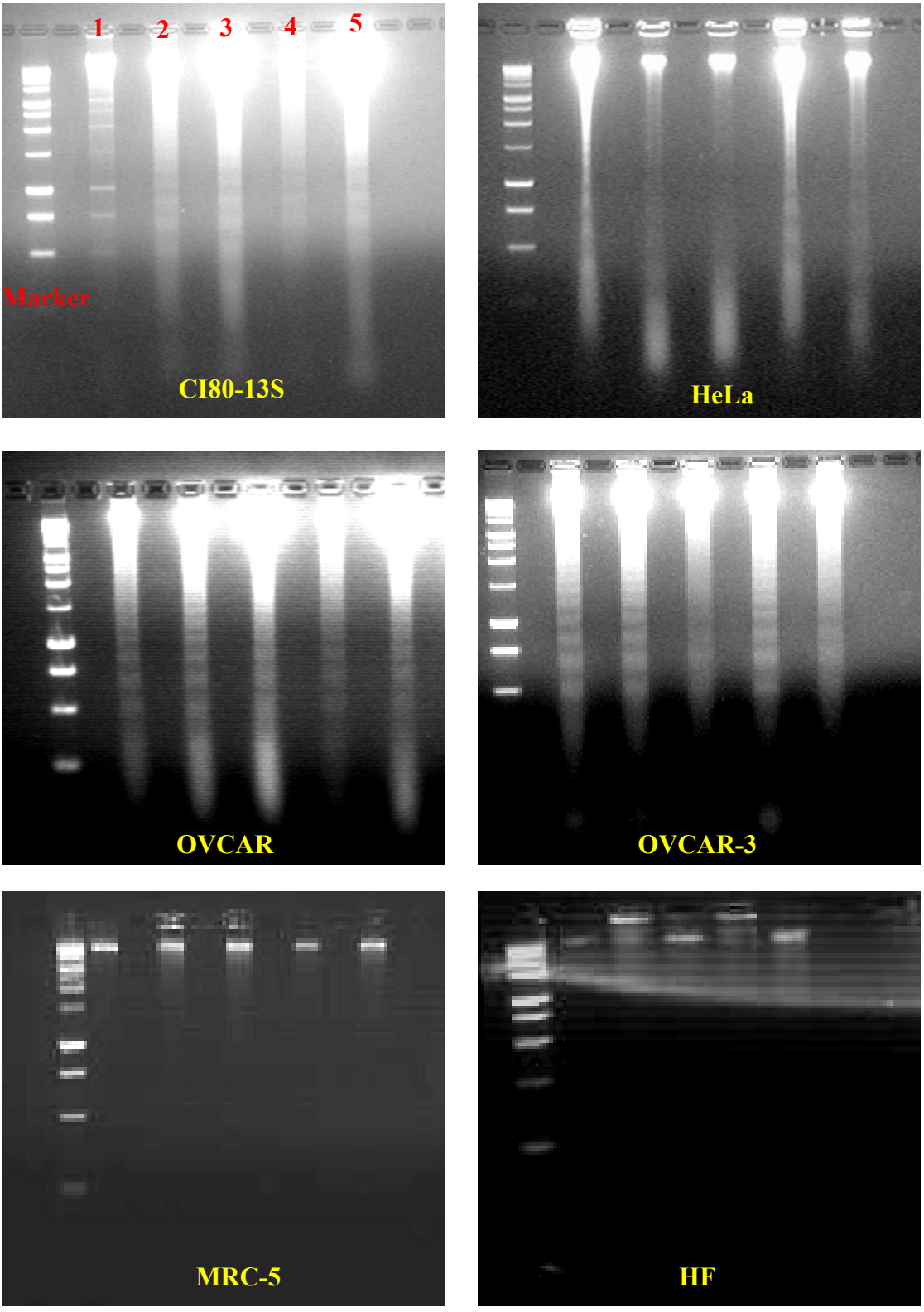

Figure 8. DNA fragmentation in the tested cell lines treated with different realgar nanoparticles for 72 h at respective concentration of around IC_{50}. Lane 1 to 5: original realgar, realgar ground alone, R/PVP, R/SDS, and R/PVP/SDS.

Both arsenite and arsenic trioxide are known to activate the G_2 phase checkpoint and induce mitotic arrest and apoptosis in a variety of cell lines including HeLa [Huang SC and Lee TC, 1998], U937 [Halicka HD et al., 2002; McCabe MJ Jr et al., 2000], and several prostate and ovarian carcinoma cells [Uslu R et al., 2000]. Arsenic trioxide has been suggested to induce apoptosis through three major apoptotic mechanisms as identified by using pharmacologic inhibitors to: 1) mitogen-activated protein kinases, caspase, and reactive oxygen species (ROS). Mitogen-activated protein kinases include c-Jun-N-terminal kinase (JNK), p38, and extracellular signal-regulated kinase (ERK) [Garban HJ and Bonavida B, 1999; Hedlund TE et al., 1998; Frei K et al., 1998; Huang C et al., 1999; Namgung U and Xia Z, 2000]; 2) cascade reaction of caspases, a family of aspartate-specific cysteine proteases [Zhu J et al., 2003; Chen YC et al., 1998]. Functionally, these caspases are divided into two subgroups: initiator (caspase-8, -9, and -10) and effector (caspase-3, -6, and -7) caspases; and 3) ROS, such as hydrogen peroxide, superoxide, hydroxyl radicals, and nitric oxide [Halliwell B and Gutteridge JM, 1990]. To date, the most critical mechanism and the interactions between the mechanisms involved in the arsenic induced apoptosis are still not clear, especially in solid cancers. The actual mechanisms could be compound, dose, duration of exposure and cell-type dependent.

3.3.4 *In vivo* bioavailability investigations

Numerous studies have shown that the particle size is crucial for uptake and transport of fine particles across the GI tract mucosal barrier [Katharine EC et al., 1996]. It is known as microparticle size-dependent exclusion phenomena in the GI mucosal tissue that particles less than 100 nm in size show significantly greater tissue uptake than the larger particles [Desai MP et al., 1996; Liversidge GG and Cundy KC,

1995]. Nanoparticles (NP) could reduce the adverse effects of a drug associated with its use under conventional pharmaceutical dosage forms and improve its bioavailability [Mainardes RM et al., 2005]. Formulating poorly water-soluble drugs as nanosized crystals can have a dramatic effect on the bioavailability [Bittner B and Mountfield RJ, 2002]. It should be noted that size reduction to nanocrystals will not be of value, when bioavailability is limited by the metabolic- and/or permeation-related factors.

It has been suggested that urinary excretion is the major pathway of arsenic elimination from system circulation [Frankenberger WT Jr, 2002c]. Therefore, short-term exposure of humans to arsenic can be evaluated by measuring urinary arsenic as a marker of exposure and the extent of absorption. The biological half-life of ingested inorganic arsenic in humans is about 10 h, and 50-80% of arsenic absorbed is excreted in urine in about 3 days [Goyer RA, 1991]. Absolute bioavailability of arsenic is the fraction or percentage of the absorbed dose to the administered dose [Candy AC et al., 1997]. To date, the bioavailability of arsenic has been determined in a number of animal models, including juvenile swines [Lorenza ML et al., 1996], monkeys [Freeman GB et al., 1995], rabbits [Davis A et al., 1992], dogs [Hollins JG et al., 1979], and rats [Cui X et al., 2004]. Most of these findings indicated that majority of absorbed arsenic could be recovered in urine. Thus, measuring arsenic recovery in urine is a convenient and acceptable method of evaluating bioavailability of arsenic. In this study, the *in vivo* bioavailability was estimated from the urinary recovery of arsenic. The results are shown in Table 4. The urinary arsenic level was normalized with creatinine concentration and was presented as mg of arsenic/mmol of creatinine. Ranging from 58.5 to 69.6% of the administered dose of arsenic was recovered in urine in the first 48 h from the PVP and/or SDS co-ground preparations; whereas the

original realgar powder gave a urinary recovery of only 24.9%. In 96 h, up to 85.4% of the dose was recovered in urine after oral administration of R/PVP/SDS; whereas the original realgar powder gave a urinary recovery of 31.9%. Our results showed that nano-sizing realgar particles enhanced the bioavailability. The co-ground realgar preparations consistently gave higher arsenic urinary recoveries, indicating better bioavailability of these preparations.

Table 4. Cumulated urinary arsenic recoveries from rats treated with the respective realgar suspensions. Values are mean ± SD for *n* = 6 rats.

Drug (50 mg /kg)	Arsenic excretion in urine (mg As_2S_2/mmol creatinine); recovery (%)		
	0-24 h	0-48 h	0-96 h
Original reaglar	49.6 ± 21.2; 16.5 ± 7.0%	68.4 ± 29.2 24.9 ± 10.6%	79.1 ± 33.8 31.9 ± 13.6%
Realgar ground alone	81.9 ± 17.2; 26.1 ± 6.1%	114.2 ± 27.9 38.7 ± 9.5%	125.7 ± 33.9 46.6 ± 12.6%
R/PVP	107.2 ± 28.8; 37.2 ± 10.0%	163.4 ± 43.8 59.8 ± 16.0%	183.6 ± 51.4 72.5 ± 20.3%
R/SDS	90.0 ± 17.2; 38.2 ± 7.6%	137.8 ± 29.9 58.5 ± 12.7%	155.4 ± 43.9 69.9 ± 19.7%
R/PVP/SDS	108.9 ± 15.6; 55.9 ± 6.4%	156.1 ± 27.3 69.6 ± 12.2%	179.5 ± 51.3 85.4 ± 24.4%

3.4 Conclusions

Nanosized realgar particles were successfully produced by cryo-grinding method. With the assistance of PVP and/or SDS, the grinding efficiency was enhanced and the physical properties of the nanoparticles, including the sizes, polydispersity and zeta potentials were improved.

In *in vitro* study, the realgar nanoparticles were used to treat some human gynecological cancer cell lines, and significant anti-proliferation effects comparable to arsenic trioxide were observed. One of the arsenic sensitive ovarian cancer cell

lines CI80-13S was even more sensitive to realgar than to arsenic trioxide. Through cell cycle analysis, apoptosis induced by realgar nanoparticles was concluded from the appearance of the characterized sub-G_1 phase in cell cycle histogram. This result was further confirmed by DNA laddering analysis.

In this study, the extent of absorption was evaluated from the urinary recovery of arsenic. Since the *in vivo* bioavailability studies were carried out under the same experimental conditions, any difference in the urinary recoveries from various preparations would be caused by the difference in the extent of absorption. The compound that is not orally absorbed could be passed out in the feces. Despite this model could estimate the extent of availability of arsenic to the body, it gave no information on the concentrations of the compound in blood and various tissues. To determinate arsenic in blood and various tissues, a more specific and sensitive analytic technique than GFAAS used in this study, such as high-performance liquid chromatography (HPLC) – inductively coupled argon plasma mass spectrometry (ICP MS) could be applied in the future studies [Mandal BK et al., 2004].

After oral administration of the ground realgar preparation, the urinary arsenic excretion was significantly increased compared with that in rats given orally with the original realgar powder. The improvement in bioavailability was attributed to the realgar particles size reduction. Realgar has been suggested to be a less toxic compound in arsenic superfamily. The usage of realgar nanoparticles could overcome the usage limitation associated with its poor water-solubility and allow it being used clinically.

CHAPTER FOUR

Evaluation of the *in vitro* activity and *in vivo* bioavailability of orpiment nanoparticles prepared by cryo-grinding

CHAPTER FOUR

4.1 Introduction

Orpiment (O) (As_2S_3) is a monoclinic crystal with orange-yellow color. The unit cell of orpiment is shown in Figure 1.

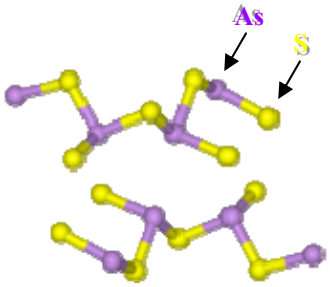

Figure 1. The unit cell of orpiment.

Inspired by the promising results of arsenic trioxide and realgar in the treatment of APL, orpiment was tested in the present study for *in vitro* activity on some solid cancer cell lines and *in vivo* bioavailability after oral administration of its reduced sized particles. The nanosized orpiment particles were prepared by the cryo-grinding approach with the assistance of PVP and SDS. The *in vitro* cytotoxicity of the orpiment nanoparticles was assessed on human ovarian (OVCAR-3) and cervical (HeLa) cancer cell lines with two normal human fibroblast cell lines (MRC-5 and HF) as controls. For the *in vivo* study, a SD rat model was selected to estimate the oral bioavailability of the reduced sized orpiment particles based on the urinary recovery of arsenic.

4.2 Materials and methods

The materials and methods could be referred to Section of 3.2 in Chapter 3.

4.3 Results and discussion

4.3.1 Submicron/nanoparticles formation using cryo-grinding technique

The filtrates of the original orpiment course powder (sieved through 150 μm pore size mesh before weighing), ground orpiment alone particles, and co-ground O/PVP/SDS preparation were obtained, and some physical properties were analyzed as shown in Table 1.

According to the increased amounts of soluble arsenic in the O/PVP/SDS filtrate, the presence of PVP and SDS facilitated the production of the larger amounts of orpiment fine particles of 200 nm or less during cryo-grinding process (Table 1).

Table 1. Physical properties of the orpiment nanoparticles in the filtrates collected after filtering the respective orpiment suspensions through the 0.2 μm filter membranes. Values are mean ± SD (*n* = 3).

Analyte filtrate	Arsenic concentration (ppm)	Particle size (nm)	Polydispersity index (PI)	Zeta potential (mV)
Original orpiment particles	0.51 ± 0.03	296.8 ± 22.5	0.79 ± 0.12	0.30 ± 0.10
Orpiment particles ground without additive	2.78 ± 0.16	310.3 ± 29.6	0.78 ± 0.33	0.40 ± 0.20
O/PVP/SDS ground mixture (1/3/1, w/w/w)	152.8 ± 5.54	222.4 ± 5.70	0.21 ± 0.02	-8.50 ± 2.90

Judging from the particle size ($p < 0.05$, O/PVP/SDS vs original orpiment; $p < 0.01$, O/PVP/SDS vs ground original without additives) and PI values ($p < 0.05$, O/PVP/SDS vs original orpiment; $p < 0.05$, O/PVP/SDS vs groud orpiment without additives), more homogeneous particles were produced after co-grinding with the additives (Table 1).

After pulverizing with PVP and SDS, the negative zeta potential value of the O/PVP/SDS nanoparticle indicated that both PVP and the negatively charged SDS were adsorbed onto the orpiment particle surface similar to the observation for co-

ground R/PVP/SDS preparation as shown in Chapter 3 (Table 1). The orpiment nanosuspension was thus stabilized by steric and ionic barriers formed on the particle surface by adsorption of PVP and SDS. Similar effects of PVP and SDS on stabilization of drugs nanosuspensions were previously reported [Koichi I et al., 2003].

TEM was used to examine the morphology of orpiment nanoparticles from the ternary O/PVP/SDS preparation. Figure 2 displays the TEM image of the O/PVP/SDS filtrate. Once again, the particle sizes measured by the TEM were found to be smaller than those observed by Zetasizer, in consistent with the observation for the R/PVP/SDS filtrate (see Chapter 3).

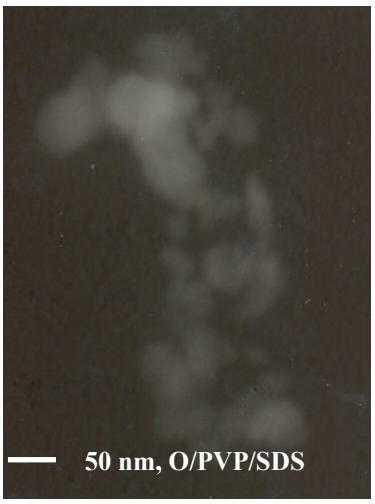

Figure 2. TEM image of the orpiment nanoparticles from the O/PVP/SDS filtrate.

To study the crystallinity of the orpiment after the cryo-grinding treatment, the XRDs of the respective orpiment powders were scanned. Figure 3 shows that the XRD patterns of the ground orpiment alone and ternary O/PVP/SDS preparations almost overlaid each other, indicating there was no change in the crystallinity of the orpiment after cryo-grinding.

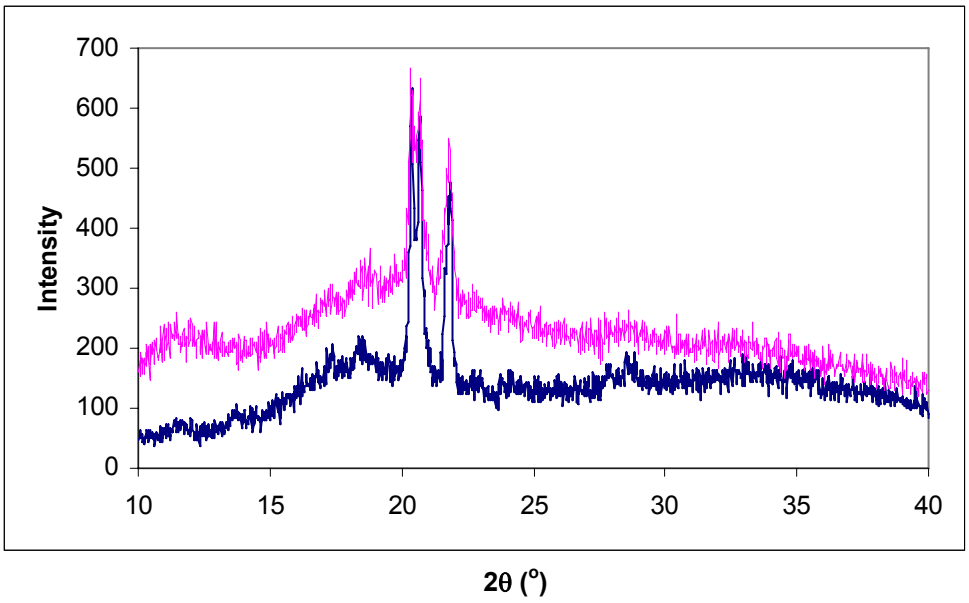

Figure 3. Powder XRD patterns of various orpiment preparations: Orpiment particles ground without additive (top); and O/PVP/SDS (bottom).

In summary, orpiment nanocrystals were formed successfully by cryo-grinding technique. PVP and SDS not only enhanced the grinding efficiency, but also helped to stabilize the corresponding orpiment nanosuspension.

4.3.2 *In vitro* activities of the nanosized orpiment particles on human ovarian and cervical cancer cell lines

For this purpose, both OVCAR-3 and HeLa cancer cell lines were chosen, whilst normal fibroblast MRC-5 and HF cell lines were tested as controls. Exposure of these cancer cell lines to the filtrates of the different orpiment preparations caused inhibited growth in a dose-dependent manner, and the respective IC_{50} values are summarized in Table 2. Comparing the IC_{50} values of O/PVP/SDS nanosuspension (3.11 ± 0.44 μM on OVCAR-3 cells; 3.21 ± 0.46 μM on HeLa cells) with those of R/PVP/SDS nanosuspension (4.06 ± 0.45 μM on OVCAR-3 cells; 3.51 ± 0.48 μM on HeLa cells) and arsenic trioxide (2.37 ± 0.33 μM on OVCAR-3 cells; 1.85 ± 0.54 μM

on HeLa cells), the effect of orpiment nanoparticles on OVCAR-3 cells is not significantly different from those of realgar ($p > 0.05$, orpiment vs realgar) and arsenic trioxide ($p > 0.05$, orpiment vs arsenic trioxide); orpiment nanosuspension had similar cytotoxic effect to realgar on HeLa cells ($p > 0.05$), but it was less cytotoxic than arsenic trioxide ($p < 0.05$). Different types of orpiment formulations did not show significant differences on the anti-proliferation effect on the target cancer cells in terms of the IC_{50} values ($p > 0.05$).

Table 2. IC_{50} (μM as As_2S_3) of different orpiment particles in OVCAR-3 and HeLa cells exposed for 3 days. Results are the mean ± SD from at least three independent experiments.

	IC_{50} (μM as As_2S_3)			
	OVCAR-3	**HeLa**	**MRC-5**	**HF**
Original orpiment particles	3.54 ± 0.50	3.01 ± 0.39	*	*
Orpiment ground alone particles	3.01 ± 0.40	3.12 ± 0.31	*	*
O/PVP/SDS	3.11 ± 0.44	3.21 ± 0.46	*	*

* IC_{50} could not be reached in the test dose range.

4.3.3 Assessment of the apoptotic effects of the orpiment nanosuspension

The distribution of the target cancer cells in the various phases of cell cycle was analyzed after treatment with the filtrate of the O/PVP/SDS preparation for 72 h as shown in Figure 4. DNA content distribution histograms clearly indicated that exposure of all cancer cells to the O/PVP/SDS filtrate resulted in the appearance of cells with a fractional DNA content forming a well-defined sub-G_1 peak, a typical profile of apoptotic cells. The proportions of all cancer cell lines tested in the G_2/M phase were also increased. This result suggested that orpiment induced apoptosis probably through delay in G_2/M phase cell in the cell cycle. However, after the same

treatment, no major variation in the cell phase distribution was noted in the MRC-5 and HF cells (not shown).

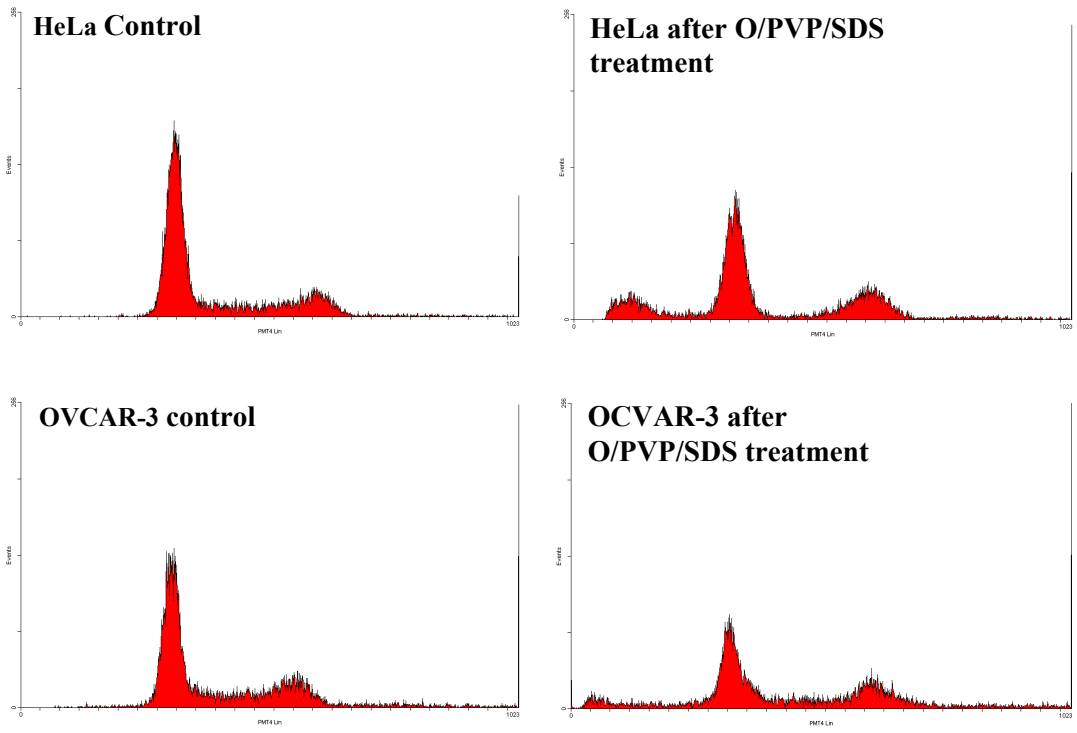

Figure 4. Histograms of the cell cycle distribution of the cell lines treated with the O/PVP/SDS nanoparticles at the concentration of IC_{50} for 72 h.

4.3.4 *In vivo* bioavailability investigations

In this study, the *in vivo* bioavailability was estimated based on the urinary recovery of arsenic. The results are shown in Table 3. After oral administration of the O/PVP/SDS suspension, most of the ingested arsenic (75.8 ± 27.2% of the total dose) was recovered in the urine within 96 h, more than twice than the arsenic recovery of the original orpiment course powder (33.2 ± 14.2% of the total dose). The increased arsenic urinary recovery after oral administration of the reduced sized orpiment indicated the consequent enhanced bioavailability.

Table 3. Cumulated urinary arsenic recoveries from rats orally given original orpiment and O/PVP/SDS. Values are mean ± SD for *n* = 6.

Drug (50 mg /kg)	Arsenic excretion in urine (mg As_2S_2/mmol creatinine; recovery %)		
	0-24 h	0-48 h	0-96 h
Original orpiment particle	44.2 ± 14.6; 14.7 ± 7.0%	62.9 ± 26.4 22.9 ± 10.0%	82.3 ± 33.9 33.2 ± 14.2%
O/PVP/SDS	92.8 ± 18.2; 47.6 ± 9.8%	117.8 ± 25.8 60.9 ± 16.4%	160.4 ± 45.7 75.8 ± 27.2%

4.4 Conclusions

Nanosized orpiment particles were successfully produced by cryo-grinding method with the assistance of PVP and SDS. In the *in vitro* study, the orpiment nanoparticles were used to treat some human gynecological cancer cell lines, and significant anti-proliferation effects comparable to realgar nanoparticles and arsenic trioxide were observed. Through cell cycle analysis, apoptosis induced by the orpiment nanosuspension was concluded from the appearance of the characterized sub-G_1 phase in the cell cycle histogram.

In this study, the extent of absorption was evaluated from the urinary recovery of arsenic. After oral administration of the co-ground orpiment particles, the urinary arsenic excretion was significantly increased, when compared to the rats given orally with the original orpiment course powder. The improvement in bioavailability was attributed to the orpiment particles size reduction. Orpiment has been suggested to be a less toxic compound in arsenic superfamily. The usage of orpiment nanoparticles could overcome the usage limitation associated with its poor water-solubility and allow it being used clinically.

CHAPTER FIVE

Gene expression profiles of HeLa cells after treatment with arsenic compounds

CHAPTER FIVE

5.1 Introduction

Arsenic has sustained a mysterious and quixotic public image for a number of centuries. The action mechanisms of arsenic are very complex. In addition, the effects of arsenicals are dose [Barchowsky A et al., 1999], time [Roboz GJ et al., 2000], and species dependent [Styblo M et al., 2000]. In particular, several arsenic-induced effects exhibit a biphasic characteristic. For example, low doses of arsenic in cell culture increase cell proliferation and enhance endocrine signaling, whereas higher but still noncytotoxic doses suppress these same pathways [Barchowsky A et al., 1999]. Likewise, patterns of altered gene expression, as detected by microarray studies, demonstrated very different patterns at low versus high doses [Andrew AS, 2003].

Cancer is a disease caused, at least in part, by somatic and inherited mutations in genes called oncogenes and tumor suppressor genes. Microarray is a new powerful tool for studying the molecular basis of interactions on a scale that is impossible using conventional analysis [van't Veer LJ et al., 2002]. This technology promises to lead to improvement in developing rational approaches to therapy as well as to improvement in cancer diagnosis and prognosis.

There are two main types of microarray: cDNA and oligonucleotide microarrays. The major advantages of oligonucleotide microarray might minimize any cross-hybridization between spots on the same array despite the representation of closely related members of the same gene families [Kreil DP et al., 2006].

To better characterize the transcriptional response to realgar, orpiment, arsenic trioxide and arsenite, we employed oligonucleotide microarrays to assess gene expression profiles of cultured cervical cancer cell, HeLa. To our knowledge, this is the first report that provides insights into the potential anticancer effects of realgar

and orpiment and arsenic trioxide in HeLa.

5.2 Materials and methods

5.2.1 Cell lines and drug treatments

HeLa cell line was chosen for assessment of gene expression profiles change after drug treatments. Stock solutions of nanosized realgar from the R/PVP/SDS preparation and nanosized orpiment from the O/PVP/SDS preparation each with a concentration of 100.0 ppm were made according to the procedures indicated in Chapter 3 and 4. As_2O_3 stock solution was prepared by directly dissolving As_2O_3 in PBS at a concentration of 100.0 ppm. Arsenite stock solution with a concentration of 100.0 ppm was obtained by dissolving appropriate amount of As_2O_3 in 10 mM NaOH followed by pH adjustment using concentrated HCl to pH 7.0 ± 0.2. All were diluted to the respective working concentrations with culture medium before use, and the actual concentrations were further confirmed by GFAAS. The actual treatment concentrations were 1.5 and 4.5 μM for realgar, 2.0 and 6.0 μM for orpiment, 3.5 μM for As_2O_3, and 3.0 μM for arsenite. The treatment durations were kept for 24 h. Approximate 80% cells were live after high dose realgar and orpiment treatments, almost same as those after arsenic trioxide and arsenite treatments.

5.2.2 Microarray analysis procedure

Oligo GEArray® Human Cancer Microarray chips (OHS-802) were supplied by SuperArray Bioscience Corp. (Frederick, MD, USA), containing 440 genes that include members of several different pathways frequently altered during the progression of cancer. The corresponding gene lists could be found on the company's website, http://www.superarray.com/gene_array_product/HTML/OHS-802.html. This

Oligo GEArray contains a pre-biotinylated oligonucleotide with an artificial sequence in the lower right-hand corner of the membrane. Spots immediately to the left of the corner contain smaller amounts of the same oligonuceotide as shown in Picture below. These spots are detection controls, showing whether the detection steps were performed properly. A specific set of housekeeping genes (darkly circled in Picture, at positions of 1, 2, 14, 15, 16, 17, 164, 181, 198, 363, 378, 393, 408, 433, 449, 465, 466, 467) was used as landmarks to insure that the array image has been placed in the correct orientation for data analysis as well as positive controls for the success of the microarray experiment.

The experiments were conducted in duplicates.

Overview of the oligo GEArray® procedure was schemed as below:

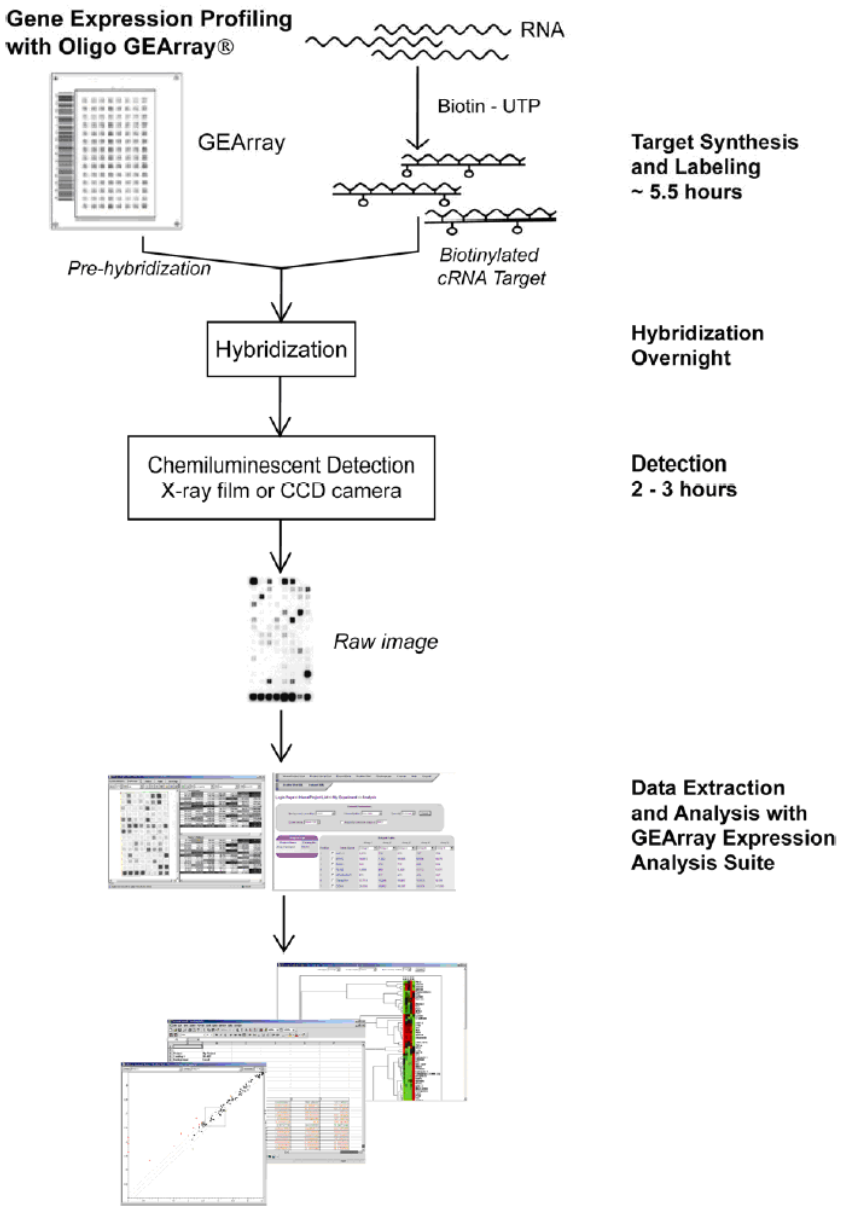

In detail, the entire protocol mainly includes:

1) Total RNA preparation and quality control.

High quality RNA is essential for obtaining good microarray results. Total RNA from drug treated and untreated (as control) cancer cells were isolated and purified using a QIAGEN RNeasy Mini Kit from QIAGEN Inc. (Valencia, CA, USA)

following manufacturer's protocols. Purity and concentration of RNA were assessed by NanoDrop® ND-1000 Spectrophotometer (NanoDrop Technologies Inc., Wilmington, Delaware, USA) through determination of absorbance at 230 (A_{230}), 260 (A_{260}) and 280 nm (A_{280}). All RNA samples must meet all of the following criteria: 1) concentration by A_{260} should be greater than 11 ng/µl total RNA; 2) A_{260}/A_{280} ratio should be greater than 2.0; and 3) A_{260}/A_{230} ratio should be greater than 1.7. In addition, ribosomal RNA band integrity was also required and tested by agarose gel electrophoresis. The appearance of a sharp distinction at the small side of both the 18S and 28S ribosomal RNA (rRNA) bands/peaks was verified to indicate that nondegradation has occurred in the RNA sample as shown in Figure below.

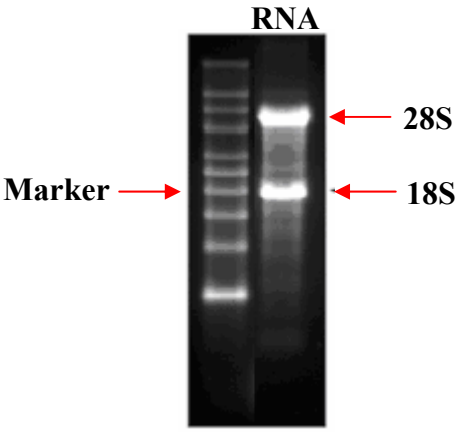

2) cRNA synthesis and labeling.

TrueLabeling-AMP™ 2.0 Kit from SuperArray Bioscience Corp. was used for conversion of experimental RNA to biotinylated UTP labeled cDNA target based on the manufacturer's instructions. A new proprietary *in vitro* transcription (IVT)-based RNA linear amplification technique was involved in such kit. The synthesis was processed in MyCycler™ thermal cycler (BioRad Laboratories, Hercules, CA, USA). Because the reaction mixture still contains protein and a large excess of

unincorporated nucleotide that will interfere with the calculation of the actual yield of the purified cRNA product required for Oligo GEArray hybridization. Therefore, before characterizing the cRNA yield and purity, cRNA purification was proceed by using SuperArray ArrayGrade cRNA Cleanup kit. Thereafter, the quantification and quality of the purified cRNA was assessed by NanoDrop® ND-1000 spectrophotometer.

3) Hybridization.

GEAhyb Hybridization Solution from SuperArray Bioscience Corp. was used for hybridization of the designated microarray chip with the labeled cDNA probes synthesized strictly according to the manufacturer's guidelines. Prehybridization of the chip was required. The hybridization process was conducted in a hybridization oven (ProBlot 12S, Labnet International Inc., Woodbridge, NJ, USA). After hybridization, the chip was washed strictly following the manufacturer's manual.

4) Chemiluminescent detection.

Chemiluminescent Detection Kit from SuperArray Bioscience Corp. was used.

5) Image and data acquisition.

A cooled CCD camera from Alpha Innotech Corp. (FluorChem^{TM} 9900, San Leandro, CA, USA) was used for image acquisition. Their advantages include lower backgrounds and good dynamic ranges. Fifteen minutes exposure time was set for each image taken.

5.2.3 Microarray data analysis

The microarray data were analyzed by means of GEArray Expression Analysis Suite 2.0. The "minimum value" was selected for background correction, and housekeeping genes which have stable expression so called "selected genes" were chosen for normalization to eliminate as much systematic variation as possible. This software provides a statistical means to determine the presence or absence of a gene in a sample. The definition of "absent/present" is based on two reasons. First, there is about 10% covariance in microarray printing; second, it is an empirically-derived value based on a lot of experiments in Superarray. In detail, a spot is considered "absent" if the average intensity of the spot is less than the mean value of the local backgrounds of the lower 75% of all non-bleeding spots. All other spots are considered "present". The fold change of the DNA level was calculated by dividing the mean signal value of drug-treated cells by that of the control cells. The gene probes whose signal values were statistically different from those of the corresponding controls, and the fold change between the drug-treated and the control cells were determined to be above 2 (up-regulated genes) or below 0.5 (down-regulated genes). Finally, gene probes whose Detection Calls gave presence in all the drug-treated or control cells for the above selected up- or down-regulated gene probes, respectively, were selected.

5.3 Results and discussion

The representative images of membrane array from the control and drug-treated HeLa cells are shown in Figure 1 (a-g). The intensity of the signal for all the housekeeping genes was similar in untreated and arsenic-treated cells ($p > 0.05$), indicating intra-assay variation was acceptable.

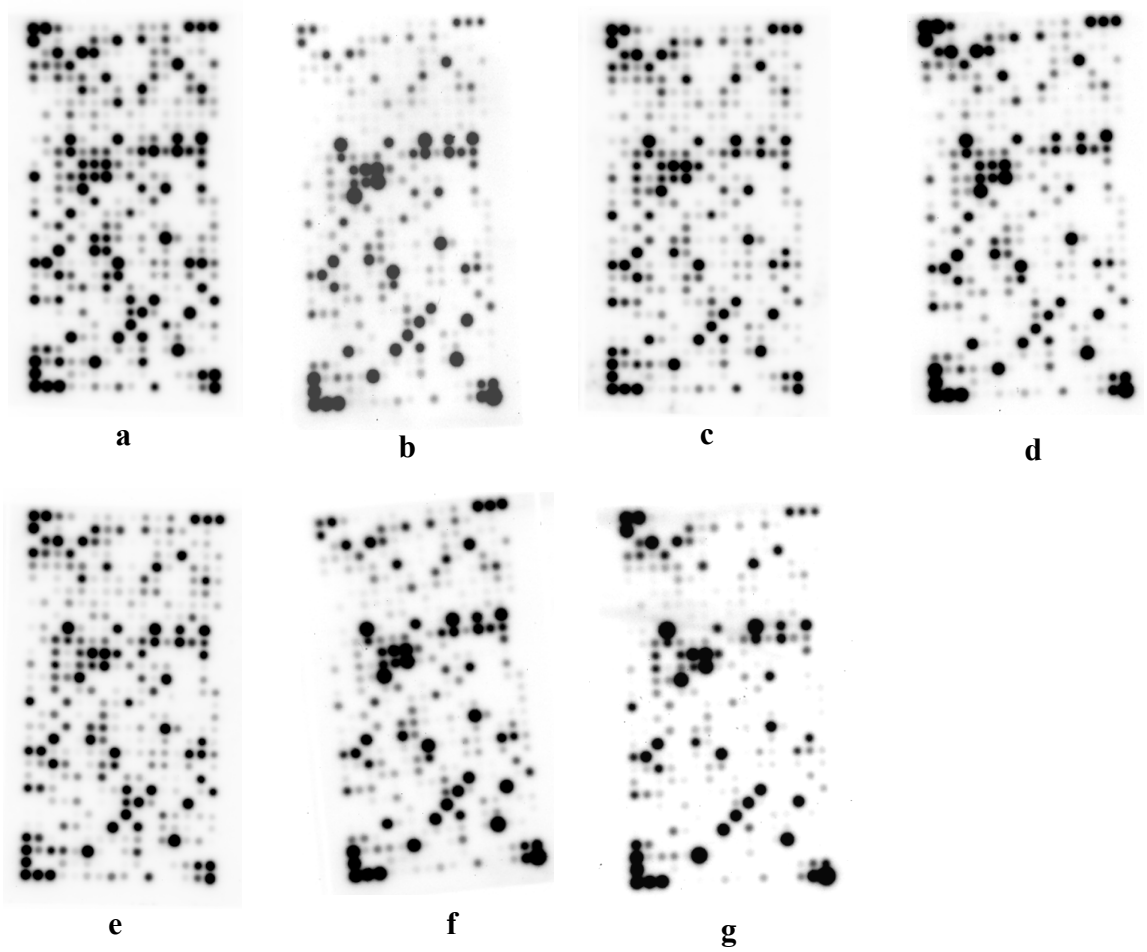

Figure 1. The scanning results of hybridizing signals on gene chips displaying the gene expression alteration: (a) HeLa control; (b) after realgar treatment with low concentration; (c) after realgar treatment with high concentration; (d) after orpiment treatment with low concentration; (e) after orpiment treatment with high concentration; (f) after As_2O_3 treatment; and (g) after arsenite treatment.

Under the criteria of ≥ 2-fold and ≤ 0.05-fold differences, arsenic-treated HeLa cells had up-regulated genes and down-regulated genes, comparing to the control cells, as summarized in Table 1 (a-f). Blank, housekeeping genes, and genes which are absent in either control or sample group are not included in Table 1.

CHAPTER FIVE

==========

Table 1a. The differently expressed genes (fold change ≥ 2.0) after realgar treatment with low concentration.

Chip b			
GeneBank	**Symbol Functional gene grouping; Description**	**Fold change**	**GO term**
NM_006644	HSPH1 **Other cancer-related genes;** Heat shock 105kDa/110kDa protein 1	2.62	ATP binding;Cytoplasm;Heat shock protein activity;
NM_002266	KPNA2 **Other cancer-related genes;** Karyopherin alpha 2 (RAG cohort 1, importin alpha 1)	2.47	Protein binding;Cytoplasm;Nucleoplasm;DNA metabolism;Regulation of DNA recombination;Intracellular protein transport;Protein transporter activity;Nuclear localization sequence binding;G2 phase of mitotic cell cycle;M phase specific microtubule process;NLS-bearing substrate-nucleus import;
NM_020300	MGST1 **Other cancer-related genes;** Microsomal glutathione S-transferase 1	2.25	Transferase activity;Mitochondrion;Membrane;Glutathione transferase activity;Microsome;
NM_003330	TXNRD1 **Other cancer-related genes;** Thioredoxin reductase 1	2.25	Signal transduction;Cytoplasm;Electron transport;Metal ion binding;Disulfide oxidoreductase activity;Oxidoreductase activity, acting on NADH or NADPH, disulfide as acceptor;Thioredoxin-disulfide reductase activity;
NM_001605	AARS **Other cancer-related genes;** Alanyl-tRNA synthetase	0.30	ATP binding;Nucleic acid binding;Cytoplasm;Ligase activity;Soluble fraction;TRNA binding;Protein biosynthesis;Alanine-tRNA ligase activity;Alanyl-tRNA aminoacylation;TRNA processing;
NM_183356	ASNS **Other cancer-related genes;** Asparagine synthetase	0.43	Ligase activity;Soluble fraction;Metabolism;Glutamine metabolism;Asparagine synthase (glutamine-hydrolyzing) activity;Asparagine biosynthesis;
NM_001746	CANX **Other cancer-related genes;** Calnexin	0.50	Integral to plasma membrane;Sugar binding;Heterophilic cell adhesion;Chaperone activity;Protein secretion;Endoplasmic reticulum membrane;Calcium ion storage activity;

NM_004421	DVL1 **Signal transduction;** Signal transduction: Dishevelled, dsh homolog 1 (Drosophila)	0.48	Protein binding;Cytoplasm;Intracellular signaling cascade;Signal transducer activity;Development;Morphogenesis;Heart development;Frizzled signaling pathway;
NM_003641	IFITM1 **Cell cycle, cell growth and differentiation, signal transduction;** Interferon induced transmembrane protein 1 (9-27)	0.42	Receptor signaling protein activity;Plasma membrane;Integral to membrane;Immune response;Negative regulation of cell proliferation;Regulation of cell cycle;Cell surface receptor linked signal transduction;Response to biotic stimulus;
NM_000598	IGFBP3 **Cell growth and differentiation;** Insulin-like growth factor binding protein 3	0.33	Regulation of cell growth;Extracellular;Cell growth and/or maintenance;Metal ion binding;Insulin-like growth factor binding;Protein tyrosine phosphatase activator activity;Negative regulation of signal transduction;Positive regulation of apoptosis;Positive regulation of myoblast differentiation;
NM_002467	MYC **Cell cycle, cell growth and differentiation;** V-myc myelocytomatosis viral oncogene homolog (avian)	0.35	Cell proliferation;Nucleus;Transcription factor activity;Regulation of transcription from Pol II promoter;Cell cycle arrest;Iron ion homeostasis;

Table 1b. The differently expressed genes (fold change ≥ 2.0) after realgar treatment with high concentration.

Chip c			
GeneBank	**Symbol & Description**	**Fold change**	**GO term**
NM_183356	ASNS **Other cancer-related genes;** Asparagine synthetase	2.62	Ligase activity;Soluble fraction;Metabolism;Glutamine metabolism;Asparagine synthase (glutamine-hydrolyzing) activity;Asparagine biosynthesis;
NM_001789	CDC25A **cell cycle, cell growth and differentiation;**	2.37	Hydrolase activity;Cell proliferation;Intracellular;Regulation of cyclin dependent protein kinase activity;Mitosis;Protein amino acid dephosphorylation;Protein tyrosine phosphatase activity;M phase of

	Cell division cycle 25A		mitotic cell cycle;
NM_001806	CEBPG **Other cancer-related genes;** CCAAT/enhancer binding protein (C/EBP) gamma	2.30	DNA binding;Regulation of transcription, DNA-dependent;Nucleus;
NM_001964	EGR1 **Other cancer-related genes;** Early growth response 1	3.36	Regulation of transcription, DNA-dependent;Nucleus;Transcription factor activity;Zinc ion binding;
NM_005438	FOSL1 **Cell growth and differentiation;** FOS-like antigen 1	4.65	Nucleus;Transcription factor activity;Positive regulation of cell proliferation;Response to virus;Regulation of transcription from Pol II promoter;Chemotaxis;Cellular defense response;
NM_004864	GDF15 **Cell growth and differentiation;** Growth differentiation factor 15	2.05	Signal transduction;Extracellular;Growth factor activity;Cell-cell signaling;Cytokine activity;Transforming growth factor beta receptor signaling pathway;
NM_000876	IGF2R **Other cancer-related genes;** Insulin-like growth factor 2 receptor	2.30	Signal transduction;Receptor activity;Lysosome;Integral to plasma membrane;Insulin-like growth factor receptor activity;Transporter activity;Receptor mediated endocytosis;Transport;
NM_002228	JUN **Cell growth and differentiation;** V-jun sarcoma virus 17 oncogene homolog (avian)	2.58	Regulation of transcription, DNA-dependent;Cell growth and/or maintenance;Transcription factor activity;RNA polymerase II transcription factor activity;Nuclear chromosome
NM_003768	PEA15 **Apoptosis;** Phosphoprotein enriched in astrocytes 15	3.55	Protein binding;Regulation of apoptosis;Anti-apoptosis;Transport;Sugar porter activity;Negative regulation of glucose import;Microtubule associated complex;
NM_003842	TNFRSF10B **Apoptosis;** Tumor necrosis factor receptor superfamily, member 10b	2.63	Integral to membrane;Signal transduction;Protein binding;Electron transporter activity;Induction of apoptosis;Regulation of apoptosis;Induction of apoptosis via death domain receptors;Positive regulation of I-kappaB kinase/NF-kappaB cascade;Receptor activity;Iron ion binding;Electron transport;TRAIL binding;Caspase activator activity;Caspase activation;Activation of NF-kappaB-inducing kinase;

NM_001605	AARS **Other cancer-related genes;** Alanyl-tRNA synthetase	0.39	ATP binding;Nucleic acid binding;Cytoplasm;Ligase activity;Soluble fraction;TRNA binding;Protein biosynthesis;Alanine-tRNA ligase activity;Alanyl-tRNA aminoacylation;TRNA processing;
NM_000927	ABCB1 **Other cancer-related genes;** ATP-binding cassette, sub-family B (MDR/TAP), member 1	0.41	ATP binding;Integral to membrane;Membrane fraction;Transporter activity;Transport;ATP-binding cassette (ABC) transporter activity;Nucleotide binding;Response to drug;
NM_001610	ACP2 **Other cancer-related genes;** Acid phosphatase 2, lysosomal	0.37	Hydrolase activity;Integral to membrane;Acid phosphatase activity;Lysosomal membrane;
NM_000666	ACY1 **Cell motility;** Aminoacylase 1	0.26	Hydrolase activity;Proteolysis and peptidolysis;Cytosol;Metallopeptidase activity;Amino acid metabolism;Aminoacylase activity;
NM_003670	BHLHB2 **Other cancer-related genes;** Basic helix-loop-helix domain containing, class B, 2	0.19	Regulation of transcription, DNA-dependent;Nucleus;Transcription factor activity;
NM_000386	BLMH **Other cancer-related genes;** Bleomycin hydrolase	0.42	Hydrolase activity;Aminopeptidase activity;Proteolysis and peptidolysis;Nucleus;Cytoplasm;Bleomycin hydrolase activity;Carboxypeptidase activity;
NM_005186	CAPN1 **Cell growth and differentiation;** Calpain 1, (mu/I) large subunit	0.44	Hydrolase activity;Calcium ion binding;Proteolysis and peptidolysis;Positive regulation of cell proliferation;Intracellular;Calpain activity;
NM_000611	CD59 **Signal transduction;** CD59 antigen p18-20 (antigen identified by monoclonal antibodies 16.3A5, EJ16, EJ30, EL32 and G344)	0.41	Plasma membrane;Immune response;Membrane fraction;Cell surface receptor linked signal transduction;Blood coagulation;
NM_001255	CDC20 **Cell cycle;** CDC20 cell division cycle 20 homlog (S. cerevisiae)	0.38	Regulation of cell cycle;Mitosis;Ubiquitin-dependent protein catabolism;Spindle;

NM_004358	CDC25B **Cell cycle, cell growth and differentiation;** Cell division cycle 25B	0.33	Hydrolase activity;Regulation of cell cycle;Positive regulation of cell proliferation;Intracellular;Mitosis;Protein amino acid dephosphorylation;Protein tyrosine phosphatase activity;M phase of mitotic cell cycle;
NM_003718	CDC2L5 **Cell growth and differentiation;** Cell division cycle 2-like 5 (cholinesterase-related cell division controller)	0.38	ATP binding;Transferase activity;Protein amino acid phosphorylation;Protein serine/threonine kinase activity;Positive regulation of cell proliferation;Development;Regulation of mitosis;
NM_004064	CDKN1B **Cell cycle, cell growth and differentiation;** Cyclin-dependent kinase inhibitor 1B (p27, Kip1)	0.46	Nucleus;Negative regulation of cell proliferation;Cell cycle arrest;Cyclin-dependent protein kinase inhibitor activity;Regulation of cyclin dependent protein kinase activity;Transforming growth factor beta receptor, cytoplasmic mediator activity;
NM_006384	CIB1 **Other cancer-related genes;** Calcium and integrin binding 1 (calmyrin)	0.30	Calcium ion binding;Cell adhesion;Protein binding;Double-strand break repair;
NM_020990	CKMT1B **Other cancer-related genes;** Creatine kinase, mitochondrial 1B	0.17	Mitochondrion;Creatine kinase activity;Transferase activity, transferring phosphorus-containing groups;
NM_001291	CLK2 **Other cancer-related genes;** CDC-like kinase 2	0.10	ATP binding;Transferase activity;Protein amino acid phosphorylation;Nucleus;Protein serine/threonine kinase activity;Protein-tyrosine kinase activity;
NM_001293	CLNS1A **Cell growth and differentiation;** Chloride channel, nucleotide-sensitive, 1A	0.32	Plasma membrane;Nucleus;Transport;Circulation;Visual perception;Chloride transport;Auxiliary transport protein activity;Regulation of cell volume;
NM_004374	COX6C **Other cancer-related genes;** Cytochrome c oxidase subunit VIc	0.38	Energy pathways;Integral to membrane;Oxidoreductase activity;Mitochondrion;Electron transport;Inner membrane;Cytochrome-c oxidase activity;
NM_001319	CSNK1G2	0.30	ATP binding;Transferase activity;Protein amino acid

	Signal transduction; Casein kinase 1, gamma 2		phosphorylation;Signal transduction;Protein serine/threonine kinase activity;Wnt receptor signaling pathway;Protein kinase activity;Casein kinase I activity
NM_001905	CTPS **Other cancer-related genes;** CTP synthase	0.19	Ligase activity;Nucleobase, nucleoside, nucleotide and nucleic acid metabolism;Response to drug;CTP synthase activity;Glutamine metabolism;Pyrimidine nucleotide biosynthesis;
NM_001814	CTSC **Other cancer-related genes;** Cathepsin C	0.12	Hydrolase activity;Immune response;Proteolysis and peptidolysis;Lysosome;Cysteine-type endopeptidase activity;Dipeptidyl-peptidase I activity;
NM_003592	CUL1 **Apoptosis, cell cycle, cell growth and differentiation;** Cullin 1	0.48	Protein binding;Negative regulation of cell proliferation;Cell cycle arrest;G1/S transition of mitotic cell cycle;Cell cycle;Induction of apoptosis by intracellular signals;
NM_001920	DCN **Other cancer-related genes;** Decorin	0.13	Extracellular matrix;Organogenesis;
NM_001360	DHCR7 **Other cancer-related genes;** 7-dehydrocholesterol reductase	0.08	Integral to membrane;Oxidoreductase activity;Endoplasmic reticulum;Cholesterol biosynthesis;7-dehydrocholesterol reductase activity;
NM_004421	DVL1 **Signal transduction;** Dishevelled, dsh homolog 1 (Drosophila)	0.26	Protein binding;Cytoplasm;Intracellular signaling cascade;Signal transducer activity;Development;Morphogenesis;Heart development;Frizzled signaling pathway;
NM_005225	E2F1 **Apoptosis, cell cycle, cell growth and differentiation;** E2F transcription factor 1	0.14	Regulation of transcription, DNA-dependent;Nucleus;Apoptosis;Regulation of cell cycle;Transcription factor activity;Negative regulation of transcription from Pol II promoter;G1 phase of mitotic cell cycle;Transcription corepressor activity;Transcription factor complex;
NM_000122	ERCC3 **Other cancer-related genes;** Excision repair cross-complenenting rodent repair deficiency, complementation group 3 (xeroderma	0.46	ATP binding;Hydrolase activity;Regulation of transcription, DNA-dependent;Nucleus;Protein binding;Induction of apoptosis;Transcription from Pol II promoter;Damaged DNA binding;Perception of sound;DNA unwinding;3' to 5' DNA helicase activity;ATP-dependent DNA helicase activity;Helicase activity;Type

	pigmentosum group B complementing)		III site-specific deoxyribonuclease activity;DNA restriction;Transcription-coupled nucleotide-excision repair;Transcription factor TFIIH complex;
NM_001992	F2R **Apoptosis, cell cycle, cell motility, signal transduction;** Coagulation factor II (thrombin) receptor	0.41	Golgi apparatus;Receptor binding;Signal transduction;Apoptosis;Regulation of cell cycle;G-protein coupled receptor protein signaling pathway;Positive regulation of I-kappaB kinase/NF-kappaB cascade;Integral to plasma membrane;Response to wounding;Cell motility;Blood coagulation;Caspase activation;Rhodopsin-like receptor activity;Thrombin receptor activity;STAT protein nuclear translocation;Morphogenesis;Tyrosine phosphorylation of STAT protein;
NM_000138	FBN1 **Other cancer-related genes;** Fibrillin 1 (Marfan syndrome)	0.44	Calcium ion binding;Development;Extracellular matrix;Extracellular space;Extracellular matrix structural constituent;Skeletal development;Visual perception;
NM_004958	FRAP1 **Cell cycle;** FK506 binding protein 12-rapamycin associated protein 1	0.44	Transferase activity;Regulation of cell cycle;DNA recombination;DNA repair;Inositol or phosphatidylinositol kinase activity;Phosphoinositide 3-kinase complex;
NM_001518	GTF2I **Other cancer-related genes;** General transcription factor II, i	0.28	Signal transduction;Regulation of transcription, DNA-dependent;Nucleus;Protein binding;Transcription factor activity;Transcription initiation from Pol II promoter;General RNA polymerase II transcription factor activity;
NM_004494	HDGF **Cell growth and differentiation;** Hepatoma-derived growth factor (high-mobility group protein 1-like)	0.44	Cell proliferation;Signal transduction;Cytoplasm;Extracellular space;Heparin binding;Growth factor activity;
NM_002127	HLA-G **Other cancer-related genes;** HLA-G histocompatibility antigen, class I, G	0.40	Integral to membrane;Cellular defense response;Antigen processing, endogenous antigen via MHC class I;MHC class I receptor activity;Antigen presentation, endogenous antigen;Detection of pest, pathogen or parasite;
NM_003641	IFITM1	0.27	Receptor signaling protein activity;Plasma membrane;Integral to

	Cell cycle, cell growth and differentiation, signal transduction; Interferon induced transmembrane protein 1 (9-27)		membrane;Immune response;Negative regulation of cell proliferation;Regulation of cell cycle;Cell surface receptor linked signal transduction;Response to biotic stimulus;
NM_000598	IGFBP3 **Cell growth and differentiation;** Insulin-like growth factor binding protein 3	0.20	Regulation of cell growth;Extracellular;Cell growth and/or maintenance;Metal ion binding;Insulin-like growth factor binding;Protein tyrosine phosphatase activator activity;Negative regulation of signal transduction;Positive regulation of apoptosis;Positive regulation of myoblast differentiation;
NM_004517	ILK **Cell motility, signal transduction;** Integrin-linked kinase	0.31	ATP binding;Transferase activity;Protein amino acid phosphorylation;Protein serine/threonine kinase activity;Cell-matrix adhesion;Integrin-mediated signaling pathway;
NM_001571	IRF3 **Other cancer-related genes;** Interferon regulatory factor 3	0.37	Regulation of transcription, DNA-dependent;Nucleus;Transcription factor activity;RNA polymerase II transcription factor activity;Transcription from Pol II promoter;Transcription cofactor activity;
NM_002204	ITGA3 **Cell motility, signal transduction;** Integrin, alpha 3 (antigen CD49C, alpha 3 subunit of VLA-3 receptor)	0.47	Integral to membrane;Protein binding;Receptor activity;Cell-matrix adhesion;Integrin-mediated signaling pathway;Integrin complex
NM_002291	LAMB1 **Other cancer related genes;** Laminin, beta 1	0.33	Structural molecule activity;Cell adhesion;Protein binding;Basement membrane;
NM_002337	LRPAP1 **Cell growth and differentiation;** Low density lipoprotein receptor-related protein associated protein 1	0.32	Plasma membrane;Integral to membrane;Calcium ion binding;Cell proliferation;Heparin binding;Endoplasmic reticulum;Protein folding;Chaperone activity;Asialoglycoprotein receptor activity;Lipoprotein binding;Vesicle-mediated transport;
NM_030662	MAP2K2 **Other cancer-related genes;** Mitogen-activated protein kinase kinase 2	0.37	ATP binding;Transferase activity;Protein amino acid phosphorylation;Extracellular;Protein serine/threonine kinase activity;Protein-tyrosine kinase activity;
NM_004635	MAPKAPK3 **Other cancer-related genes;**	0.45	ATP binding;Transferase activity;Protein amino acid phosphorylation;Signal transduction;Nucleus;Protein serine/threonine

	Mitogen-activated protein kinase-activated protein kinase 3		kinase activity;Response to stress;MAP kinase kinase activity;
NM_004526	MCM2 **Cell cycle;** MCM2 minichromosome maintenance deficient 2, mitotin (S. cerevisiae)	0.38	ATP binding;DNA binding;Regulation of transcription, DNA-dependent;Nucleus;DNA replication;Chromatin;Cell cycle;DNA-dependent ATPase activity;DNA replication initiation;
NM_002467	MYC **Cell cycle, cell growth and differentiation;** V-myc myelocytomatosis viral oncogene homolog (avian)	0.09	Cell proliferation;Nucleus;Transcription factor activity;Regulation of transcription from Pol II promoter;Cell cycle arrest;Iron ion homeostasis;
NM_006097	MYL9 **Other cancer-related genes;** Myosin, light polypeptide 9, regulatory	0.32	Calcium ion binding;Muscle development;Structural constituent of muscle;Regulation of muscle contraction;Muscle myosin;Myosin;
NM_000268	NF2 **Cell cycle, cell growth and differentiation;** Neurofibromin 2 (bilateral acoustic neuroma)	0.33	Plasma membrane;Structural molecule activity;Negative regulation of cell cycle;Negative regulation of cell proliferation;Cytoskeleton;Cytoskeletal protein binding;Perception of sound;
NM_000269	NME1 **Cell cycle, cell growth and differentiation;** Non-metastatic cells 1, protein (NM23A) expressed in	0.32	ATP binding;Transferase activity;Nucleus;Negative regulation of cell cycle;Negative regulation of cell proliferation;Kinase activity;Nucleoside-diphosphate kinase activity;CTP biosynthesis;GTP biosynthesis;UTP biosynthesis;Nucleoside triphosphate biosynthesis;
NM_002512	NME2 **Cell cycle, cell growth and differentiation;** Non-metastatic cells 2, protein (NM23B) expressed in	0.39	ATP binding;Transferase activity;Regulation of transcription, DNA-dependent;Nucleus;Negative regulation of cell cycle;Negative regulation of cell proliferation;Transcription factor activity;Kinase activity;Nucleoside-diphosphate kinase activity;CTP biosynthesis;GTP biosynthesis;UTP biosynthesis;Nucleoside triphosphate biosynthesis;
NM_002513	NME3 **Apoptosis;**	0.08	ATP binding;Transferase activity;Induction of apoptosis;Apoptosis;Kinase activity;Nucleoside-diphosphate kinase

	Non-metastatic cells 3, protein expressed in		activity;CTP biosynthesis;GTP biosynthesis;UTP biosynthesis;
NM_005654	NR2F1 **Other cancer-related genes;** Nuclear receptor subfamily 2, group F, member 1	0.08	Signal transduction;Regulation of transcription, DNA-dependent;Nucleus;Transcription factor activity;Transcription coactivator activity;Steroid hormone receptor activity;Ligand-regulated transcription factor activity;
NM_005234	NR2F6 **Other cancer-related genes;** Nuclear receptor subfamily 2, group F, member 6	0.16	Signal transduction;Regulation of transcription, DNA-dependent;Nucleus;Transcription factor activity;Steroid hormone receptor activity;Thyroid hormone receptor activity;
NM_182649	PCNA **Cell cycle, cell growth and differentiation;** Proliferating cell nuclear antigen	0.20	Cell proliferation;DNA binding;Nucleus;Regulation of cell cycle;DNA replication;DNA polymerase processivity factor activity;DNA repair;Regulation of DNA replication;Delta-DNA polymerase cofactor complex;
NM_002596	PCTK3 **Other cancer-related genes;** PCTAIRE protein kinase 3	0.16	ATP binding;Transferase activity;Protein amino acid phosphorylation;Signal transduction;Protein serine/threonine kinase activity;Cellular_component unknown;Signal transducer activity;
NM_002649	PIK3CG **Signal transduction;** Phosphoinositide-3-kinase, catalytic, gamma polypeptide	0.43	Transferase activity;G-protein coupled receptor protein signaling pathway;Inositol or phosphatidylinositol kinase activity;Phosphatidylinositol 3-kinase activity;Phosphatidylinositol-4,5-bisphosphate 3-kinase activity;Phosphoinositide 3-kinase complex;
NM_006238	PPARD **Other cancer-related genes;** Peroxisome proliferative activated receptor, delta	0.32	Energy pathways;Nucleus;Transcription factor activity;Regulation of transcription from Pol II promoter;Steroid hormone receptor activity;Lipid metabolism;
NM_002734	PRKAR1A **Signal transduction;** Protein kinase, cAMP-dependent, regulatory, type I, alpha (tissue specific extinguisher 1)	0.31	Protein amino acid phosphorylation;Intracellular signaling cascade;Regulation of transcription from Pol II promoter;CAMP-dependent protein kinase regulator activity;CAMP-dependent protein kinase complex;3',5'-cAMP binding;
NM_000962	PTGS1	0.39	Oxidoreductase activity;Peroxidase activity;Membrane;Physiological

	Other cancer-related genes; Prostaglandin-endoperoxide synthase 1 (prostaglandin G/H synthase and cyclooxygenase)		process;Lipid metabolism;Oxidoreductase activity, acting on single donors with incorporation of molecular oxygen, incorporation of two atoms of oxygen;Prostaglandin-endoperoxide synthase activity;Prostaglandin biosynthesis;
NM_002823	PTMA **Cell cycle;** Prothymosin, alpha (gene sequence 28)	0.22	Nucleus;Regulation of cell cycle;Development;Transcription;
NM_002880	RAF1 **Apoptosis, cell growth and differentiation, signal transduction;** V-raf-1 murine leukemia viral oncogene homolog 1	0.34	Receptor signaling protein activity;ATP binding;Transferase activity;Protein amino acid phosphorylation;Cell proliferation;Protein binding;Diacylglycerol binding;Protein serine/threonine kinase activity;Intracellular signaling cascade;Apoptosis;Mitochondrial outer membrane;
NM_002884	RAP1A **Cell cycle, signal transduction;** RAP1A, member of RAS oncogene family	0.20	GTP binding;GTPase activity;Small GTPase mediated signal transduction;Signal transduction;Negative regulation of cell cycle;
NM_000964	RARA **Cell growth and differentiation;** Retinoic acid receptor, alpha	0.33	Signal transduction;Regulation of transcription, DNA-dependent;Nucleus;Cell growth and/or maintenance;Transcription factor activity;Transcription coactivator activity;Steroid hormone receptor activity;Retinoic acid receptor activity;
NM_000321	RB1 **Cell cycle;** Retinoblastoma 1 (including osteosarcoma)	0.35	Regulation of transcription, DNA-dependent;Nucleus;Negative regulation of cell cycle;Transcription factor activity;Negative regulation of transcription from Pol II promoter;Chromatin;Cell cycle checkpoint;
NM_005610	RBBP4 **Cell cycle, cell growth and differentiation;** Retinoblastoma binding protein 4	0.16	Regulation of transcription, DNA-dependent;Nucleus;Negative regulation of cell proliferation;DNA replication;Cell cycle;DNA repair;
NM_007273	PHB2 **Cell growth and differentiation;** Prohibitin 2	0.31	Cellular_component unknown;Receptor activity;Negative regulation of transcription;Estrogen receptor binding;
NM_021975	RELA	0.38	Regulation of transcription, DNA-dependent;Nucleus;Protein

	Apoptosis; V-rel reticuloendotheliosis viral oncogene homolog A, nuclear factor of kappa light polypeptide gene enhancer in B-cells 3, p65 (avian)		binding;Anti-apoptosis;Transcription factor activity;Signal transducer activity;Positive regulation of I-kappaB kinase/NF-kappaB cascade;Transcription from Pol II promoter;Transcription factor complex;Response to toxin;
NM_002951	RPN2 **Other cancer-related genes;** Ribophorin II	0.39	Transferase activity;Integral to membrane;Protein modification;Dolichyl-diphosphooligosaccharide-protein glycotransferase activity;N-linked glycosylation via asparagine;Oligosaccharyl transferase complex;
NM_003944	SELENBP1 **Other cancer-related genes;** Selenium binding protein 1	0.44	Selenium binding;
NM_015129	SEPT6 **Cell cycle;** Septin 6	0.50	GTP binding;Protein binding;Cellular_component unknown;Cell cycle;Cytokinesis;
NM_006142	SFN **Cell cycle, cell growth and differentiation;** Stratifin	0.38	Cell proliferation;Signal transduction;Cytoplasm;Regulation of cell cycle;Extracellular space;Protein domain specific binding;Protein kinase C inhibitor activity;Negative regulation of protein kinase activity;
NM_006427	SIVA **Apoptosis;** CD27-binding (Siva) protein	0.33	Receptor signaling protein activity;Cytoplasm;Apoptosis;Induction of apoptosis by extracellular signals;Positive regulation of apoptosis;CD27 receptor binding;Defense response;
NM_005415	SLC20A1 **Other cancer-related genes;** Solute carrier family 20 (phosphate transporter), member 1	0.49	Phosphate metabolism;Signal transducer activity;Positive regulation of I-kappaB kinase/NF-kappaB cascade;Receptor activity;Membrane;Integral to plasma membrane;Transport;Phosphate transport;Inorganic phosphate transporter activity;Sodium:phosphate symporter activity;
NM_014390	SND1 **Other cancer-related genes;** Staphylococcal nuclease domain containing 1	0.35	
NM_003092	SNRPB2	0.48	Nucleus;RNA binding;Ribonucleoprotein complex;Pre-mRNA

	Other cancer-related genes; Small nuclear ribonucleoprotein polypeptide B”		splicing factor activity;RNA splicing;Nuclear mRNA splicing, via spliceosome;SnRNP U2;
NM_003150	STAT3 **Cell motility, signal transduction;** Signal transducer and activator of transcription 3 (acute-phase response factor)	0.29	Regulation of transcription, DNA-dependent;Nucleus;Cytoplasm;Intracellular signaling cascade;Transcription factor activity;Negative regulation of transcription from Pol II promoter;Signal transducer activity;Acute-phase response;Cell motility;JAK-STAT cascade;Neurogenesis;Hematopoietin/interferon-class (D200-domain) cytokine receptor signal transducer activity;
NM_004749	TBRG4 **Cell cycle, cell growth and differentiation;** Transforming growth factor beta regulator 4	0.27	Positive regulation of cell proliferation;Cell cycle arrest;G1 phase of mitotic cell cycle;
NM_000545	TCF1 **Other cancer-related genes;** Transcription factor 1, hepatic; LF-B1, hepatic nuclear factor (HNF1), albumin proximal factor	0.49	Nucleus;Transcription factor activity;Regulation of transcription from Pol II promoter;RNA polymerase II transcription factor activity;Transcriptional activator activity;Positive regulation of transcription;
NM_007111	TFDP1 **Cell cycle, cell growth and differentiation;** Transcription factor Dp-1	0.04	Nucleus;Regulation of cell cycle;Transcription factor activity;Regulation of transcription from Pol II promoter;Transcription factor complex;Transcription coactivator activity;
NM_003243	TGFBR3 **Other cancer-related genes;** Transforming growth factor, beta receptor III (betaglycan, 300kDa)	0.26	Integral to membrane;Signal transduction;Development;Receptor activity;Glycosaminoglycan binding;Transforming growth factor beta receptor signaling pathway;
NM_003258	TK1 **Other cancer-related genes;** Thymidine kinase 1, soluble	0.39	ATP binding;Transferase activity;Cytoplasm;Kinase activity;DNA metabolism;Thymidine kinase activity;
NM_001066	TNFRSF1B	0.34	Integral to membrane;Apoptosis;Receptor activity;Tumor necrosis

	Apoptosis; Tumor necrosis factor receptor superfamily, member 1B		factor receptor activity;Cytokine and chemokine mediated signaling pathway;
NM_000546	TP53 **Apoptosis, cell cycle;** Tumor protein p53 (Li-Fraumeni syndrome)	0.20	ATP binding;Cell proliferation;Regulation of transcription, DNA-dependent;Protein binding;Negative regulation of cell cycle;Apoptosis;Mitochondrion;Transcription factor activity;Zinc ion binding;DNA damage response, signal transduction resulting in induction of apoptosis;Cell cycle arrest;Nucleolus;Cell cycle checkpoint;DNA strand annealing activity;Copper ion binding;Nuclease activity;DNA recombination;Base-excision repair;Caspase activation via cytochrome c;Cell aging;Cell differentiation;Induction of apoptosis by hormones;Negative regulation of cell growth;Nucleotide-excision repair;Regulation of mitochondrial membrane permeability;Protein tetramerization activity;Negative regulation of helicase activity;
NM_004881	TP53I3 **Other cancer-related genes;** Tumor protein p53 inducible protein 3	0.38	Cellular_component unknown;Zinc ion binding;Alcohol dehydrogenase activity, zinc-dependent;Induction of apoptosis by oxidative stress;
NM_003470	USP7 **Other cancer-related genes;** Ubiquitin specific peptidase 7 (herpes virus-associated)	0.47	Hydrolase activity;Nucleus;Ubiquitin-dependent protein catabolism;Cysteine-type endopeptidase activity;Ubiquitin thiolesterase activity;
NM_003374	VDAC1 **Apoptosis;** Voltage-dependent anion channel 1	0.35	Integral to membrane;Mitochondrial outer membrane;Mitochondrion;Apoptotic program;Apoptogenic cytochrome c release channel activity;Voltage-dependent anion channel porin activity;Voltage-dependent ion-selective channel activity;Anion transport;
NM_006347	PPIH **Other cancer-related genes;** Peptidylprolyl isomerase H (cyclophilin H)	0.39	Protein complex assembly;Protein folding;Isomerase activity;Chaperone activity;Peptidyl-prolyl cis-trans isomerase activity;Nuclear mRNA splicing, via spliceosome;Spliceosome complex;Cyclosporin A binding;SnRNP protein-nucleus import;
NM_021141	XRCC5	0.27	Nucleus;DNA recombination;ATP-dependent DNA helicase

	Other cancer-related genes; X-ray repair complementing defective repair in Chinese hamster cells 5 (double-strand-break rejoining; Ku autoantigen, 80kDa)		activity;Helicase activity;Double-stranded DNA binding;Double-strand break repair via nonhomologous end-joining;Regulation of DNA repair;DNA-dependent protein kinase complex;
NM_003404	YWHAB **Other cancer-related genes;** Tyrosine 3-monooxygenase/tryptophan 5-monooxygenase activation protein, beta polypeptide	0.46	Protein domain specific binding;

Table 1c. The differently expressed genes (fold change ≥ 2.0) after orpiment treatment with low concentration.

Chip d			
GeneBank	**Symbol & Description**	**Fold change**	**GO term**
NM_001605	AARS **Other cancer-related genes;** Alanyl-tRNA synthetase	2.25	ATP binding;Nucleic acid binding;Cytoplasm;Ligase activity;Soluble fraction;TRNA binding;Protein biosynthesis;Alanine-tRNA ligase activity;Alanyl-tRNA aminoacylation;TRNA processing;
NM_000927	ABCB1 **Other cancer-related genes;** ATP-binding cassette, sub-family B (MDR/TAP), member 1	2.74	ATP binding;Integral to membrane;Membrane fraction;Transporter activity;Transport;ATP-binding cassette (ABC) transporter activity;Nucleotide binding;Response to drug;
NM_005759	ABI2 **Other cancer-related genes;** AbI interactor 2	2.28	DNA binding;Cytoplasm;SH3/SH2 adaptor protein activity;Kinase activity;SH3 domain binding;Biological_process unknown;
NM_001154	ANXA5 **Other cancer-related genes;** Annexin A5	2.51	Calcium ion binding;Blood coagulation;Calcium-dependent phospholipid binding;Phospholipase inhibitor activity;Negative regulation of coagulation;
NM_004034	ANXA7 **Other cancer-related genes;**	2.26	Calcium ion binding;Calcium-dependent phospholipid binding;Negative regulation of coagulation;Voltage-gated calcium channel activity;

	Annexin A7		
NM_183356	ASNS **Other cancer-related genes;** Asparagine synthetase	2.01	Ligase activity;Soluble fraction;Metabolism;Glutamine metabolism;Asparagine synthase (glutamine-hydrolyzing) activity;Asparagine biosynthesis;
NM_001746	CANX **Other cancer-related genes;** Calnexin	2.44	Integral to plasma membrane;Sugar binding;Heterophilic cell adhesion;Chaperone activity;Protein secretion;Endoplasmic reticulum membrane;Calcium ion storage activity
NM_006367	CAP1 **Other cancer-related genes;** CAP, adenylate cyclase-associated protein 1 (yeast)	3.79	Signal transduction;Membrane;Establishment and/or maintenance of cell polarity;Adenylate cyclase activation;
NM_005186	CAPN1 **Cell growth and differentiation;** Calpain 1, (mu/I) large subunit	3.03	Hydrolase activity;Calcium ion binding;Proteolysis and peptidolysis;Positive regulation of cell proliferation;Intracellular;Calpain activity;
NM_001749	CAPNS1 **Cell growth and differentiation;** Calpain, small subunit 1	2.39	Calcium ion binding;Positive regulation of cell proliferation;Calpain activity;
NM_001255	CDC20 **Cell cycle;** CDC20 cell division cycle 20 homolog (S, cerevisiae)	3.81	Regulation of cell cycle;Mitosis;Ubiquitin-dependent protein catabolism;Spindle;
NM_004358	CDC25B **Cell cycle, cell growth and differentiation;** Cell division cycle 25B	2.40	Hydrolase activity;Regulation of cell cycle;Positive regulation of cell proliferation;Intracellular;Mitosis;Protein amino acid dephosphorylation;Protein tyrosine phosphatase activity;M phase of mitotic cell cycle;
NM_001790	CDC25C **Cell growth and differentiation;** Cell division cycle 25C	2.03	Hydrolase activity;Cell proliferation;Nucleus;Regulation of cyclin dependent protein kinase activity;Protein amino acid dephosphorylation;Protein tyrosine phosphatase activity;Regulation of mitosis;Traversing start control point of mitotic cell cycle;
NM_006384	CIB1 **Other cancer-related genes;** Calcium and integrin binding 1	2.37	Calcium ion binding;Cell adhesion;Protein binding;Double-strand break repair;

	(calmyrin)		
NM_001319	CSNK1G2 **Signal transduction;** Casein kinase 1, gamma 2	2.36	ATP binding;Transferase activity;Protein amino acid phosphorylation;Signal transduction;Protein serine/threonine kinase activity;Wnt receptor signaling pathway;Protein kinase activity;Casein kinase I activity
NM_004941	DHX8 **Other cancer-related genes;** DEAH (Asp-Glu-Ala-His) box polypeptide 8	2.09	ATP binding;RNA binding;Pre-mRNA splicing factor activity;RNA splicing;ATP-dependent RNA helicase activity;Hydrogen-transporting ATP synthase activity, rotational mechanism;Hydrogen-transporting ATPase activity, rotational mechanism;ATP synthesis coupled proton transport;Nuclear mRNA splicing, via spliceosome;Proton-transporting two-sector ATPase complex;Spliceosome complex;
NM_005225	E2F1 **Apoptosis, and cell cycle, and cell growth and differentiation;** E2F transcription factor 1	2.17	Regulation of transcription, DNA-dependent;Nucleus;Apoptosis;Regulation of cell cycle;Transcription factor activity;Negative regulation of transcription from Pol II promoter;G1 phase of mitotic cell cycle;Transcription corepressor activity;Transcription factor complex;
NM_002026	FN1 **Cell motility;** Fibromectin 1	0.34	Cell adhesion;Extracellular;Oxidoreductase activity;Collagen binding;Extracellular matrix structural constituent;Heparin binding;Acute-phase response;Cell migration;Metabolism;Response to wounding
NM_002127	HLA-G **HLA-G histocompatibility antigen, class I, G**	0.38	Integral to membrane;Cellular defense response;Antigen processing, endogenous antigen via MHC class I;MHC class I receptor activity;Antigen presentation, endogenous antigen;Detection of pest, pathogen or parasite
NM_006389	HYOU1 **Other cancer-related genes;** Hypoxia up-regulated 1	0.44	ATP binding;Response to stress;Endoplasmic reticulum;Chaperone activity;
NM_003897	IER3 **Apoptosis, and cell growth and differentiation;** Immediate early response 3	0.39	Integral to membrane;Cell growth and/or maintenance;Molecular_function unknown;Apoptosis;Anti-apoptosis;Morphogenesis;
NM_002467	MYC **Cell cycle, and cell growth and differentiation;** V-myc myelocytomatosis viral	0.47	Cell proliferation;Nucleus;Transcription factor activity;Regulation of transcription from Pol II promoter;Cell cycle arrest;Iron ion homeostasis;

	oncogene homolog (avian)		
NM_024408	NOTCH2 **Apoptosis, cell cycle, cell growth and differentiation, signal transduction;** Notch homolog 2 (Drosophila)	0.36	Calcium ion binding;Regulation of transcription, DNA-dependent;Nucleus;Protein binding;Induction of apoptosis;Anti-apoptosis;Negative regulation of cell proliferation;Cell cycle arrest;Receptor activity;Integral to plasma membrane;Cell differentiation;Neurogenesis;Protein heterodimerization activity;Cell fate determination;Cell growth;Regulation of development;Hemopoiesis;Cell surface;Morphogenesis of an epithelial sheet;Ligand-regulated transcription factor activity;Notch signaling pathway;Determination of left/right symmetry;Positive regulation of RAS protein signal transduction;Stem cell maintenance;
NM_003768	PEA15 **Apoptosis;** Phosphoprotein enriched in astrocytes 15	0.31	Protein binding;Regulation of apoptosis;Anti-apoptosis;Transport;Sugar porter activity;Negative regulation of glucose import;Microtubule associated complex;
NM_015869	PPARG **Other cancer-related genes;** Peroxisome proliferative activated receptor, gamma	0.33	Energy pathways;Response to nutrients;Signal transduction;Nucleus;Transcription factor activity;Regulation of transcription from Pol II promoter;Steroid hormone receptor activity;Lipid metabolism;White adipocyte differentiation;
NM_004162	RAB5A **Signal transduction;** RAB5A, member RAS oncogene family	0.41	GTP binding;GTPase activity;Protein transport;Small GTPase mediated signal transduction;Protein binding;Endocytosis;Early endosome;
NM_002880	RAF1 **Apoptosis, cell growth and differentiation, signal transduction;** V-raf-1 murine leukemia viral oncogene homolog 1	0.47	Receptor signaling protein activity;ATP binding;Transferase activity;Protein amino acid phosphorylation;Cell proliferation;Protein binding;Diacylglycerol binding;Protein serine/threonine kinase activity;Intracellular signaling cascade;Apoptosis;Mitochondrial outer membrane
NM_007273	PHB2 **Cell growth and differentiation;** Prohibitin 2	0.50	Cellular_component unknown;Receptor activity;Negative regulation of transcription;Estrogen receptor binding;
NM_002951	RPN2	0.48	Transferase activity;Integral to membrane;Protein modification;Dolichyl-

	Other cancer-related genes; Ribophorin II		diphosphooligosaccharide-protein glycotransferase activity;N-linked glycosylation via asparagine;Oligosaccharyl transferase complex;

Table 1d. The differently expressed genes (fold change ≥ 2.0) after orpiment treatment with high concentration.

Chip e			
GeneBank	**Symbol & Description**	**Fold change**	**GO term**
NM_183356	ASNS **Other caner-related genes;** Asparagine synthetase	2.68	Ligase activity;Soluble fraction;Metabolism;Glutamine metabolism;Asparagine synthase (glutamine-hydrolyzing) activity;Asparagine biosynthesis;
NM_004936	CDKN2B **Cell cycle, and cell growth and differentiation;** Cyclin-dependent kinase inhibitor 2B (p15, inhibits CDK4)	2.28	Nucleus;Cytoplasm;Negative regulation of cell cycle;Negative regulation of cell proliferation;Cell cycle arrest;Cell cycle;Cyclin-dependent protein kinase inhibitor activity;Regulation of cyclin dependent protein kinase activity;
NM_001806	CEBPG **Other cancer-related genes;** CCAAT/enhancer binding protein (C/EBP), gamma	3.27	DNA binding;Regulation of transcription, DNA-dependent;Nucleus;
NM_000755	Crat **Other cancer-related genes;** Carmitine acetyltransferase	2.42	Transferase activity;Mitochondrion;Endoplasmic reticulum;Transport;Acyltransferase activity;Carnitine O-acetyltransferase activity;Acyl-CoA metabolism;Energy derivation by oxidation of organic compounds;Peroxisome
NM_001554	CYR61 **Cell growth and differentiation;** Cysteine-rich, angiogenic inducer, 61	2.90	Cell adhesion;Cell proliferation;Regulation of cell growth;Extracellular;Heparin binding;Chemotaxis;Insulin-like growth factor binding;Morphogenesis
NM_001999	FBN2 **Other cancer-related genes;** Fibrillin 2 (congenital contractual arachnodactyly)	2.36	Calcium ion binding;Extracellular matrix;Extracellular matrix structural constituent;Morphogenesis;

NM_005438	FOSL1 **Cell growth and differentiation;** FOS-like antigen 1	6.36	Nucleus;Transcription factor activity;Positive regulation of cell proliferation;Response to virus;Regulation of transcription from Pol II promoter;Chemotaxis;Cellular defense response;
NM_006389	HYOU1 **Other cancer-related genes;** Hypoxia up-regulated 1	2.65	ATP binding;Response to stress;Endoplasmic reticulum;Chaperone activity;
NM_000876	IGF2R **Other cancer-related genes;** Insulin-like growth factor 2 receptor	2.38	Signal transduction;Receptor activity;Lysosome;Integral to plasma membrane;Insulin-like growth factor receptor activity;Transporter activity;Receptor mediated endocytosis;Transport;
NM_005564	LCN2 **Other cancer-related genes;** Lipocalin 2 (oncogene 24p3)	2.18	Cytoplasm;Soluble fraction;Transporter activity;Transport;Binding;
NM_003768	NFKB2 **Cell growth and differentiation;** Phosphoprotein enriched in astrocytes 15	2.69	Protein binding;Regulation of apoptosis;Anti-apoptosis;Transport;Sugar porter activity;Negative regulation of glucose import;Microtubule associated complex;
NM_003768	PEA15 **Apoptosis;** Phosphoprotein enriched in astrocytes 15	3.55	Protein binding;Regulation of apoptosis;Anti-apoptosis;Transport;Sugar porter activity;Negative regulation of glucose import;Microtubule associated complex;
NM_183079	PRNP **Other cancer-related genes;** Prion protein (p27-30) (Creutzfeld-Jakob disease, Gerstmann-Strausler-Scheinker syndrome, fatal familial insomnia)	2.09	Metabolism;
NM_006509	RELB **Other cancer-related genes;** V-rel reticuloendotheliosis viral oncogene homolog B, nuclear factor of kappa light polypeptide gene enhancer in B-cells 3 (avian)	2.94	Regulation of transcription, DNA-dependent;Nucleus;Protein binding;Transcription factor activity;Transcription corepressor activity;
NM_006513	SARS **Other cancer-related genes;**	2.46	ATP binding;Cytoplasm;Ligase activity;Soluble fraction;Protein biosynthesis;RNA binding;TRNA processing;Serine-tRNA ligase

	Seryl-tRNA synthetase		activity;Seryl-tRNA aminoacylation;
NM_003028	SHB **Signal transduction;** Src homology 2 domain containing adaptor protein B	2.08	Intracellular signaling cascade;SH3/SH2 adaptor protein activity;
NM_003842	TNFRSF10B **Apoptosis;** Tumor necrosis factor receptor superfamily, member 10b	2.56	Integral to membrane;Signal transduction;Protein binding;Electron transporter activity;Induction of apoptosis;Regulation of apoptosis;Induction of apoptosis via death domain receptors;Positive regulation of I-kappaB kinase/NF-kappaB cascade;Receptor activity;Iron ion binding;Electron transport;TRAIL binding;Caspase activator activity;Caspase activation;Activation of NF-kappaB-inducing kinase;
NM_014294	TRAM1 **Other cancer related genes;** Translocation associated membrane protein 1	4.21	Integral to membrane;Receptor activity;Endoplasmic reticulum;Cotranslational membrane targeting;Protein targeting;
NM_003330	TXNRD1 **Other cancer-related genes;** Thioredoxin reductase 1	2.39	Signal transduction;Cytoplasm;Electron transport;Metal ion binding;Disulfide oxidoreductase activity;Oxidoreductase activity, acting on NADH or NADPH, disulfide as acceptor;Thioredoxin-disulfide reductase activity;
NM_000666	ACY1 **Cell motility;** Aminoacylase 1	0.34	Hydrolase activity;Proteolysis and peptidolysis;Cytosol;Metallopeptidase activity;Amino acid metabolism;Aminoacylase activity;
NM_003670	BHLHB2 **Other cancer-related genes;** Basic helix-loop-helix domain containing, class B, 2	0.30	Regulation of transcription, DNA-dependent;Nucleus;Transcription factor activity;
NM_000386	BLMH **Other cancer-related genes;** Bleomycin hydrolase	0.34	Hydrolase activity;Aminopeptidase activity;Proteolysis and peptidolysis;Nucleus;Cytoplasm;Bleomycin hydrolase activity;Carboxypeptidase activity;
NM_001238	CCNE1	0.32	Nucleus;Regulation of cell cycle;G1/S transition of mitotic cell cycle;

	Cell cycle; Cyclin E1		
NM_000611	CD59 **Signal transduction;** CD59 antigen p18-20 (antigen identified by monoclonal antibodies 16.3A5, EJ16, EJ30, EL32 and G344)	0.35	Plasma membrane;Immune response;Membrane fraction;Cell surface receptor linked signal transduction;Blood coagulation;
NM_004358	CDC25B **Cell cycle, and cell growth and differentiation;** Cell division cycle 25B	0.32	Hydrolase activity;Regulation of cell cycle;Positive regulation of cell proliferation;Intracellular;Mitosis;Protein amino acid dephosphorylation;Protein tyrosine phosphatase activity;M phase of mitotic cell cycle;
NM_020990	CKMT1B **Other cancer-related genes;** Creatine kinase, mitochondrial 1B	0.34	Mitochondrion;Creatine kinase activity;Transferase activity, transferring phosphorus-containing groups;
NM_001291	CLK2 **Other cancer-related genes;** CDC-like kinase 2	0.34	ATP binding;Transferase activity;Protein amino acid phosphorylation;Nucleus;Protein serine/threonine kinase activity;Protein-tyrosine kinase activity;
NM_001905	CTPS **Other cancer-related genes;** CTP synthase	0.39	Ligase activity;Nucleobase, nucleoside, nucleotide and nucleic acid metabolism;Response to drug;CTP synthase activity;Glutamine metabolism;Pyrimidine nucleotide biosynthesis;
NM_001814	CTSC **Other cancer-related genes;** Cathepsin C	0.15	Hydrolase activity;Immune response;Proteolysis and peptidolysis;Lysosome;Cysteine-type endopeptidase activity;Dipeptidyl-peptidase I activity;
NM_001920	DCN **Other cancer-related genes;** Decorin	0.08	Extracellular matrix;Organogenesis;
NM_001360	DHCR7 **Other cancer-related genes;** 7-dehydrocholesterol reductase	0.14	Integral to membrane;Oxidoreductase activity;Endoplasmic reticulum;Cholesterol biosynthesis;7-dehydrocholesterol reductase activity;
NM_001992	F2R **Apoptosis, cell cycle, cell motility, signal transduction;**	0.44	Golgi apparatus;Receptor binding;Signal transduction;Apoptosis;Regulation of cell cycle;G-protein coupled receptor protein signaling pathway;Positive regulation of I-kappaB

	Coagulation factor II (thrombin) receptor		kinase/NF-kappaB cascade;Integral to plasma membrane;Response to wounding;Cell motility;Blood coagulation;Caspase activation;Rhodopsin-like receptor activity;Thrombin receptor activity;STAT protein nuclear translocation;Morphogenesis;Tyrosine phosphorylation of STAT protein;
NM_021078	GCN5L2 **Other cancer-related genes;** GCN5 general control of amino-acid synthesis 5-like 2 (yeast)	0.44	Transferase activity;Nucleus;Regulation of transcription from Pol II promoter;Transcription coactivator activity;Chromatin remodeling;N-acetyltransferase activity;Histone acetyltransferase activity;Protein amino acid acetylation;
NM_001518	GTF2I **Other cancer-related genes;** General transcription factor II, i	0.41	Signal transduction;Regulation of transcription, DNA-dependent;Nucleus;Protein binding;Transcription factor activity;Transcription initiation from Pol II promoter;General RNA polymerase II transcription factor activity
NM_002127	HLA-G **HLA-G histocompatibility antigen, class I, G**	0.49	Integral to membrane;Cellular defense response;Antigen processing, endogenous antigen via MHC class I;MHC class I receptor activity;Antigen presentation, endogenous antigen;Detection of pest, pathogen or parasite;
NM_003641	IFITM1 **Cell cycle, cell growth and differentiation, signal transduction;** Interferon induced transmembrane protein 1 (9-27)	0.30	Receptor signaling protein activity;Plasma membrane;Integral to membrane;Immune response;Negative regulation of cell proliferation;Regulation of cell cycle;Cell surface receptor linked signal transduction;Response to biotic stimulus;
NM_000598	IGFBP3 **Cell growth and differentiation;** Insulin-like growth factor binding protein 3	0.19	Regulation of cell growth;Extracellular;Cell growth and/or maintenance;Metal ion binding;Insulin-like growth factor binding;Protein tyrosine phosphatase activator activity;Negative regulation of signal transduction;Positive regulation of apoptosis;Positive regulation of myoblast differentiation;
NM_002291	LAMB1 **Other cancer-related genes;** Laminin, beta 1	0.28	Structural molecule activity;Cell adhesion;Protein binding;Basement membrane;
NM_002337	LRPAP1 **Cell growth and differentiation;** Low	0.47	Plasma membrane;Integral to membrane;Calcium ion binding;Cell proliferation;Heparin binding;Endoplasmic reticulum;Protein

	density lipoprotein receptor-related protein associated protein 1		folding;Chaperone activity;Asialoglycoprotein receptor activity;Lipoprotein binding;Vesicle-mediated transport;
NM_002467	MYC **Cell cycle, cell growth and differentiation;** V-myc myelocytomatosis viral oncogene homolog (avian)	0.20	Cell proliferation;Nucleus;Transcription factor activity;Regulation of transcription from Pol II promoter;Cell cycle arrest;Iron ion homeostasis;
NM_002513	NME3 **Apoptosis;** Non-metastatic cells 3, protein expressed in	0.27	ATP binding;Transferase activity;Induction of apoptosis;Apoptosis;Kinase activity;Nucleoside-diphosphate kinase activity;CTP biosynthesis;GTP biosynthesis;UTP biosynthesis;
NM_005654	NR2F1 **Other cancer-related genes;** Nuclear receptor subfamily 2, group F, member 1	0.21	Signal transduction;Regulation of transcription, DNA-dependent;Nucleus;Transcription factor activity;Transcription coactivator activity;Steroid hormone receptor activity;Ligand-regulated transcription factor activity;
NM_005234	NR2F6 **Other cancer-related genes;** Nuclear receptor subfamily 2, group F, member 6	0.36	Signal transduction;Regulation of transcription, DNA-dependent;Nucleus;Transcription factor activity;Steroid hormone receptor activity;Thyroid hormone receptor activity;
NM_182649	PCNA **Cell cycle, cell growth and differentiation;** Proliferating cell nuclear antigen	0.50	Cell proliferation;DNA binding;Nucleus;Regulation of cell cycle;DNA replication;DNA polymerase processivity factor activity;DNA repair;Regulation of DNA replication;Delta-DNA polymerase cofactor complex;
NM_002596	PCTK3 **Other cancer-related genes;** PCTAIRE protein kinase 3	0.25	ATP binding;Transferase activity;Protein amino acid phosphorylation;Signal transduction;Protein serine/threonine kinase activity;Cellular_component unknown;Signal transducer activity;
NM_002884	RAP1A **Cell cycle, signal transduction;** RAP1A, member of RAS oncogene family	0.31	GTP binding;GTPase activity;Small GTPase mediated signal transduction;Signal transduction;Negative regulation of cell cycle
NM_003944	SELENBP1 **Other cancer-related genes;**	0.22	Selenium binding;

	Selenium binding protein 1		
NM_015129	SEPT6 **Cell cycle;** Septin 6	0.48	GTP binding;Protein binding;Cellular_component unknown;Cell cycle;Cytokinesis;
NM_007111	TFDP1 **Cell cycle, cell growth and differentiation;** Transcription factor Dp-1	0.25	Nucleus;Regulation of cell cycle;Transcription factor activity;Regulation of transcription from Pol II promoter;Transcription factor complex;Transcription coactivator activity;
NM_003243	TGFBR3 **Other cancer-related genes;** Transforming growth factor, beta receptor III (betaglycan, 300kDa)	0.26	Integral to membrane;Signal transduction;Development;Receptor activity;Glycosaminoglycan binding;Transforming growth factor beta receptor signaling pathway;
NM_001066	TNFRSF1B **Apoptosis;** Tumor necrosis factor receptor superfamily, member 1B	0.16	Integral to membrane;Apoptosis;Receptor activity;Tumor necrosis factor receptor activity;Cytokine and chemokine mediated signaling pathway;
NM_000546	TP53 **Apoptosis, cell cycle;** Tumor protein p53 (Li-Fraumeni syndrome)	0.38	ATP binding;Cell proliferation;Regulation of transcription, DNA-dependent;Protein binding;Negative regulation of cell cycle;Apoptosis;Mitochondrion;Transcription factor activity;Zinc ion binding;DNA damage response, signal transduction resulting in induction of apoptosis;Cell cycle arrest;Nucleolus;Cell cycle checkpoint;DNA strand annealing activity;Copper ion binding;Nuclease activity;DNA recombination;Base-excision repair;Caspase activation via cytochrome c;Cell aging;Cell differentiation;Induction of apoptosis by hormones;Negative regulation of cell growth;Nucleotide-excision repair;Regulation of mitochondrial membrane permeability;Protein tetramerization activity;Negative regulation of helicase activity;
NM_006297	XRCC1 **Other cancer-related genes;** X-ray repair complementing defective repair in Chinese hamster cells 1	0.45	Nucleus;Damaged DNA binding;Single strand break repair

Table 1e. The differently expressed genes (fold change ≥ 2.0) after As_2O_3 treatment.

Chip f			
GeneBank	**Symbol & Description**	**Fold change**	**GO term**
NM_000611	CD59 **Signal transduction;** CD59 antigen p18-20 (antigen identified by monoclonal antibodies 16.3A5, EJ16, EJ30, EL32 and G344)	2.00	Plasma membrane;Immune response;Membrane fraction;Cell surface receptor linked signal transduction;Blood coagulation;
NM_005438	FOSL1 **Cell growth and differentiation;** FOS-like antigen 1	2.31	Nucleus;Transcription factor activity;Positive regulation of cell proliferation;Response to virus;Regulation of transcription from Pol II promoter;Chemotaxis;Cellular defense response;
NM_006644	HSPH1 **Other cancer-related genes;** Heat shock 105kDa/110kDa protein 1	2.20	ATP binding;Cytoplasm;Heat shock protein activity;
NM_183356	ASNS **Other cancer-related genes;** Asparagine synthetase	0.44	Ligase activity;Soluble fraction;Metabolism;Glutamine metabolism;Asparagine synthase (glutamine-hydrolyzing) activity;Asparagine biosynthesis;
NM_001746	CANX **Other cancer-related genes;** Calnexin	0.49	Integral to plasma membrane;Sugar binding;Heterophilic cell adhesion;Chaperone activity;Protein secretion;Endoplasmic reticulum membrane;Calcium ion storage activity;
NM_004421	DVL1 **Signal transduction;** Dishevelled, dsh homolog 1 (Drosophila)	0.38	Protein binding;Cytoplasm;Intracellular signaling cascade;Signal transducer activity;Development;Morphogenesis;Heart development;Frizzled signaling pathway;
NM_002026	FN1 **Cell motility;** Fibromectin 1	0.44	Cell adhesion;Extracellular;Oxidoreductase activity;Collagen binding;Extracellular matrix structural constituent;Heparin binding;Acute-phase response;Cell migration;Metabolism;Response to wounding;
NM_003641	IFITM1 **Cell cycle, cell growth and differentiation, signal transduction;**	0.29	Receptor signaling protein activity;Plasma membrane;Integral to membrane;Immune response;Negative regulation of cell proliferation;Regulation of cell cycle;Cell surface receptor linked

	Interferon induced transmembrane protein 1 (9-27)		signal transduction;Response to biotic stimulus;
NM_000598	IGFBP3 **Cell growth and differentiation;** Insulin-like growth factor binding protein 3	0.25	Regulation of cell growth;Extracellular;Cell growth and/or maintenance;Metal ion binding;Insulin-like growth factor binding;Protein tyrosine phosphatase activator activity;Negative regulation of signal transduction;Positive regulation of apoptosis;Positive regulation of myoblast differentiation;
NM_002291	LAMB1 **Other cancer-related genes;** Laminin, beta 1	0.42	Structural molecule activity;Cell adhesion;Protein binding;Basement membrane;
NM_002294	LAMP2 **Other cancer-related genes;** Lysosomal-associated membrane protein 2	0.46	Integral to plasma membrane;Lysosomal membrane;
NM_004990	MARS **Other cancer-related genes;** Methionine-tRNA synthetase	0.41	ATP binding;Cytoplasm;Ligase activity;Soluble fraction;Methionine-tRNA ligase activity;TRNA binding;Methionyl-tRNA aminoacylation;Protein biosynthesis;
NM_002467	MYC **Cell cycle, cell growth and differentiation;** V-myc myelocytomatosis viral oncogene homolog (avian)	0.25	Cell proliferation;Nucleus;Transcription factor activity;Regulation of transcription from Pol II promoter;Cell cycle arrest;Iron ion homeostasis;
NM_003998	NFKB1 **Apoptosis;** Nuclear factor of kappa light polypeptide gene enhancer in B-cells 1 (p105)	0.36	Signal transduction;Regulation of transcription, DNA-dependent;Nucleus;Protein binding;Cytoplasm;Apoptosis;Anti-apoptosis;Transcription factor activity;Inflammatory response;Transcription from Pol II promoter;Response to pathogenic bacteria;Antibacterial humoral response (sensu Vertebrata);
NM_002513	NME3 **Apoptosis;** Non-metastatic cells 3, protein expressed in	0.37	ATP binding;Transferase activity;Induction of apoptosis;Apoptosis;Kinase activity;Nucleoside-diphosphate kinase activity;CTP biosynthesis;GTP biosynthesis;UTP biosynthesis;
NM_015869	PPARG	0.42	Energy pathways;Response to nutrients;Signal

	Other cancer-related genes; Peroxisome proliferative activated receptor, gamma		transduction;Nucleus;Transcription factor activity;Regulation of transcription from Pol II promoter;Steroid hormone receptor activity;Lipid metabolism;White adipocyte differentiation;
NM_003321	TUFM **Other cancer-related genes;** Tu translation elongation factor, mitochondrial	0.45	GTP binding;Mitochondrion;Protein biosynthesis;Translational elongation;Translation elongation factor activity;

Table 1f. The differently expressed genes (fold change ≥ 2.0) after arsenite treatment.

Chip g			
GeneBank	**Symbol & Description**	**Fold change**	**GO term**
NM_000927	ABCB1 **Other cancer-related genes;** ATP-binding cassette, sub-family B (MDR/TAP), member 1	3.23	ATP binding;Integral to membrane;Membrane fraction;Transporter activity;Transport;ATP-binding cassette (ABC) transporter activity;Nucleotide binding;Response to drug;
NM_005759	ABI2 **Other cancer-related genes;** AbI interactor 2	3.17	DNA binding;Cytoplasm;SH3/SH2 adaptor protein activity;Kinase activity;SH3 domain binding;Biological_process unknown;
NM_005157	ABL1 **Apoptosis, cell cycle, cell growth and differentiation, signal transduction;** V-abl Abelson murine leukemia viral oncogene homolog 1	2.43	ATP binding;Transferase activity;Protein amino acid phosphorylation;DNA binding;Regulation of transcription, DNA-dependent;Nucleus;Cell growth and/or maintenance;Intracellular signaling cascade;Protein-tyrosine kinase activity;Regulation of cell cycle;DNA damage response, signal transduction resulting in induction of apoptosis;S-phase-specific transcription in mitotic cell cycle;Mismatch repair;
NM_005158	ABL2 **Signal transduction;** V-abl Abelson murine leukemia viral oncogene homolog 2 (arg, Abelson-	3.40	ATP binding;Transferase activity;Protein amino acid phosphorylation;Cytoplasm;Cell growth and/or maintenance;Intracellular signaling cascade;Protein-tyrosine kinase activity;

	related gene)		
NM_001154	ANXA5 **Other cancer-related genes;** Annexin A5	2.38	Calcium ion binding;Blood coagulation;Calcium-dependent phospholipid binding;Phospholipase inhibitor activity;Negative regulation of coagulation;
NM_001746	CANX **Other cancer-related genes;** Calnexin	2.32	Integral to plasma membrane;Sugar binding;Heterophilic cell adhesion;Chaperone activity;Protein secretion;Endoplasmic reticulum membrane;Calcium ion storage activity;
NM_006367	CAP1 **Other cancer-related genes;** CAP, adenylate cyclase-associated protein 1 (yeast)	5.58	Signal transduction;Membrane;Establishment and/or maintenance of cell polarity;Adenylate cyclase activation;
NM_001749	CAPNS1 **Cell growth and differentiation;** Calpain, small subunit 1	2.04	Calcium ion binding;Positive regulation of cell proliferation;Calpain activity;
NM_001789	CDC25A **Cell cycle, cell growth and differentiation;** Cell division cycle 25A	9.41	Hydrolase activity;Cell proliferation;Intracellular;Regulation of cyclin dependent protein kinase activity;Mitosis;Protein amino acid dephosphorylation;Protein tyrosine phosphatase activity;M phase of mitotic cell cycle;
NM_001790	CDC25C **Cell growth and differentiation;** Cell division cycle 25C	3.42	Hydrolase activity;Cell proliferation;Nucleus;Regulation of cyclin dependent protein kinase activity;Protein amino acid dephosphorylation;Protein tyrosine phosphatase activity;Regulation of mitosis;Traversing start control point of mitotic cell cycle;
NM_000389	CDKN1A **Apoptosis, cell cycle, cell growth and differentiation;** Cyclin-dependent kinase inhibitor 1A (p21, Cip1)	2.10	Nucleus;Negative regulation of cell proliferation;Cell cycle arrest;Protein kinase activity;Cyclin-dependent protein kinase inhibitor activity;Regulation of cyclin dependent protein kinase activity;Kinase activity;Induction of apoptosis by intracellular signals;
NM_001903	CTNNA1 **Other cancer-related genes;** Catenin (cadherin-associated protein), alpha 1, 102kDa	2.75	Structural molecule activity;Cell adhesion;Protein binding;Cytoskeleton;
NM_004941	DHX8	2.56	ATP binding;RNA binding;Pre-mRNA splicing factor activity;RNA

	Other cancer-related genes; DEAH (Asp-Glu-Ala-His) box polypeptide 8		splicing;ATP-dependent RNA helicase activity;Hydrogen-transporting ATP synthase activity, rotational mechanism;Hydrogen-transporting ATPase activity, rotational mechanism;ATP synthesis coupled proton transport;Nuclear mRNA splicing, via spliceosome;Proton-transporting two-sector ATPase complex;Spliceosome complex;
NM_004423	DVL3 **Signal transduction;** Dishevelled, dsh homolog 3 (Drosophila)	3.04	Protein binding;Intracellular signaling cascade;Signal transducer activity;Development;Intracellular;Kinase activity;Neurogenesis;Heart development;Frizzled signaling pathway;
NM_001949	E2F3 **Cell cycle;** E2F transcription factor 3	2.60	Regulation of transcription, DNA-dependent;Nucleus;Protein binding;Regulation of cell cycle;Transcription factor activity;Transcription factor complex;Transcription initiation from Pol II promoter;
NM_001964	EGR1 **Other cancer-related genes;** Early growth response 1	2.49	Regulation of transcription, DNA-dependent;Nucleus;Transcription factor activity;Zinc ion binding;
NM_005240	ETV3 **Other cancer-related genes;** Ets variant gene 3	16.11	Regulation of transcription, DNA-dependent;Nucleus;Transcription factor activity;
NM_001987	ETV6 **Cell growth and differentiation;** Ets variant gene 6 (TEL oncogene)	4.84	Regulation of transcription, DNA-dependent;Nucleus;Cell growth and/or maintenance;Transcription factor activity;
NM_005438	FOSL1 **Cell growth and differentiation;** FOS-like antigen 1	2.59	Nucleus;Transcription factor activity;Positive regulation of cell proliferation;Response to virus;Regulation of transcription from Pol II promoter;Chemotaxis;Cellular defense response;
NM_003468	C2orf31 **Chromosome 2 open reading frame 31**	3.45	Wnt receptor signaling pathway;G-protein coupled receptor protein signaling pathway;Development;Integral to plasma membrane;G-protein coupled receptor activity;Non-G-protein coupled 7TM receptor activity;Establishment of tissue polarity;
NM_003508	FZD9 **Signal transduction;** Frizzled homolog 9 (Drosophila)	2.71	Plasma membrane;Integral to membrane;G-protein coupled receptor protein signaling pathway;Development;Neurogenesis;G-protein coupled receptor activity;Wnt receptor activity;Frizzled signaling pathway;

NM_002154	HSPA4 **Other cancer-related genes;** Heat shock 70kDa protein 4	2.11	ATP binding;Cytoplasm;Heat shock protein activity;
NM_006644	HSPH1 **Other cancer-related genes;** Heat shock 105kDa/110kDa **protein 1**	3.13	ATP binding;Cytoplasm;Heat shock protein activity;
NM_000876	IGF2R **Other cancer-related genes;** Insulin-like growth factor 2 receptor	2.25	Signal transduction;Receptor activity;Lysosome;Integral to plasma membrane;Insulin-like growth factor receptor activity;Transporter activity;Receptor mediated endocytosis;Transport;
NM_003768	PEA15 **Apoptosis;** Phosphoprotein enriched in astrocytes 15	2.15	Protein binding;Regulation of apoptosis;Anti-apoptosis;Transport;Sugar porter activity;Negative regulation of glucose import;Microtubule associated complex;
NM_001664	RHOA **Cell growth and differentiation, signal transduction;** Ras homolog gene family, member A	0.48	GTP binding;GTPase activity;Protein transport;Small GTPase mediated signal transduction;Rho protein signal transduction;Signal transducer activity;Positive regulation of I-kappaB kinase/NF-kappaB cascade;Membrane;Cytoskeleton;Magnesium ion binding;Actin cytoskeleton organization and biogenesis;Positive regulation of NF-kappaB-nucleus import;
NM_004040	RHOB **Cell growth and differentiation, signal transduction;** Ras homolog gene family, member B	0.28	GTP binding;GTPase activity;Rho protein signal transduction;Cell growth and/or maintenance;
NM_003670	BHLHB2 **Other cancer-related genes;** Basic helix-loop-helix domain containing, class B, 2	0.40	Regulation of transcription, DNA-dependent;Nucleus;Transcription factor activity;
NM_000386	BLMH **Other cancer-related genes;** Bleomycin hydrolase	0.40	Hydrolase activity;Aminopeptidase activity;Proteolysis and peptidolysis;Nucleus;Cytoplasm;Bleomycin hydrolase activity;Carboxypeptidase activity;
NM_000077	CDKN2A **Cell cycle, cell growth and**	0.47	Nucleus;Negative regulation of cell cycle;Negative regulation of cell proliferation;Cell cycle arrest;Cell cycle;Cyclin-dependent protein

	differentiation; Cyclin-dependent kinase inhibitor 2A (melanoma, p16, inhibits CDK4)		kinase inhibitor activity;Regulation of cyclin dependent protein kinase activity;Kinase activity;Cell cycle checkpoint;
NM_001293	CLNS1A **Cell growth and differentiation;** Chloride channel, nucleotide-sensitive, 1A	0.26	Plasma membrane;Nucleus;Transport;Circulation;Visual perception;Chloride transport;Auxiliary transport protein activity;Regulation of cell volume;
NM_001865	COX7A2 **Other cancer-related genes;** Cytochrome c oxidase subunit VIIa polypeptide 2 (liver)	0.40	Electron transporter activity;Oxidoreductase activity;Mitochondrion;Electron transport;Inner membrane;Cytochrome-c oxidase activity;
NM_001814	CTSC **Other cancer-related genes;** Cathepsin C	0.19	Hydrolase activity;Immune response;Proteolysis and peptidolysis;Lysosome;Cysteine-type endopeptidase activity;Dipeptidyl-peptidase I activity;
NM_003592	CUL1 **Apoptosis, cell cycle, cell growth and differentiation;** Cullin 1	0.50	Protein binding;Negative regulation of cell proliferation;Cell cycle arrest;G1/S transition of mitotic cell cycle;Cell cycle;Induction of apoptosis by intracellular signals;
NM_003472	DEK **Cell growth and differentiation;** DEK oncogene (DNA binding)	0.31	GTP binding;Signal transduction;DNA binding;Nucleus;Cell growth and/or maintenance;Specific RNA polymerase II transcription factor activity;Regulation of transcription from Pol II promoter;Viral genome replication;RNA binding;Histone binding;SRP-dependent cotranslational membrane targeting;Signal recognition particle;
NM_006389	HYOU1 **Other cancer-related genes;** Hypoxia up-regulated	0.47	ATP binding;Response to stress;Endoplasmic reticulum;Chaperone activity;
NM_003641	IFITM1 **Cell cycle, cell growth and differentiation, signal transduction;** Interferon induced transmembrane protein 1 (9-27)	0.34	Receptor signaling protein activity;Plasma membrane;Integral to membrane;Immune response;Negative regulation of cell proliferation;Regulation of cell cycle;Cell surface receptor linked signal transduction;Response to biotic stimulus;
NM_000598	IGFBP3	0.21	Regulation of cell growth;Extracellular;Cell growth and/or

	Cell growth and differentiation; Insulin-like growth factor binding protein 3		maintenance;Metal ion binding;Insulin-like growth factor binding;Protein tyrosine phosphatase activator activity;Negative regulation of signal transduction;Positive regulation of apoptosis;Positive regulation of myoblast differentiation;
NM_002291	LAMB1 **Other cancer-related genes;** Laminin, beta 1	0.14	Structural molecule activity;Cell adhesion;Protein binding;Basement membrane;
NM_002337	LRPAP1 **Cell growth and differentiation;** Low density lipoprotein receptor-related protein associated protein 1	0.30	Plasma membrane;Integral to membrane;Calcium ion binding;Cell proliferation;Heparin binding;Endoplasmic reticulum;Protein folding;Chaperone activity;Asialoglycoprotein receptor activity;Lipoprotein binding;Vesicle-mediated transport;
NM_004635	MAPKAPK3 **Other cancer-related genes;** Mitogen-activated protein kinase-activated protein kinase 3	0.46	ATP binding;Transferase activity;Protein amino acid phosphorylation;Signal transduction;Nucleus;Protein serine/threonine kinase activity;Response to stress;MAP kinase kinase activity;
NM_004526	MCM2 **Cell cycle;** MCM2 minichromosome maintenance deficient 2, mitotin (S. cerevisiae)	0.46	ATP binding;DNA binding;Regulation of transcription, DNA-dependent;Nucleus;DNA replication;Chromatin;Cell cycle;DNA-dependent ATPase activity;DNA replication initiation;
NM_002467	MYC **Cell cycle, cell growth and differentiation;** V-myc myelocytomatosis viral oncogene homolog (avian)	0.07	Cell proliferation;Nucleus;Transcription factor activity;Regulation of transcription from Pol II promoter;Cell cycle arrest;Iron ion homeostasis;
NM_003998	NFKB1 **Apoptosis;** Nuclear factor of kappa light polypeptide gene enhancer in B-cells 1 (p105)	0.44	Signal transduction;Regulation of transcription, DNA-dependent;Nucleus;Protein binding;Cytoplasm;Apoptosis;Anti-apoptosis;Transcription factor activity;Inflammatory response;Transcription from Pol II promoter;Response to pathogenic bacteria;Antibacterial humoral response (sensu Vertebrata);
NM_000269	NME1 **Cell cycle, cell growth and differentiation;**	0.29	ATP binding;Transferase activity;Nucleus;Negative regulation of cell cycle;Negative regulation of cell proliferation;Kinase activity;Nucleoside-diphosphate kinase activity;CTP

	Non-metastatic cells 1, protein (NM23A) expressed in		biosynthesis;GTP biosynthesis;UTP biosynthesis;Nucleoside triphosphate biosynthesis;
NM_002512	NME2 **Cell growth and differentiation;** Non-metastatic cells 2, protein (NM23B) expressed in	0.35	ATP binding;Transferase activity;Regulation of transcription, DNA-dependent;Nucleus;Negative regulation of cell cycle;Negative regulation of cell proliferation;Transcription factor activity;Kinase activity;Nucleoside-diphosphate kinase activity;CTP biosynthesis;GTP biosynthesis;UTP biosynthesis;Nucleoside triphosphate biosynthesis;
NM_002513	NME3 **Apoptosis;** Non-metastatic cells 3, protein expressed in	0.10	ATP binding;Transferase activity;Induction of apoptosis;Apoptosis;Kinase activity;Nucleoside-diphosphate kinase activity;CTP biosynthesis;GTP biosynthesis;UTP biosynthesis;
NM_024408	NOTCH2 **Cell cycle, cell growth and differentiation, signal transduction;** Notch homolog 2 (Drosophila)	0.47	Calcium ion binding;Regulation of transcription, DNA-dependent;Nucleus;Protein binding;Induction of apoptosis;Anti-apoptosis;Negative regulation of cell proliferation;Cell cycle arrest;Receptor activity;Integral to plasma membrane;Cell differentiation;Neurogenesis;Protein heterodimerization activity;Cell fate determination;Cell growth;Regulation of development;Hemopoiesis;Cell surface;Morphogenesis of an epithelial sheet;Ligand-regulated transcription factor activity;Notch signaling pathway;Determination of left/right symmetry;Positive regulation of RAS protein signal transduction;Stem cell maintenance;
NM_015869	PPARG **Other cancer-related genes;** Peroxisome proliferative activated receptor, gamma	0.32	Energy pathways;Response to nutrients;Signal transduction;Nucleus;Transcription factor activity;Regulation of transcription from Pol II promoter;Steroid hormone receptor activity;Lipid metabolism;White adipocyte differentiation;
NM_182649	PCNA **Cell cycle, cell growth and differentiation;** Proliferating cell nuclear antigen	0.20	Cell proliferation;DNA binding;Nucleus;Regulation of cell cycle;DNA replication;DNA polymerase processivity factor activity;DNA repair;Regulation of DNA replication;Delta-DNA polymerase cofactor complex;
NM_006406	PRDX4 **Other cancer-related genes;**	0.37	Oxidoreductase activity;Peroxidase activity;Thioredoxin peroxidase activity;I-kappaB phosphorylation;

	Peroxiredoxin 4		
NM_000962	PTGS1 **Other cancer-related genes;** Prostaglandin-endoperoxides synthase 1 (prostaglandin G/H synthase and cyclooxygenase)	0.48	Oxidoreductase activity;Peroxidase activity;Membrane;Physiological process;Lipid metabolism;Oxidoreductase activity, acting on single donors with incorporation of molecular oxygen, incorporation of two atoms of oxygen;Prostaglandin-endoperoxide synthase activity;Prostaglandin biosynthesis;
NM_002823	PTMA **Cell cycle;** Prothymosin, alpha (gene sequence 28)	0.29	Nucleus;Regulation of cell cycle;Development;Transcription;
NM_004162	RAB5A **Signal transduction;** RAB5A, member RAS oncogene family	0.45	GTP binding;GTPase activity;Protein transport;Small GTPase mediated signal transduction;Protein binding;Endocytosis;Early endosome;
NM_006908	RAC1 **Cell motility, signal transduction;** Ras-related C3 botulinum toxin substrate 1 (rho family, small GTP binding protein Rac1)	0.47	GTP binding;GTPase activity;Protein transport;Small GTPase mediated signal transduction;Cell adhesion;Inflammatory response;Cell motility;Morphogenesis;
NM_002880	RAF1 **Apoptosis, cell growth and differentiation, signal transduction;** V-raf-1 murine leukemia viral oncogene homolog 1	0.42	Receptor signaling protein activity;ATP binding;Transferase activity;Protein amino acid phosphorylation;Cell proliferation;Protein binding;Diacylglycerol binding;Protein serine/threonine kinase activity;Intracellular signaling cascade;Apoptosis;Mitochondrial outer membrane;
NM_005610	RBBP4 **Cell cycle, cell growth and differentiation;** Retinoblastoma binding protein 4	0.24	Regulation of transcription, DNA-dependent;Nucleus;Negative regulation of cell proliferation;DNA replication;Cell cycle;DNA repair;
NM_007273	PHB2 **Cell growth and differentiation;** Probibitin 2	0.29	Cellular_component unknown;Receptor activity;Negative regulation of transcription;Estrogen receptor binding;
NM_002951	RPN2 **Other cancer-related genes;** Ribophorin II	0.30	Transferase activity;Integral to membrane;Protein modification;Dolichyl-diphosphooligosaccharide-protein glycotransferase activity;N-linked glycosylation via

			asparagine;Oligosaccharyl transferase complex;
NM_006142	SFN **Cell cycle, cell growth and differentiation;** Stratifin	0.21	Cell proliferation;Signal transduction;Cytoplasm;Regulation of cell cycle;Extracellular space;Protein domain specific binding;Protein kinase C inhibitor activity;Negative regulation of protein kinase activity;
NM_006427	SIVA **Apoptosis;** CD27-binding (Siva) protein	0.30	Receptor signaling protein activity;Cytoplasm;Apoptosis;Induction of apoptosis by extracellular signals;Positive regulation of apoptosis;CD27 receptor binding;Defense response;
NM_005415	SLC20A1 **Other cancer-related genes;** Solute carrier family 20 (phosphate transporter), member 1	0.39	Phosphate metabolism;Signal transducer activity;Positive regulation of I-kappaB kinase/NF-kappaB cascade;Receptor activity;Membrane;Integral to plasma membrane;Transport;Phosphate transport;Inorganic phosphate transporter activity;Sodium:phosphate symporter activity;
NM_004749	TBRG4 **Cell cycle, cell growth and differentiation;** Transforming growth factor beta regulator 4	0.27	Positive regulation of cell proliferation;Cell cycle arrest;G1 phase of mitotic cell cycle;
NM_000358	TGFBI **Cell growth and differentiation;** Transforming growth factor, beta-induced 68kDa	0.45	Cell adhesion;Cell proliferation;Protein binding;Negative regulation of cell adhesion;Extracellular matrix;Extracellular space;Integrin binding;Visual perception;Extracellular matrix (sensu Metazoa);
NM_003254	TIMP1 **Cell growth and differentiation, cell motility;** TIMP metallopeptidase inhibitor 1	0.48	Proteolysis and peptidolysis;Positive regulation of cell proliferation;Development;Extracellular matrix;Metalloendopeptidase inhibitor activity;Extracellular matrix (sensu Metazoa);Negative regulation of membrane protein ectodomain proteolysis;
NM_001066	TNFRSF1B **Apoptosis;** Tumor necrosis factor receptor superfamily, member 1B	0.29	Integral to membrane;Apoptosis;Receptor activity;Tumor necrosis factor receptor activity;Cytokine and chemokine mediated signaling pathway;
NM_000546	TP53 **Apoptosis, cell cycle;**	0.49	ATP binding;Cell proliferation;Regulation of transcription, DNA-dependent;Protein binding;Negative regulation of cell

	Tumor protein p53 (Li-Fraumeni syndrome)		cycle;Apoptosis;Mitochondrion;Transcription factor activity;Zinc ion binding;DNA damage response, signal transduction resulting in induction of apoptosis;Cell cycle arrest;Nucleolus;Cell cycle checkpoint;DNA strand annealing activity;Copper ion binding;Nuclease activity;DNA recombination;Base-excision repair;Caspase activation via cytochrome c;Cell aging;Cell differentiation;Induction of apoptosis by hormones;Negative regulation of cell growth;Nucleotide-excision repair;Regulation of mitochondrial membrane permeability;Protein tetramerization activity;Negative regulation of helicase activity;
NM_004881	TP53I3 **Other cancer-related genes;** Tumor protein p53 inducible protein 3	0.21	Cellular_component unknown;Zinc ion binding;Alcohol dehydrogenase activity, zinc-dependent;Induction of apoptosis by oxidative stress;
NM_003321	TUFM **Other cancer-related genes;** Tu translation elongation factor, mitochondrial	0.37	GTP binding;Mitochondrion;Protein biosynthesis;Translational elongation;Translation elongation factor activity;
NM_003374	VDAC1 **Apoptosis;** Voltage-dependent anion channel 1	0.23	Integral to membrane;Mitochondrial outer membrane;Mitochondrion;Apoptotic program;Apoptogenic cytochrome c release channel activity;Voltage-dependent anion channel porin activity;Voltage-dependent ion-selective channel activity;Anion transport;
NM_021141	XRCC5 **Other cancer-related genes;** X-ray repair complementing defective repair in Chinese hamster cells (double-strand-break rejoining; Ku autoantigen 80kDa)	0.29	Nucleus;DNA recombination;ATP-dependent DNA helicase activity;Helicase activity;Double-stranded DNA binding;Double-strand break repair via nonhomologous end-joining;Regulation of DNA repair;DNA-dependent protein kinase complex;

For realgar-treated HeLa cells, there were 4 up-regulated and 7 down-regulated genes after low dose treatment, whilst at high dose treatment, more genes altered, i.e. 10 up-regulated and 86 down-regulated genes. This finding further indicates that the effect of realgar on cancer cell is dose-dependent. All changed genes were categorized based on their specific functions as respective functional gene groups, i.e. apoptosis, cell cycle, cell growth and differentiation, cell motility, signal transduction, and other cancer-related genes, as summarized in Table 1 as well.

For orpiment-treated HeLa cells, from Table 1 (c and d), high dose did cause more genes changed than low dose, similar to the observation for realgar-treated cells. There were 17 up-regulated and 12 down-regulated genes after low dose treatment compared to 19 up-regulated and 34 down-regulated genes after high dose treatment.

For As_2O_3-treated HeLa cells, total 18 genes altered including 3 up-expressed genes and 15 down-expressed genes.

Arsenite induced 25 genes up expressed and 46 genes down expressed.

In order to diminish the impact of dose variation on the results, the drug concentrations chosen were those which could cause about 80% cells alive after 24 h treatment. For realgar and orpiment, the lower concentrations were one third of respective higher concentrations. Therefore, omitting the dose effects on gene expression, the effects of arsenic compounds on cancer cells did be species-dependent.

In order to clearly view them, Table 2 outlines the altered gene profiles of cells after high dose realgar, high dose orpiment, arsenic trioxide, and arsenite treatments, respectively. From Table 1 and Table 2, it could be seen that the mechanisms of actions of arsenical compounds are very complicated.

Table 2. Gene profiles after corresponding arsenicals treatments.

Gene	Realgar	Orpiment	Arsenite	As_2O_3
	High concentration	High concentration		
AARS	↓↓	–	–	–
ABCB1	↓	–	↑↑↑	–
ABI2	–	–	↑↑↑	–
ABL1	–	–	↑	–
ABL2	–	–	↑↑↑	–
ACP2	↓↓	–	–	–
ACY1	↓↓↓	↓↓	–	–
ANXA5	–	–	↑	–
RHOA	–	–	↓	–
RHOB	–	–	↓↓↓	–
ASNS	↑↑	↑↑	–	↓
BHLHB2	↓↓↓	↓↓↓	↓	–
BLMH	↓	↓↓	↓	–
CANX	–	–	↑	↓
CAP1	–	–	↑↑↑	–
CAPN1	↓	–	–	–
CAPNS1	–	–	↑	–
CCNE1	–	↓↓↓	–	–
CD59	↓	↓↓	–	↑
CDC20	↓↓	–	–	–
CDC25A	↑	–	↑↑↑	–
CDC25B	↓↓↓	↓↓↓	–	–
CDC25C	–	–	↑↑↑	–
CDC2L5	↓↓	–	–	–
CDKN1A	–	–	↑	–
CDKN1B	↓	–	–	–
CDKN2A	–	–	↓	–
CDKN2B	–	↑	–	–
CEBPG	↑	↑↑↑	–	–
CIB1	↓↓↓	–	–	–
CKMT1B	↓↓↓	↓↓	–	–
CLK2	↓↓↓	↓↓	–	–
CLNS1A	↓↓↓	–	↓↓↓	–
COX6C	↓↓	–	–	–
COX7A2	–	–	↓	–
Crat	–	↑	–	–
CSNK1G2	↓↓↓	–	–	–
CTNNA1	–	–	↑↑	–
CTPS	↓↓↓	↓↓	–	–
CTSC	↓↓↓	↓↓↓	↓↓↓	–
CUL1	↓	–	↓	–
CYR61	–	↑↑	–	–
DCN	↓↓↓	↓↓↓	–	–
DEK	–	–	↓↓↓	–
DHCR7	↓↓↓	↓↓↓	–	–

DHX8	–	–	↑↑	–
DVL1	↓↓↓	–	–	↓↓
DVL3	–	–	↑↑↑	–
E2F1	↓↓↓	–	–	–
E2F3	–	–	↑↑	–
EGR1	↑↑↑	–	↑	–
ERCC3	↓	–		–
ETV3	–	–	↑↑↑	–
ETV6	–	–	↑↑↑	–
F2R	↓	↓	–	–
FBN1	↓	–	–	–
FBN2	–	↑	–	–
FN1	–	–	–	↓
FOSL1	↑↑↑	↑↑↑	↑↑	↑
FRAP1	↓	–		–
C2orf31	–	–	↑↑↑	–
FZD9	–	–	↑↑	–
GCN5L2	–	↓	–	–
GDF15	↑	–	–	–
GTF2I	↓↓↓	↓	–	–
HDGF	↓	–	–	–
HLA-G	↓	↓	–	–
HSPA4	–	–	↑	–
HSPH1	–	–	↑↑↑	↑
HYAL1	–	–	–	–
HYOU1	–	↑↑	↓	–
IER3	–	–	–	–
IFITM1	↓↓↓	↓↓↓	↓↓	↓↓↓
IGF2R	↑	↑	↑	–
IGFBP3	↓↓↓	↓↓↓	↓↓↓	↓↓↓
ILK	↓↓↓	–	–	–
IRF3	↓↓	–	–	–
ITGA3	↓	–	–	–
JUN	↑↑	–	–	–
KPNA2	–	–	–	–
LAMB1	↓↓↓	↓↓↓	↓↓↓	↓
LAMP2	–	–	–	↓
LCN2	–	↑	–	–
LRPAP1	↓↓↓	↓	↓↓↓	–
MAP2K2	↓↓	–		–
MAPKAPK3	↓	–	↓	–
MARS	–	–	–	↓
MCM2	↓↓	–	↓	–
MGST1	–	–	–	–
MYC	↓↓↓	↓↓↓	↓↓↓	↓↓↓
MYL9	↓↓↓	–	–	–
NF2	↓↓↓	–	–	–
NFKB1	–	–	↓	↓↓
NFKB2	–	↑↑	–	–

NME1	↓↓↓	–	↓↓↓	–
NME2	↓↓	–	↓↓	–
NME3	↓↓↓	↓↓↓	↓↓↓	↓↓
NOTCH2	–	–	↓	–
NR2F1	↓↓↓	↓↓↓	–	–
NR2F6	↓↓↓	↓↓	–	–
PCNA	↓↓↓	↓	↓↓↓	–
PCTK3	↓↓↓	↓↓↓	–	–
PEA15	↑↑↑	↑↑↑	↑	–
PIK3CG	↓	–	–	–
PPARD	↓↓↓	–	–	–
PPARG	–	–	↓↓↓	↓
PRDX4	–	–	↓↓	–
PRKAR1A	↓↓↓	–	–	–
PRNP	–	↑	–	–
PTGS1	↓↓	–	↓	–
PTMA	↓↓↓	–	↓↓↓	–
RAB5A	–	–	↓	–
RAC1	–	–	↓	–
RAF1	↓↓	–	↓	–
RAP1A	↓↓↓	↓↓↓	–	–
RARA	↓↓↓	–	–	–
RB1	↓↓	–	–	–
RBBP4	↓↓↓	–	↓↓↓	–
PHB2	↓↓↓	–	↓↓↓	–
RELA	↓↓	–	–	–
RELB	–	↑↑	–	–
RPN2	↓↓	–	↓↓↓	–
SARS	–	↑	–	–
SELENBP1	↓	↓↓↓	–	–
SEPT6	↓	↓	–	–
SFN	↓↓	–	↓↓↓	–
SHB	–	↑	–	–
SIVA	↓↓↓	–	↓↓↓	–
SLC20A1	↓	–	↓↓	–
SND1	↓↓	–	–	–
SNRPB2	↓	–	–	–
STAT3	↓↓↓	–	–	–
TBRG4	↓↓↓	–	↓↓↓	–
TCF1	↓	–	–	–
TFDP1	↓↓↓	↓↓↓	–	–
TGFBI	–	–	↓	–
TGFBR3	↓↓↓	↓↓↓	–	–
TIMP1	–	–	↓	–
TK1	↓↓	–	–	–
TNFRSF10B	↑↑	↑↑	–	–
TNFRSF1B	↓↓	↓↓↓	↓↓↓	–
TP53	↓↓↓	↓↓	↓	–
TP53I3	↓↓	–	↓↓↓	–

TRAM1	–	↑↑↑	–	–
TUFM	–	–	↓↓	↓
TXNRD1	–	↑	–	–
USP7	↓	–	–	–
VDAC1	↓↓	–	↓↓↓	–
PPIH	↓↓	–	–	–
XRCC1	–	↓	–	–
XRCC5	↓↓↓	–	↓↓↓	–
YWHAB	↓	–	–	–

↓: Down-regulated gene (fold change between 2.0-2.5); ↓↓: Down-regulated gene (fold change between 2.5-3.0); ↓↓↓: Down-regulated gene (fold change > 3.0).
↑: Up-regulated gene (fold change between 2.0-2.5); ↑↑: Up-regulated gene (fold change between 2.5-3.0); ↑↑↑: Up-regulated gene (fold change > 3.0).
–: Insignificantly changed gene.

Special concern was focused on those selected genes (total 25 genes with yellow background highlight in Table 2) which were expressed significantly (fold change ≥ 5.0 and ≤ 0.2). Here we try to explain the possible underlying biological process of those significantly altered genes involved in one by one as follow:

1. BHLHB2

Of class B of basic helix-loop-helix (bHLH) proteins binding to the E box sequence (5'-CANNTG-3'), BHLHB2 (also referred to as DEC1/Eip1/SHARP-2/Stra13/Clast5) is transcription factor that contains a unique orange domain. It represses the transcription of target gene not only via binding to the E box sequence but also via protein-protein interactions with other transcription factors. BHLHB2 is widely expressed in both embryonic and adult tissues.

BHLHB1 expression is regulated in a cell type-specific manner by various extracellular stimuli including growth factors, serum starvation, hypoxia, hormones, nutrient, cytokines, light, and infection etc [Yamada K and Miyamoto K, 2005]. Therefore, it plays pivotal role in multiple signalling pathways that impact many

biological processes including development, cell differentiation, cell growth, cell death, oncogenesis, immune systems, circadian rhythm, and homeostasis.

The cellular BHLHB2 expression level was significantly decreased after reaglar treatment. Similar responses with the lower expression levels from orpiment- and arsenite-treated cells were also observed.

In a recent study, researchers identified BHLHB2 as a STAT3 partner and provided a consistent line of evidence for BHLHB2 involvement into regulation of apoptosis via the STAT pathways [Ivanova AV et al., 2004]. In our study, decreased STATS expression induced by realgar was also observed. STAT3 has been classified as an oncogene because constitutively active STAT3 can mediate oncogenic transformation in cell culture and in nude mice [Turkson J and Jove R, 2000]. Whether there is an association between these two genes in the current study co-mediated by realgar need to be further investigated.

2. CAP1

Many extracellular signals elicit changes in the actin cytoskeleton. One family of proteins that plays a role in regulating actin remodelling in response to cellular signals are the cyclise-associated proteins (CAPs). CAPs are highly conserved monomeric actin binding proteins present in a wide range of organisms including yeast, fly, plants, and mammals. Two different CAP genes, CAP1 and CAP2, share at least 64% amino acid identity in mammals [Yu G et al, 1994].

The significant up-expression of CAP1 gene was found for arsenite treated cells compared to non-change for other arsenicals treated cells. Actin filaments provide basic infrastructure for maintaining cell morphology and functions such as adhesion, motility, exocytosis, endocytosis, and cell division. Growing evidence

shows that actin remodelling plays a pivotal role in regulating the morphologic and phenotypic events of a malignant cell. Since CAP1 has a central role in actin remodelling, it could be assumed that arsenite probably stimulated actin remodelling to inhibit cell growth.

3. CDC25A

CDC25A is a member of the CDC25 (cell division cycle) family of phosphatases. CDC25A is required for progression from G1 to the S phase of the cell cycle. It activates the cyclin-dependent kinases (CDKs) by removing two phosphate groups. CDC25A is specifically degraded in response to DNA damage, which prevents cells with chromosomal abnormalities from progressing through cell division. A regulatory role of CDC25A in the G2-M transition has also been suggested. CDC25A is an oncogene, although its exact role in oncogenesis has not been demonstrated. Two transcript variants encoding different isoforms have been found for this gene.

CDC25 has been shown to be overexpressed in a number of cancers [Kristjansdottir K and Rudolph J, 2004]. The central role of CDC25A in the cell cycle makes it a potential target for novel anti-cancer drugs. However, to date, no clinically-viable compounds targeting this enzyme have been described. The over-expression of CDC25A of cells after arsenite treatment probably indicated that arsenite might inhibit cell proliferation through CDC25A-independent pathway.

4. CKMT1B

Official full name of CKMT1B is creatine kinase, mitochondrial 1 B. Mitochondrial creatine kinase (MtCK as known as CKMT) is responsible for the

transfer of high energy phosphate from mitochondria to the cytosolic carrier, creatine. It belongs to the creatine kinase (CK) isoenzyme family. It exists as two isoenzymes, sarcomeric and ubiquitous forms, encoded by separate genes. CKMT occurs in two different oligomeric forms: dimers and octamers, in contrast to the exclusively dimeric cytosolic CK isoenzymes. Many malignant cancers with poor prognosis have shown overexpression of ubiquitous CKMT; this may be related to high energy turnover and failure to eliminate cancer cells via apoptosis. Ubiquitous CKMT has 80% homology with the coding exons of sarcomeric mitochondrial creatine kinase. Two genes located near each other on chromosome 15 have been identified which encode identical mitochondrial creatine kinase proteins.

In addition, CTMK1B has been implicated in the regulation of the Ca^{2+}-induced mitochondrial permeability transition pore (PTP) [O'Gorman E et al., 1997]. PTP is involved in triggering apoptosis by releasing proapoptotic factor into the cytosol [Crompton M, 1999].

The response of CKMT1B gene of HeLa cells to realgar was obviously down-regulated, but not to arsenic trioxide and arsenite. There was an opposite observation in oral squamous cell carcinoma reported by Onda T et al. [Onda T et al., 2006], where researcher found that down-regulation of CKMT1B was involved in the oral carcinogenesis and they also concluded that epigenetic mechanism may regulate loss of its expression, leading to block apoptosis through specialized systems such as mitochondrial PTP in oral cancer cells.

5. CLK2

CDC-line kinase 2 (CLK2) encodes a member of the CLK family of dual specificity protein kinases. CLK family members have shown to interact with, and

phosphorylate, serine- and arginine-rich (SR) proteins of the spliceosomal complex, which is a part of the regulatory mechanism that enables the SR proteins to control RNA splicing. This protein kinase is involved in the regulation of several cellular processes and may serve as a link between cell cycle progression, apoptosis, and telomere length regulation.

Recent studies on human tumor cells demonstrated that over-expression of CLK2 renders the cell hypersensitive to apoptosis triggered by oxidative stress or DNA replication block and gradually increases telomere length [Jiang N et al., 2003].

Only realgar significantly induced CLK2 expression down-regulated.

6. CTPS

The catalytic conversion of UTP to CTP is accomplished by the enzyme cytidine-5-prime-triphosphate synthetase (CTPS). The enzyme is important in the biosynthesis of phospholipids and nucleic acids, and plays a key role in cell growth, development, and tumorigenesis. The region to which the CTPS gene has been mapped is the location of breakpoints involved in several tumor types.

CTPS is a key enzyme in nucleic acid and phospholipid biosythesis and its activity is increased in certain human cancers, making it a promising drug target [Verschuur AC et al., 2000]. Antiproliferative drugs targeted specifically towards CTPS have been developed, with the aim of depleting cancer cells of CTP and thus slowing down tumour growth, such as cyclopentenyl cytosine (CPEC), acivicin and 3-deazauridine [Verschuur AC et al., 2000]. Down-regulation of CTPS was observed for realgar treated HeLa cells, indicating that the activity of CTPS in cancerous cells could be inhibited by realgar.

7. CTSC

The protein encoded by cathepsin C (CTSC), a member of the peptidase C1 family, is a lysosomal cysteine proteinase that appears to be a central coordinator for activation of many serine proteinases in immune/inflammatory cells. It is composed of a dimer of disulfide-linked heavy and light chains, both produced from a single protein precursor. It requires chloride ions for activity and can degrade glucagon. Defects in the encoded protein have been shown to be a cause of Papillon-Lefevre syndrome, an autosomal recessive disorder characterized by palmoplantar keratosis and periodontitis. Two transcript variants encoding different isoforms have been found for this gene.

High expression of CTSC in human skin cancer was reported [Dang C et al., 2006]. Except arsenic trioxide, other arsenicals inactivated CTSC significantly.

8. DCN

Decorin (DCN) is a proteoglycan on average 90-140 kD in size. The protein encoded by this gene is a small cellular or pericellular matrix proteoglycan that is closely related in structure to biglycan protein. The encoded protein and biglycan are thought to be the result of gene duplication. This protein is a component of connective tissue, binds to type I collagen fibrils, and plays a role in matrix assembly. It contains one attached glycosaminoglycan chain. This protein is capable of suppressing the growth of various tumor cell lines. There are multiple alternatively spliced transcript variants known for this gene. This gene is a candidate gene for Marfan syndrome.

DCN belongs to tumor suppressing gene. Inhibition of growth of different cancer cells by DCN has been reported, by neutralizing the epidermal growth factor receptor-dependent kinases, by up-regulating $p21^{CIP1/WAF1}$ through interaction with the

epidermal growth factor receptor [Lozzo RV et al., 1999], or by a mechanism involving the SMAD4 transduction pathway [Chen WB et al., 2002]. In this study, however, the down-regulation of DCN after realgar and orpiment treatments likely indicated that realgar and orpiment induced the cells death through DCN-independent pathways. In some publications, DCN could influence bioactivity of TGF-β1 positively or negatively. Similar response trend of TGF-β receptor-TGFBP3 with slightly lower expression levels to realgar and orpiment probably implied that regulation of cell growth by DCN could be involved in TGF-β signaling pathway.

9. DHCR7

In mammals, 7-dehydroxholesterol reductase (DHCR7) is the terminal enzyme in cholesterol biosynthesis. Smith-Lemli-Opitz syndrome (SLOS) is a severe developmental disorder caused by mutations in the DHCR7 gene, which is also current research focus.

Both realgar and orpiment significantly down-regulated DHCR7 compared to arsenic trioxide and arsenite. The association between this down expression and inhibition of cell growth is not clear yet.

10. E2F1

E2F stands for family of transcription factors in higher eukaryotes. E2F1 is one of three activators. The E2F family plays a crucial role in the control of cell cycle and action of tumor suppressor proteins and is also a target of the transforming proteins of small DNA tumor viruses. The E2F proteins contain several evolutionally conserved domains found in most members of the family. These domains include a DNA binding domain, a dimerization domain which determines interaction with the

differentiation regulated transcription factor proteins (DP), a transactivation domain enriched in acidic amino acids, and a tumor suppressor protein association domain which is embedded within the transactivation domain. This protein and another 2 members, E2F2 and E2F3, have an additional cyclin binding domain. This protein binds preferentially to retinoblastoma protein pRB in a cell-cycle dependent manner. It can mediate both cell proliferation and p53-dependent/independent apoptosis.

It should be emphasized that some E2F family members behave as both oncogene and tumor suppressor gene [Johnson DG and Degregori J, 2006]. For example, down-regulated E2F1 expression can either promote or inhibit tumorigenesis depending on the nature of the other oncogenic mutations that are present.

In this study, only realgar induced E2F1 down-regulation.

11. ETV3

Full name of ETV3 is ETS variation gene 3. ETS transcription factors family plays important roles in cell development, cell differentiation, cell proliferation, apoptosis and tissue remodelling. Most of them are downstream nuclear targets of Ras-MAP kinase signalling, and the deregulation of ETS genes results in malignant transformation of cells. Considering that some ETS transcription factors are involved in malignant transformation and tumor progression, including invasion, metastasis and neo-angiogenesis through the activation of cancer-related genes, they could be potential molecular targets for selective cancer therapy [Oikawa T, 2004]. ETV3 functions as repressors to inhibit growth-related genes such as c-myc and cdc2 but they do not inhibit differentiation-related genes [Klappacher GW et al., 2002]. Thus, it is possible that they could be used as antagonists against ETS transcriptional

activators.

Only arsenite obviously increased ETV3 expression.

12. FOSL1

The Fos gene family consists of 4 members: FOS, FOSB, FOSL1, and FOSL2. These genes encode leucine zipper proteins that can dimerize with proteins of the JUN family, thereby forming the transcription factor complex AP-1. As such, the FOS proteins have been implicated as regulators of cell proliferation, differentiation, and transformation.

There was a summary reporting that misregulated activation of AP-1 can lead to tumorigenesis and that JUN and FOS can function as oncogenic transcription factors [Young MR and Colburn NH, 2006]. Therefore, up-regulation of FOSL1 after arsenicals treatments especially orpiment possibly suggests the oncogenic properties of arsenicals.

13. IGFBP3

This gene is a member of the insulin-like growth factor binding protein (IGFBP) family and encodes a protein with an IGFBP domain and a thyroglobulin type-I domain. The protein forms a ternary complex with insulin-like growth factor acid-labile subunit (IGFALS) and either insulin-like growth factor (IGF) I or II. In this form, it circulates in the plasma, prolonging the half-life of IGFs and altering their interaction with cell surface receptors. IGFBP3 is the most abundant protein, accounting for 80% of all IGF binding. Alternate transcriptional splice variants, encoding different isoforms, have been characterized.

IGF-I and its main binding protein IGFBP3 modulate cell growth and survival,

and are thought to be important in tumour development. Early studies on risk of several cancers suggested that high circulating IGF-I concentrations are associated with an increased risk of cancer, whereas high IGFBP3 concentrations are associated with a decreased risk [Renehan AG et al., 2004]. Down-regulation of IGFBP3 induced by all four types of arsenicals was observed, positively influencing the cell growth.

14. LAMB1

Laminins, a family of extracellular matrix glycoproteins, are the major noncollagenous constituent of basement membranes. They have been implicated in a wide variety of biological processes including cell adhesion, differentiation, migration, signaling, neurite outgrowth and metastasis. Laminins are composed of 3 non identical chains: laminin alpha, beta and gamma (formerly A, B1, and B2, respectively) and they form a cruciform structure consisting of 3 short arms, each formed by a different chain, and a long arm composed of all 3 chains. Each laminin chain is a multidomain protein encoded by a distinct gene. Several isoforms of each chain have been described. Different alpha, beta and gamma chain isomers combine to give rise to different heterotrimeric laminin isoforms which are designated by Arabic numerals in the order of their discovery, i.e. alpha1beta1gamma1 heterotrimer is laminin 1. The biological functions of the different chains and trimer molecules are largely unknown, but some of the chains have been shown to differ with respect to their tissue distribution, presumably reflecting diverse functions in vivo. This gene encodes the beta chain isoform laminin, beta 1. The beta 1 chain has 7 structurally distinct domains which it shares with other beta chain isomers. The C-terminal helical region containing domains I and II are separated by domain alpha, domains III and V

contain several EGF-like repeats, and domains IV and VI have a globular conformation. Laminin, beta 1 is expressed in most tissues that produce basement membranes, and is one of the 3 chains constituting laminin 1, the first laminin isolated from Engelbreth-Holm-Swarm (EHS) tumor. A sequence in the beta 1 chain that is involved in cell attachment, chemotaxis, and binding to the laminin receptor was identified and shown to have the capacity to inhibit metastasis.

Integrin- and non-integrin-mediated laminin signalling activate several regulatory pathways that are involved in metastasis of cancer cells [Patarroyo M et al., 2002; Givant-Horwitz V et al., 2005]. All arsenicals seem to trigger down-regulated alteration of LAMB1 gene, especially for arsenite, meaning that they positively inhibit the possible metastasis of cancer cells.

15. MYC

Full name of MYC is v-myc myelocytomatosis viral oncogene homology. The protein encoded by this gene is a multifunctional, nuclear phosphoprotein that plays a role in cell cycle progression, apoptosis and cellular transformation. It functions as a transcription factor that regulates transcription of specific target genes. Mutations, overexpression, rearrangement and translocation of this gene have been associated with a variety of hematopoietic tumors, leukemias and lymphomas, including Burkitt lymphoma. There is evidence to show that alternative translation initiations from an upstream, in-frame non-AUG (CUG) and a downstream AUG start site result in the production of two isoforms with distinct N-termini. The synthesis of non-AUG initiated protein is suppressed in Burkitt's lymphomas, suggesting its importance in the normal function of this gene.

MYC oncogene is deregulated in a wide variety of human tumors hence the

MYC pathway is an attractive target for tailored cancer treatment. Significant down-regulation of MYC induced by arsenicals tested probably suggested that arsenicals killed the cells via MYC-dependent pathways.

16. NME3

nm23 gene family has been associated with metastasis suppression and differentiation. nm23 proteins have functional characteristics, such as kinase activity, leucine-zipper motif for transcriptional factor dimerization, and the integrin binding dowain arginine-glycine-aspartic acid (RGD), suggesting that they are multiple role proteins. NME3 (also called DR-nm23) is the third member of nm23 gene family, which shows 70% homology with other two members of nm23-H1 and nm23-H2 [Amendola R et al., 2001]. Reportedly, DR-nm23 is involved in differentiation and apoptotic process in myeloid and neuroblastoma cells [Venturelli D et al., 1995; Amendola R et al., 1997]. DR-nm23 possesses NDP kinase activity.

Both realgar and arsenite caused reduced expression of NME3.

17. NR2F1

Steroid/thyroid hormones play an important role in regulating cellular differentiation, development and homeostasis in eukaryotes. They function through binding to their cognate nuclear receptors which are ligand-inducible transcription factors. Chicken ovalbumin upstream promoter-transcription factors (COUP-TFs) are the orphan memebers of the nuclear receptor superfamily [Tsai SY and Tsai MJ, 1997]. Two COUP-TFs members are identified, COUP-TFI (also called NR2F1) and COUP-TFII (also called NR2F6).

In this study, only realgar significantly caused both NR2F1 and NR2F6 down-

regulated.

18. NR2F6

19. PCNA

The protein encoded by proliferating cell nuclear antigen (PCNA) is found in the nucleus and is a cofactor of DNA polymerase delta. The encoded protein acts as a homotrimer and helps increase the processivity of leading strand synthesis during DNA replication. In response to DNA damage, this protein is ubiquitinated and is involved in the RAD6-dependent DNA repair pathway. Two transcript variants encoding the same protein have been found for this gene. Pseudogenes of this gene have been described on chromosome 4 and on the X chromosome.

PCNA in mammalian cells plays a key role in controlling several reactions through the coordination and organization of different partners. Down-regulation of PCNA mediated by realgar and arsenite were observed. Reduced PCNA expression and inhibited cell growth by arsenical in nasopharyngeal cancer xenografted SCID mice were reported [Li D et al., 2002].

20. PCTK3

PCTK3, also called PCTAIRE3, is a CDC2 family protein kinase.

An overexpression of PCTK3 was found in sporadic breast cancer in Mexican women [Valladares A et al., 2006]. In our study, only realgar significantly reduced PCTK3 expression.

21. RAP1A

The product of this gene belongs to the family of RAS-related proteins. These proteins share approximately 50% amino acid identity with the classical RAS proteins and have numerous structural features in common. The most striking difference between RAP proteins and RAS proteins resides in their 61st amino acid: glutamine in RAS is replaced by threonine in RAP proteins. The product of this gene counteracts the mitogenic function of RAS because it can interact with RAS GAPs and RAF in a competitive manner. Two transcript variants encoding the same protein have been identified for this gene.

RAS and RAS-related proteins are often deregulated in cancers, leading to increased invasion and metastasis, and decreased apoptosis. Down-regulation of RAP1A induced by realgar was observed.

22. RBBP4

Retinoblastoma binding protein 4 (RBBP4) encodes a ubiquitously expressed nuclear protein which belongs to a highly conserved subfamily of WD-repeat proteins. Another name of RBBP4 is RBAP48. It is present in protein complexes involved in histone acetylation and chromatin assembly. It is part of the Mi-2 complex which has been implicated in chromatin remodeling and transcriptional repression associated with histone deacetylation. This encoded protein is also part of co-repressor complexes, which is an integral component of transcriptional silencing. It is found among several cellular proteins that bind directly to retinoblastoma protein to regulate cell proliferation. This protein also seems to be involved in transcriptional repression of E2F-responsive genes.

Very little is known about the role of RBB4 in cancers, although its expression has been found elevated in different human tumors including lung, liver, AML, and

acute lymphoblastic leukemia [Fukuoka J et al., 2004; Song H et al., 2003; Casas S et al., 2003]. Only realgar stimulated RBBP4 down-expressed.

23. TFDP1

The E2F transcription factor family (see MIM 189971) regulates the expression of various cellular promoters, particularly those involved in the cell cycle. E2F factors bind to DNA as homodimers or heterodimers in association with dimerization partner DP1. TFDP1 function as binding partner for E2F transcription factor and may be the first example of a family of related transcription factors; see TFDP2 (MIM 602160).

The association of TFDP with E2F directly enhances both DNA binding affinity ad the transactivation function of the heterodimer. Although DP proteins might not possess a biological function on their own, they are indispensable for regulating E2F activity and thus play a central role in important cellular functions such as apoptosis. Furthermore, active TFDP1/E2F1 promotes apoptosis in both a p53-dependent and –independent manners [Hitchens MR and Robbins PD, 2003]. Down-regulation of TFDP1 was triggered by realgar treatment, same trend were found for the change of E2F1 gene.

24. TNFRSF1B

The protein encoded by this gene is a member of tumor necrosis factor receptor (TNFR) superfamily. This protein and TNF-receptor 1 form a heterocomplex that mediates the recruitment of two anti-apoptotic proteins, c-IAP1 and c-IAP2, which possess E3 ubiquitin ligase activity. The function of IAPs in TNF-receptor signalling is unknown, however, c-IAP1 is thought to potentiate TNF-induced

apoptosis by the ubiquitination and degradation of TNF-receptor-associated factor 2, which mediates anti-apoptotic signals. Knockout studies in mice also suggest a role of this protein in protecting neurons from apoptosis by stimulating antioxidative pathways.

TNFR superfamily members can induce a context-dependent apoptosis or cell activation. However, the mechanisms by which these opposing programs are selected remain unclear. Particularly, the mechanism of TNFRSF1B-mediated cell death remains under-investigated. Influence of orpiment on TNFRSF1B was to down-regulate its expression, probably showing that orpiment induced cell death through TNFRSF1B-dependent pathways.

25. TP53

Tumor protein 53 (TP53), a nuclear protein, plays an essential role in the regulation of cell cycle, specifically in the transition from G0 to G1. It is found in very low levels in normal cells, however, in a variety of transformed cell lines, it is expressed in high amounts, and believed to contribute to transformation and malignancy. p53 is a DNA-binding protein containing DNA-binding, oligomerization and transcription activation domains. It is postulated to bind as a tetramer to a p53-binding site and activate expression of downstream genes that inhibit growth and/or invasion, and thus function as a tumor suppressor. Mutants of p53 that frequently occur in a number of different human cancers fail to bind the consensus DNA binding site, and hence cause the loss of tumor suppressor activity. Alterations of the TP53 gene occur not only as somatic mutations in human malignancies, but also as germline mutations in some cancer-prone families with Li-Fraumeni syndrome.

In this study, only realgar significantly caused TP53 down-expressed,

probably indicating that realgar stimulated the cell death via P53-independent pathways.

5.4 Conclusions

Although most of altered genes need to be further confirmed by other methods such as RT-PCR, the microarray analysis has provided a global view of molecular alterations induced by specific arsenic compounds. Furthermore, the microarray data also suggest the complexity of tumor suppression of arsenic compounds, which likely involves the multitude of molecular alterations that require further investigation.

CHAPTER SIX

Urinary 8-hydroxy-2’-deoxyguanosine determined by isotope dilution LC/MS/MS in rats after oral administrations of arsenic compounds

CHAPTER SIX

6.1 Introduction

Currently there is evidence that ROS can cause cell and tissue damage, consequently leading to various diseases including cancer [Hu CW et al., 2004]. There is great interest in studying the DNA damage caused by oxidation and various biomarkers associated with the damage. Urinary 8-hydroxy-2'-deoxyguanosine (8-OH-dGuo) is reported to be the most acceptable biomarker of the oxidative DNA damage, because of its good water-solubility, stability, non-invasive sampling, absence of artifacts as encountered in DNA extraction, relatively high abundance, and more importantly etiological role in mutations and gene expression (causing G:C to T:A transversion) [Cheng KC et al., 1992; Kasai H, 1997]. Urinary 8-OH-dGuo also represents the average rate of damage in the total body. Therefore, determination of urinary 8-OH-dGuo can be used for investigation of different types of exposure to DNA-damaging factors, such as carcinogen and body irradiation [Cheng KC et al., 1992; Kasai H, 1997; Peoples MC and Karnes HT, 2005]. 8-OH-dGuo has as well been identified as a biomarker for a few types of cancers including breast, lung, and liver cancers [Ma YF et al., 2004]. Therefore, determination of urinary 8-OH-dGuo has been considered as a noninvasive method for cancer diagnosis. Mei SR et al [Mei SR et al., 2005] analyzed 9 urine samples of healthy persons and 28 of cancer patients, and found that the excretion level of 8-OH-dGuo in cancer patients was significantly higher than in healthy persons, suggesting that the routine clinical determination of urinary 8-OH-dGuo could be a useful cancer biomarker. However, the concentration of 8-OH-dGuo in urine is normally as low as 1-10 nM, which makes detection difficult in most cases [Ma YF et al., 2004].

6.1.1 Analytical methods for determination of 8-OH-dGuo

8-OH-dGuo has been analyzed using various instruments, mainly including HPLC with electrochemical detection (ECD) [Helbock HJ et al., 1998], enzyme-linked immunosorbent assays (ELISA) [Kubota R et al., 2006], gas chromatography with mass spectrometry (GC/MS) [Dizdaroglu M, 1998], and HPLC with tandem mass spectrometry (LC/MS/MS) [Li CS et al., 2005]. GC-MS is currently the most commonly used method for analysis of modified nucleobase and nucleoside. However, artificial oxidation during sample preparation and analysis procedures has been reported [Cadet J et al., 1998; Dizdaroglu M, 1998]. From a practical point of view, an ideal method of analysis should include a minimum sample preparation, fast analysis time, and specific and sensitive detection. LC/MS/MS has the advantages over GC/MS of not requiring analyte derivatization to avoid artifact formation, and over HPLC/ECD of being chemospecific. Comparisons between LC/MS/MS method and commercial ELISA kit method on analysis of 8-OH-dGuo have been made by Hu CW et al. [2004]. In that study, the researchers found that the commercial ELISA kit method could have over-estimated the 8-OH-dGuo levels in urine. The reason might be due to the monoclonal antibody N45.1, used for the commercial ELISA kit, being not sufficiently specific toward urinary 8-OH-dGuo; the crude urine samples could contain considerable amounts of cross-reacting substances and other structurally related compounds competing for the N45.1 antibody.

Comprehensively considering the unique advantages and instrumental availability, in this study, LC/MS/MS was selected to determine the changes of urinary 8-OH-dGuo in rats after drug treatments. Urine is a very complex matrix containing numerous endogenous compounds. When co-eluted with the analyte urinary matrix can cause electrospray ionization (ESI) suppression or enhancement, thus adversely affecting the reproducibility and accuracy of the mass detection,

leading to serious quantitation errors. To solve such problem, our method involves solid-phase extraction to remove intensively the urine matrix contaminations.

6.1.2 Objectives of this study

Arsenic is a well-established human carcinogen based on epidemiological studies, although the underlying mechanisms of carcinogenesis remain unclear. Induction of ROS by arsenic has been observed in some *in vitro* and *in vivo* experiments [Hei TK and Filipic M, 2004; Yamanaka K et al., 1989]. In spite of such evidences, it is still difficult to accurately assess health effects of arsenic on human, because its therapeutic applications also have a long history. It is well known that the toxicity of arsenicals depends on their chemical states [Tchounwou PB et al., 2003]. In addition, the toxicity of arsenicals depends on the exposure dose, frequency and duration, the biological species, age and gender, as well as on individual susceptibilities, genetic and nutritional factors [Tchounwou PB et al., 2003].

In order to examine possible associations between arsenic intake and the possible oxidative stress caused, we compared the urinary levels of the commonly accepted DNA damage biomarkers, 8-OH-dGuo, in rats after arsenite, realgar and orpiment administrations with control rats. The findings would add valuable information to the toxicity of arsenite, realgar and orpiment and safety in their future clinical applications.

6.2 Materials and methods

6.2.1 Chemicals

8-Hydroxy-2'-deoxyguanosine (8-OH-dGuo, 100% in purity) with molecular weight of 283.2 and 8-hydroxy-2'-deoxyadenosine (8-OH-dAdo, 100% in purity)

with molecular weight of 267.2 were purchased from Berry & Associates Inc. (Ann Arbor, MI, USA). Stable heavy isotope labeled [^{15}N5]-8-OH-dGuo (98% in purity) with molecular weight of anhydrous basis of 288.2 was obtained from Cambridge Isotope Laboratories (Andover, MA, USA). 2'-Deoxyguanosine monohydrate (dGuo, 99-100% in purity) with molecular weight of 267.2 and formic acid of mass spectrometry grade were purchased from Sigma Chemical Corp. (St. Louis, MO, USA). Methanol of HPLC grade was obtained from Merck Corp. (Darmstadt, Germany). Milli-Q water was used throughout experiment. Aqueous stock standard solutions of 8-OH-dGuo and [^{15}N5]-8-OH-dGuo, dGuo, and 8-OH-dAdo were prepared by dissolving them respectively in Milli-Q water to give a concentration of 10 μg/ml, and stored at –80 ^{o}C (under these conditions, the stocks were stable over at least six months). The concentration of 8-OH-dGuo could be further confirmed by UV spectrophotometry using the absorption coefficient of 9908 M^{-1} cm^{-1} at 245 nm, and that of 8-OH-dAdo could be further determined using the absorption coefficient of 12764 M^{-1} cm^{-1} at 270 nm [Cavalieri LF and Bendich A, 1950]. Working standard solutions of 8-OH-dGuo (0.5 to 10 ng/ml) were freshly prepared by series dilution with Milli-Q water.

The respective suspensions of realgar (R/PVP/SDS) and orpiment (O/PVP/SDS) were prepared by individually dispersing the R/PVP/SDS and O/PVP/SDS preparations into Milli-Q water at a concentration of 4.0 mg drug/ml (the details could be referred to Chapter 3). Arsenite solution with a concentration of 2.0 mg arsenite/ml was prepared by firstly dissolving exact amount of arsenic trioxide into 1 N NaOH followed by adjustment of pH to 7.0 ± 0.2 with concentrated HCl.

6.2.2 Animal model and arsenic compounds administrations

Healthy male Sprague-Dawley (SD) rats (6-7 weeks of age, with average body weight of 200 ± 20 g) were purchased from Laboratory Animals Center, Singapore. They were randomly selected and housed individually in polycarbonate metabolic cages and provided with a standard diet (Mouse pellets, Laboratory Animals Centre, Singapore) and water *ad libitum*. The housing conditions were kept on a 12/12-h light/dark cycle at a temperature of 23 ± 1 ^{o}C and relative humidity of 50 ± 10%. At least one week of acclimatization period was allowed for rats prior to drug administration experiments. The animal experiment protocol followed the guidelines for proper and humane care of animals in scientific research.

Rats were divided randomly into four groups of six rats each: one control group and three experimental groups. The three experimental groups received individual arsenic compounds by gavage administration for consecutive 15 days, whilst the control group received drinking water instead. Dosages were 20 mg pure drug/kg body weight for realgar and orpiment suspensions, and 10 mg arsenite/kg body weight for arsenite solution. After the experiment, all rats were euthanized by carbon dioxide gas inhalation.

6.2.3 Urine sample collection, normalization and purification

Every 24 hour urine outputs were collected and stored frozen at –80 ^{o}C until analysis. Prior to analysis, each sample was thawed at 37 ^{o}C for 10 min to re-dissolve possible 8-OH-dGuo precipitate during freezing storage [Weimann A et al., 2001], vigorously mixed, and then centrifuged at 1500 g for 10 min to obtain a clear supernatant.

Since the urine concentration is highly variable between different subjects and in the same subject at different time points, the volume of urine was adjusted

according to its creatinine concentration level measured by Jaffe method after slight modification [Chan MH, 2004]. Briefly, the formation of acid-sensitive chromogen after reduction of the urine sample with picrate was measured at UV absorbance of 500 nm. The different creatinine concentration can be reflected by different color by the present modified Jaffe method as shown in picture below. The urine was then normalized according to creatinine concentration by adding appropriate amount of 10% formic acid. Normalized urine samples were then subjected to further purification steps.

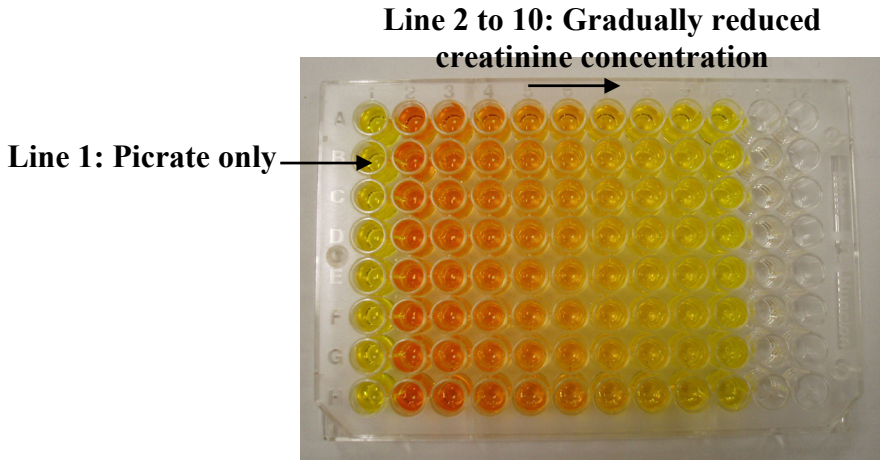

The solid phase extraction (SPE) clean-up procedure was processed and optimized by Waters Oasis® HLB Vac cartridges (Waters Corp., Milford, MA, USA) according to the standard protocol after slight modification. A volume of 1 ml of the normalized urine was loaded into a preconditioned SPE cartridge. The cartridge was then washed with 2 ml of water. The fraction containing 8-OH-dGuo was eluted with 1 ml of HPLC running buffer. To optimize and evaluate the recovery of 8-OH-dGuo after clean-up procedure, isotope labeled [^{15}N5]-8-OH-dGuo equaling to 10 ng/ml was added to urine sample as an internal standard.

6.2.4 Analysis of 8-OH-dGuo by LC/MS/MS

The HPLC system used was Agilent 1200 Series LC systems (Agilent Technologies Inc., Santa Clara, CA, USA). A Waters Symmetry300^{TM} C18 column (150 × 1.0 mm i.d., 3.5 μm particle size) (Waters Ltd., Watford, UK) with an identical guard column (10 × 2.0 mm, 3.5 μm) was used. The isocratic mobile phase was 30% methanol with 0.1% formic acid, delivered at a flow rate of 50 μl/min. The HPLC was connected to an API 3200 Qtrap® mass spectrometer (Applied Biosystems, Foster, CA, USA) equipped with a TurboIonSpray^{TM} source. Electrospray ionization (ESI) was performed. Multiple reaction monitoring (MRM) mode with positive ionization was used. Optimization of mass responses (compound parameters) was achieved by infusion of the 8-OH-dGuo solution in mobile phase with 1 μg/ml at a flow rate of 10 μl/min by using a syringe pump. Major mass conditions used include: curtain gas at 40 psi, ionspray source voltage at 5500 V, ionspray probe temperature at 450 ^{o}C, ion source gas 1 at 50 psi and gas 2 at 30 psi, declustering potential at 25 V, entrance potential at 4.0 V, collision energy at 15.4 V, and collision cell exit potential at 8.0 V. A volume of 10 μl of purified urine sample was injected into the LC/MS/MS instrument for urinary 8-OH-dGuo determination.

Data were acquired and processed with Analyst® 1.4.2 software (Applied Biosystems, Foster, CA, USA). The urinary concentration of 8-OH-dGuo was corrected by using individual urinary creatinine concentration (ng/mg creatinine).

6.2.5 Measurement of urinary arsenic concentration by GFAAS

Determination of urinary arsenic concentration by GFAAS could be referred to 3.2.2.1 (2) in Chapter 3.

6.2.6 Statistical methods

The results were presented as mean ± standard deviation (SD). Differences among data were determined using one-way ANOVA with the post hoc Tukey's multiple comparison test (GraphPad Prism V4.0). Linear regression model was applied to study the association of the urinary arsenic recovery levels with urinary 8-OH-dGuo levels (GraphPad Prism 4.0). A p-value < 0.05 was considered a significant difference.

6.3 Results and discussion

6.3.1 8-OH-dGuo and [^{15}N5]-8-OH-dGuo: Typical mass spectra and chromatograms

Production-ion spectra of 8-OH-dGuo and [^{15}N5]-8-OH-dGuo were acquired respectively at optimum MS/MS conditions as shown in Figures 1a and 1b. The most abundant fragment of 8-OH-dGuo was detected at *m/z* 168, resulting from cleavage of the N-glycosidic bond accompanied by transfer of a hydrogen atom from the sugar moiety. A following intense daughter ion was observed at *m/z* 117, molecular ion $[M+H]^+$ at *m/z* 284 was also observed. Corresponding fragmentation scheme was proposed in Figure 1a, and consistent with previous reports [Serrano J et al., 1996; Pietta PG et al., 2003]. [^{15}N5]-8-OH-dGuo has been reported to be a stable internal standard [Frelon S et al., 2000; Singh R et al., 2003] and was thus selected in this study, yielding a same fragmentation pattern as 8-OH-dGuo (Figure 1b). The advantages of the isotope-dilution method are to correct for losses during the sample preparation and variations in the mass spectrometric response by calibration with isotopically labeled internal standard. In a recent study it was shown that tandem mass spectrometry for 8-OH-dGuo in MRM mode provided a significant increase in

sensitivity over in selected ion monitoring (SIM) mode, mainly because using MRM mode led to a significant reduction in background noise to consequently generate an apparently overall increase in sensitivity [Podmore ID et al., 2000]. Therefore, the MRM mode was selected in the present study, and according to the individual production-ion spectra transition ion pairs chosen were 284/168 for 8-OH-dGuo and 289/173 for [^{15}N5]-8-OH-dGuo.

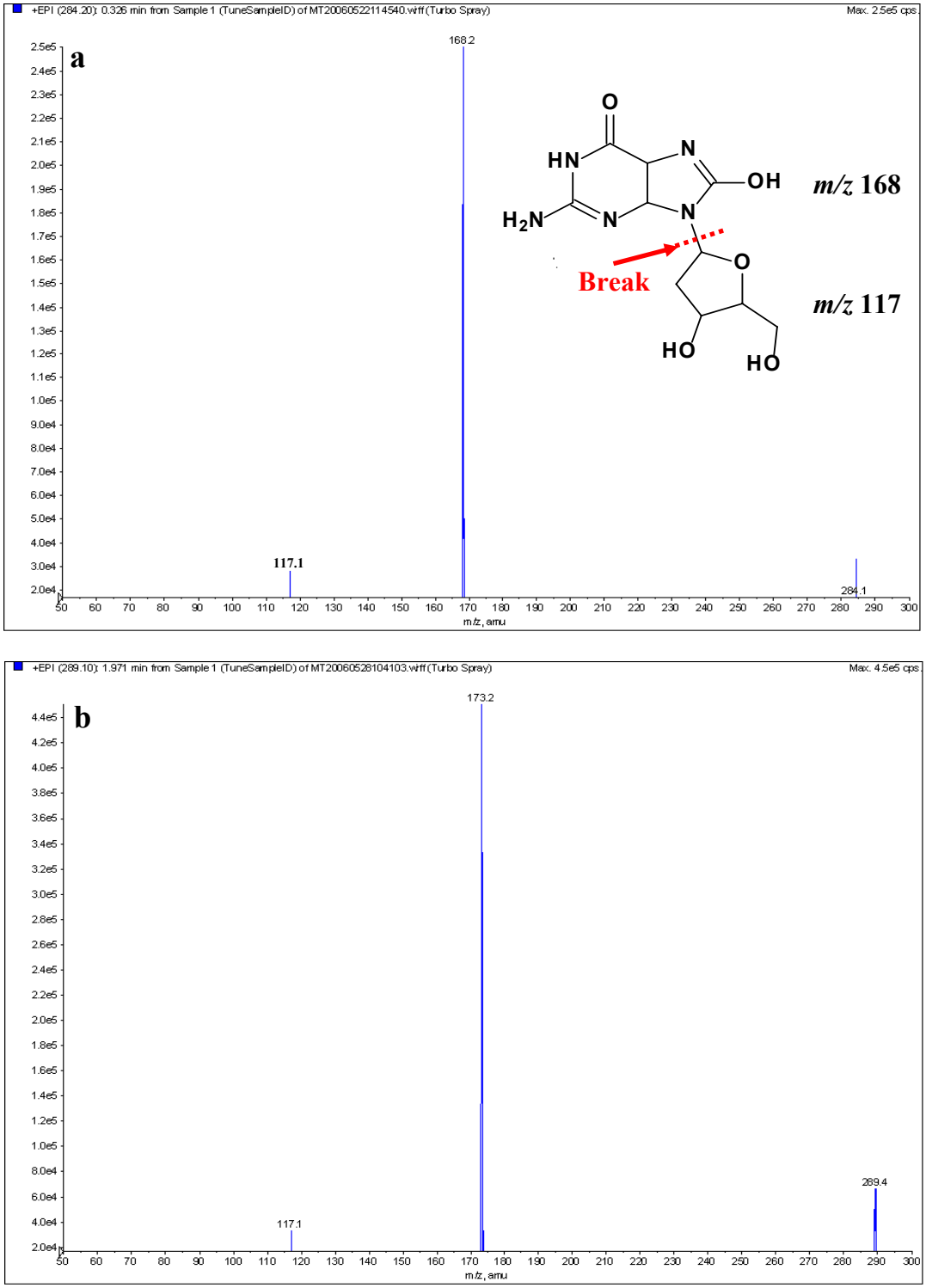

Figure 1. Positive production-ion spectra of 8-OH-dGuo (a, product ion scan of $[M+H]^+$ at *m/z* 284) and [^{15}N5]-8-OH-dGuo (b, product ion scan of $[M+H]^+$ at *m/z* 289).

Chromatographic conditions for LC were established by using several types of solvent conditions. Considering both separation and sensitivity in response of the

mass spectrometer, 70% 0.1% formic acid with 30% methanol was selected. This elution system was simple and well suited for LC/MS. A typical chromatogram of a mixture of 8-OH-dGuo and [^{15}N5]-8-OH-dGuo in standard aqueous solution is shown in Figure 2. Both 8-OH-dGuo and [^{15}N5]-8-OH-dGuo were simultaneously eluted at the same retention time of 3.5 min, which also makes the isotope internal standard as an extra control in case the retention time of the analyte would somehow change during a run.

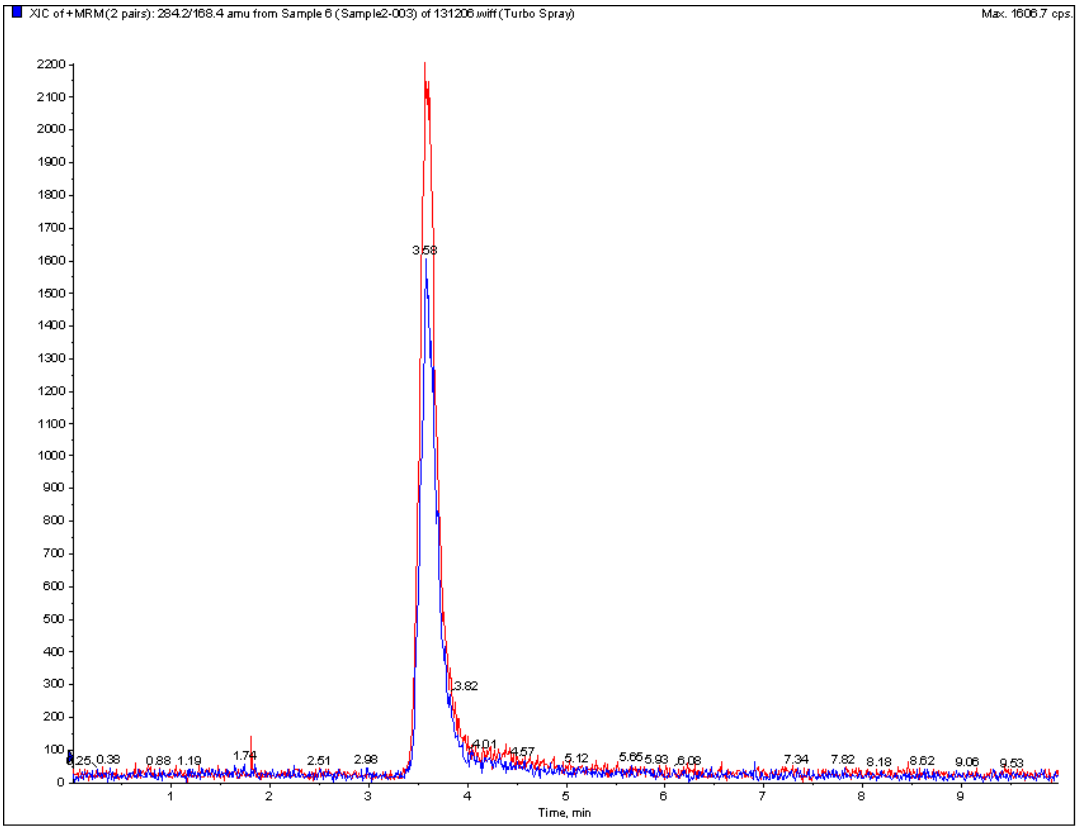

Figure 2. MRM chromatogram for an aqueous standard solution of 8-OH-dGuo (4.0 ng/ml, blue line) and [^{15}N5]-8-OH-dGuo (5.0 ng/ml, red line).

A separation chromatogram of purified urine sample spiked with 8-OH-dGuo and [$^{15}N_5$]-8-OH-dGuo is shown in Figure 3. The rat urine sample was randomly selected from the corresponding sample pools. As indicated, base line separation of 8-

OH-dGuo and [^{15}N5]-8-OH-dGuo from interferences in the urine matrix was obtained, indicating the urine matrix did not affect the detection of the analytes, although SPE clean-up procedure did not remove the urine matrix entirely. LOD value for [$^{15}N_5$]-8-OH-dGuo in urine matrix was about 0.5 ng/ml, which was comparable with that in the aqueous standard, suggesting that urinary contaminants left after clean-up of the urine matrix with SPE did not much affect the detection sensitivity of analyte. However, both peaks of urinary 8-OH-dGuo and [^{15}N5]-8-OH-dGuo became broader compared with those in corresponding aqueous solutions. For comparison, zero blank and double blank chromatograms of purified urine samples randomly selected from control group were displayed (Figures 4a and 4b).

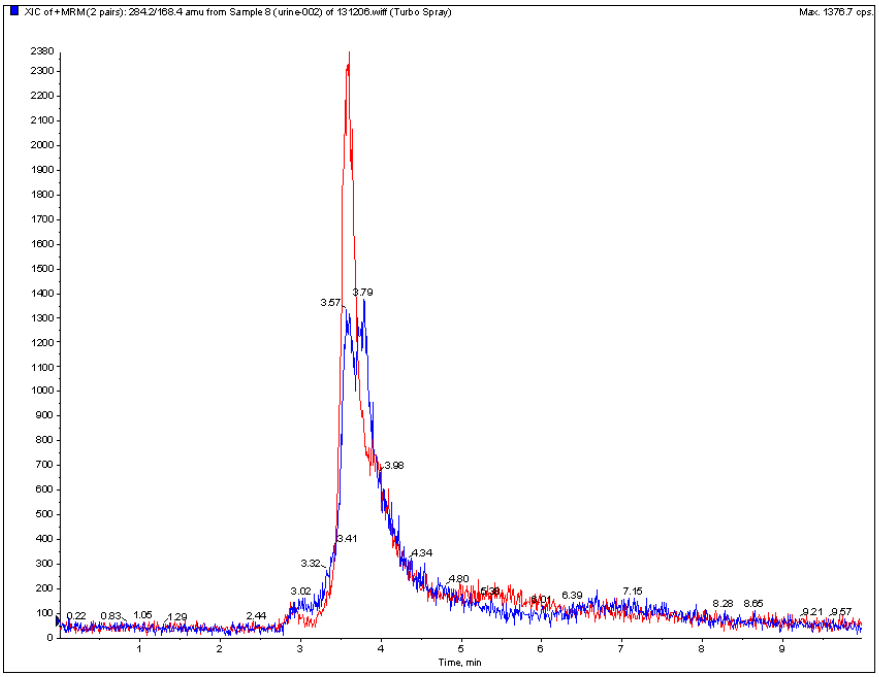

Figure 3. MRM chromatogram for 8-OH-dGuo (1.0 ng/ml added, blue line) and [^{15}N5]-8-OH-dGuo (5.0 ng/ml, red line) in urine matrix.

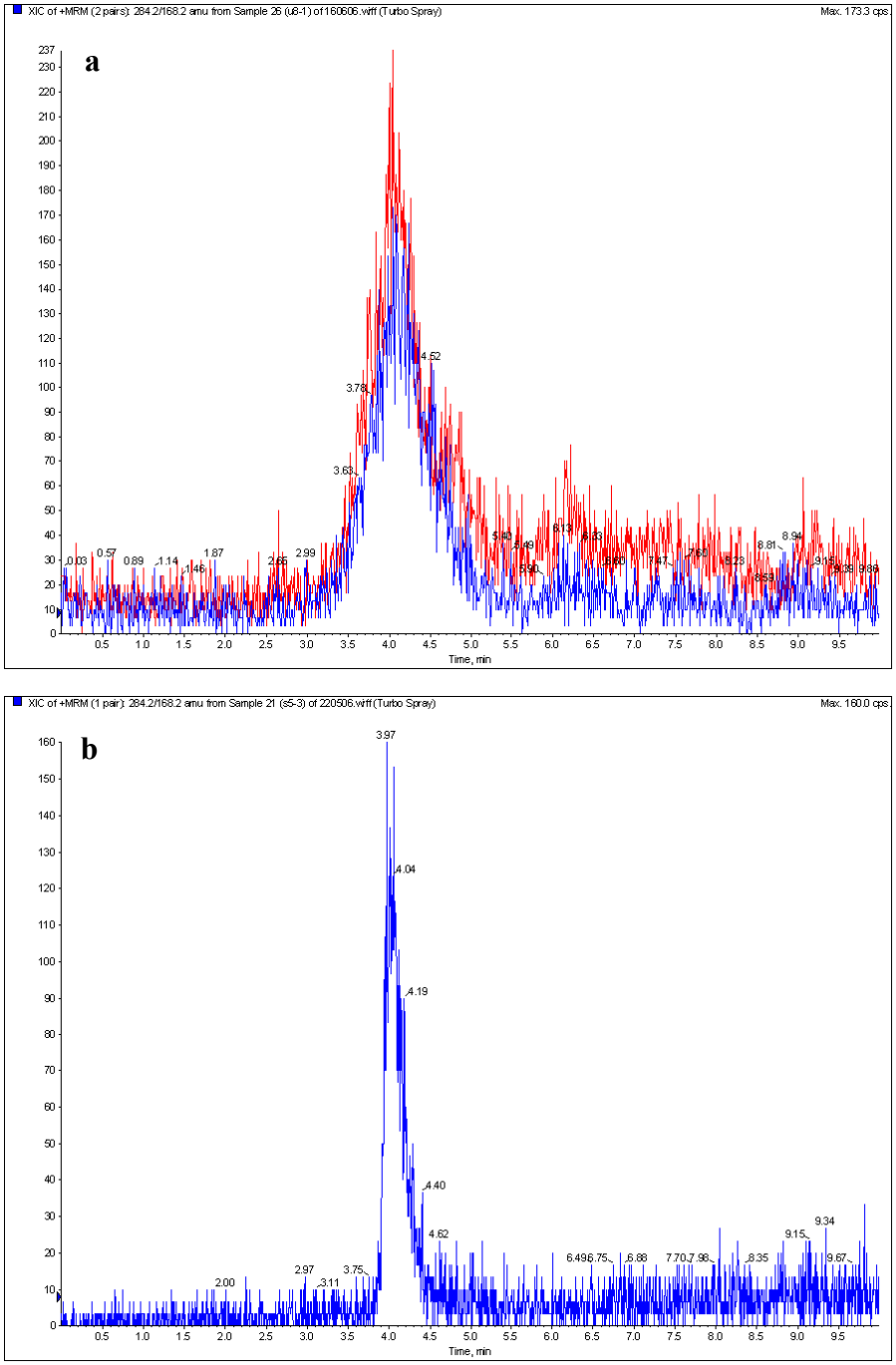

Figure 4. Zero blank (a, with addition of 1.0 ng/ml isotope, red line) and double blank (b) chromatograms of purified control urine sample randomly selected from control group.

Besides 8-OH-dGuo, dozens of different forms of DNA damage products are known to be produced by oxygen radicals. 2-Hydroxy-2'-deoxyadenosine (2-OH-dAdo) and 8-hydroxy-2'-deoxyadenosine (8-OH-dAdo) are the major oxidative damage products of adenine [Kamiya H and Kasai H, 1995]. However, the yield of 2-

OH-dAdo in DNA is much lower than that of 8-OH-dAdo after external stimulation as determined by GC/MS [Jaruga P et al., 2001]. For LC/MS analysis, there was no authentic compound available for 2-OH-dAdo probably because of its too low concentration [Jaruqa P et al., 2001]. Therefore, 8-OH-dAdo becomes study focus, and it has been implicated in mutagenesis, carcinogenesis, and aging [Tan XZ et al., 1999]. For example, lesions induce A → G and A→ C mutations in mammalian cells [Tan XZ et al., 1999]. In addition, adenosine works as a universal protective agent against hypoxia, ischemia, excitotoxicity, toxicities induced by other substances and trauma [Engler RL, 1991]. The measurement of urinary adenosine can contribute to evaluation of renal injury in various clinical settings [Katholi RE et al., 1995; Heyne N et al., 2004]. Therefore, the primary aim of this study was to measure simultaneously the urinary 8-OH-dGuo and 8-OH-dAdo.

Since 8-OH-dAdo has the same molecular weight as dGuo, for identification purpose, dGuo was included for the initial method development. According to the product ion spectra and proposed fragmental schemes of 8-OH-dAdo and dGuo (Figures 5a and 5b), their transition ion pairs were same, i.e. 268/152. Figure 6 gives the chromatogram of an aqueous mixture of 8-OH-dGuo, [^{15}N5]-8-OH-dGuo, dGuo and 8-OH-dAdo. It could be seen that 8-OH-dGuo/[^{15}N5]-8-OH-dGuo, dGuo and 8-OH-dAdo were well separated, following the eluting order of dGuo, 8-OH-dGuo/[^{15}N5]-8-OH-dGuo, and 8-OH-dAdo. The eluting order was confirmed by chromatographic analysis of the individual analytes. In order to improve the separation, the mobile phase was changed to 80% 0.1% formic acid with 20% methanol, whilst the operation parameters were also adjusted accordingly. The different chromatographic retention time of 8-OH-dAdo from that of dGuo may be explained by differences in intramolecular hydrogen bonding. During reversed phase

HPLC, isomeric 8-OH-dAdo elutes later than dGuo probably because the 8-hydroxy group and oxygen on the sugar chain mask some of its polar groups, making 8-OH-dAdo more nonpolar than dGuo.

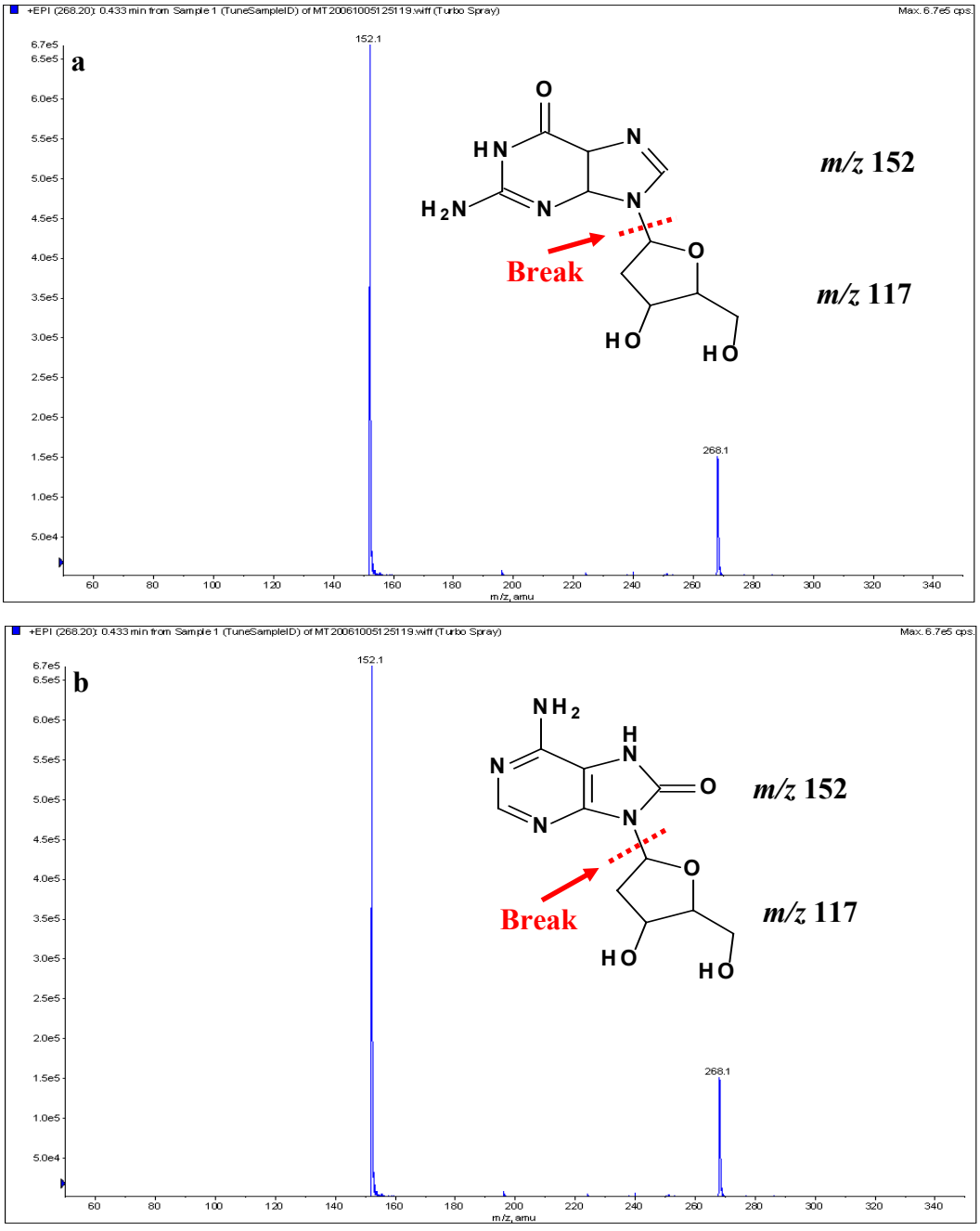

Figure 5. Positive product-ion spectra of dGuo (a, production-ion scan of $[M+H]^+$ at *m/z* 268) and 8-OH-dAdo (b, production-ion scan of $[M+H]^+$ at *m/z* 268).

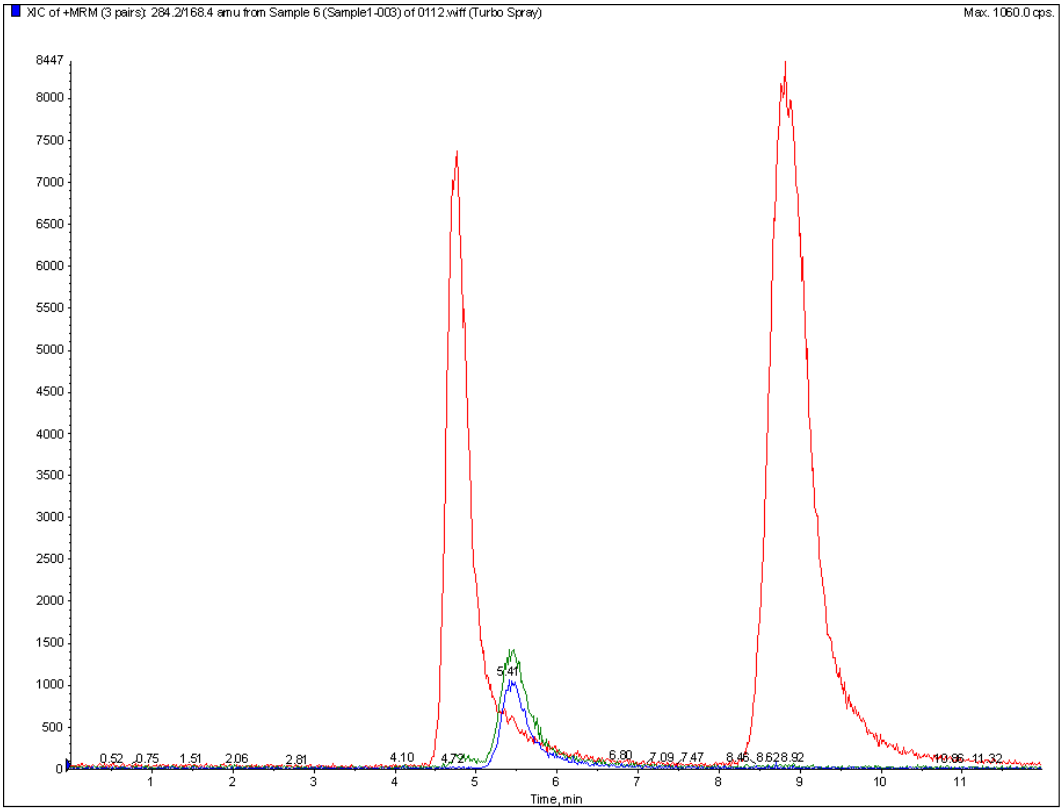

Figure 6. MRM chromatogram for an aqueous standard solution of dGuo (5.0 ng/ml, first red line), 8-OH-dGuo (3.0 ng/ml, blue line), [^{15}N5]-8-OH-dGuo (4.0 ng/ml, green line), and 8-OH-dAdo (5.0 ng/ml, last red line).

However, it was found in this study that 8-OH-dAdo was undetectable in the urine samples. It was due to the low concentration less than the limit of quantitation of our assay. Our finding is consistent with the observations by Weimann A et al. [Weimann A et al., 2001; Cadet J et al., 2002], but in contrast to the findings by GC/MS [Rehman A et al., 1998; Podmore ID et al., 1998], which could be due to artifacts from oxidation during derivatizaiton for GC/MS method and/or the GC run. Our finding is also in agreement with the fact that ·OH-mediated oxidation of the adenine moiety as inferred from the measured formation of 8-OH-dAdo is, at least, 10-fold lower than that of 8-OH-dGuo within both isolated and cellular DNA [Cadet J et al., 2002]. Therefore, only the concentration of 8-OH-dGuo in the urine samples was subsequently measured in our study.

6.3.2 Characteristics of SPE LC/MS/MS method for quantification of urinary 8-OH-dGuo

It is troublesome and unnecessary to completely remove the endogenous 8-OH-dGuo in the urine matrix. Therefore, for the accurate determination of 8-OH-dGuo in the urine samples, its stable isotope was used as an internal standard [Frelon S et al., 2000; Singh R et al., 2003].

In this study, urinary calibration curve for 8-OH-dGuo measurement was built on [^{15}N5]-8-OH-dGuo spiked urine samples. A linear urinary calibration curve, Y = 0.7126 X, with correlation coefficient (r^2) better than 0.995 was obtained in the selected concentration range from 1.0 to 10.0 ng/ml of [^{15}N5]-8-OH-dGuo (calibration samples at 1.0, 2.0, 4.0, 6.0, 8.0, 10.0 ng/ml were conducted in triplicate respectively). The calibration range was chosen to match the range of concentrations actually measured. The limit of quantitation (LOQ) of 1 ng/ml for [^{15}N5]-8-OH-dGuo was determined as the concentration that gave signal to noise (S/N) ratio of 10.5 in rat urine matrix. The adverse effects of interference from urine matrix could be clearly demonstrated by disappearance of the analyte peak for intact urine samples without SPE purification even after spiked with a high concentration of the 8-OH-dGuo standard solution (data not shown). The present recovery of 8-OH-dGuo after SPE was more than 65%.

In order to verify the diminishment of matrix effects after SPE treatment, the accuracy and recovery of the present method was ascertained by performing five replicate determinations of spiked [^{15}N5]-8-OH-dGuo in four different urine samples on the same day. The results are shown in Table 1. As can be seen, all spiked urine samples had [^{15}N5]-8-OH-dGuo recoveries of more than 90%, and the coefficient of

variation were less than 7.31% for the analysis of urinary [^{15}N5]-8-OH-dGuo.

Table 1. Accuracy and recovery of the SPE isotope dilution LC/MS/MS method for analyzing spiked [^{15}N5]-8-OH-dGuo in urine samples.

Added [^{15}N5]-8-OH-dGuo (ng/ml)	Measured value[1] (mean ± SD, ng/ml)	Recovery (%)	CV (%)
1.0	0.93 ± 0.07	93.0	7.31
5.0	5.12 ± 0.30	102.4	5.78

[1] There were four urine samples tested which were randomly selected from 6 rats from the respective control group, arsenite-, realgar- and orpiment-treated groups on the same day; 1.0 ng/ml [^{15}N5]-8-OH-dGuo was added to individual urine samples selected from day zero, and 5.0 ng/ml [^{15}N5]-8-OH-dGuo was added to individual urine samples chosen from day seven. Each sample was measured for five replicates.

The methodological reproducibility was examined by repeated measurements of [^{15}N5]-8-OH-dGuo spiked urine samples on the same day (intra-day) and on three consecutive days (inter-day) (Table 2). In all cases, the reproducibilities expressed by the coefficient of variation for [^{15}N5]-8-OH-dGuo were less than 10%.

Table 2. Reproducibility of the SPE isotope dilution LC/MS/MS method for analyzing spiked [^{15}N5]-8-OH-dGuo in urine samples.

Added [^{15}N5]-8-OH-dGuo (ng/ml)		Measured value[1] (mean ± SD, ng/ml)	CV (%)
1.0	**Intra-day**	0.96 ± 0.06	6.67
	Inter-day	0.93 ± 0.09	9.14
5.0	**Intra-day**	5.11 ± 0.26	5.00
	Inter-day	5.07 ± 0.42	8.22

[1] One urine sample for inter-day and intra-day studies was randomly selected among 24 rats from four groups on the same day; 1.0 ng/ml [^{15}N5]-8-OH-dGuo was added to the urine sample selected from day zero, and 5.0 ng/ml [^{15}N5]-8-OH-dGuo was added to the one chosen from day seven. Each sample was measured for five replicates.

The method developed in the present study is fast, robust, and easily automated to measure two and potentially more oxidative DNA products, and is thus applicable to large scale epidemiological studies. Furthermore, the possibility of using stable isotopically marked internal standard in mass spectrometry (isotope dilution) adds increased reliability to the method. A drawback of the method is that the equipment is expensive.

6.3.3 Concentrations of 8-OH-dGuo in rats urines before and after arsenic compounds administrations

Arsenic is unusual, as it is one of the few demonstrated human carcinogens for which carcinogenicity in laboratory animals has not been firmly established [Goeing PL et al., 1999; Basu A et al., 2001]. Recent studies have reported that some arsenic compounds such as dimenthylarsinic acid (DMA) induced elevated formation of 8-OH-dGuo in rodent animals [Wanibuchi H et al., 1997; Vijayaraghavan M et al., 2001; Patlolla AK and Tchounmou PB, 2005].

The concentrations of urinary 8-OH-dGuo for control and treated rats were measured by the established SPE isotope dilution LC/MS/MS method. In most studies, urinary 8-OH-dGuo levels were normalized with corresponding urinary creatinine levels [Dizdaroglu M, 1998; Li CS et al., 2005], which was adopted in this study. Table 3 lists the creatinine-adjusted urinary 8-OH-dGuo concentrations in the rats studied. A large inter-individual variation in terms of mean urinary 8-OH-dGuo concentrations was found, with the values of coefficient of variation (CV) up to 40%. Despite the relatively high CVs among the individuals, comparison analysis by one-way ANOVA showed that all arsenic compounds-treated rats had significantly higher mean urinary 8-OH-dGuo concentrations, more than 10 times, than the control rats

(control vs arsenite-treated group, $p < 0.001$; control vs realgar-treated group, $p < 0.001$; control vs orpiment-treated group, $p < 0.001$); at current dosages, arsenite released more urinary 8-OH-dGuo than both realgar ($p < 0.01$) and orpiment ($p < 0.01$), and there was no significant difference between realgar and orpiment on the induction of urinary 8-OH-dGuo ($p > 0.05$). Arsenite induced the elevated formation of urinary 8-OH-dGuo instantly at day 1 ($p < 0.01$) but not further increased thereafter ($p > 0.05$), so did realgar and orpiment. In addition, the mean urinary 8-OH-dGuo concentrations (ng/mg creatinine) of all intact rats including the control rats and experimental rats before treatment were in the range of 3.70 - 4.30, comparable with the reported values [Yasuhara T et al., 2007; Zhou H et al., 2006].

Table 3. Urinary 8-OH-dGuo production in rats before and after arsenic administrations, measured by current SPE LC/MS/MS method. Data are presented as mean ± SD (n = 6).

Duration	Urinary 8-OH-dGuo (ng/mg creatinine)			
	Control group	Arsenite administration	Realgar administration	Orpiment administration
Day 0	3.86 ± 1.06	3.94 ± 1.19	4.00 ± 1.23	3.73 ± 1.19
Day 1	3.94 ± 1.22	57.44 ± 24.55	40.26 ± 17.39	42.05 ± 18.92
Day 2	4.27 ± 1.26	60.89 ± 20.80	43.43 ± 17.16	44.19 ± 17.67
Day 3	4.10 ± 1.28	59.78 ± 24.12	42.41 ± 18.74	45.70 ± 17.64
Day 4	3.75 ± 1.31	61.23 ± 25.83	46.89 ± 18.19	42.40 ± 18.28
Day 5	3.90 ± 1.13	63.19 ± 19.40	43.99 ± 18.37	44.66 ± 18.92
Day 6	3.95 ± 1.15	58.06 ± 25.27	46.72 ± 17.04	45.00 ± 18.19
Day 7	4.07 ± 1.20	61.78 ± 19.10	42.31 ± 17.78	47.33 ± 17.94
Day 8	3.94 ± 1.18	59.93 ± 24.38	44.64 ± 15.52	47.80 ± 18.30
Day 9	3.82 ± 1.13	64.49 ± 23.08	44.99 ± 16.67	44.96 ± 17.98
Day 10	4.01 ± 1.23	60.11 ± 26.31	47.00 ± 18.41	43.99 ± 18.07
Day 11	3.78 ± 1.24	59.91 ± 22.49	49.30 ± 17.19	42.38 ± 17.98
Day 12	3.86 ± 1.32	62.30 ± 19.40	45.09 ± 17.74	45.80 ± 18.55
Day 13	4.19 ± 1.13	63.17 ± 19.18	46.38 ± 16.96	46.01 ± 18.55
Day 14	4.19 ± 1.16	60.38 ± 22.38	49.22 ± 18.85	48.37 ± 17.85

After oral ingestion, over 90% of inorganic arsenics are absorbed [Le XC et al., 1994]. The ingested inorganic arsenics undergo methylation metabolism in the liver and about 60-70% is excreted in the urine [Vahter M, 2002]. The rest may then be deposited in other tissues. Since arsenic is rapidly metabolized and excreted into urine, detection of arsenic in urine thus has been used as a marker of recent arsenic exposure [Hwang YH et al., 1997]. Therefore, in the present study, the urinary arsenic recovery in rats after the arsenic compounds administrations was measured as shown in Table 4. In order to adjust the variability of urinary volume among individuals, the urinary arsenic concentrations were also corrected with corresponding urinary creatinine concentrations.

Table 4. The urinary arsenic recovery in rats after the arsenic compounds administrations. Data are presented as mean ± SD (*n* = 6).

Duration	Arsenic urinary recovery (μg/mg creatinine)		
	Arsenite administration	Realgar administration	Orpiment administration
Day 1	70.38 ± 21.01	77.88 ± 22.25	67.75 ± 22.54
Day 2	71.62 ± 22.69	78.21 ± 23.04	68.21 ± 19.47
Day 3	71.93 ± 22.92	78.78 ± 25.00	68.96 ± 19.01
Day 4	72.99 ± 21.78	78.98 ± 25.28	68.76 ± 20.96
Day 5	73.21 ± 19.76	77.62 ± 23.45	70.23 ± 20.16
Day 6	73.27 ± 20.64	79.01 ± 23.10	69.89 ± 20.45
Day 7	74.01 ± 19.85	78.21 ± 24.93	70.21 ± 20.60
Day 8	74.17 ± 19.89	79.01 ± 25.84	70.33 ± 21.38
Day 9	75.64 ± 22.09	78.21 ± 23.26	69.41 ± 20.86
Day 10	75.71 ± 20.14	79.37 ± 23.77	69.21 ± 20.08
Day 11	77.21 ± 20.42	80.01 ± 23.77	70.89 ± 20.66
Day 12	77.88 ± 26.74	78.54 ± 23.81	69.81 ± 19.59
Day 13	78.21 ± 24.73	78.14 ± 24.49	70.26 ± 20.03
Day 14	78.32 ± 24.56	79.61 ± 23.28	71.77 ± 19.21

It should be mentioned that the urinary arsenic concentrations in all intact rats including the control and experimental rats before arsenic dosing were too low to be

detectable under current instrumental conditions. Theoretically, urinary arsenic recovery should gradually increase with daily arsenic compounds intake, because the reported biological half-life for arsenic has been estimated to between 1 to 3 days [Hwang YH et al., 1997]. However, in this study, from the statistical point of view, similar increase of daily urinary arsenic recovery with time (~70 μg/mg creatinine) were not found for each study group ($p > 0.05$). This result probably was due to the fact that the doses used were so low that they would be mostly and promptly eliminated by rats within 24 h. Dosages were 20 mg pure drug/kg body weight for realgar and orpiment suspensions, and 10 mg arsenite/kg body weight for arsenite solution. About 50% of daily administered arsenite was excreted into the urine, compared to around 20% of daily administered realgar and orpiment. The relatively lower urinary arsenic recoveries for realgar and orpiment suspensions when compared to arsenite solution probably were resulted from the extra dissolution step involved with the suspending particles.

Besides urinary excretion, the real body distribution and elimination by other pathways such as feces except urine of daily dosed arsenic compounds were not determined in the present study. Table 3 showed that consecutive administration of arsenicals for 15 days did not significantly change the production of 8-OH-dGuo, the indicator of the whole body oxidative damage rate. Data in Table 3 and Table 4 indicated there were likely positive correlations between urinary arsenic levels and corresponding urinary 8-OH-dGuo levels in each study group. Therefore, the urinary arsenic-adjusted 8-OH-dGuo concentrations were also calculated and listed in Table 5. Comparison analysis again showed similar results to what have been obtained with the creatinine-adjusted 8-OH-dGuo concentrations. That is, arsenite triggered more 8-OH-dGuo production than realgar ($p < 0.001$) and orpiment ($p < 0.001$), but, in

contrast, there was significant difference between realgar and orpiment on the formation of 8-OH-dGuo ($p < 0.001$). It might be concluded that arsenite caused more oxidative DNA damage, and therefore, was more toxicogenic than both realgar and orpiment.

Table 5. The urinary arsenic-corrected 8-OH-dGuo concentrations. Data are presented as mean ± SD ($n = 6$).

Duration	Urinary 8-OH-dGuo (ng/μg urinary arsenic)		
	Arsenite administration	Realgar administration	Orpiment administration
Day 1	0.86 ± 0.21	0.55 ± 0.29	0.58 ± 0.16
Day 2	0.87 ± 0.21	0.54 ± 0.13	0.62 ± 0.13
Day 3	0.83 ± 0.21	0.51 ± 0.12	0.64 ± 0.12
Day 4	0.83 ± 0.22	0.59 ± 0.16	0.58 ± 0.14
Day 5	0.86 ± 0.10	0.54 ± 0.13	0.60 ± 0.16
Day 6	0.76 ± 0.29	0.57 ± 0.07	0.61 ± 0.13
Day 7	0.83 ± 0.15	0.52 ± 0.12	0.65 ± 0.10
Day 8	0.77 ± 0.21	0.56 ± 0.08	0.66 ± 0.11
Day 9	0.86 ± 0.22	0.57 ± 0.08	0.62 ± 0.12
Day 10	0.75 ± 0.25	0.57 ± 0.09	0.61 ± 0.13
Day 11	0.77 ± 0.14	0.61 ± 0.11	0.58 ± 0.22
Day 12	0.82 ± 0.12	0.55 ± 0.10	0.65 ± 0.18
Day 13	0.83 ± 0.17	0.58 ± 0.07	0.67 ± 0.22
Day 14	0.85 ± 0.45	0.60 ± 0.10	0.68 ± 0.20

In order to further examine whether there are positive correlations existing between urinary 8-OH-dGuo and urinary arsenic levels as assumed earlier, a linear regression analysis was used. Figure 7 gives correlations between urinary arsenic recovery values and urinary 8-OH-dGuo concentrations in each experimental group. Positive correlations were obtained (arsenite-treated group, $n = 84$, $r^2 = 0.5946$, $p < 0.001$; realgar-treated group, $n = 84$, $r^2 = 0.7883$, $p < 0.001$; orpiment-treated group, $n = 84$, $r^2 = 0.8426$, $p < 0.001$), in agreement with the reported findings [Fujino Y et al., 2005; Yamauchi H et al., 2004].

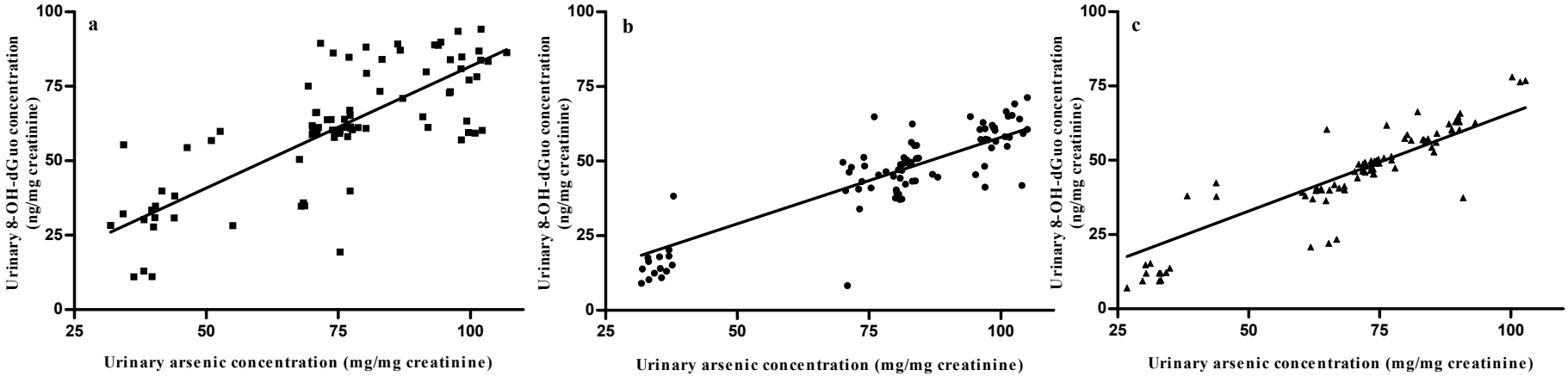

Figure 7. Correlation between urinary 8-OH-dGuo and urinary arsenic recovery levels in three arsenic compounds-treated groups (a, arsenite-treated group; b, realgar-treated group; c, orpiment-treated group.).

It should be mentioned that so far the measured urinary 8-OH-dGuo values in both intact animal and healthy human samples were quite variable even after normalized with creatinine. Some reported results are summarized in Table 6. That can be explained by the variability between animals and humans, the different methodology used for 8-OH-dGuo and creatinine analysis, the different sample extraction and cleanup procedures performed and by the reduced number of experiments done. In general, the range of the 8-OH-dGuo levels analyzed differs 10-1000-fold depending on the analysis method used [Kasai H, 1997].

Table 6. Summary of recent reported urinary 8-OH-dGuo in intact animal and healthy human samples.

Animals	8-OH-dGuo (ng/mg creatinine)	Approach	Ref.
Male SD rats, 8 weeks, 200-250g	2.0 ± 0.4	ELISA	Yasuhara T et al., 2007
Male SD rats, 230-250g	7.05 ± 1.49	ELISA	Zhou H et al., 2006
Male Wistar rats, 10-11 weeks	3.7 ± 0.6	HPLC-ECD	Svoboda P and Kasai H, 2004
Male Wistar rats, 10 weeks, 200 g around	89.34 ± 27.34	HPLC-ECD	De Martinis BS and Bianchi MD, 2001
Male Wistar rats, 10 weeks, 200g around	89.3 ± 23.7/75.9 ± 15.3	HPLC-ECD	De Martinis BS and de Lourdes Piers Bianchi M, 2002
Male Wistar rats, 10-11 weeks	3.7 ± 0.6	HPLC-ECD	Svoboda P and Kasai H, 2004
Male Wistar rats, 8 weeks, 240 g around	10.89 ± 2.59	ELISA	Sakamoto W et al., 2003
Male Long-Evans pigmented rats, 50-55 days, 226-250 g	22.2 ± 6.8	ELISA	Van Campen LE et al., 2002
49 male healthy workers, 44.7 years	5.69 ± 3.34 14.69 ± 12.84	LC/MS/MS ELISA	Hu CM et al., 2004
3 healthy persons	3.8 ± 1.66	LC/MS/MS	Sabatimi L et al., 2005

6.4 Conclusions

The SPE isotope dilution LC/MS/MS method for quantitative analysis of urinary 8-OH-dGuo was established. Practical application of the present method on the analysis of association of arsenic intake and the biomarkers of DNA oxidative damage imply that the evaluation of such biomarkers in body after invasion is an effective method to understand the *in vivo* response to potential drug candidate. Urinary 8-OH-dGuo analysis could be used to assess the responses to therapy and help to know the effect of the therapy for the next treatment. To our knowledge, this is the first study concerning the potential oxidative stress caused by realgar and orpiment. Our findings pointed out in certain dose range, arsenite could cause more oxidative DNA damage indicated by the induction of more urinary 8-OH-dGuo than realgar and orpiment. It has been recognized that increased levels of DNA base oxidation products such as 8-OH-dGuo do not always lead to malignancy [Halliwell B, 2007]. The nature of the DNA damages and the effectiveness of their subsequent repair could determine the outcomes.

CHAPTER SEVEN

Conclusions and future studies

CHAPTER SEVEN

7.1 Final conclusions

For identifying the components in the alkali extracts of realgar and orpiment, a CZE assay with indirect UV detector by using the PDC/CTAOH as a BGE was established. The developed CZE method provided excellent linearity, intra-day and inter-day variation, sensitivity to identify the components in the alkali extracts of realgar and orpiment. The main components in both extracts were found to be iAs^{III} and iAs^{V}. The finding also showed that the method was suitable for simultaneous separation and determination of the inorganic and organic arsenic compounds, including arsenite, arsenate, MMA^{V} and DMA^{V}. The method could be applied to standardize pharmaceutical arsenic formulations. Since the major components in the alkali extracts of realgar and orpiment were arsenite and arsenate instead of the intact realgar and orpiment, alkali extraction could not be an appropriate approach to solubilize realgar/orpiment powder. The findings thus suggested that other approaches should be employed to improve the water-solubility of realgar and orpiment.

In order to improve the water-solubility of realgar and orpiment, cryo-grinding technique was used to mechanically reduce their particle sizes to nanograde with the assistance of PVP and/or SDS. The presence of PVP and/or SDS was found not only to enhance the grinding efficiency but also to stabilize realgar/orpiment colloidal solution. The adsorption of PVP and/or SDS onto the surface of the realgar/orpiment particle was able to form a coating, that provided steric and/or ionic barrier to prevent aggregation and/or agglomeration.

The cytotoxicity of the realgar nanoparticle preparations, i.e. realgar ground alone, R/PVP, R/SDS, R/PVP/SDS, on the selected cell lines were evaluated. In *in vitro* study, the realgar nanoparticle preparations were used to treat some human gynecological cancer cell lines including HeLa, CI80-13S, OVCAR, and OVCAR-3,

and significant anti-proliferation effects comparable to arsenic trioxide were observed, whereas they did not cause much cytotoxicity on two control human fibroblast cell lines, MRC-5 and HF. Through cell cycle analysis, apoptosis induced by realgar nanoparticles was concluded depending on the appearance of the characterized sub-G_1 phase in cell cycle histograms. The induction of apoptosis was further confirmed by the morphological observation and DNA fragmentation assay. Similar results were found when using the orpiment nanoparticle preparations (orpiment ground alone and O/PVP/SDS) to treat the HaLa and OVCAR-3 cells.

In *in vivo* studies, the extent of absorption and bioavailability were estimated based on the urinary recovery of arsenic. After oral administrations of the ground realgar and orpiment preparations, the urinary arsenic excretions in SD rats were significantly increased when compared to those in rats after oral administrations of the corresponding original realgar and orpiment powders. The improvement in absorption and bioavailability was attributed to the particle size reduction of realgar and orpiment. Both realgar and orpiment have been considered to be less toxic compounds in arsenic superfamily. The usage of realgar and orpiment nanoparticles could overcome the usage limitations associated with the poor water-solubility and the consequent poor absorption and bioavailability and allow them being used clinically.

In order to clearly understand the possible underlying action mechanisms of realgar and orpiment and arsenite, microarray technique was used. The altered gene expression profiles of HeLa cells after these arsenical treatments were different. These suggested that their effects were very complicated and compound-dependent. Further confirmation studies would be required to verify the microarray findings before the exact mechanisms of action could be proposed.

Although both realgar and orpiment have long been considered as mild-toxic

compounds, the partial reason of such classification probably is due to their poor water-solubility and the consequent low absorption instead of their intrinsic toxicity. In recent years, the urinary 8-OH-dGuo was used as the most commonly acceptable biomarker of oxidative DNA damage. The oxidative DNA damage has been proved to be associated with many types of diseases. Therefore, it is important to find out the association of the arsenical intake and the resulting urinary 8-OH-dGuo level, an indicator of oxidative DNA damage by the arsenicals. For this purpose, a LC/MS/MS method for quantitative analysis of urinary 8-OH-dGuo was established. By using the established LC/MS/MS method, urinary 8-OH-dGuo levels in rats after oral administrations of arsenite, realgar, and orpiment were measured. In terms of the urinary 8-OH-dGuo levels, the findings suggested that both realgar and orpiment could cause oxidative DNA damage to the similar extent, but slightly less than that caused by arsenite.

7.2 Proposed future studies

In this study, the grinding yield of the cryo-grinding approach is low. Therefore, it warrants increasing the grinding efficiency, e.g., the selection and optimization of stabilizers such as polymers and surfactants for further improvement of the productivity. With suitable solvents for recrystalizing realgar and orpiment, nanosized realgar and orpiment particles could be produced chemically. Generally, chemical method has advantages over mechanical method, as the former approach gives more homogeneous and controllable particle distribution. The productivity of realgar and orpiment nanoparticles could also be easily enhanced by the chemical method. However, the potential toxicity of the solvent used could be a concern.

The multiple mechanisms of action of realgar and orpiment have not yet been

elucidated in this study. It warrants putting more efforts in this area, because understanding of the mechanisms provides the foundation for the potential combination therapies for better treatment outcomes. The preliminary microarray study gave some valuable information on some most affected cancer-related genes regulated by realgar and orpiment. Future study could focus on these genes and verify the involvement of these genes in the activities.

In this study, the urinary arsenic recovery was used to reflect the extent of the absorption and bioavailability of realgar and orpiment. However, the disposition and metabolism profiles of realgar and orpiment after oral administration are unknown. It would be especially important to study the metabolism and tissue distribution of arsenicals when they are used as therapeutics, and the relationship of DMPK profiles to their therapeutic efficacy and toxicity.

BIBLIOGRAPHY

BIBLIOGRAPHY

Abernathy CO, Calderon RL, Chappell WR, (1997), Arsenic: Exposure and Health Effects, Chapman & Hall, London, p. 363.

Akao Y, Nakagawa Y, Akiyama K, (1999), Arsenic trioxide induces apoptosis in neuroblastoma cell lines through the activation of caspase 3 in vitro, FEBS lett., 455: 59-62.

Akay C, Thomas C 3rd, Gazitt Y, (2004), Arsenic trioxide and paclitaxel induce apoptosis by different mechanisms, Cell Cycle, 3: 324-334.

Alison MR, Sarraf CE, (1995), Apoptosis: regulation and relevance to toxicology, Hum Exp Toxicol., 14: 234-247.

Amendola R, Martinez R, Negroni A, Venturelli D, Tanno B, Calabretta B, Raschella G, (2001), DR-nm23 expression affects neutoblastoma cell differentiation, integrin expression, and adhesion characteristics, Med Pediatr Oncol, 36: 93-96.

Amendola R, Martinez R, Negroni A, Ventruelli D, Tanno B, Calabretta B, Raschella G, (1997), DR-nm23 gene expression in neuroblastoma cells: relationship to integrin expression, adhesion characteristics, and differentiation, J Natl Cancer Inst, 89: 1300-1310.

Anderson KC, Boise LH, Louie R, Waxman S, (2002), Arsenic trioxide in multiple myeloma: rationale and future directions, Cancer J., 8: 12-25.

Andrew AS, Warren AJ, Barchowsky A, Temple KA, Klei L, Soucy NV, O'Hara KA, Hamilton JW, (2003), Genomic and proteomic profiling of responses to toxic metals in human lung cells, Environ Health Perspect., 111: 825-835.

Argos M, Kibriya MG, Parvez F, Jasmine F, Rakibuz-Zaman M, Ahsan H, (2006), Gene expression profiles in peripheral lymphocytes by arsenic exposure and skin lesion status in a Bangladeshi population, Cancer Epidemiol Biomarkers Prev., 15: 1367-1375.

Barchowsky A, Roussel RR, Klei LR, James PE, Ganju N, Smith KR, Dudek EJ, (1999), Low levels of arsenic trioxide stimulate proliferative signals in primary vascular cells without activating stress effector pathways, Toxicol Appl Pharmacol., 159: 65-75.

Basu A, Mahata J, Gupta S, Giri AK, (2001), Genetic toxicology of a paradoxical human carcinogen, arsenic: a review, Mutat Res., 488: 171-194.

Benramdane L, Bressolle F, Vallon JJ, (1999), Arsenic speciation in humans and food products: a review, J Chromatogr Sci., 37: 330-344.

Bittner B, Mountfield RJ, (2002), Intravenous administration of poorly soluble new drug entities in early drug discovery: The potential impact of formulation on pharmacokinetic parameters, Cur Opin Drug Discov, Dev. 5: 59-71.

BIBLIOGRAPHY

Bode AM, Dong ZG, (2002), The paradox of arsenic: molecular mechanisms of cell transformation and chemotherapeutic effects, Crit Rev Oncol Hematol., 42: 5-24.

Boffetta P, (2006), Human cancer from environmental pollutants: the epidemiological evidence, Mutat Res., 608: 157-162.

Cadet J, D'Ham C, Douki T, Pouget JP, Ravanat JL, Sauvaigo S, (1998), Facts and artifacts in the measurement of oxidative base damage to DNA, Free Radic Res., 29: 541-550.

Cadet J, Douki T, Frelon S, Sauvaigo S, Pouget JP, Ravanat JL, (2002), Assessment of oxidative base damage to isolated and cellular DNA by HPLC-MS/MS measurement, Free Radic Biol Med., 33: 441-449.

Candy AC, Hanley JE, Susten AS, (1997), ATSDR science panel on bioavailability of mercury in soil-lessons learned, Risk Anal., 17: 527-532.

Casas S, Ollila J, Aventin A, Vihinen M, Sierra J, Knuutila S, (2003), Changes in apoptosis-related pathways in acute myelocytic leukemia, Cancer Genet Cytogenet, 146: 89-101.

Cavalieri LF, Bendich A, (1950), The ultraviolet absorption spectra of pyrimidines and purines, J Am Chem Soc., 72: 2587-2594.

Chan JY, Siu KP, Fung KP, (2006), Effect of arsenic trioxide on multidrug resistant hepatocellular carcinoma cells, Cancer Lett., 236: 250-258.

Chan MH, Ng KF, Szeto CC, Lit LC, Chow KM, Leung CB, Suen MW, Li PK, Lam CW, (2004), Effect of a compensated Jaffe creatinine method on the estimation of glomerular filtration rate, Ann Clin Biochem., 41: 482-484.

Chen CJ, Chen CW, Wu MM, Kuo TL, (1992), Cancer potential in liver, lung, bladder and kidney due to ingested inorganic arsenic in drinking water. Br J Cancer, 66: 888-892.

Cheng KC, Cahill DS, Kasai H, Nishinura S, Loeb LA, (1992), 8-Hydroxyguanine, an abundant form of oxidative DNA damage, causes G $\rightarrow$ T and A $\rightarrow$ C substitutions, J Biol Chem., 267: 166-172.

Chen SY, Liu SX, Li XM, (2002), In vitro study on realgar induced apoptosis of all-trans acid resistant acute promyelocytic leukemia cell line (MR2), Zhongguo Zhong Yao Za Zhi (中国中药杂志), 27: 211-215.

Chen WB, Lenschow W, Tiede K, Fischer JW, Kalthoff H, Ungefroren H, (2002), Smad4/DPC4-dependent regulation of bioglycan gene expression by transforming growth factor-β in pancreatic tumor cells, J Biol Chem, 277: 36118-35128.

Chen X, Young TJ, Sarkari M, Williams RO, Johnston KP, (2002), Preparation of

cyclosporine A nanoparticles by evaporative precipitation into aqueous solution, Int J Pharm., 242: 3-14.

Chen YC, Lin-Shiau SY, Lin JK, (1998), Involvement of reactive oxygen species and caspase 3 activation in arsenite-induced apoptotis, J Cell Physiol., 177: 324-333.

Chen Z, Chen GQ, Shen ZX, Chen SJ, Wang ZY, (2001), Treatment of acute promyelocytic leukemia with arsenic compounds: in vitro and in vivo studies, Semin Hematol., 38: 26-36.

Cheung WM, Chu PW, Kwong YL, (2006), Effects of arsenic trioxide on the cellular proliferation, apoptosis and differentiation of human neuroblastoma cells, Cancer Lett., [Epub ahead of print].

Chow SK, Chan JY, Fung KP, (2004), Inhibition of cell proliferation and the action mechanisms of arsenic trioxide on human breast cancer cells, J Cell Biochem., 93: 173-187.

Chun YJ, Park IC, Park MJ, Woo SH, Hong SI, Chung HY, Kim TH, Lee YS, Rhee CH, Lee SJ, (2002), Enhancement of radiation response in human cervical cancer cells in vitro and in vivo by arsenic trioxide, FEBS Lett., 519: 195-200.

Cooke MS, Evans MD, Dizdaroglu M, Lunec J, (2003), Oxidative DNA damage: mechanisms, mutation, and disease, FASEB J., 17: 1195-1214.

Corsini E, Asti L, Viviani B, Marinovich M, Galli CL, (1999), Sodium arsenate induces overproduction of interleukin-1alpha in murine keratinocytes: role of mitochondria, J Invest Dermatol., 113: 760-765.

Costantino HR, Firouzabadian L, Hogeland K, Wu C, Beganski C, Carrasquillo KG, Cordova M, Griebenow K, Zale SE, Tracy MA, (2000), Protein spray-freeze drying. Effect of atomization conditions on particle size and stability, Pharm Res., 17: 1374-1383.

Crompton M, (1999), The mitochondrial permeability transition pore and its role in cell death, Biochem J, 341: 233-249.

Cui X, Kobayashi Y, Hayakawa T, Hirano S, (2004), Arsenic speciation in bile and urine following oral and intravenous exposure to inorganic and organic arsenics in rats, Toxicol Sci., 82: 478-487.

Dai J, Weinberg RS, Waxman S, Jing Y, (1999), Malignant cells can be sensitized to undergo growth inhibition and apoptosis by arsenic trioxide through modulation of the glutathione redox system, Blood, 93: 268-277.

Dang C, Gottschling M, Manning K, O'Currain E, Schneider S, Sterry W, Stockfleth E, Nindl I, (2006), Identificaiton of dysregulated genes in cutaneous squamous cells carcinoma, Oncol Rep, 16: 513-519.

BIBLIOGRAPHY

Davis A, Ruby MV, Bergestrom PD, (1992), Bioavailability of arsenic and lead in soils from butte, Montana, mining district, Environ Sci and Tochnol., 26: 461-468.

de Garavilla L, Peltier N, Merisko-Liversidge E, (1996), Controlling the acute hemodynamic effects associated with IV administration of particulate drug dispersions in dogs, Drug Develop Res, 37: 86-96.

Degos L, Wang ZY, (2001), All trans retinoic acid in acute promyelocytic leukemia, Oncogene, 20: 7140-7145.

Del Razo LM, Quintanilla-Vega B, Brambila-Colombres E, Calderon-Aranda ES, Manno M, Albores A, (2001), Stress proteins induced by arsenic, Toxicol Appl Pharmacol., 177: 132-148.

De Martinis BS, de Lourdes Pires Bianchi M, (2002), Methodology for urinary 8-hydroxy-2'-deoxyguanosine analysis by HPLC with electrochemical detection, Pharmacol Res, 46: 129-131.

De Martinis BS, Bianchi MD, (2001), Effect of vitamin C supplementation against cisplatin-induced toxicity and oxidative DNA damage in rats, Pharmacol Res, 44: 317-320.

Deng Y, Xu HB, Huang KX, Yang XL, Xie CS, Wu J, (2001), Size effects of realgar particles on apoptosis in a human umbilical vein endothelial cell line: ECV-304, Pharmacol Res., 44: 513-518.

Desai MP, Labhasetwar V, Amidon GL, Levy RJ, (1996), Gastrointestinal uptake of biodegradable microparticless: effect of particles size, Pharm Res., 13: 1838-1845.

Dizdaroglu M, (1998), Facts about the artifacts in the measurement of oxidative DNA base damage by gas chromatography-mass spectrometry, Free Radic Res., 29: 551-563.

Dizdaroglu M, Jaruga P, Rodriquez H, (2001), Measurement of 8-hydroxy-2'-deoxyguanosine in DNA by high-performance liquid chromatography-mass spectrometry: comparison with measurement by gas chromatography-mass spectrometry, Nucleic Acids Res, 29: E12 (8 pages).

Do B, Alet P, Pradeau D, Poupon J, Guilley-Gaillot M, Guyon F, (2000), On-line reversed-phase liquid chromatography hydride generation emission spectrometry: speciation of arsenic in urine of patients intravenously treated with As_2O_3, J Chromatogr B Biomed Sci Appl., 740:179-186.

Dong JT, Luo XM, (1993), Arsenic-induced DNA-strand breaks associated with DNA-protein crosslinks in human fetal lung fibroblasts, Mutat Res., 302: 97-102.

Dopp E, Hartmann LM, von Recklinghausen U, Florea AM, Rabieh S, Zimmermann

U, Shokouhi B, Yadav S, Hirner AV, Retternmeier AW, (2005), Forced uptake of trivalent and pentavalent methylated and inorganic arsenic and its cyto-/genotoxicity in fibroblasts and hepatoma cells, Toxicol Sci., 87: 46-56.

Douer D, (2006), ATO: the forefront of APL treatment, Blood, 107: 2588-2589.

Du YH and Ho PC, (2001), Arsenic compounds induce cytotoxicity and apoptosis in cisplatin-sensitive and –resistant gynecological cancer cell lines, Cancer Chemother Pharmacol., 47: 481-490.

Duker AA, Carranza EJ, Hale M, (2005), Arsenic geochemistry and health, Environ Int, 31: 631-641.

Elmore S, (2007), Apoptosis: a review of programmed cell death, Toxicol Pathol., 35: 495-516.

Engler RL, (1991), Adenosine: the signal of life?, Circulation, 84: 951-954.

Foa V, Colombi A, Maroni M, Buratti M, Calzaferri G, (1984), The speciation of the chemical forms of arsenic in the biological monitoring of exposure to inorganic arsenic, Sci Total Environ., 34: 241-259.

Foret F, Krivankova L, Bocek P (1993), Capillary zone electrophoresis, VCH, Weinheim, ch. 3, p.13.

Foret F, Fanali S, Nardi A, Bocek P, (1990), Capillary zone electrophoresis of rare earth metals with indirect UV absorbance detection, Electrophoresis, 11: 780-783.

Francesconi KA and Kuehnelt D, (2004), Determination of arsenic species: a critical review of methods and applications, 2000-2003, Analyst, 129: 373-395.

Frankenberger WT Jr., (2002a), Environmental Chemistry of Arsenic, Marcel Dekker, Inc., New York, p.22.

Frankenberger WT Jr., (2002b), Environmental Chemistry of Arsenic, Marcel Dekker, Inc., New York, p.55.

Frankenberger WT Jr (2002c), Environmental Chemistry of Arsenic, Marcel Dekker, NY, ch. 4, p. 96.

Frankenberger WT Jr (2002d), Environmental Chemistry of Arsenic, Marcel Dekker, NY, ch. 4, p. 97.

Freeman GB, Schoof RA, Ruby MV, Davis AO, Dill JA, Lia SC, Lapin CA, Bergstrom PD, (1995), Bioavailability of arsenic in soil and house dust impacted by smelter activities following oral administration in cynomolgus monkeys, Fund Appl Toxicol., 28: 215-222.

Frei K, Ambar B, Adachi N, Yonekawa Y, Fontana A, (1998), Ex vivo malignant

glioma cells are sensitve to Fas (CD95/APO-1) ligand-mediated apoptosis, J Neuroimmunol., 87: 105-113.

Frelon S, Douki T, Ravanat JL, Pouget JP, Tornabene C, Cadet J, (2000), High-performance liquid chromatography--tandem mass spectrometry measurement of radiation-induced base damage to isolated and cellular DNA, Chem Res Toxicol., 13: 1002-1010.

Fujino Y, Guo X, Liu J, Matthews IP, Kusuda T, Shirane K, Wu K, Kasai H, Miyatake M, Tanabe K, Kusuda T, Yoshimura T, (2005), Japan inner Mongolia arsenic pollution study group, J Exposure Anal Environ Epidemiol., 15: 147-152.

Fukuoka J, Fujii T, Shih JH, Dracheva T, Meerzaman D, Player A, Hong K, Settnek S, Gupta A, Buetow K, Hewitt S, Travis WD, Jen J, (2004), Chromatin remodeling factors and BRM/BRG1 expression as prognostic indicators in non-small cell lung cancer, Clin Cancer Res, 10: 4314-4324.

Garban HJ, Bonavida B, (1999), Nitric oxide sensitizes ovarian tumor cells to Fas-induced apoptosis, Cynecol Oncol., 73: 257-264.

Givant-Horwitz V, Davidson B, Reich R, (2005), Laminin-induced signaling in tumor cells, Cancer Lett, 223: 1-10.

Goering PL, Aposhian HV, Mass MJ, Cebrian M, Beck BD, Waalkes MP, (1999), The enigma of arsenic carcinogenesis: role of metabolism, Toxicol Sci., 49: 5-14.

Goyer RA, (1991), Toxic Effects of Metals, 4th edition, McGraw-Hill, New York.

Groopman J, Ellman L, (1979), Acute promyelocytic leukemia, Am J Hematol, 7: 395-408.

Haga N, Fujita N, Tsuruo T, (2005), Involvement of mitochondrial aggregation in arsenic trioxide-induced apoptosis in human glioblastoma cells, Cancer Sci., 96: 825-833.

Halicka HD, Smolewski P, Darzynkiewcz Z, Dai W, Traganos F, (2002), Arsenic trioxide arrests cells early in mitosis leading to apoptosis, Cell Cycle, 1: 201-209.

Halliwell B, Gutteridge JM, (1990), Role of free radicals and catalytic metal ions in human disease: an overview, Methods Enzymol., 186: 1-85.

Halliwell B, (2007), Oxidative stress and cancer: have we moved forward? Biochem J., 401: 1-11.

Hao HY, Teng ZP, Lu DP, (2002), Study on the role of PML-RAPalpha and RARalpha fusion protein in NB4 cell apoptosis induced by arsenic trisulfide, Zhongguo Shi Yan Xue Ye Xue Za Zhi (中国实验血液学杂志), 10: 108-111.

BIBLIOGRAPHY

Harris GK, Shi X, (2003), Signaling by carcinogenic metals and metal-induced reactive oxygen species, Mutat Res., 533: 183-200.

He B, Jiang GB, Xu X, (2000), Arsenic speciation based on ion exchange high-performance liquid chromatography hyphenated with hydride generation atomic fluorescence and on-line UV photo oxidation, Fresenius J Anal Chem., 368: 803-808.

Hedlund TE, Duke RC, Schleicher MS, Miller JG, (1998), Fas-mediated apoptosis in seven human prostate cancer cell lines: correlation with tumor stage, Prostate, 36: 92-101.

Hei TK, Filipic M, (2004), Role of oxidative damage in the genotoxicity of arsenic, Free Radical Biol Med., 37: 574-581.

Helbock HJ, Beckman KB, Shigenaga MK, Walter PB, Woodall AA, Yeo HC, Ames BN, (1998), DNA oxidation matters: The HPLC-electrochemical detection assay of 8-oxo-deoxyguanosine and 8-oxo-guanine, Proc Natl Acad Sci USA, 95: 288-293.

Heyne N, Benohr P, Muhlbauer B, Delabar U, Risler T, Osswald H, (2004), Regulation of renal adenosine excretion in humans-role of sodium and fluid homeostasis, Nephrol Dial Transplant, 19: 2737-2741.

Hitchens MR, Robbins PD, (2003), The role of the transcription factor DP in apoptosis, Apoptosis, 8: 461-468.

Hollins JG, Charbonneau SM, Tam GK, Bryce F, Ridgeway JM, Wiles RF, (1979), Whole body retention and excretion of arsenic acid [^{74}As] in the adult beagle dog, Toxicol Lett., 4: 7-13.

Hopenhayn-Rich C, Biggs ML, Smith AH, (1998), Lung and kidney cancer mortality associated with arsenic in drinking water in Cordoba, Argentina, Int J Epidemiol., 27: 561-569.

Huang C, Ma WY, Li J, Dong Z, (1999), Arsenic induces apoptosis through a c-Jun NH_2-terminal kinase-dependent, p53-independent pathway, Cancer Res., 59: 3053-3058.

Huang ME, Ye YC, Chen SR, Chai JR, Lu HX, Zhoa I, Gu IJ, Wang ZY, (1988), Use of all-trans-retinoic acid in the treatment of acute promyelocytic leukemia, Blood, 72: 567-572.

Huang SC, Lee TC, (1998), Arsenite inhibits mitotic division and perturbs spindle danamics in HeLa S3 cells, Carcinogenesis, 19:889-896.

Huang SL, Guo AX, Xiang Y, Wang XB, Lin HX, Fu L, (1995), Clinical study on the treatment of acute promyelocytic leukemia mainly with composite indigo naturalis tablets, 中华血液学杂志，16: 26-28.

BIBLIOGRAPHY

Huang YM, Whang CW, (1998), Capillary electrophoresis of arsenic compounds with indirect fluorescence detection, Electrophoresis, 19: 2140-2144.

Hu CW, Wu MT, Chao MR, Pan CH, Wang CJ, Swenberg JA, Wu KY, (2004), Comparison of analyses of urinary 8-hydroxy-2'-deoxyguanosine by isotope-dilution liquid chromatography with electrospray tandem mass spectrometry and by enzyme-linked immunosorbent assay, Rapid Commun Mass Spectrom., 18: 505-510.

Huilgol NG, (2006), A phase I study to study arsenic trioxide with radiation and hyperthermia in advanced head and neck cancer, Int J Hyperthermia., 22: 391-397.

Hu J, Johnston KP, Williams III RO, (2004), Nanoparticles engineering processes for enhancing the dissolution rates of poorly water soluble drugs, Drug Dev Ind Pharma., 30: 233-245.

Hwang YH, Bomschein RL, Grote J, Menrath W, Roda S, (1997), Urinary arsenic excretion as a biomarker of arsenic exposure in children, Arch Environ Health, 52: 139-147.

Itoh K, Pongpeerapat A, Tozuka Y, Oguchi T, Yamanoto K, (2003), Nanoparticles formation of poorly water-soluble drugs from ternary ground mixtures with PVP and SDS, Chem Pharm Bull., 51: 171-174.

Ivanova AV, Ivanov SV, Zhang X, Ivanov VN, Timofeeva OA, Lerman MI, (2004), STRA13 interacts with STAT3 and modulates transcription of STAT3-dependent targets, J Mol Biol, 340: 641-653.

Jaruga P, Rodriquez H, Dizdaroglu M, (2001), Measurement of 8-hydroxy-2'-deoxyadenosine in DNA by liquid chromatography/mass spectrometry, Free Radic Biol Med., 31: 336-344.

Jeffrey RM, Khaledi MG (1998), High Performance Capillary Electrophoresis: Theory, Techniques, and Applications, John Wiley & Sons, NY, ch. 24, p. 831.

Jiang N, Benard CY, Kebir H, Shoubridge EA, Hekimi S, (2003), Human CLK2 links cell cycle progress, apoptosis, and telomere length regulation, J Biol Chem, 278: 21678-21684.

Jiang Su New Medical College, (1986), Encyclopedia of Chinese Medicine, Shanghai, China, Shanghai Scientific Publishing House, p. 1620-1622.

Jing HM, Yukihiro S, Ke XY, Yoshiro K, Akiharu W, (2002), Effect of arsenic trioxide on different cell lines derived from chronic myeloid leukemia, Zhongguo Shi Yan Xue Ye Xue Za Zhi (中国实验血液学杂志), 10: 413-418.

Jolliffe DM, (1993), A history of the use of arsenicals in man, J R Soc of Med., 86: 287-289.

BIBLIOGRAPHY

Johnson DG, Degregori J, (2006), Putting the oncogenic and tumor suppressive activities of E2F into context, Curr Mol Med, 6: 731-738.

Jorgenson JW, Lukacs KD, (1981), Capillary zone electrophoresis, Science, 222: 266-272.

Jorgenson JW, Lukacs KD, (1983), Free-zone electrophoresis in glass capillaries, Clin Chem., 27: 1551-1553.

Kalman DA, Hughes J, van Belle G, Burbacher T, Bolgiano D, Coble K, Mottet NK, Polissar L, (1990), Environ Health Perspect, 89: 145-151.

Kamiya H, Kasai H, (1995), Formation of 2-hydroxydeoxyadenosine triphosphate, and oxidatively damaged nucleotide, and its incorporation by DNA polymerases: steady-state kinetics of the incorporation, J Bio Chem, 270: 19446-19450.

Kang YH, Yi MJ, Kim MJ, Park MT, Bae S, Kang CM, Cho CK, Park IC, Park MJ, Rhee CH, Hong SI, Chung HY, Lee YS, Lee SJ, (2004), Caspase-independent cell death by arsenic trioxide in human cervical cancer cells: reactive oxygen species-mediated poly(ADP-ribose) polymerase-1 activation signals apoptosis-inducing factor release from mitochondria, Cancer Res., 64: 8960-8967.

Kasai H, (1997), Analysis of a form of oxidative DNA damage, 8-hydroxy-2'-deoxyguanosine, as a marker of cellular oxidative stress during carcinogenesis, Mutat Res., 387: 147-163.

Kasai H, Nishimura, (1984), Hydroxylation of deoxyguanosine at the C-8 position by ascorbic acid and other radical agents, Nucleic Acids Res., 12: 2137-2145.

Kasten FH, (1996), Paul Ehrlich: Pathfinder in cell biology. 1. Chronicle of his life and accomplishments in immunology, cancer research, and chemotherapy, Biotechnic & histochemistry, 71: 2-37.

Katharine EC, Rosemary AH, Shane R, Gisele MH, (1996), The effect of size on uptake of orally administration latex microparticless in the small intestine and transport to mesenteric lymph nodes, Pharm Res., 13: 1205-1209.

Katholi RE, Taylor GJ, McCann WP, Woods WT Jr, Womack KA, McCoy CD, Katholi CR, Moses HW, Mishkel GJ, Lucore CL, (1995), Nephrotoxicity from contrast media: attention with theophylline, Radiology, 195: 17-22.

Keck CM, Muller RH, (2006), Drug nanocrystals of poorly soluble drugs produced by high pressure homogenization, Eur J Pharm Biopharm., 62: 3-16.

Kerr JF, Wyllie AH, Currie AR, (1972), Apoptosis: a basic biological phenomenon with wide-range implications in tissue kinetics, Br J Cancer, 26: 239-257.

BIBLIOGRAPHY

Kibbe AH, (2000), Handbook of Pharmaceutical Excipients, 3rd Edition, AphA and PhP, Washington, DC.

Kipp JP, (2004), The role of solid nanoparticles technology in the parenteral delivery of poorly water-soluble drugs, Int J Pharm., 284: 109-122.

Klappacher GW, Lunyak VV, Sykes DB, Sawka-Verhelle D, Sage J, Brard G, Ngo SD, Gangadharan D, Jacks T, Kamps MP, Rose DW, Rosenfeld MG, Glass CK, (2002), An induced ETS repressor complex regulates growth arrest during terminal macrophage differentiation, Cell, 109: 169-180.

Koichi I, Adchara P, Yuichi T, Toshio O, Keiji Y, (2003), Nanoparticle formation of poorly water-soluble drugs from ternary ground mixtures with PVP and SDS, Chem. Pharm. Bull., 51: 171-174.

Kong AN, Yu R, Hebbar V, Chen C, Owuor E, Hu R, Ee R, Mandlekar S, (2001), Signal transduction events elicited by cancer prevention compounds, Mutat Res., 481: 231-241.

Krause KP, Muller RH, (2001), Production and characterization of highly concentrated nanosuspensions by high pressure homogenization, Int J Pharm., 214: 21-24.

Kreil DP, Russell RR, Russell S, (2006), Microarray oligonucleotide probes, Methods Enzymol., 410: 73-98.

Kristjansdottir K, Rudolph J, (2004), CDC25 phosphatases and cancer, Chem Biol, 11: 1043-1051.

Kubota R, Kunito T, Agusa T, Fujihara J, Monirith I, Iwata H, Subramanian A, Tana TS, Tanabe S, (2005), Urinary 8-hydroxy-2'-deoxyguanosine in inhabitants chronically exposed to arsenic in groundwater in Cambodia, J Environ Monit., 8: 293-299.

Kuhr WG, Yeung ES, (1988), Indirect fluorescence detection of native amino acids in capillary zone electrophoresis, Anal Chem., 60: 1831-1834.

Kunio E, Mari I, Kanjiro T, (2000), Kinetics of simultaneous adsorption of poly(vinylpyrrolidone) and sodium dodecyl sulfate on alumina particles, J Colloid Interface Sci., 232: 71-75.

Kurttio P, Pukkala E, Kahelin H, Auvinen A, Pekkanen J, (1999), Arsenic concentrations in well water and risk of bladder and kidney cancer in Finland, Environ Health Perspect., 107: 705-710.

Larsson R, Nygren P, (1989), A rapid fluorometric method for semiautomated determination of cytotoxicity and cellular proliferation of human tumor cell lines in microculture, Anticancer Res., 9: 1111-1120.

Le XC, Cullen WR, Reimer KJ, (1994), Human urinary arsenic excretion after one-

time ingestion of seaweed, crab, and shrimp, Clin Chem., 40: 617-624.

Lee TC, Ho IC, (1995), Modulation of cellular antioxidant defense activities by sodium arsenite in human fibroblasts, Arch Toxicol., 69: 498-504.

Li CS, Wu KY, Chang-chien GP, Chou CC, (2005), Analysis of oxidative DNA damage 8-hydroxy-2'-deoxyguanosine as a biomarker of exposures to persistent pollutants for marine mammals, Environ Sci Technol., 39: 2455-2460.

Li D, Du C, Lin Y, Wu M, (2002), Inhibition of growth of human nasopharyngeal cancer xenografts in SCID mice by arsenic trioxide, Tumori, 88: 522-526.

Li JE, Wu WL, Wang ZY, Sun GL, (2002), Apoptosis effect of As_2S_2 on K562 cells and its mechanism, Acta Pharmacol Sin., 23: 991-996.

Li SZ, (1593),Compendium of Materia Medica.

Lin TH, Huang YL, Tseng WC, (1995), Arsenic and lipid peroxidation in patients with blackfoot disease, Bull Environ Contam Toxicol., 54: 488-493.

List M, Sucker H, (1988), In GB Patent 2200048, Sandoz LTD. CH, GB.

Liversidge GG, Cundy KC, (1995), Particle size reduction for improvement of oral bioavailability of hydrophobic drugs: I. Absolute oral bioavailability of nanocrystalline danazol in beagle dogs, Int J Pharm., 125: 91-97.

Liversidge GG, Cundy KC, Bishop JF, Zekai DA, (1992), Surface modified drug nanoparticless, U.S. Patent No. 5, 145,684.

Lorenza ML, Ketterer M, Lowry J, Simon J, Dawson M, Poppenga R, (1996), Bioavailability of arsenic and lead in environmental substrates, EPA 910/R-96-002. USEPA Region 10, Seattle.

Lozzo RV, Moscatello DK, McQuillan DJ, Eichstetter I, (1999), Decorin is a biological ligand for the epidermal growth factor receptor, J Biol Chem, 274: 4489-4492.

Lu DP, Qiu JY, Jiang B, Wang Q, Liu KY, Liu YR, Chen SS, (2002), Tetra-arsenic tetra-sulfide for the treatment of acute promyelocytic leukemia: a pilot report, Blood, 99: 3136-3143.

Lu DP, Wang Q, (2002), Current study of APL treatment in China, Int J Hematol., 76 Suppl. 1: 316-318.

Lu M, Xia L, Luo D, Waxman S, Jing Y, (2004), Dual effects of glutathione-S-transferase pi on As_2O_3 action in prostate cancer cells: enhancement of growth inhibition and inhibition of apoptosis, Oncogene, 23: 3945-3952.

Lundstrom NG, Englyst V, Gerhardsson L, Jin T, Nordberg G, (2006), Lung cancer

development in primary smelter workers: a nested case-referent study, J Occup Environ Med., 48: 376-380.

Lunec J, Herbert K, Blount S, Griffiths HR, Emery P, (1994), 8-Hydroxydenoxyguanosine: A marker of oxidative DNA damage in systemic lupus erythematosus, FEBS lett., 348: 131-138.

Luo LY, Zhang TL, Wang K, (2006a), Differentiation of HL-60 cells induced by realgar nano-particles, Zhongguo Zhong Yao Za Zhi (中国中药杂志), 31: 1343-1346.

Luo LY, Huang J, Gou BD, Zhang TL, Wang K, (2006b), Induction of human promyelocytic leukemia HL-60 cell differentiation into monocytes by arsenic sulphide: involvement of serine/threonine protein phosphatases, Leuk Res., 30: 1399-1405.

Lynn S, Gurr JR, Lai HT, Jan KY, (2000), NADH oxidase activation is involved in arsenite-induced oxidative DNA damage in human vascular smooth muscle cells, Circ Res., 86: 514-519.

Ma CM, Li CL, (1989), Interaction between polyvinylpyrrolidone and sodium dodecyl sulfate at solid/liquid interface, J Colloid Interface Sci., 131: 485-492.

Mahieux R, Pise-Masision C, Gessain A, Brady JN, Olivier R, Perret E, Misteli T, Nicot C, (2001), Arsenic trioxide induces apoptosis in human T-cell leukemia virus type-1 and type-2 infected cells by a caspase-3-dependent mechanism involving bcl-2 cleavage, Blood, 98: 3762-3769.

Mainardes RM, Urban MC, Cinto PO, Khalil NM, Chaud MV, Evangelista RC, Gremiao MP, (2005), Colloidal carriers for ophthalmic drug delivery, Curr Drug Targets., 6: 363-371.

Ma M, Le XC, (1998), Effect of arsenosugar ingestion on urinary arsenic speciation, Clin Chem., 44: 539-550.

Ma YF, Liu GS, Du M, Stayton I, (2004), Recent developments in the determination of urinary cancer biomarkers by capillary electrophoresis, Electrophoresis, 25: 1473-1484.

Mandal BK, Ogra Y, Anzai K, Suzuki KT, (2004), Speciation of arsenic in biological samples, Toxicol Appl Pharmacol., 198: 307-318.

Masaaki S, Takuya O, Shinji N, Yoshiyuki K, Kingo N, (1998), Improvement of dissolution characteristics and bioavailability of poorly water-soluble drugs by novel cogrinding method using water-soluble polymer, Int J Pharm., 160: 11-19.

McCabe MJ Jr, Singh KP, Reddy SA, Chelladurai B, Pounds JG, Reners JJ Jr, States JC, (2000), J Pharmacol Exp Ther, 295: 724-733.

BIBLIOGRAPHY

McSheehy S, Pohl P, Velez D, Szpunar J, (2002), Multidimensional liquid chromatography with parallel ICP MS and electrospray MS/MS detection as a tool for the characterization of arsenic species in algae, Anal Bioanal Chem., 372: 457-466.

Mei SR, Yao QH, Wu CY, Xu GW, (2005), Determination of urinary 8-hydroxy-2'-deoxyguanosine by two approaches-capillary electrophoresis and GC/MS: an assay for in vivo oxidative DNA damage in cancer patients, J Chromatogr B Analyt Technol Biomed Life Sci., 827: 83-87.

Mendel J, Bugner D, Bermel AD, (1999), Particles generation and ink particles size effects in pigmented inkjet inks. Part II, J Nanoparticles Res., 1: 421-424.

Miller WH Jr, (2002), Molecular targets of arsenic trioxide in malignant cells, Oncologist, 7 Suppl.: 14-19.

Moghimi SM, Hunter AC, Murray JC, (2005), Nanomedicine: current status and future prospects, FASEB J., 19: 311-330.

Mosharraf MN, (1995), The effect of particle size and shape on the surface specific dissolution rate of microsized practically insoluble drugs, Int J Pharm., 122: 35-47.

Mosmann T, (1983), Rapid colorimetric assay for cellular growth and survival: Application to proliferation and cytotoxicity assays, J Immunol Meth., 65: 55-63.

Muller RH, Keck CM, (2004), Challenges and solutions for the delivery of biotech drugs---a review of drug nanocrystal technology and lipid nanoparticles, J Biotechnol., 113: 151-170.

Muller RH, Peters K, (1998), Nanosuspensions for the formulation of poorly soluble drugs I. Preparation by a size-reduction technique, Int J Pharm., 160: 229-237.

Mura P, Faucci MT, Parrini PL, (2001), Effects of grinding with microcrystalline cellulose and cyclodextrins on the ketaprofen physicochemical properties, Drug Dev Ind Pharm., 27: 119-128.

Namgung U, Xia Z, (2000), Arsenite-induced apoptosis in cortical neurons is mediated by c-Jun N-terminal protein kinase 3 and p38 mitogen-activated protein kinase, J Neurosci., 20: 6442-6451.

Niu C, Yan H, Yu T, Sun HP, Liu JX, Li XS, Wu W, Zhang FQ, Chen Y, Zhou L, Li JM, Zeng XY, Yang RRO, Yuan MM, Ren MY, Gu FY, Cao Q, Gu BW, Su XY, Chen GQ, Xiong SM, Zhang TD, Waxman S, Wang ZY, Chen Z, Hu J, Shen ZX, Chen SJ, (1999), Studies on treatment of acute promyelocytic leukemia with arsenic trioxide: Remission induction, follow-up, and molecular monitoring in 11 newly diagnosed and 47 relapsed acute promyelocytic leukemia patients, Blood, 94: 3315-3324.

BIBLIOGRAPHY

O'Gorman E, Beutner G, Dolder M, Korestky AP, Bridiczka D, Wallimann T, (1997), The role of creatine kinase in inhibition of mitochondrial permerbility transition, FEBS Lett, 414: 253-257.

Oikawa T, (2004), ETS transcription factors: possible targets for cancer therapy, Cancer Sci, 95: 626-633.

Olefirowicz TM, Ewing AG, (1990), Capillary electrophoresis with indirect amperometric detection, J Chromatogr., 499: 713-719.

Onda T, Uzawa K, Endo Y, Bukawa H, Yokoe H, Shibahara T, Tanzawa H, (2006), Ubiquitous mitochondrial creatine kinase downregulaiton in oral squamous cell carcinoma, Br J Cancer, 94: 698-709.

Otsuka M, Ofusa T, Matsuda Y, (1999), Physicochemical characterization of glybuzole polymorphs and their pharmaceutical properties, Drug Dev Ind Pharm., 25: 197-203.

Otsuka M, Matsuda Y, (1995), Effect of cogrinding with various kinds of surfactants on the dissolution behavior of phenytoin, J Pharm Sci., 84: 1434-1437.

Pan B, Xu L, Yang X, (2004), Advances in the study on antineoplastic action of realgar, Zhong Yao Cai (中药材), 27: 226-229.

Park JW, Choi YJ, Jang MA, Baek SH, Lim JH, Passaniti T, Kwon TK, (2001), Arsenic trioxide induces G2/M growth arrest and apoptosis after caspase-3 activation and bcl-2 phosphorylation in promonocytic U937 cells, Biochem Biophys Res Commun., 286: 726-734.

Park MJ, Lee JY, Kwak HJ, Park CM, Lee HC, Woo SH, Jin HO, Han CJ, An S, Lee SH, Chung HY, Park IC, Hong SI, Rhee CH, (2005), Arsenic trioxide inhibits invasion of HT1080 human fibrosarcoma cells: role of nuclear factor-kappaB and reactive oxygen species, J Cell Biochem., 95: 955-969.

Patarroyo M, Tryggvason K, Virtanen I, (2002), Laminin isoforms in tumor invasion, angiogenesis and metastasis, Semin Cancer Biol, 12: 197-207.

Patlolla AK, Tchounwou PB, (2005), Cytogenetic evaluation of arsenic trioxide toxicity in Sprague-Dawley rats, Mutat Res, 587: 126-133.

Patton SE, Hall MC, Ozen H, (2002), Bladder cancer, Curr Opin Oncol., 14: 265-272.

Peoples MC, Karnes HT, (2005), Recent developments in analytical methodology for 8-hydroxy-2'-deoxyguanosine and related compounds, J Chromatogr B Analyt Technol Biomed Life Sci., 827: 5-15.

Pietta PG, Simonetti P, Gardana C, Cristoni S, Bramati L, Mauri PL, (2003), LC-APCI-MS/MS analysis of urinary 8-hydroxy-2'-deoxyguanosine, J Pharm Biomed Anal., 32: 657-661.

BIBLIOGRAPHY

Podmore ID, Cooper D, Evans MD, Wood M, Lunec J, (2000), Simultaneous measurement of 8-oxo-2'-deoxyguanosine and 8-oxo-2'-deoxyadenosine by HPLC-MS/MS, Biochem Biophys Res Commun., 277: 764-770.

Podmore ID, Griffiths HR, Herbert KE, Minstry N, Mistry P, Lunec J, (1998), Vitamin C exhibits pro-oxidant properties, Nature, 392: 559-559.

Prentis RA, Lis Y, Walker SR, (1998), Pharmaceutical innovation by the seven U.K.-owned pharmaceutical companies (1964-1984), Br J Clin Pharmacol, 25: 387-396.

Pu YS, Hour TC, Chen J, Huang CY, Guan JY, Lu SH, (2002), Cytotoxicity of arsenic trioxide to transitional carcinoma cells, Urology, 60: 346-350.

Rasenack N, Muller BW, (2002), Dissolution rate enhancement by in situ micronization of poorly water-soluble drugs, Pharm Res., 19: 1894-1900.

Rehman A, Collis CS, Yang M, Kelly M, Diplock AT, Halliwell B, Rice-Evans C, (1998), The effects of iron and vitamin C co-supplementation on oxidative damage to DNA in healthy volunteers, Biochem Biophys Res Commun., 246: 293-298.

Renehan AG, Zwahlen M, Minder C, O'Dwyer ST, Shalet SM, Egger M, (2004), Insulin-like growth factor (IGF)-I, IGF binding protein-3, and cancer risk: systematic review and meta-regression analysis, Lancet, 363: 1346-1353.

Robertson AJB, (1983), The development of ideas on heterogeneous catalysis: Progress from Davy to Langmuir, Platimun Met Rev., 27: 31-39.

Roboz GJ, Dias S, Lam G, Lane WJ, Soignet SL, Warrell RP Jr, Rafii S, (2000), Arsenic trioxide induces dose- and time-dependent apoptosis of endothelium and may exert an antileukemia effect via inhibition of angiogenesis, Blood, 96: 1525-1530.

Rossman TG, Uddin AN, Burns FJ, (2004), Evidence that arsenite acts as a cocarcinogen in skin cancer. Toxicol Appl Pharmacol., 198: 394-404.

Rousselot P, Larghero J, Arnulf B, Poupon J, Rover B, Tibi A, Madelaine-Chambrin I, Cimerman P, Chevret S, Hermine O, Dombret H, Claude Brouet J, Paul Fermand J, (2004), A clinical and pharmacological study of arsenic trioxide in advanced multiple myeloma patients, Leukemia, 18: 1518-1521.

Roy K, Mao HQ, Huang SK, Leong KW, (1999), Oral gene delivery with chitosan-DNA nanoparticles generates immunologic protection in a murine model of peanut allergy, Nature Medicine, 5: 387-391.

Sabatini L, Barbieri A, Tosi M, Roda A, Violante FS, (2005), A method for routine quantitation of urinary 8-hydroxy-2'-deoxyguanosine based on solid-phase extraction and micro-high-performance liquid chromatography/electrospray ionization tandem mass spectrometry, Rapid Commun Mass Spectrom, 19:

147-152.

Sakamoto W, Isomura H, Fujie K, Nishihira J, Ozaki M, Yukawa S, (2003), Coffee increases levels of urinary 8-hydroxydeoxyguanosine in rats, Toxicology, 183: 255-263.

Schlegel D, Mattusch J, Wennrich R, (1996), Speciation analysis of arsenic and selenium compounds by capillary electrophoresis, Anal Bioanal Chem., 354: 535-539.

Seo T, Urasaki Y, Takemura H, Ueda T, (2005), Arsenic trioxide circumvents multidrug resistance based on different mechanisms in human leukemia cell lines, Anticancer Res., 25: 991-998.

Serrano J, Palmeira CM, Wallace KB, Kuehl DW, (1996), Determination of 8-hydroxydeoxyguanosine in biological tissue by liquid chromatography/electrospray ionization-mass spectrometry/mass spectrometry, Rapid Commun Mass Spectrom., 10: 1789-1791.

Shen ZX, Chen GQ, Ni JH, Li XS, Xiong SM, Qiu QY, Zhu J, Tang W, Sun GL, Yang KQ, Chen Y, Zhou L, Fang ZW, Wang YT, Ma J, Zhang P, Zhang TD, Chen SJ, Chen Z, Wang ZY, (1997), Use of arsenic trioxide (As_2O_3) in the treatment of acute promyelocytic leukemia (APL). 2. Clinical efficacy and pharmacokenetics in relapsed patients, Blood, 89: 3354-3360.

Shen ZY, Shen J, Cai WJ, Hong C, Zheng MH, (2000), The alteration of mitochondria is an early event of arsenic trioxide induced apoptosis in esophageal carcinoma cells, Int J Mol Med., 5: 155-158.

Shi H, Shi X, Liu KJ, (2004), Oxidative mechanism of arsenic toxicity and carcinogenesis, Mol Cell Biochem., 255: 67-78.

Simonelli AP, Mehta SC, Higuchi WI, (1970), Inhibition of sulfathiazole crystal growth by polyvinylpyrrolidone, J Pharm Sci., 59: 633-638.

Singh R, McEwan M, Lamb JH, Santella RM, Farmer PB, (2003), An improved liquid chromatography/tandem mass spectrometry method for the determination of 8-oxo-7,8-dihydro-2'-deoxyguanosine in DNA samples using immunoaffinity column purification, Rapid Commun Mass Spectrom., 17: 126-134.

Soga T, Imaizumi M, (2001), Capillary electrophoresis method for the analysis of inorganic anions, organic acids, amino acids, nucleotides, carbohydrates and other anionic compounds, Electrophoresis 22: 3418-3425.

Soignet SL, Maslak P, Wang ZG, Jhanwar S, Calleja E, Dardashti LJ, Corso D, DeBlasio A, Gabrilove J, Scheinberg DA, Pandolfi PP, Warrell RP Jr, (1998), Complete remission after treatment of acute promyelocytic leukemia with arsenic trioxide, N Engl J Med., 339: 1341-1348.

BIBLIOGRAPHY

Song H, Xia SL, Liao C, Li YL, Wang YF, Li TP, Zhao MJ, (2003), Genes encoding Pir51, Beclin 1, RbAp48 and aldolase b are up or down-regulated in human primary hepatocellular carcinoma, World J Gastroenterol, 10: 509-513.

Stella B, Arpicco S, Peracchia MT, Desmaele D, Hoebeke J, Renoir M, D'Angelo J, Cattel L, Couvreur P, (2000), Design for folic acid-conjugated nanoparticles for drug targeting, J Pharm Sci., 29: 1452-1464.

Sternmaus C, Moore L, Hopenhayn-Rich C, Biggs ML, Smith AH, (2000), Arsenic in drinking water and bladder cancer, Cancer Invest., 18: 174-182.

Styblo M, Del Razo LM, Vega L, Germolec DR, LeCluyse EL, Hamilton GA, Reed W, Wang C, Cullen WR, Thomas DJ, (2000), Comparison toxicity of trivalent and pentavalent inorganic and methylated arsenicals in rat and human cells, Arch Toxicol., 74: 289-299.

Sun B, Macka M, Haddad PR, (2002), Separation of organic and inorganic arsenic species by capillary electrophoresis using directed sepctrophotometric detection, Electrophoresis, 23: 2430-2438.

Svoboda P, Kasai H, (2004), Simultaneous HPLC analysis of 8-hydroxydeoxyguanosien and 7-methylguanine in urine from human and rodents, Anal Biochem, 334: 239-250.

Tan XZ, Grollman AP, Shibutani S, (1999), Comparison of the mutagenic properties of 8-oxo-7,8-dihydro-2'-deoxyadenosine and 8-oxo-7,8-dihydro-2'-deoxyguanosine DNA lesions in mammalian cells, Carcinogenesis, 20: 2287-2292.

Tchounwou PB, Patlolla AK, Centeno JA, (2003), Carcinogenic and systemic health effects associated with arsenic exposure-a critical review, Toxicol Pathol., 31: 575-588.

Tom JW, Bebededetti PG, (1991), Particle formation with supercritical fluids-a review, J Aerosol Sci., 22: 555-584.

Tsai SY, Tsai MJ, (1997), Chick ovalbumin upstream promoter-transcription factors (COUP-TFs): coming of age, Endocr Rev, 18: 229-240.

Tseng WC, Yang MH, Chen TP, Huang YL, (2002), Automated, continuous, and dynamic speciation of urinary arsenic in the bladder of living organisms using microdialysis sampling coupled on-line with high performance liquid chromatography and hydride generation atomic absorption spectrometry, Analyst, 127: 560-564.

Turkson J, Jove R, (2000), STAT protein: novel molecular targets for cancer drug discovery, Oncongene, 19: 6613-6626.

User's Manual of CE-L1 Instrument (version 2.3), CE Resource Pte Ltd, Singapore.

BIBLIOGRAPHY

United States Environmental Protection Agency, (2003), http://www.epa.gov/safewater/arsenic/regulations.html

Urso ML, Clarkson PM, (2001), Oxidative stress, exercise, and antioxidant supplementation, Toxicology, 189: 41-54.

Uslu R, Sanli UA, Sezgin C, Karabulut B, Terzioglu E, Omay SB, Goker E, (2000), Arsenic trioxide-mediated cytotoxicity and apoptosis in prostate and ovarian carcinoma cell lines, Clin Cancer Res., 6: 4957-4964.

Vahter M, (2002), Mechanisms of arsenic biotransformation, Toxicology, 27: 211-217.

Valladares A, Hernandez NG, Gomez FS, Curiel-Quezada E, Madrigal-Bujaidar E, Vergara MD, Martinez MS, Arenas Aranda DJ, (2006), Genetic expression profiles and chromosomal alterations in sporadic breast cancer in Mexican women, Cancer Genet Cytogenet, 170: 147-151.

Van Campen LE, Murphy WJ, Franks JR, Mathias PI, Toraason MA, (2002), Oxidative DAN damage is associated with intense noise exposure in the rat, Hear Res, 164: 29-38.

van't Veer LJ, Dai H, van de Vijver MJ, He YD, Hart AA, Mao M, Peterse HL, van der Kooy K, Marton MJ, Witteveen AT, Schreiher GJ, Kerbhoven RM, Roberts C, Linsley PS, Bernards R, Friend SH, (2002), Gene expression profiling predicts clinical outcome of breast cancer, Nature, 415: 530-536.

Venturelli D, Martinez R, Melotti P, Casella I, Peschle C, Cucco C, Spampinato G, Darzynkiewicz Z, Calbretta B, (1995), Overexpression of DR-nm23, a protein encoded by a member of the nm23 gene family, inhibits granulocyte differentiation and induces apoptosis in 32Dc13 myeloid cells, Proc Natl Acad Sci USA, 92: 7435-7439.

Verschuur AC, Van Gennip AH, Leen R, Muller EJ, Elzinga L, Voute PA, Van Kuilenburg AB, (2000), Cyclopentenyl cytosine inhibits cytidine triphosphate synthetase in paediatric acute non-lymphocytic leukaemia: a promising target for chemotherapy, Eur J Cancer, 36: 627-635.

Vijayaraghavan M, Wanibuchi H, Karim R, Yamamoto S, Masuda C, Nakae D, Konishi Y, Fukushima S, (2001), Dimethylarsinic acid induces 8-hydroxy-2'-deoxyguanosine formation in the kidney of NCI-Black-Reiter rats, Cancer Lett, 165: 11-17.

Vuky J, Yu R, Schwartz L, Motzer RJ, (2002), Phase II trials of arsenic trioxide in patients with metastatic renal cell carcinoma, Invest New Drugs, 20: 327-330.

Wang H, Liu S, Lu X, Zhao X, Chen S, Li X, (2003), Gene expression profile changes in NB4 cells induced by realgar, Chin Med J., 116: 1074-1077.

Wang HY, Liu SX, (2002), Investigation on NB4 cell responses to realgar by cDNA

microarray, Zhongguo Zhang Yao Za Zhi (中国中药杂志), 27: 600-604.

Wang MC, Liu SX, Liu PB, (2006), Effect of realgar on the gene expression profile of multiple myeloma cell line RPMI 8226, Zhong Nan Da Xue Xue Bao Yi Xue Ban (中南大学学报医学版), 31: 24-27.

Wang ZY, (2001), Arsenic compounds as anticancer agents, Cancer Chemother Pharmacol., 48 Suppl. 1: S72-76.

Wanibuchi H, Hori T, Meenakshi V, Ichihara T, Yamanoto S, Yano Y, Otani S, Nakae D, Konishi Y, Fukushima S, (1997), Promotion of rat hepatocarcinogenesis by demethylarsinic acid: association with elevated ornithine decarboxylase activity and formation of 8-hydroxydeoxyguanosine in the liver, Jpn J Cancer Res, 88: 1149-1154.

Waxman S, Anderson KC, (2001), History of the development of arsenic derivatives in cancer therapy, Oncologist, 6 (Suppl. 2): 3-10.

Weimann A, Belling D, Poulsen HE, (2001), Measurement of 8-oxo-2'-deoxyguanosine and 8-oxo-2'-deoxyadenosine in DNA and human urine by high performance liquid chromatography-electrospray tandem mass spectrometry, Free Radic Biol Med., 30: 757-764.

Wiseman H, Kaur H, Halliwell B, (1995), DNA damage and cancer: measurement and mechanism, Cancer Lett., 93: 113-120.

Woo SH, Park IC, Park MJ, Lee HC, Lee SJ, Chun YJ, Lee SH, Hong SI, Rhee CH, (2002), Arsenic trioxide induces apoptosis through a reactive oxygen species-dependent pathway and loss of mitochondrial membrane potential in HeLa cells, Int J Oncol., 21: 57-63.

Wu LL, Chiou CC, Chang PY, Wu JT, (2004), Urinary 8-OHdG: a marker of oxidative stress to DNA and a risk factor for cancer, atherosclerosis and diabetics, Clin Chim Acta, 339: 1-9.

Xiao YF, Liu Y, Liu SX, Ren LF, (2005), Effect of realgar on expression of survivin in leukemia cell lines and its significance, Zhongguo Shi Yan Xue Ye Xue Za Zhi (中国实验血液学杂志), 13: 389-390.

Zhang C, Huang SL, Xiang Y, Guo AX, (2003), Study on realgar inducing apoptosis in T lymphocutic cell line CEM, Zhong Xi Yi Jie He Xue Bao (中西医结合学报), 1: 42-43.

Zhang J, Wang JC, Han YH, Wang LF, Ji SP, Liu SX, Liu XP, Yan LB, (2005), High expression of bcl-x(L) in K562 cells and its role in the low sensitivity of K562 to realgar-induced apoptosis, Acta Haematol., 113: 247-254.

Zhang P, (1999), The use of arsenic trioxide in the treatment of acute promyelocytic leukemia, J Biol Regul Homeost Agents, 13: 195-200.

BIBLIOGRAPHY

Zhang P, Wang S, Hu L, Qiu F, Yang H, Xiao Y, Li X, Han X, Zhou J, Liu P, (2000), Seven year's summary report on the treatment of acute promyolocytic leukemia with arsenic trioxide-an anlysis of 242 cases, Zhonghua Xue Ye Xue Za Zhi (中华血液学杂志), 21: 67-70.

Zhang TC, Cao EH, Li JF, Ma W, Qin JF, (1999), Induction of apoptosis and inhibition of human gastric cancer MGC-803 cell growth by arsenic trioxide, Eur J Cancer, 35: 1258-1263.

Zhang TD, Chen GQ, Wang ZG, Wang ZY, Chen SJ, Chen Z, (2001), Arsenic trioxide, a therapeutic agent for APL, Oncogene, 20: 7146-7153.

Zhao XA, Liu SX, (2003), Effects of realgar on tissue factor expression of NB4 and MR2 cells, Zhongguo Zhong Yao Za Zhi (中国中药杂志), 28: 553-556.

Zhong L, Chen F, Han J, Shao N, Ouyang R, (2003), Effects of red orpiment on cell morphology and expression of PML mRNA and protein in NB4 and HL-60 cels, Chinese Med J., 116: 148-150.

Zhong L, Chen FY, Han JY, Shao NX, Ouyang RR, (2001), Effects of red orpiment on cell morphology and expression of PML mRNA and protein in NB4 and HL-60 cells, Zhongguo Shi Yan Xue Ye Xue Za Zhi (中国实验血液学杂志), 9: 223-227.

Zhou H, Kato A, Miyaji T, Yasuda H, Fujigaki Y, Yamamoto T, Yonemura K, Takebayashi S, Mineta H, Hishida A, (2006), Urinary marker for oxidative stress in kidneys in cisplatin-induced acute renal failure in rats, Nephrol Dial Transplant, 21: 616-623.

Zhu J, Lallemand-Breitenbach V, de The H, (2001), Pathways of retinoic acid- or arsenic trioxide-induced PML/RARalpha catabolism, role of oncogene degradation in disease remission, Oncogene, 20: 7257-7265.

Zhu J, Okumura H, Ohtake S, Nakamura S, Nakao S, (2003), Arsenic trioxide induces apoptosis in leukemia/lymphoma cell lines via the CD95/CD95L system, Oncol Rep., 10: 705-709.

Zhu XH, Shen YL, Jing YK, Cai X, Jia PM, Huang Y, Tang W, Shi GY, Sun YP, Dai J, Wang ZY, Chen SJ, Zhang TD, Waxman S, Chen Z, Chen GQ, (1999), Apoptosis and growth inhibition in malignant lymphocytes after treatment with arsenic trioxide at clinically achievable concentrations, Journal of the National Cancer Institute, 91: 772-778.

Zornig M, Hueber A, Baum W, Evan G, (2001), Apoptosis regulators and their role in tumorigenesis, Biochim Biophys Acta, 1551: F1-F37.

Yamada K, Miyamoto K, (2005), Basic helix-loop-helix transcription factors, BHLHB2 and BHLHB3; their gene expressions are regulated by multiple extracellular stimuli, Front Biosci, 10: 3151-3171.

BIBLIOGRAPHY

Yamanaka K, Hasegawa A, Sawamura R, Okada S, (1989), Dimethylated arsenic induce DNA strand breaks in lung via the production of active oxygen in mice, Biochem Biophys Res Commun., 165: 43-50.

Yamauchi H, Aminaka Y, Yoshida K, Sun G, Pi J, Waalkes MP, (2004), Evaluation of DNA damage in patients with arsenic poisoning: urinary 8-hydroxydeoxyguanine, Toxicol Appl Pharnacol., 198: 291-296.

Yamauchi H, Takahashi K, Mashiko M, Yamamura Y, (1989), Biological monitoring of arsenic exposure of gallium arsenide- and inorganic arsenic-exposed workers by determination of inorganic arsenic and its metabolites in urine and hair, Am Ind Hyg Assoc J., 50: 606-612.

Yasuhara T, Hara K, Sethi KD, Morgan JC, Borlongan CV, (2007), Increased 8-OHdG levels in the urine, serum, and substantia nigra of hemiparkinsonian rats, Brain Res, 1133: 49-52.

Ye HQ, Gan L, Yang XL, Xu HB, (2006), Membrane-associated cytotoxicity induced by realgar in promyelocytic leukemia HL-60 cells, J Ethnopharmacol., 103: 366-371.

Ye HQ, Gan L, Yang XL, Xu HB, (2005), Membrance toxicity accounts for apoptosis induced by realgar nanoparticles in promyelocytic leukemia HL-60 cells, Biol Trace Elem Res., 103: 117-132.

Yonemochi E, Kitahara S, Maeda S, Yamamura S, Oguchi T, Yamamoto K, (1999), Physicochemical properties of amorphous clarithromycin obtained by grinding and spray drying, Eur J Pharm Sci., 7: 331-338.

Yoshida K, Kuroda K, Zhou X, Inoue Y, Date Y, Wanibuchi H, Fukushima S, Endo G, (2003), Urinary sulfer-containing metabolite produced by intestinal bacteria following oral administration of dimethylarsinic acid to rats, Chem Res Toxicol., 16: 1124-1129.

Young MR, Colburn NH, (2006), Fra-1 a target for cancer prevention or intervention, Gene, 379: 1-11.

Yu G, Swiston J, Young D, (1994), Comparison of human CAP and CAP2, homologs of the yeast adenylyl cyclase-associated proteins, J Cell Sci, 107: 1671-1678.

Publications

1. Wu JZ, Ho PC, (2004), Speciation of inorganic and methylated arsenic compounds by capillary zone electrophoresis with indirect UV detection. Application to the analysis of alkali extracts of As_2S_2 (realgar) and As_2S_3 (orpiment), J Chromatogr A, 1026: 261-270.

2. Wu JZ, Ho PC, (2006), Evaluation of the *in vitro* activity and *in vivo* bioavailability of realgar nanoparticles prepared by cryo-grinding, Eur J Pharm Sci., 29: 35-44.

3. Li HY, Lai CS, Wu JZ, Ho PC, de Vos D, Tiekink ERT, (2007), Cytotoxicity, quantitative structure-activity relationship (QSAR), and anti-tumor activity of bismuth dithiocarbamate complexes, J Inorg Biochem., 101: 809-816.

4. Wu JZ, Ho PC, (2005), Identification of the main components in the alkali extracts of realgar and orpiment by capillary zone electrophoresis, *17th Singapore Pharmacy Congress*, Singapore, July 1-4. (Poster presentation)

5. Wu JZ, Ho PC, (2006), Evaluation of the *in vitro* activity and *in vivo* bioavailability of realgar nanoparticles prepared by cryo-grinding, *18th Singapore Pharmacy Congress*, Singapore, June 30-July 3. (Oral presentation)